Technische Universität München
TUM School of Engineering and Design

Characterization of hydraulic and biogeochemical processes in the subsurface related to anthropogenic impacts and the potential use of managed aquifer recharge

Anne Sophie Charlotte Imig

Vollständiger Abdruck der von der TUM School of Engineering and Design der Technischen Universität München zur Erlangung einer

Doktorin der Naturwissenschaften (Dr. rer. nat.)

genehmigten Dissertation.

Vorsitz: apl. Prof. Dr. Thomas Baumann

Prüfer*innen der Dissertation:

1. Priv.-Doz. Dr. Arno Rein
2. Priv.-Doz. Dr. Gabriele Chiogna

Die Dissertation wurde am 07.11.2022 bei der Technischen Universität München eingereicht und durch die TUM School of Engineering and Design am 15.12.2022 angenommen.

Interpretation of dissertation content by an artificial intelligence program that generates images from textual descriptions

Abstract

About half of the world's population depends on groundwater for drinking water supply. Therefore, protecting our global groundwater resources is of tremendous importance to sustain life on earth. Impacts of climate change, such as lower frequency but higher intensities of rain events, can lead to decreased infiltration and, thus, severe soil water and groundwater droughts. Moreover, groundwater resources can be contaminated by various pollutants like agrochemicals or effluents from wastewater treatment plants, leading to decreased groundwater quality. Preventing and mitigating groundwater contamination is essential for avoiding adverse effects on human health and the environment.

A technical solution to address quantitative and qualitative protection of groundwater resources is managed aquifer recharge (MAR). MAR refers to a suite of methods that are increasingly being used worldwide. Excess water from rainfall or flooding is infiltrated in an aquifer and stored for recovery at a future need. To implement MAR solutions safely and sustainably, infiltration processes, as well as transport and fate of contaminants within the subsurface, must be understood. Otherwise, MAR operation can negatively affect groundwater and soil resources instead of protecting them.

Investigating the hydraulic and biogeochemical processes in the subsurface remains challenging. Soil samples can be taken, which on the downside, disturb the natural soil system. In laboratory experiments with soil samples, influences of hydraulic and biogeochemical processes and their rates can be determined. However, such investigations often fall short of capturing the subsurface’s heterogeneous conditions. Studies of proxies, such as tracers, can allow leaving the subsurface undisturbed to obtain hints on subsurface processes and characteristics. Further, lysimeter experiments enable the investigation of field conditions and have the advantage that measurements, such as drainage samples, can be collected.

In addition to measurements, mechanistic descriptions of subsurface processes and their representation with different computational models have been developed. These models attempt to simplify the consideration of subsurface processes appropriately and efficiently. Combining observations and mathematical modelling is often the only way to improve process understanding and obtain information on involved processes and their rates. Within mechanistic models, flow and (reactive) transport in the subsurface are usually described with differential equations, including several independent parameters (partial differential equations). For some specific, well-defined problems, analytical solutions were found. For example, lumped-parameter models (LPM), incorporating analytical solutions for tracer transport, can be used to obtain information on subsurface flow and transport characteristics. Compared to numerical models, LPM require only a limited number of input data (tracer input and output) and fitting parameters (“lumped” parameters).

Abstract

Lumped-parameter and numerical models are applied to investigate lysimeter experiments in the first part of this thesis. The overall objective is to contribute to an improved understanding of hydraulic and biogeochemical processes in the subsurface using observations and modelling.

The two investigated lysimeters are located at a test field in Wielenbach, southern Germany, and consist of stainless-steel cylinders with a surface area of 1 m² and a length of 2 m each. The lysimeters are filled with undisturbed monolithic soil cores from two different locations. Lysimeter 1 (Ly1) contains sandy gravels from a former target shooting range near Garching, Germany. Lysimeter 2 (Ly2) contains clayey sandy silt, and the soil core was excavated from an agricultural site at Hutthurm-Auberg, Germany. The study site and data set represented a unique research opportunity, as the measurements were taken over several years. To the best of our knowledge, few lysimeter studies with stable water isotopes are available that consider the same vegetation for different soil types as well as the measurements over several years.

First, stable water isotope data ($\delta^{18}O$ and $\delta^{2}H$), taken over three years in precipitation and lysimeter drainage, were investigated. Simulation results from an improved LPM approach mimicking variable soil water flow were compared to numerical simulation of unsaturated flow and stable water isotope transport using HYDRUS-1D. Both approaches were extended by the consideration of preferential flow paths. Finally, although LPM requires fewer input data than numerical models, both approaches achieve comparable decision-support integrity.

Next, an aim was to improve the description of the stable water isotope transport in the numerical model of Ly2. Since the objective was no longer to compare the numerical model setup to the LPM approach, we wondered if we could achieve an improved model performance by considering a multi-process modelling approach including immobile water and preferential flow processes. For Ly1, modelling results were satisfactory without considering immobile water. For Ly2, however, the damping observed in the isotope signature of the drainage could not be fully covered. Moreover, model performance improved by considering immobile water with a dual-porosity setup. Further, the description of short-term fluctuations of the measured stable water isotopes, which were related to preferential flow, seemed generally not well described. Neither for Ly1 nor Ly2, with approaches currently available in HYDRUS-1D, an adequate description was possible. Accounting for the fractionation of stable water isotopes due to evaporation did not lead to improved model performance in both model setups. Consequentially, the differences in soil hydraulic properties between the two lysimeters seem to impact water flow processes dominantly.

Third, a focus was set on the investigation and description of biodegradation and sorption processes in the lysimeters: the fate and transport of four herbicides applied at the lysimeter site were investigated. For this task, the HYDRUS-1D models were extended by reactive transport. Herbicide concentrations monitored weekly in lysimeter drainage over 4.5 years were analysed and modelled. Recovery rates of 0.9-15.9% of applied herbicides in lysimeter drainage were found (up to 20.9%, including measured metabolites). Metabolites formation and accumulation were observed in lysimeter drainage. Moreover, biodegradation was also indicated by small changes in the stable carbon isotope composition of herbicides between input and drainage. Model setups could well describe the dynamics of herbicide concentrations in lysimeter drainage. Concentration peaks in drainage were connected in time with higher amounts of precipitation, indicating an influence of preferential flow. The soil with a coarser texture (Ly1) showed less herbicide leaching in contrast to the soil with a finer texture (Ly2), which can be explained by a larger mobile phase in the coarser texture (Ly1).

The findings of this work show that the calibration of an unsaturated flow and transport model with stable water isotopes was successful. Further, considering multi-process modelling to describe water flow and solute transport in the unsaturated zone is a helpful tool to identify dominant processes and should be an integral part of model calibration.

The second part of this thesis addresses potential risks related to soil and groundwater systems during the application of MAR. Knowledge about the unsaturated zone is essential for designing and implementing MAR schemes because potential risks, such as the infiltration of pollutants into the soil and groundwater, are connected. In addition, an improved understanding of flow and transport processes can help mitigate these risks since the prediction of contamination spreading or clogging processes will be possible in greater detail.

One approach to enable the safe and accepted use of MAR could be to provide comprehensive risk management, including identifying, analysing, and evaluating potential risks related to MAR. We aimed to summarize existing MAR risk assessment methodologies and to identify frequently considered risks. Further, we highlighted limitations and lessons learned from MAR risk assessment documented in the literature. As a state of the art description, this part of the thesis may serve as a starting point for further evaluating potentially suitable methods for MAR risk assessment to improve safety and decrease risks to soil and groundwater systems related to MAR schemes.

Overall, the findings of this thesis will support modellers and decision-makers in determining the contamination potentials of groundwater resources and identifying risks to soil and groundwater systems.

Zusammenfassung

Für circa die Hälfte der Weltbevölkerung basiert die Trinkwasserversorgung mit Grundwasser. Der Schutz unserer Grundwasserressourcen ist deshalb von enormer Bedeutung, auch um menschliches Leben auf der Erde zu ermöglichen. Auswirkungen des Klimawandels, wie z.B. eine geringere Häufigkeit, aber höhere Intensität von Regenereignissen, führen zu einer verringerten Infiltration und damit zu einer bedeutsamen Bodenwasser- und Grundwasserknappheit. Außerdem können Grundwasserressourcen durch Agrochemikalien oder Abwässer aus Kläranlagen verunreinigt werden, was zu einer Verschlechterung der Grundwasserqualität führt. Grundwasserkontamination hat negative Auswirkungen auf die menschliche Gesundheit und die Umwelt, deshalb ist deren Verhinderung und Eindämmung von entscheidender Bedeutung.

Eine technische Lösung für den quantitativen und qualitativen Schutz der Grundwasserressourcen ist künstliche Grundwasseranreicherung (managed aquifer recharge MAR). MAR bezieht sich auf eine Reihe von Methoden, die weltweit zunehmend eingesetzt werden. Überschüssiges Wasser aus Regenfällen oder Überschwemmungen wird in einen Grundwasserleiter infiltriert und gespeichert, damit es bei späterem Bedarf wieder genutzt werden kann. Um MAR Lösungen sicher und nachhaltig umzusetzen, müssen die Infiltrationsprozesse sowie der Transport von Schadstoffen im Untergrund nachvollzogen werden. Andernfalls kann die Anwendung von MAR die Grundwasser- und Bodenressourcen kontaminieren, anstatt sie zu schützen.

Die Untersuchung der hydraulischen und biogeochemischen Prozesse im Untergrund stellt, nach wie vor, eine Herausforderung dar. Es können Bodenproben entnommen werden, die jedoch das natürliche Bodensystem stören. In Laborexperimenten mit Bodenproben können Beiträge von hydraulischen und biogeochemischen Prozessen und deren Raten bestimmt werden. Allerdings reichen solche Untersuchungen oft nicht aus, um die heterogenen Bedingungen im Untergrund zu erfassen. Untersuchungen mit Proxies, wie z. B. Tracern, können es ermöglichen, den Untergrund ungestört zu belassen, und dennoch Hinweise auf Prozesse und Eigenschaften des Untergrunds zu erhalten. Darüber hinaus ermöglichen Lysimeterexperimente die Untersuchung von Feldbedingungen und haben den Vorteil, dass Messungen, etwa Proben im Lysimeterausfluss, gesammelt werden können.

Zusätzlich zu den Messtechniken wurden mechanistische Beschreibungen des Untergrundes sowie deren Darstellungen in Rechenmodelle entwickelt, die versuchen, die Vorgänge im Untergrund in geeigneter und effizienter Weise zu vereinfachen. Die Kombination von Messdaten und mathematischen Modellen ist oft die einzige Möglichkeit, das Verständnis der Prozesse zu verbessern oder Informationen über die beteiligten Prozesse und deren Raten zu erhalten. In mechanistischen Modellen werden Strömung und (reaktiver) Transport im Untergrund in der Regel durch Differentialgleichungen mit mehreren unabhängigen Parametern (partielle Differentialgleichungen)

beschrieben. Für einige spezifische, wohldefinierte Probleme wurden analytische Lösungen gefunden. Sogenannte Lumped-Parameter Modelle, LPM (Modelle mit zusammengefassten Parametern), die analytische Lösungen für den Tracertransport enthalten, können verwendet werden, um Informationen über die Strömungseigenschaften des Untergrundes zu erhalten. Im Vergleich zu numerischen Modellen erfordern LPM nur eine begrenzte Anzahl von Eingangsdaten (Tracerinput und -output) und Anpassungsparametern.

Im ersten Teil dieser Arbeit werden Lumped-Parameter und numerische Modelle angewandt, um Lysimeterexperimente zu untersuchen. Das übergeordnete Ziel ist es, mit Hilfe von Beobachtungen und Modellierung zu einem besseren Verständnis der hydraulischen und biogeochemischen Prozesse im Untergrund beizutragen.

Die beiden untersuchten Lysimeter sind auf einem Testfeld in Wielenbach in Süddeutschland, Oberbayern, installiert. Die Lysimeter bestehen aus Edelstahlzylindern mit einer Oberfläche von je 1 m² und einer Länge von 2 m und sind mit ungestörten monolithischen Bodenkernen von zwei verschiedenen Standorten gefüllt. Lysimeter 1 (Ly1) enthält sandige Kiese, die von einem ehemaligen Schießplatz in der Nähe von Garching bei München, Deutschland, stammen. Lysimeter 2 (Ly2) enthält einen lehmigen, sandigen Schluff, und der Bodenkern wurde auf einer landwirtschaftlichen Fläche in Hutthurm-Auberg bei Passau, Deutschland, entnommen. Der Untersuchungsstandort und der Datensatz stellen eine einzigartige Forschungsmöglichkeit dar, da der Messzeitraum mehrere Jahre abdeckt. Nach Kenntnissen der Autoren, gibt es nur wenige Lysimeterstudien mit stabilen Wasserisotopen, die dieselbe Vegetation und meteorologischen Bedingungen für verschiedene Bodentypen, sowie die Messungen über einen Zeitraum von mehreren Jahren berücksichtigen.

Es wurden stabile Wasserisotopendaten ($\delta^{18}O$ und $\delta^{2}H$) im Niederschlag und im Sickerwasser der beiden Lysimeter über einen Zeitraum von drei Jahren untersucht. Zunächst wurden Ergebnisse eines verbesserten LPM, dass zeitlich variable Strömung im Untergrund nachahmt, mit einer numerischen Simulation (HYDRUS-1D) der ungesättigten Strömung und des Transports stabiler Wasserisotope verglichen. Darüber hinaus wurden beide Ansätze um die Berücksichtigung von präferentiellen Fließpfade erweitert. Obwohl LPM- Ansätze im Vergleich zu numerischen Modellen weniger Eingangsdaten benötigen, erzielte beide Modellansätze vergleichbar gute Beschreibungen der gemessenen Daten.

Als nächstes wurde versucht, die Beschreibung des Transports stabiler Wasserisotope im numerischen Modell von Ly2 zu verbessern. Da das Ziel nicht mehr darin bestand, den numerischen Modellaufbau mit dem LPM-Ansatz zu vergleichen, fragten wir uns, ob wir eine verbesserte Modellbeschreibung erreichen könnten, indem wir einen Multiprozess-Modellierungsansatz in Betracht ziehen, der immobiles Wasser und präferentielle Strömungsprozesse einschließt. Für Ly1 waren die Modellierungsergebnisse ohne Berücksichtigung von immobilem Wasser zufriedenstellend. Für Ly2

konnte die saisonale Dämpfung der Isotopensignatur im Lysimeterausfluss nicht vollständig erfasst werden. Durch die Berücksichtigung von immobilem Wasser mit einem Doppelporositätsansatz verbesserte sich die Modellbeschreibung. Darüber hinaus konnten kurzfristiger Fluktuationen der gemessenen stabilen Wasserisotope, die wir mit Einflüssen von präferentiellen Fließpfande erklären, mit den verfügbaren Ansätzen in HYDRUS-1D weder für Ly1 noch für Ly2 gut beschrieben werden. Die Berücksichtigung von Fraktionierung stabiler Wasserisotope durch die Evaporation führte zu keiner verbesserten Beschreibung durch das Modell. Folglich schienen sich die unterschiedlichen hydraulischen Eigenschaften des Bodens zwischen den beiden Lysimetern in erster Linie auf die Strömungsprozesse auszuwirken.

Ein weiterer Schwerpunkt wurde auf die Untersuchung und Beschreibung von Bioabbau- und Sorptionsprozessen von Herbiziden in den Lysimetern gelegt. Die mit den stabilen Wasserisotopen kalibrierten Strömungs- und Transportmodelle wurden um den reaktiven Transport erweitert. Herbizidkonzentrationen im Lysimeterausfluss, die über einen Zeitraum von viereinhalb Jahren wöchentlich gemessenen wurden, wurden analysiert und modelliert. Es wurden Rückgewinnungsraten von 0,9-15,9 % der ausgebrachten Herbizide im Lysimeterausfluss festgestellt (bis zu 20,9 %, wenn man die gemessenen Metaboliten mit einbezieht). Die Bildung und Akkumulation von Metaboliten wurde im Lysimeterausfluss beobachtet und auf das Vorhandensein eines biologischen Abbaus deuteten auch die beobachteten geringen Veränderungen in der Signatur stabiler Kohlenstoffisotope der Herbizide zwischen Eintrag und Lysimeterausfluss hin. Die Dynamik der Herbizidkonzentrationen im Lysimeterausfluss konnte mit den Modellansätzen gut beschrieben werden. Konzentrationsspitzen im Lysimeterausfluss waren zeitlich mit höheren Niederschlagsmengen verbunden, was auf einen Einfluss der präferentiellen Strömung hinweist. Der Boden mit der gröberen Textur (Ly1) wies eine geringere Herbizidauswaschung auf als der Boden mit der feineren Textur (Ly2), was durch eine ausgeprägte mobile Phase in Ly1 erklärt werden kann.

Die Ergebnisse dieser Arbeit zeigen, dass die Kalibrierung eines Modells für Strömung und Transport in der ungesättigten Zone mit stabilen Wasserisotopen möglich ist. Darüber hinaus ist die Berücksichtigung von Multiprozessmodellen zur Beschreibung des Wasserflusses und des Transports gelöster Stoffe in der ungesättigten Zone ein hilfreiches Instrument zur Identifizierung dominanter Prozesse und sollte ein integraler Bestandteil der Modellkalibrierung sein.

Der zweite Teil dieser Arbeit befasst sich mit potenziellen Risiken für Boden und Grundwasser bei der Anwendung von MAR. Kenntnisse über die ungesättigte Zone sind wichtig für die Planung und Umsetzung von MAR-Systemen, da potenzielle Risiken wie die Infiltration von Schadstoffen in den Boden und das Grundwasser damit verbunden sind. Ein verbessertes Verständnis der Fließ- und Transportprozesse kann dazu beitragen, diese Risiken zu mindern, da eine detailliertere Vorhersage der Kontaminationsausbreitung möglich wird.

Ein Ansatz, um den sicheren und akzeptierten Einsatz von MAR zu ermöglichen, könnte ein umfassendes Risikomanagement sein, einschließlich der Identifizierung, Analyse und Bewertung potenzieller Risiken im Zusammenhang mit MAR. Unser Ziel war es, die bestehenden Methoden zur Risikobewertung von MAR zusammenzufassen und häufig betrachtete Risiken zu identifizieren. Außerdem haben wir die in der Literatur dokumentierten Einschränkungen und Lehren aus den gegenwärtig angewandten MAR-Risikobewertung aufgezeigt. Als Beschreibung des aktuellen Stands der Technik kann dieser Teil der Arbeit als Ausgangspunkt für die weitere Evaluierung potenziell geeigneter Methoden zur MAR-Risikobewertung dienen, um die Sicherheit im Hinblick auf Wasserverfügbarkeit und-qualität zu verbessern und die Risiken im Zusammenhang mit MAR-Systemen zu verringern.

Insgesamt unterstützen die Ergebnisse dieser Arbeit Modellierer und Entscheidungsträger dabei, das Kontaminationspotenzial für Grundwasserressourcen zu ermitteln und Risiken für Boden- und Grundwassersysteme zu identifizieren.

Acknowledgements

I am grateful for many people who have been part of my PhD thesis journey in the last 3,5 years. Without them, the thesis time would not have been the same.

First, I would like to thank my supervisors, Dr. Arno Rein and Prof. Dr. Florian Einsiedl, for giving me the possibility to conduct this research. I strongly appreciate your devotion of time and efforts to help me complete this thesis. I am very happy to have been introduced to the managed aquifer recharge topic and have improved my environmental modelling skills. Thank you, Arno, for your constant patience and support in realizing many ambitious ideas.

Furthermore, I would like to thank my mentor, Prof. Gabriele Chiogna, for his advice and taking over my mentorship and his participation as an examiner. Thank you very much for your insightful comments and suggestions and always on-time feedback. Moreover, I want to thank Prof. Zoi Dokou for welcoming me to Sacramento. My stay in the USA motivated me to continue working in sustainable groundwater resources management to battle climate change effects. I want to thank my co-authors, Dr. Jannis Groh and Dr. Thomas Pütz, for explaining lysimeter modelling and helping me manoeuvre and avoid trap doors.

Thanks to Florian Konrad and Theis Winter, who were always supportive office mates. You always had time for a cup of coffee, a chat, or advice, making office time much more fun. But also all my other colleagues with whom I shared many cherished hours during lunch breaks, parties, volleyball, squash, hiking, and skiing weekends. Thank you all for your support during my PhD with your time and kind words: Alejandra Pena, Tamara Michaelis, Christine Haas, Fabian Böttcher, Manuel Gossler, Felix Schölderle, Florian Heine, and all other colleagues at the Chair of Hydrogeology. I am also very thankful for the support of my dear fellow PhD students: Anica Mayer, Francesca Perosa, and Sonja Teschemacher. They helped me to endure the frustrating moments of this thesis work and to see the parts of my work that motivated me. Special thanks go to two phenomenal master's students, Lea Augustin and Sophia Klausner; without them, many ideas would not have been realized.

Finally, I would like to thank my family and friends for being part of my life and making free time and weekends a source of energy to continue the thesis work.

Table of Contents

List of figures

List of tables

Chapter 1 General Introduction

Groundwater accounts for 97% of the utilizable freshwater resources worldwide. Estimations of the world population relying on groundwater as drinking water supply ranges between 20-40 % (Kundzewicz and Döll, 2009) and 50 % (Shah et al., 2007; UN, 2022). In Germany, about 74% of and in the European Union, about 65% of the drinking water is supplied by groundwater (BMU, 2008; EEA, 2022).

Groundwater resources are challenged worldwide by different threats. Impacts of climate change, such as lower frequency but higher intensities of rain events (extreme rain events), lead to decreased infiltration and can locally lead to a decrease in groundwater recharge (e.g., Biswas and Tortajada, 2018; Green et al., 2007; Woldeamlak et al., 2007). Consequences are more intense and prolonged soil water and groundwater droughts, which have been documented and are expected to exacerbate worldwide, e.g., in the United States (Mann and Gleick, 2015), Thailand (Seeboonruang, 2016), or Germany (Neukum and Azzam, 2012). Furthermore, sea level rise can cause an increased intrusion of saltwater into freshwater resources on low-lying land, where regions are risked of getting uninhabitable in the upcoming years and decades (Storlazzi et al., 2018).

Unsustainable management of groundwater resources by overexploitation of an aquifer can have numerous negative effects, such as declining quantities (up to the necessity of abandoning groundwater wells), saltwater intrusion (in coastal areas), deterioration of water quality or increase in pumping costs (e.g., Alfarrah and Walraevens, 2018; Custodio, 2002; Rodríguez-Estrella, 2012). Wada et al. (2010) predicted that non-renewable groundwater abstraction contributes to 20 % of the global irrigation water demand.

Another main threat to groundwater resources is contamination with agrochemicals. In Europe, the contamination of groundwater resources by agricultural practices that lead to the leaching of pollutants, like nitrate, from applied fertilizer and pesticides has been identified as a key water management challenge (EEA, 2022). But also, contamination from anthropogenic activities can reach the soil and groundwater, e.g., industrial and household wastewater (e.g., Igboama et al., 2022; Lapworth et al., 2012; Van Stempvoort et al., 2013). A prominent example is the Fukushima nuclear accident, where radionuclides infiltrated into the soil and were transported to the ocean through groundwater (Gallardo and Marui, 2016).

Within the previous decades, intensive research has highlighted the adverse effects of such contamination on human health (e.g., Fantke et al., 2012; Genuis et al., 2016; Nicolopoulou-Stamati et al., 2016) or the soil ecosystem (e.g., Arias-Estévez et al., 2008; Ikoyi et al., 2018; Michel et al., 2021). Policymakers have taken action to address these threats to groundwater, soil resources, and human health. In Europe, the REACH regulation aims to ensure chemical safety assessment (EC, 2006). The Water

Framework Directive (EUCO, 2000) aims at chemical protection of all surface water, and the Drinking Water Directive focuses on the quality of water for human consumption (EUCO, 1998). Furthermore, the Environmental Liability and Industrial Emission Directive focuses on maintaining soil functions and soil quality (EUCO, 2004; 20010). Nevertheless, concentrations of individual pesticides and their metabolites measured in drinking water are often exceeding the limit of 0.1 µg/L established by the European Council (e.g., Delgado-Moreno and Peña, 2009; EUCO, 1998; Guzzella et al., 2006; Hildebrandt et al., 2008).

A technical solution to address quantitative and qualitative protection of groundwater resources is Managed Aquifer Recharge (MAR). Excess water from, e.g., rainfall, flooding, water treatment plants, rivers, and desalinated seawater can be infiltrated into an aquifer to store and recharge groundwater (e.g., Dillon et al., 2019; Gale, 2005). As a result, groundwater availability is enhanced, and groundwater can be extracted in a time of need. Moreover, water quality can be increased by (engineered) natural attenuation processes of the aquifer and soil matrix. Several authors describe water treatment due to sorption or degradation processes in the unsaturated and saturated zone (e.g., Barba et al., 2019; Barbagli et al., 2019; Bekele et al., 2011; Yamaguchi et al., 1998).

The hydraulic and biogeochemical processes in the subsurface must be understood for the design, implementation, and management of a MAR scheme. This is required, among others, for the prediction of groundwater flow direction originating from the recharge location (e.g., Ganot et al., 2017, 2018; Nicolas et al., 2019), for evaluating effects on water quality of recovered water (e.g., Barbagli et al., 2019; Jeong et al., 2018; Tzoraki et al., 2018) and for the investigation of compliance with water or soil quality regulations (Fernández Escalante et al., 2020). A profound understanding of subsurface flow and chemical fate is equally valuable for the evaluation of climate change impacts (such as droughts), adverse effects on agricultural production, or groundwater recharge (Blanchoud et al., 2007; Kundzewicz and Döll, 2009; Vrba, 2002; Woldeamlak et al., 2007).

A difficulty in investigating hydraulic and biogeochemical processes in the subsurface is how to conduct (representative) observations. Soil samples can be taken, which on the downside, disturb the natural soil system. In laboratory experiments with soil samples, influences of hydraulic and biogeochemical processes and their rates can be determined (under micro/meso-scale conditions). However, such investigations have shortcomings when a transfer to field conditions is intended, where, e.g., soil water contents or atmospheric conditions are subject to spatial and temporal changes (Isch et al., 2019; Šimůnek et al., 2001). To leave the subsurface undisturbed and thus enable more realistic observations, infiltration processes or biogeochemical reactions in the soil can be observed with non-invasive measurement techniques on the field scale. These can, for instance, be resistivity tomography, or the measurements of proxies, such as electrical resistivity or tracers, for obtaining hints on subsurface processes and characteristics (e.g., Fetter, 2001; Leibundgut et al., 2009).

Despite the available invasive and non-invasive measurement techniques, a representative observation of parameters under conditions of subsurface heterogeneity and temporal changes, under reasonable effort, usually proves challenging. Carrying out detailed observations and monitoring, with an adequate spatial and temporal resolution, to describe parameters such as soil water content or chemical concentrations can require substantial resources. Where measurements are unavailable, models can be deployed to describe subsurface contamination over a temporal and spatial evolution. Models vary in complexity from simpler conceptual over empirical to detailed mechanistic models. For example, mechanistic descriptions of the highly non-linear flow and transport processes in the subsurface, as well as their representation with computational approaches, are incorporated within the models, attempting to simplify subsurface processes appropriately and efficiently. Often, the combination of measurements and modelling is the only way to improve processes understanding and obtain information on involved processes and their rates (Anderson et al., 2015; Haws et al., 2005; Jirí Šimůnek et al., 2008; Šimůnek et al., 2003).

To solve the governing equations of models, boundary conditions must be specified to describe the boundaries of the model domain. For time-dependent problems also, initial conditions must be set. Ideally, a model's initial and boundary conditions shall be determined by observations. Lysimeter experiments can be performed and combined with field measurements or observations of environmental tracers, such as stable water isotopes, to set initial and boundary conditions (Groh et al., 2018, 2016; Sprenger et al., 2015; Stumpp et al., 2009c).

Such mechanistic models' accuracy depends on the uncertainty related to the model input (initial and boundary conditions, model parameters) and the model setup (e.g., Dell’Oca et al., 2020; Doherty, 2015; Moeck et al., 2018). Therefore, it is essential to understand the influences of the different flow and transport processes in the subsurface to choose an appropriate mechanistic model that can adequately describe the study case and maintain prediction integrity based on the available experimental or field data.

This thesis addresses the characterization of hydraulic and biogeochemical processes in the subsurface related to anthropogenic impacts and the potential use of managed aquifer recharge (MAR). Different mechanistic models are deployed to describe unsaturated flow and stable water isotope and herbicide transport. Reactive transport processes are also analysed by interpreting measured contents of stable carbon isotopes of herbicides and recovery rates of herbicides and metabolites. The overall objective is to contribute to an improved understanding of fate and transport processes in the subsurface using observations and modelling. In addition, an improved understanding of these processes will advance the analysis and prediction of groundwater contamination and thus will assist in assessing potential impacts on soil functions or risks related to the implementation of MAR schemes.

Chapter 2 Background and state of the art

This chapter shall allow the reader of this publication-based dissertation to get additional insight into applied methods and their significance in the presented research articles in Chapters 4-7. Only a short introductive overview is intended. The author is aware that it is not a detailed description but rather a support to understand the research conducted within this thesis. Emphasis is given to unsaturated flow and transport in connection to groundwater quantity and quality rather than soil ecosystems or soil functions to establish a link to the introduced method of managed aquifer recharge.

2.1 Unsaturated flow and chemical transport and fate

The subsurface can be separated by the groundwater table into two zones. The saturated zone lies below the groundwater table and is fully saturated with water. The unsaturated zone, or vadose zone, is defined as the area between the land surface and the groundwater table. In contrast to the saturated zone, water and air may be present in the soil pores in the unsaturated zone. The unsaturated zone also includes the capillary fringe and area above the water table where water temporarily fills soil pores (up to saturated conditions) by capillary action (Fetter, 1999; Freeze and Cherry, 1979).

In the saturated zone, the hydraulic potential (which can be represented by the hydraulic head) is defined as the sum of the pressure potential and elevation potential (the latter can be represented by the elevation of the groundwater table from a reference datum). This relationship leads to a positive hydraulic head in the saturated zone, whereas the hydraulic head at the groundwater table is zero. In the unsaturated zone, water flow is mainly driven by elevation and matric potential. Contributions to the matric potential are surface tension forces or capillary actions holding water in soil pores. Smaller contributions, such as osmotic and electrochemical potentials, might be relevant in some cases. Under these partially saturated conditions, the pore water is under a negative pressure leading to a negative hydraulic head.

Darcy's law was formulated in 1856 by Henry Darcy (Darcy, 1856) to describe water flow in saturated porous media and can be written for a 1D case (Fetter, 2001):

$$q = -K \times \frac{dh}{dl} \tag{2.1}$$

where q, is the water flux (or Darcy flux) in saturated porous media [LT^{-1}], $\frac{dh}{dl}$ the hydraulic gradient [-] and K, the hydraulic conductivity [LT^{-1}]. It is applicable for laminar flow and incompressible fluids.

In the unsaturated zone, hydraulic conductivity is a function of water content: unsaturated hydraulic conductivity changes as water and air may be present in the soil pores, and soil water content varies over depth and time. Furthermore, the hydraulic potential depends on the water content, where the relationship can be determined from water retention curves.

Richards (1931) formulated an equation to describe flow in the unsaturated zone. It is derived from the continuity equation of water flow and Darcy's law. It includes the formulation of the hydraulic conductivity and water content depending on the hydraulic potential for a 1D case as follows (Fetter, 1999):

$$\frac{\partial \theta(h)}{\partial t} = \frac{\partial}{\partial z}\left(K(h)\left(\frac{\partial h}{\partial z} + 1\right)\right) - S \tag{2.2}$$

in which *θ* is the volumetric water content [L^3L^{-3}], *h* is the hydraulic head [L], *t* is time [T], *z* is the vertical coordinate [L], *K* is hydraulic conductivity [LT^{-1}], and *S* [T^{-1}] is a term representing hydraulic sources and/or sinks.

Richard's equation includes two soil-hydraulic functions, $\theta(h)$ (relationship between water content and hydraulic head) and $K(h)$ (relationship between the hydraulic conductivity and hydraulic head). Experimental studies on the field and laboratory scale with, e.g., tensiometers or pressure chamber methods can be deployed for measuring these dependencies. Furthermore, empirical functions have been derived to describe the two soil-hydraulic functions in the unsaturated zone (also called pedo-transfer functions). Widely applied functions are the Brooks and Corey model (1964), the Durner model (1994), and the van Genuchten-Mualem model (1976; 1980) (Eq. 4.4 and 4.5 in Chapter 4).

2.1.1 Transport processes

To describe the transport of dissolved constituents in the subsurface, three fundamental transport processes are considered. First, dissolved constituents are transported with soil water (or groundwater) flow, named **advection**. Second, constituents move along a concentration gradient by Brownian motion, known as **diffusion.** Third, constituents move with different velocities causing mixing in a longitudinal and transverse direction, called **dispersion**. Dispersion effects mainly result from varying pore sizes, different lengths of flow paths (depending on the texture of the medium), and varying friction within pore spaces (e.g., Berkowitz et al., 2014; Fetter, 1999)

Transport of dissolved components in porous media can be described with the advection-dispersion equation, which in early hydrogeological literature is documented in

Bear (1972), Freeze and Cherry (1979), and Ogata (1970). For a 1D case, the advection-dispersion equation can be set up as follows (Berkowitz et al., 2014):

$$\frac{\partial(\theta C)}{\partial t} = \frac{\partial}{\partial z}\left(\theta D \frac{\partial C}{\partial z}\right) - \frac{\partial(qC)}{\partial z} - \Phi \tag{2.3}$$

where C is the concentration of a dissolved compound [ML^{-3}], D is the diffusion/dispersion coefficient that can account for molecular diffusion and hydrodynamic dispersion [L^2T^{-1}], q is the volumetric fluid flux [LT^{-1}], and Φ is a source/sink term [$ML^{-3}\,T^{-1}$].

Contamination in the subsurface includes physical contamination, e.g., problematic changes in temperature and turbidity, or chemical contamination, such as chlorinated solvents, pesticides, pharmaceuticals, or nitrate. Moreover, biological contamination can result, amongst others, from viruses or bacteria (e.g., Karim et al., 2020; Ray et al., 2003; Sharma and Bhattacharya, 2017).

Infiltration of water and contaminants into groundwater occurs through the unsaturated zone, which therefore plays an essential role in the contamination and protection of soil and groundwater. For example, the properties of the unsaturated zone govern the time and amounts of contaminants reaching groundwater. In addition, the unsaturated zone may act as a storage or reactor medium and may retard or enhance the transport of contaminations to groundwater (Nimmo, 2009; Ronen and Sorek, 2005). In the following sections, the most prominently investigated properties of the unsaturated zone and their influence on flow as well as transport and fate processes are described (as well as illustrated in Figure 2-1). As stated above, a short introductive overview is intended rather than a detailed description.

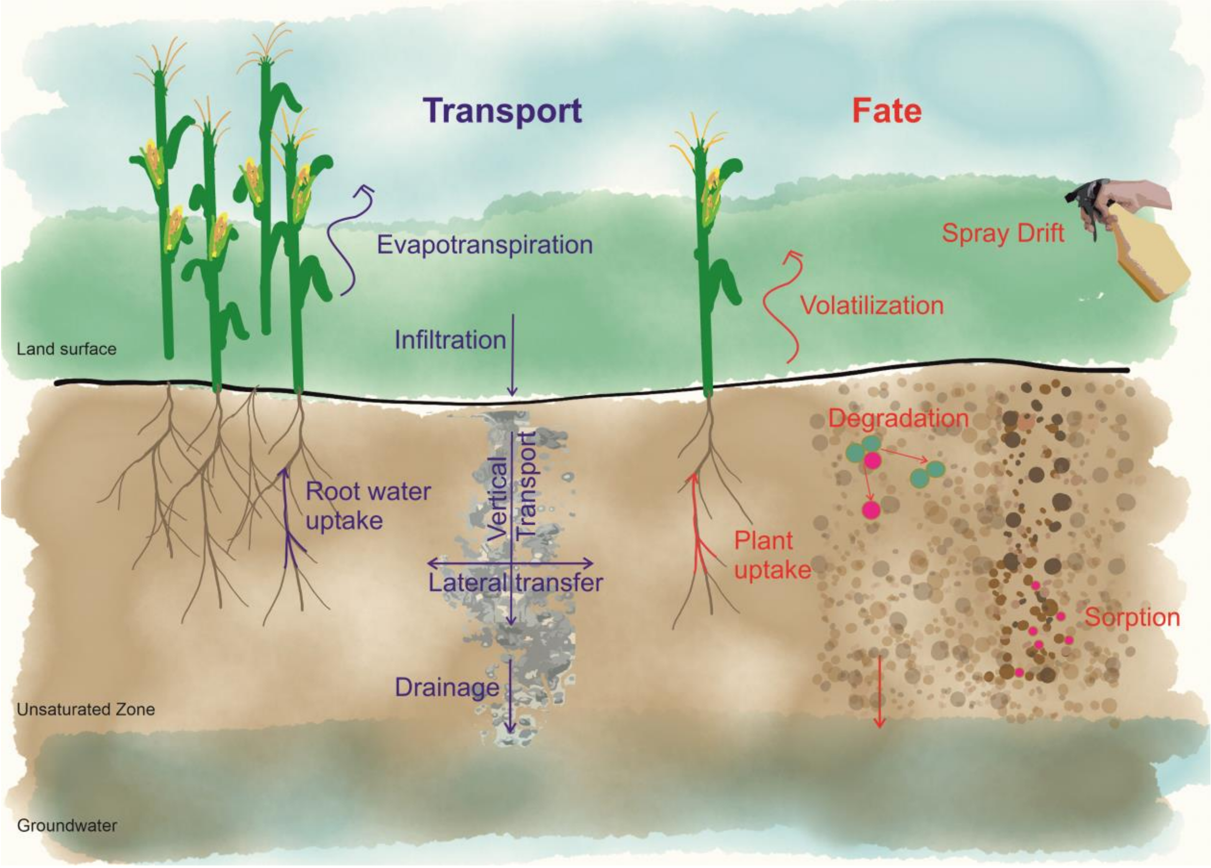

Figure 2-1: Governing processes of unsaturated flow, transport, and fate of dissolved compounds in soil, roots, and plants in an agricultural structured soil system.

2.1.1.1 *Transport along preferential flow paths*

Water and contaminants generally do not advance downward in a constant and merely vertical process. In addition to complex processes in the subsurface matrix, preferential flow paths can be important. These are created by the presence and arrangement of macropores, as well as due to channels and fractures resulting from geological/geochemical processes (weathering, freeze/thaw cycles, shrinking/swelling of clay minerals, and desiccation). Also, biological (root channels, burrowing soil organisms like earthworms) and agricultural activity such as ploughing can lead to preferential flow paths (Gazis and Feng, 2004; Van Ommen et al., 1989).

Preferential flow paths lead to a non-uniform flow and faster transport of contaminants to the groundwater table than transport within the subsurface matrix. This could contribute, e.g., to peaks of contaminant concentration reaching groundwater (DERP, 1998; Jørgensen et al., 2002; Kördel et al., 2008; McGrath et al., 2009). In his review, Jarvis (2007) found that pesticide contamination induced by preferential flow often exceeds the maximum allowed concentrations in groundwater defined by the EU drinking water standard.

2.1.1.2 Influence of immobile water on transport

In addition to water flowing through the subsurface matrix and along preferential flow paths, stagnant or immobile water can be found in soils. Porous media can be divided into mobile and immobile phases. Compared to the immobile phase, the mobile phase describes the region where flow occurs (including matrix and preferential flow). Immobile water represents water in dead-end pores (i.e., pores which are not interconnected) or water held in place by molecular or surface tension forces. Water can be removed from stagnant regions, e.g., by changing hydraulic gradients. Therefore, the term quasi-immobile water is also used. Dissolved compounds can diffuse or be transported from mobile to immobile water and vice versa. The retention of dissolved contaminants in immobile water can lead to a deterioration of soil and groundwater quality. Immobile water can, in particular, be found in soils with fine pores, such as clays or silts (Coats and Smith, 1964; James et al., 1984).

2.1.2 Reactions

Aside from the physical mechanisms of advection, dispersion, and diffusion, as well as the influence of physical properties (e.g., soil heterogeneity, leading to preferential flow or immobile water), reactions can influence contaminant transport and fate in the subsurface. Looking at reactive transport, the source/sink term of Eq. (2.3) can be formulated to account for a multitude of processes. For example, chemical transformation, including biodegradation and biogeochemical reactions (such as chemical precipitation), retardation (reversible reactions), and attenuation (irreversible reactions) in the subsurface (Berkowitz et al., 2014; Fetter, 1999). Negative impacts on groundwater and soil can be observed depending on the reaction. The attenuation of dissolved contaminants within the soil can improve groundwater quality but can negatively affect soil functions. For example, when we look at retardation, we might find the desorption of compounds from solids to the water phase, potentially decreasing the groundwater quality but mitigating soil contamination. Further, dissolution and precipitation processes can influence the chemical and physical properties of the subsurface and therefore change flow and transport over time in the subsurface (Berkowitz et al., 2014; Juraske et al., 2009).

2.1.2.1 Sorption processes

The umbrella term sorption was introduced for adsorption, absorption, desorption, chemisorption, and ion exchange processes as it is difficult to differentiate between some cases, particularly in natural soils, experimentally. **Adsorption** describes the attachment of dissolved compounds to soil particles (moving from the water to the solid phase) and **desorption** their detachment (moving from the solid to the water phase). Charged ions can be attached to opposingly charged surfaces, e.g., negatively charged clay ions, by electrostatic forces: this process is called **ion exchange**. **Chem-**

isorption (or specific adsorption) explains stronger bonds to the surface when constituent forms coordinate covalent bonds with sediment, rock surface, or soil. **Absorption** occurs when dissolved compounds diffuse into porous particles and sorb onto interior surfaces (Berkowitz et al., 2014; Fetter, 1999; Scheffer and Schachtschnabel, 2018).

Different relations and trends are documented for sorption, such as increased desorption with higher temperatures (Krieger et al., 2000; Rani and Sud Sant, 2014) or increased adsorption with higher organic matter content, presence of clay minerals and cation exchange capacity (Carbo et al., 2007; Olvera-Velona et al., 2008; Vischetti et al., 1998). For ionisable compounds (like many systemic insecticides and herbicides), electrical charge and water solubility are often the most important properties for their adsorption and desorption behaviour (Ahmad et al., 2016). Bradford et al. (2002) found that particle retention in porous media highly depends on soil grain size distribution. When the particle size is small relative to the soil pore sizes, filtration often becomes a less important mechanism of particle removal, and sorption becomes more important.

2.1.2.2 Degradation

Degradation is the decomposition of a compound into smaller molecules or elements induced by physicochemical or biological factors and processes. Abiotic degradation often results from hydrolysis and redox reactions and, to a lesser extent, from photolysis. The process where compounds are degraded by reactions with enzymes or other biogenic compounds, e.g., to serve as a substrate for microbial growth, is called biodegradation (Berkowitz et al., 2014; Trapp and Matthies, 1998). Biodegradation of, e.g., pesticides can follow different metabolic pathways, involving stepwise chemical transformations carried out by individual microbial species or consortia, resulting in the formation of metabolites (e.g., Singh and Jauhari, 2017).

A wide range of chemical and environmental factors influence degradation processes. With higher temperatures, an increase of biodegradation for organic contaminants can occur, as reported, e.g., by Dong and Sun (2016), Grünheid et al. (2007), and Krieger et al. (2000). Furthermore, other factors can affect contaminant degradation depending on the contaminant properties such as pH (Körner et al., 2019; Liu et al., 2019; Zhao et al., 2009), dissolved oxygen (Feng et al., 2017; Karakurt-Fischer et al., 2020; Shaler and Klečka, 1986) or redox potential (Ali et al., 2013; Dolfing and Harrison, 1993; Schmidt et al., 2007).

2.1.3 Water and chemical plant uptake

Plants influence the upper boundary with processes such as interception and transpiration and play an essential role in the water and chemical cycle within the subsurface. Chemical plant uptake can contribute to contaminant fate, and root water uptake can also influence the soil water content (e.g., Legind et al., 2012; Minaduola et al., 2021;

Zarebanadkouki et al., 2014). Plants take up water via the transpiration stream. Passive chemical plant uptake of dissolved compounds can occur advectively with the transpiration stream in thicker roots (transport with the xylem water). In addition, passive chemical uptake can occur by diffusion into fine roots. Differently, active plant uptake can, e.g., occur along an osmotic gradient generated by solute accumulation in the roots or by plant cell enzymatic processes (Karigar and Rao, 2011; Palmgren, 2001). Active uptake can usually be neglected for most contaminants in environmental fate evaluation (Jones, 1969; Trapp and Matthies, 1998; Weng, 2000).

2.1.4 Spray Drift

Droplets or sprayed pesticides can be carried away from the target downwind, often called spray drift. The compound can then be further distributed in the environment and, e.g., infiltrated into soil off-site or washed off, reaching surface water (Schönenberger et al., 2022; Stephenson et al., 2006).

2.1.5 Volatilization of chemicals into the atmosphere

In our context, volatilization describes the transition of a compound from the liquid (or adsorbed phase) to the gaseous phase and depends on the vapour pressure. Chemicals such as pesticides can volatilize from soil and above-ground plant parts (leaf, fruit, stem) after application (Berkowitz et al., 2014; Trapp and Matthies, 1997).

2.2 Measurement methods to investigate flow and transport

2.2.1 Lysimeter investigations

Lysimeters are measurement devices that allow the investigation of hydrological and geochemical fluxes on a quantitative and qualitative scale in the unsaturated zone. The word is derived from the Greek roots *lysis*, standing for dissolution or movement, and *metron*, meaning “to measure.” For a lysimeter, e.g., a soil volume is filled in a container or tank, for which specific boundary conditions can be defined. For example, a sampling tube, e.g., a steel cylinder, can be driven into the soil to collect undisturbed soil samples (soil cores), which can be installed in the lysimeter.

Drainage lysimeters allow the measurement of the vertically percolating water, and weighable lysimeters enable to analyse the soil-water balance. In such setups, chemical movement can be investigated, as well. Lysimeters can be installed on the field or laboratory scales (Howell, 2004; Pütz et al., 2018).

Lysimeter studies have been successfully applied in the past. They can provide important data for the investigation of soil hydraulic properties concerning water flow, the chemical cycle, as well as the dynamics of water and chemical plant uptake (e.g., Francaviglia and Capri, 2000; Leita et al., 1996; Piwowarczyk et al., 2013; Winton and Weber, 1996).

2.2.2 Tracers in hydrogeology

Tracers are substances that can be tracked in hydraulic and biogeochemical processes to investigate these. In hydrogeology, tracers are often deployed for the investigation of, e.g., groundwater age, identification of groundwater flow directions, the mean residence time of groundwater, and storage capacity of aquifers. A specific group of tracers are environmental tracers. Environmental tracers are defined as the properties or constituents of water that have not been intentionally introduced for experimental purposes (Leibundgut et al., 2009).

2.2.2.1 Stable water isotopes

Stable water isotopes are classified as environmental tracers. The abundance is stated as the ratio (R) between the less abundant species and the more abundant species of a given element. The two most abundant isotopes of a given element are chosen to compute this ratio. Measurements of absolute isotope ratios or abundances are complicated, and sophisticated measurement devices are needed. Because we are primarily interested in the variation of ratios instead of absolute values, we can compare measured isotope ratios to defined standards of these ratios. Standards, e.g., are defined by the International Atomic Energy Agency. The variations of these ratios (sample versus standard) are expressed with the δ delta notation [‰] (Clark and Fritz, 1997):

$$\delta_{\text{Isotope}}\ [‰] = \left(\frac{R_s}{R_{std}} - 1\right) \times 1000 \tag{2.4}$$

where R_s is the isotope ratio of the sample and R_{std} the isotope ratio of the standard. Stable water isotope oxygen-18 ratio is given with R = $^{18}O/^{16}O$ and deuterium with R = $^{2}H/^{1}H$. Isotopic composition changes due to fractionation processes, which can be associated with, e.g., evaporation, freezing, or melting. The fractionation factor α of isotope ratios from two compounds, the reactant R_x and the product R_y, describes these portioning processes (Clark and Fritz, 1997):

$$\alpha = \frac{1 + \frac{R_x}{1000}}{1 + \frac{R_y}{1000}} = \frac{1000 + R_x}{1000 + R_y}\ [‰] \tag{2.5}$$

Seasonal variation in isotope ratios depends on temperature, atmospheric moisture content, and trajectories of air masses. In continental stations, the isotopic signal closely follows the temperature signal. With increasing temperature, the isotopic signal is enriched in heavier isotopes, and it is isotopically depleted in heavier isotopes with decreasing temperatures. Hydrodynamic dispersion leads to a damping of the isotopic signal from precipitation within the unsaturated zone, and therefore seasonal variations often dissipate within five years in groundwater. In soil and groundwater, stable water isotopes are considered conservative tracers as they are subject to negligible reactions (Clark and Fritz, 1997; Kendall and McDonnell, 1998; Leibundgut et al., 2009).

2.2.2.2 Stable carbon isotopes

To investigate the role of biodegradation, isotope fractionation in the carbon cycle can be interpreted. Microorganisms prefer to incorporate lighter isotopes in their metabolism. In the case of carbon, this means the preferred incorporation of ^{12}C over ^{13}C isotopes (Clark and Fritz, 1997). When biodegradation takes place in the subsurface, a characteristic isotope shift due to the enrichment of heavier isotopes can be observed between input (e.g., applied herbicides) and output (e.g., herbicides dissolved in groundwater) (Mangelsdorf, 2017; Torrentó et al., 2015).

2.3 Modelling techniques of flow and (reactive) transport

When we encounter subsurface contamination, we might have measurements taken at specific locations and depths localizing the contamination or know where the contamination was released to the subsurface. Our aims as scientists or engineers would be, e.g., to assess the risk of drinking water contamination or the risks to groundwater and the soil ecosystem and to develop approaches for risk mitigation.

With a model, we aim to simplify the description of the complex environmental system. It can help us estimate subsurface contamination over a temporal and spatial evolution where measurements are unavailable. A model can be conceptual, e.g., describing hydrogeology and environmental compartments in a written text and flow chart or diagram. Mathematical descriptions of flow and (reactive) transport processes in the subsurface can be used for setting up mechanistic models. Such models describe state variables such as water content (in the unsaturated zone), hydraulic head (in the saturated zone), or chemical concentrations. Experimental data from, e.g., lysimeters or tracer tests, can be analysed and interpreted with the help of soil and groundwater models. To define the input and boundary conditions of models and model parameters, obtaining experimental data is integral for model calibration and validation (Anderson et al., 2015).

Flow and (reactive) transport in the subsurface are usually described with differential equations, including several independent parameters (partial differential equations). Analytical solutions were found for specific, well-defined problems (e.g., Bear, 1972;

Ogata and Banks, 1961). For example, lumped-parameter models (LPM) incorporating analytical solutions for tracer transport can obtain information on subsurface flow characteristics on the laboratory or field scale (Leibundgut et al., 2009). Compared to numerical models, LPM require only a limited number of input data (tracer input and output) and fitting parameters ("lumped" parameters). Depending on the hydrological conditions, different tracer transport models, such as advection-dispersion, piston-flow, or exponential models, can be combined (Einsiedl et al., 2009; Leibundgut et al., 2009; Małoszewski et al., 2002; Małoszewski and Zuber, 1982; Stumpp et al., 2009a, 2009c, 2009b).

Many problems of subsurface flow and transport can only be solved with numerical methods since analytical solutions fall short (for most cases) of describing heterogeneous conditions in the subsurface as well as initial and boundary conditions. Different numerical methods allow us to approximate the solution of differential equations when discretizing over space and time (Anderson et al., 2015; Clark and Fritz, 1997). Prominently applied numerical modelling software of unsaturated flow and transport are, e.g., HYDRUS-1D and 2D/3D (Šimůnek et al., 2022, 2018), the Root Zone Water Quality Model (RZWQM) (Ahuja et al., 2000), Finite element modelling of flow, mass and heat transport in porous and fractured Media (FEFLOW) (DHI, 2015), and R-UNSAT (Lahvis and Baehr, 1997).

2.3.1.1 *Description of unsaturated flow and transport*

Modelling approaches have been developed to describe subsurface flow and transport processes (summarized in Chapters 2.1 and 2.1.1). The single-porosity approach is based on the simplification that the complex inter- and intra-aggregation of pores can be described with only one homogenous soil porosity (Figure 2-2a). In such an approach, uniform flow and transport are considered throughout the liquid phase (Brooks and Corey, 1964; Mualem, 1976; van Genuchten, 1980). Single-porosity systems may accurately describe well-sorted soils but fall short when immobile water or preferential flow paths play an important role (Haws et al., 2005; Jiang et al., 2010; Šimůnek et al., 2001). To overcome these restrictions in a dual- or multi-porosity model, the liquid phase is portioned into mobile and immobile regions to allow the description of different flow and transport velocities (Figure 2-2b). In the immobile region, water and solutes can be stored and exchanged with the mobile region. Still, advective transport is not possible within the immobile region (e.g., van Genuchten and Wierenga, 1976). The flow domain is subdivided into a fast-flowing (preferential flow), slow-flowing (matrix), and immobile region in a dual- or multi-permeability model (Figure 2-2c). In the immobile region, water and solutes can be stored and exchanged with the mobile region. Flow is permitted in the mobile and preferential flow region, and water and solutes can exchange between both (Durner, 1994; Gerke and van Genuchten, 1996, 1993). Eq. (2.2) and (2.3) describe flow and transport in the unsaturated zone for a 1D case. Compared to single-porosity models, Dual-porosity or dual-permeability models are also described as physical non-equilibrium models (Figure 2-2). Further details on dual-porosity models are given in Chapters 5 and 6.

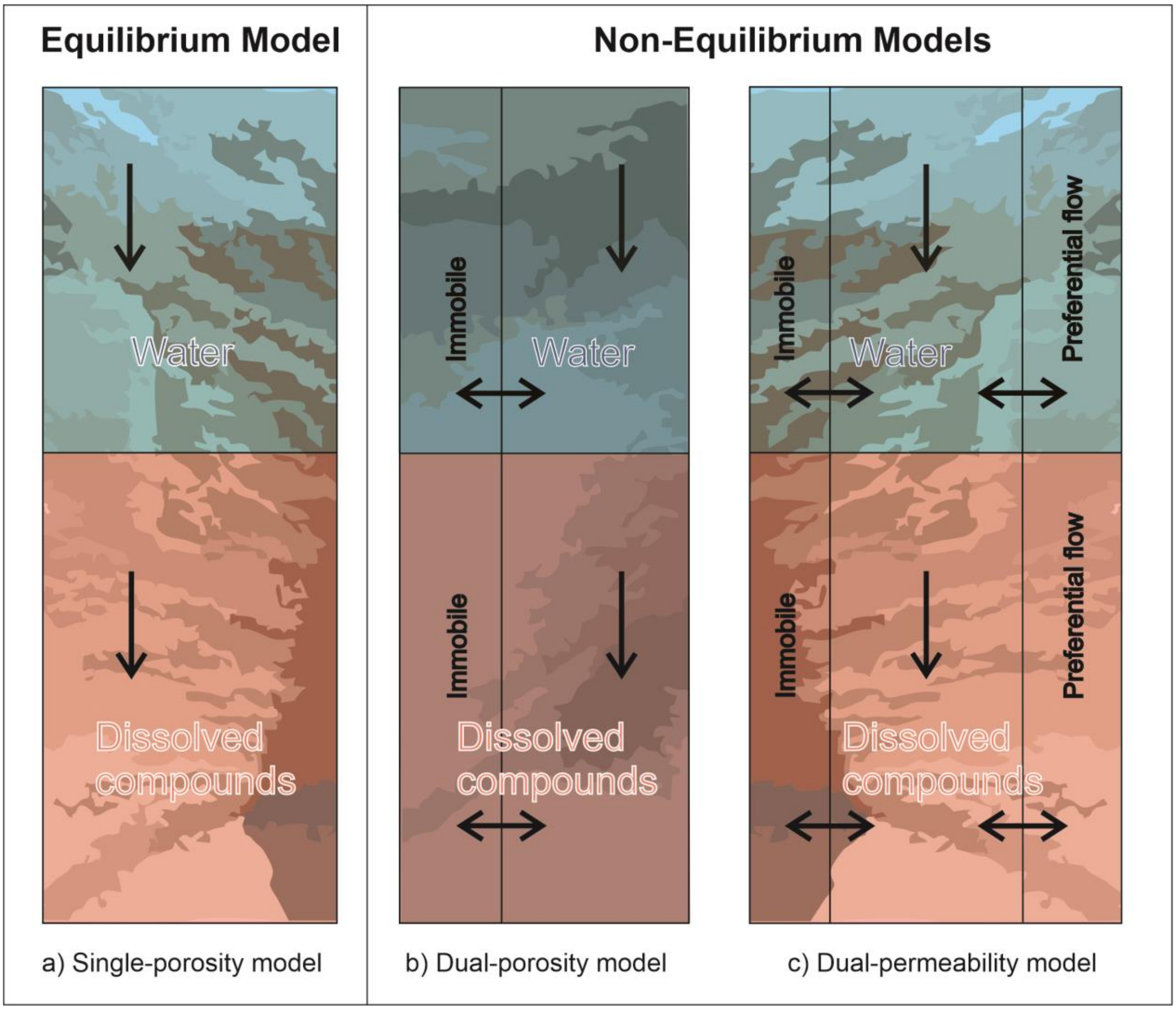

Figure 2-2: Conceptual physical (non-) equilibrium models: (a) single-porosity model, (b) dual-porosity, (c) dual-permeability consideration of the unsaturated zone are displayed. The subsurface is conceptualized to be separated into the water phase (highlighted in blue) and the dissolved compound phase (highlighted in red). The water and the dissolved compound phase are subdivided into immobile, mobile, and preferential flow regions.

2.3.1.2 Description of sorption processes

Sorption processes can be determined experimentally by measuring how much of a chemical is present in the dissolved phase versus sorbed to solids (such as soil or sediment material) over time.

Different modelling approaches for the description of sorption processes have been developed, where, as a baseline concept, the differentiation between equilibrium sorption and non-equilibrium sorption can be done. For equilibrium sorption, it is assumed that the sorption process is rapid compared with the flow velocity, and the solute will reach equilibrium with the sorbed phase rapidly. The relationship between solute concentration and the sorbed amount can be described with equilibrium sorption isotherms. A **linear sorption isotherm** describes the relationship between solute and sorbed concentration as a direct, linear relationship. Different shapes of isotherms may be needed as several mechanisms can be involved in the retention of contaminants (e.g., subsidence in adsorbing surfaces and affinity of the adsorbent at different concentrations). The **Freundlich isotherm** is a nonlinear description of the sorption process (if the Freundlich exponent is unequal to one).

Furthermore, it allows a more flexible description of the isotherm. Shortcomings of the linear sorption and Freundlich isotherms are that they do not consider limited sorption sites and, thus, a maximum adsorption capacity in soil. Therefore, the **Langmuir isotherm** was developed to overcome this restriction.

With non-equilibrium sorption models, it is assumed that an equilibrium between the solute and the sorbed phase is not attained, for example, in cases where a solute cannot be desorbed (or desorption is very slow). Non-equilibrium sorption is described using kinetic models in a time-dependent approach to describe the rate of chemical sorption (Berkowitz et al., 2014; Fetter, 1999).

2.3.1.3 *Degradation description*

Models for degradation processes describe the decomposition of a compound into smaller molecules. The velocity of a reaction, or reaction rate, is defined as the transformation per time of one reaction partner. The reaction is of zero order if a reaction is independent of the concentration of the reaction partner. For a first-order reaction, the reaction velocity depends on the concentration of one reaction partner. Second-order reactions occur when the reaction rate is proportional to the product of the concentration of both reaction partners. If the reaction depends on n concentrations of reaction partners, the reaction is called being of n^{th} order. In environmental fate models, first-order (exponential) degradation is often used to describe biodegradation (due to its mathematical simplicity).

A more accurate description of enzymatic degradation or geochemical transformation is Michaelis-Menten kinetic. Enzymatic reactions can be described using the parameters of enzyme concentration, reaction partner concentration, enzyme affinity, and degradation velocity. The Michaelis-Menten constant gives the solute concentration at which the enzyme activity is half the maximal velocity. If K_m, the Michaelis-Menten constant describing the affinity of the enzyme to the substrate, is much lower than C, the concentration of the substrate ($C \ll K_m$), then the assumption of first-order degradation can be made. If $C \gg K_m$, degradation can be assumed to be of zero order. Changing enzymatic degradation depending on solute concentration can be described with Michaelis-Menten kinetics (Berkowitz et al., 2014; Fetter, 1999). Microbial growth can be described with Monod kinetics and coupled to Michaelis Menten kinetics, e.g., for defining the enzymatic activity leading to degradation.

2.3.2 Root water uptake simulation coupled to unsaturated flow and transport models

Molz and Remson (1970) divided root water uptake approaches implemented within unsaturated flow models into macroscopic and microscopic models. The water flow in a single root is described in a microscopic model. The root is idealized as an infinitely long cylinder, and the flow from soil to the root is described with the Richards equation (such as in Eq. 2.2 for a uniform flow model). In this approach, Richard’s equation is represented in cylindrical coordinates and solved with appropriate boundary conditions at the root surface and at some distance from the root. Hence, the root water uptake is described by a flux across the soil-root interface (e.g., Gardner, 1960; Hainsworth and Aylmore, 1986). With microscopic models, it is difficult to describe the complete root system in the soil. The detailed geometry of the root system would need to be known, which is practically impossible to measure. Moreover, the spatial distribution of roots in the subsurface also changes with time. The use of macroscopic models, where the entire root system is considered a single unit to evaluate the effects of all individual roots, can be favourable as fewer soil and plant-specific parameters are needed (Ojha et al., 2009).

In a macroscopic approach, root water uptake from soil can be considered within the source/sink term of the Richards equation (such as in Eq. 2.2 for a uniform flow model) (e.g., Feddes et al., 1978; Molz and Remson, 1970). This can be done by using mechanistic or empirical assumptions. Empirical functions can, e.g., relate root uptake to soil water content (Feddes and Raats, 2004) or consider root density, root depth, and soil water stress response (Kumar et al., 2015). The root water uptake process can be described with functions following simple linear relationships (e.g., Molz and Remson, 1970) or more complex descriptions, such as mechanistic models (e.g., Trapp 2007, Rein et al. 2011, Brunetti et al. 2019) or the empirical-based Feddes model, which is implemented within HYDRUS-1D (e.g., Feddes et al., 1978; see also Appendix B).

2.3.3 Chemical plant uptake simulation coupled to unsaturated flow and transport models

For the description of chemical plant uptake in unsaturated flow models, a differentiation between the description of passive and active chemical plant uptake can be made. Passive plant uptake describes the advective or diffusive uptake of dissolved compounds into the plant's root and their transport with root water uptake. Some examples of approaches are given in the following.

A passive plant uptake model implemented within HYDRUS-1D by Šimůnek et al., (2018) describes unsaturated flow and transport with Richards and the advection-dispersion equation. Passive chemical plant uptake is calculated by multiplying the root water uptake rate (defined in the source/sink term of the Richards equation according to the Feddes et al. (1978) model) with the concentration of the dissolved solute (for concentration values below a defined concentration maximum).

In a model suggested by Šimůnek and Hopmans (2009) for the implementation within HYDRUS-1D, a differentiation between passive and active plant uptake is possible. Passive plant uptake is calculated in the same way as in the model mentioned above (Šimůnek et al., 2018), and active plant uptake is only considered if a concentration maximum for passive uptake is reached. Active plant uptake is calculated with Michaelis-Menten kinetics (considered a sink term in the advection-dispersion equation).

Further, a passive plant uptake model coupled with a water and solute transport model in the soil was proposed by Legind et al. (2012). The authors connected a tipping bucket approach to describe solute and water transport in the subsurface with a mechanistic dynamic plant uptake model considering a multitude of processes such as translocation of compounds form within the plant, volatilization, plant growth leading to dilution of the compounds or metabolization. For plant uptake and translocation within the plant, the Multi-Cascade model developed by Rein et al. (2011) was implemented. Using an analytical matrix solution, this model simulates chemical concentrations in soil, root, stem, fruit, and leaf.

In a numerical approach, Brunetti et al. (2019) set up a model that couples dynamic processes in soil and plant, including degradation processes. Unlike Legind et al. (2012), the authors described unsaturated flow and transport with the Richards and advection-dispersion equation, respectively (HYDRUS-1D); plant uptake and translocation within the plant are described numerically.

2.4 Managed Aquifer Recharge

As described above, MAR is a cross-cutting technology and can be used, among others, for drinking water supply, process water supply for industry, irrigation, sustaining groundwater-dependent ecosystems, provision of barriers to seawater intrusion in coastal areas and flood-prevention by deviating peak-flows (Dillon et al., 2009b; Gale, 2005; Kazner et al., 2012). One of the first documented MAR site was established in 1810 by the Glasgow Waterworks Company in the United Kingdom. In a perforated collector pipe parallel to the Clyde River, riverbank-filtrated water was extracted (Ray et al., 2003). MAR can be classified based on the recharge and storage type (Gale, 2005; Sprenger et al., 2017). In Table 2-1, different MAR types and their sub-types are summarized.

Table 2-1. Overview on MAR types and examples of sub-types after Gale (2005) and Sprenger et al. (2017)

	MAR type	**Examples of sub-types**
Recharge	Enhanced infiltration Surface spreading Point or line recharge In-channel modification	Infiltration ponds, soil aquifer treatment, excess irrigation, ditches, trenches, sprinkler irrigation, well/borehole infiltration, re-verse drainage, shaft recharge, check dams, riverbed scarification, sand dams
	Induced bank infiltration	Riverbank infiltration, lake bank infiltration
	Well injection	Aquifer storage and recovery, aquifer storage, transfer and recovery, aquifer storage as hydraulic barriers
Storage	In-channel modifications	Recharge dams, sub-surface dams, sand dams, channel spreading, barriers
	Runoff harvesting	Barriers, bunds, trenches

To date, various publications define selection criteria for implementing MAR schemes, which are often differentiated by the MAR type. For example, in a review by Sallway et al. (2019), selection criteria applied in the literature were summarized, categorized, and differentiated into five categories: aquifer, surface, water quality, hydrometeorological and management-related criteria. Models can be applied to assess these selection criteria and, therefore, the feasibility of a MAR scheme. Ringleb et al. (2016) reviewed modelling software's application to evaluate MAR feasibility. The authors concluded that modelling studies could reduce the need for laboratory and field work and incorporate different scenarios related to climate change impacts. Further, an increase in modelling studies since 1995 was identified and linked to increased computer capacities and the increase in MAR applications worldwide.

The successful application of models to investigate MAR feasibility implies understanding transport and fate processes in the unsaturated zone. For example, the unsaturated zone's properties govern the amount of contaminants reaching groundwater. The unsaturated zone may act as a storage or reactor medium and may retard or enhance the transport of contaminations to groundwater (Nimmo, 2009; Ronen and Sorek, 2005). Understanding governing processes in the unsaturated zone and their description in models can help to predict water quality of recovered water of MAR schemes (e.g., Barbagli et al., 2019; Jeong et al., 2018; Tzoraki et al., 2018) and for the investigation of compliance with water or soil quality regulations (Fernández Escalante et al., 2020).

Chapter 3 Objectives and aims of this thesis

Within the first part of this thesis, lysimeter experiments are investigated to contribute to an improved understanding of transport and fate processes in the unsaturated zone. The goals of such investigations include, among others, the description and prediction of groundwater contamination or the implementation of MAR schemes.

The two investigated lysimeters are installed at a test field south of Munich run by the Bavarian Environmental Agency (LfU) in Wielenbach, Germany. The lysimeters consist of stainless-steel cylinders with a surface area of 1 m² and a length of 2 m each. The lysimeters are filled with undisturbed monolithic soil cores from two different locations. Lysimeter 1 contains sandy gravels from a former target shooting range near Garching, Germany. Lysimeter 2 contains clayey sandy silt, and the soil core was excavated from an agricultural site at Hutthurm-Auberg, Germany (Figure 3-1, further details on the study site can be found in Chapters 4-6 and Appendix A-C).

Lysimeters are among the few measurement devices which allow the investigation of hydraulic and geochemical fluxes on a quantitative and qualitative scale in the unsaturated zone (Pütz et al., 2018). Moreover, the study site with the two vegetated lysimeters allows the investigation of flow and transport processes under field conditions. Natural conditions, including climate, precipitation, and vegetation, are an advantage over laboratory experiments. Further advantages over field experiments are that measurements such as weight change or the collection of discharge water are possible.

Related to the lysimeter investigations, three publications were published or submitted to scientific journals, being part of this thesis. In the following chapter, the objectives and aims of each publication will be summarized.

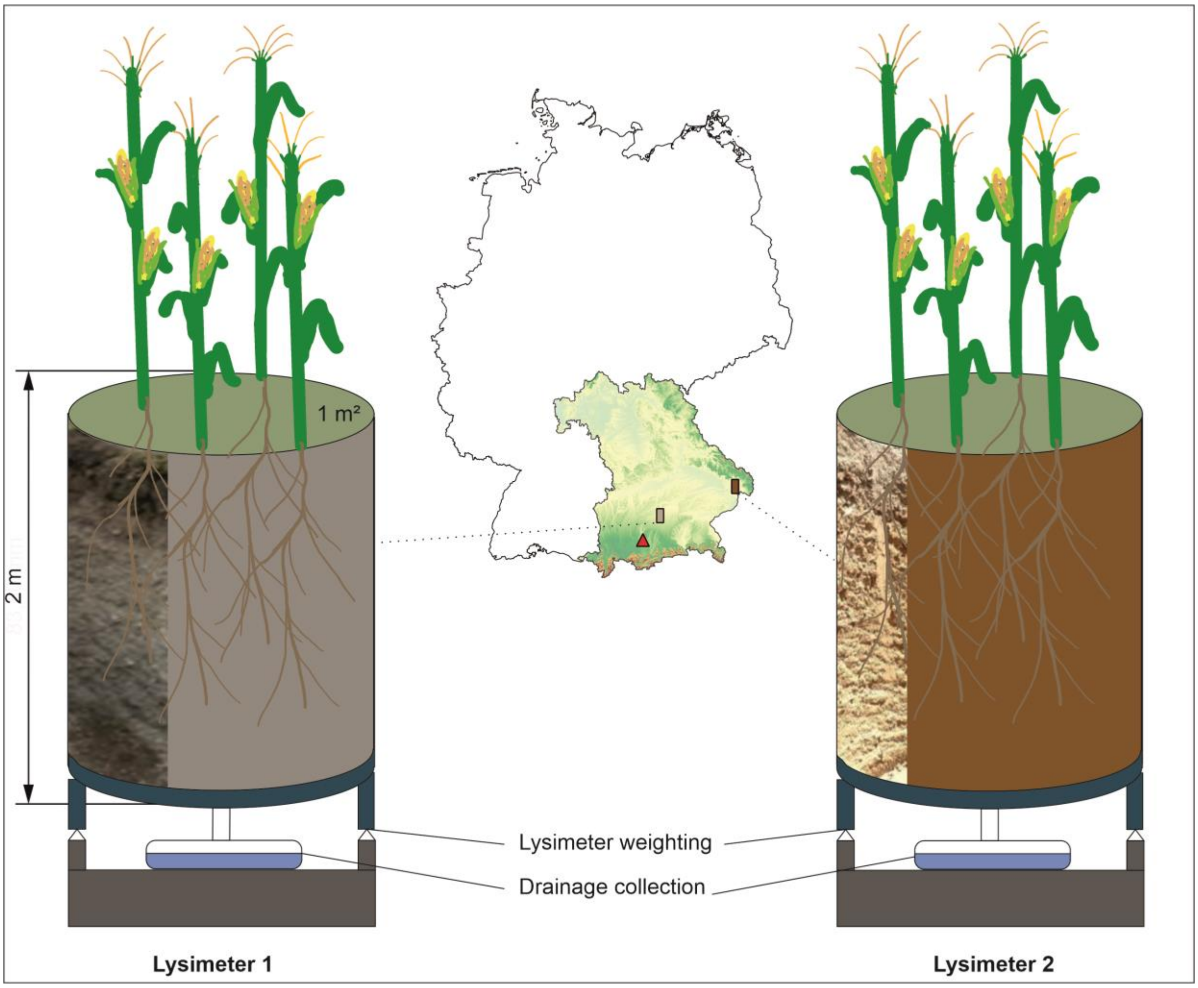

Figure 3-1: Map of Germany including elevation profile of Bavaria with the location of soil excavation site for Lysimeter 1 (filled with sandy gravel) originating from Garching (grey rectangle) and Lysimeter 2 (filled with clayey sandy silt) from Hutthurm-Auberg (brown rectangle) as well as the location of lysimeter site in Wielenbach (red triangle). Further, the experimental setup of the lysimeter, including weighting and drainage collection, its dimension, a partial display of photographed excavated soil profile, and the maize plants are displayed.

3.1 Improved lumped-parameter and numerical modelling of unsaturated water flow and stable water isotopes

The study “Improved lumped-parameter and numerical modelling of unsaturated water flow and stable water isotopes,” published in Groundwater (Imig et al., 2022a), has the objective to describe and interpret measured stable water isotopes in precipitation and lysimeter drainage with an improved lumped-lumped parameter model and, in comparison, with numerical modelling (details on this paper are given in Chapter 4).

In the study by Shajari et al. (2020), stable water isotopes were combined with lumped-parameter modelling (LPM) to characterize unsaturated flow in the two investigated cropped lysimeters in Wielenbach. With the LPM, stable water isotopes were analysed that were measured in precipitation and lysimeter drainage for 3,5 years. Mean transit times and dispersion parameters were derived for flow characterization and obtaining information on soil heterogeneity. Inherent to the LPM concept where analytical solutions are implemented, steady-state flow is considered a prerequisite (requirement of constant coefficients) (Małoszewski and Zuber, 1982). In addition to considering advective-dispersive tracer (stable water isotope) transport through the subsurface matrix, the LPM was extended by considering preferential flow as a portion of precipitation reaching lysimeter drainage rapidly.

Shortcomings in describing seasonal fluctuations of the measured stable water isotopes were observed. Therefore, as part of the publication by Imig et al. (2022a), an improved LPM was proposed. The observation period was subdivided into seasonal/vegetative periods with quasi-steady-state flow. By that, it was hypothesized that variable flow conditions could be mimicked more adequately compared to the “traditional” LPM that only considers one period with steady-state flow. Fatemeh Shajari mainly did LPM modelling, and Anne Imig carried out numerical modelling (cf. beginning of Chapter 4). To validate findings from the improved LPM approach, unsaturated flow and stable water isotope transport were also modelled numerically with the HYDRUS-1D modelling software (Šimůnek et al., 2018; Stumpp et al., 2012). To describe the measured stable water isotopes with the HYDRUS-1D model in a comparable fashion to the LPM model, preferential flow was also considered for HYDRUS-1D modelling. Like in the improved LPM model, a portion of the precipitation was assumed to pass by the subsurface matrix, rapidly flowing along preferential flow paths and thus reaching the drainage faster. Systematic underestimations of stable water isotope content in Lysimeter 2 with the improved LPM and the numerical model let us conclude that we might miss describing the influences of immobile water in our model setup. Therefore, we considered mixing processes between mobile and quasi-immobile water, presumably leading to an isotopic enrichment of heavier isotopes, represented by a constant isotopic upshift of the modelled isotopic contents (delta values).

The (improved) LPM model has the advantage of requiring fewer input parameters and computation costs than the more detailed numerical model. Thus, the aims encompassed to determine if the improved LPM can be applied to improve stable water isotope description (and therefore using a simplified approach implementing an analytical solution) comparably well as numerical modelling. We would expect that such an improved LPM would have the potential to be used as a tool for decision-makers and modellers in the prediction of groundwater contamination and its risk assessment.

Hypotheses include:

- The adaptation of the LPM for quasi-steady state flow (where flow varies between sub-periods with constant flow conditions) will improve the simulation of stable water isotopes in lysimeter seepage by accounting for seasonal hydraulic and vegetative influences.
- Preferential flow paths are essential for characterizing flow and transport in the unsaturated zone.
- The fitted flow and transport parameters from the improved LPM will be in a comparable range with fitted parameters of numerical modelling (HYDRUS-1D).

3.2 Fate of herbicides in cropped lysimeters: 1. Influence of different model setups on vadose zone flow

We found shortcomings in the numerical model work for the publication by Imig et al. (2022a) (see Chapters 3.1 and 4). Strong damping of stable water isotope contents observed in Lysimeter 2 drainage, compared to precipitation, was not represented by simulation results obtained with the chosen numerical model setup. Further, the short-term fluctuations of the measured stable water isotopes seemed generally not well described. We related short-term fluctuations to the influence of preferential flow paths. The strong damping of the isotope signal in the drainage might result, in addition to dispersion effects, from the mixing of immobile and mobile water. Since this work's objective was no longer to compare the numerical model setup to the LPM approach, we wondered if we could achieve an improved model performance if we chose a different model setup available in HYDRUS-1D. In the publication "Fate of herbicides in cropped lysimeters: 1. Influence of different model setups on vadose zone flow" submitted to Water Resources Research (Imig et al., under review, a) we, therefore, compared single- with dual-porosity model setups to investigate the influence of immobile water and preferential flow (cf. Chapter 2.4.3.1). We further extended the model setup with the consideration of root water uptake. This publication aims to identify the model setup's importance and the soil texture influence on the model setup for the description of stable water isotope contents. Additionally, we investigated if the drainage's stable water isotope signature could result from isotope fractionation by evaporation. The lighter isotope, such as ^{16}O, is more likely to evaporate than the heavier one, such as ^{18}O, leading to an enrichment of the heavier isotope in the remaining water phase and thus to an isotopic shift of $\delta^{18}O$ to more positive values (Clark and Fritz, 1997).

Hypotheses include:

- Soil hydraulic and transport parameters calibration for both lysimeters will be possible with available data.
- The dual-porosity model can adequately cover influences of preferential flow paths and immobile water on the stable water isotope signature of the drainage, and model performance will improve over the single-porosity setup.
- Models for adequately describing flow and stable water isotope transport in the unsaturated zone differ between Lysimeter 1 and 2.
- Comparing different model setups will allow us to investigate the differences between Lysimeters 1 and 2 related to soil texture.
- Parts of the input signal damping could be explained by isotope fractionation by evaporation, including the systematic underestimation of stable water isotope contents observed in the drainage of Lysimeter 2 (Imig et al., 2022a).

3.3 Fate of herbicides in cropped lysimeters: 2. Leaching of four maize herbicides considering different model setups

As described in the previous section, in Imig et al. (under review, a), we set up flow and non-reactive transport models (the latter for stable water isotope transport) in HYDRUS-1D for the two investigated lysimeters. We identified an improved model performance in Lysimeter 2 with a dual-porosity setup, whereas in Lysimeter 1, the single porosity approach adequately described measured stable water isotopes in drainage. We extended these flow models with a reactive transport description of four herbicides (terbuthylazine, nicosulfuron, prosulfuron, and metolachlor), which were applied once a year on top of the lysimeter and monitored in lysimeter drainage over 4,5 years. This was done in the paper “Fate of herbicides in cropped lysimeters: 2. Leaching of four maize herbicides considering different model setups”, submitted to the Vadose Zone Journal (Imig et al., under review, b; details see Chapter 6). The paper aimed to combine lysimeter observations and numerical modelling approaches to describe herbicide transport and to determine possible influences of sorption, interaction with immobile water, biodegradation, and plant uptake. Analyses of stable carbon isotopes of terbuthylazine and metolachlor, provided by the Institute of Groundwater Ecology, Helmholtz Zentrum München (cf. beginning of Chapter 6), were interpreted to investigate short- and long-term changes in $\delta^{13}C$ values, for evaluating the evidence of biodegradation under the influence of preferential flow and matrix flow. These findings are expected to support modellers and decision-makers in predicting the contamination potential of herbicides to groundwater resources.

Hypotheses include:

- Reaction parameters calibration for both lysimeters will be possible with available data.
- Preferential flow paths play an important role in herbicide transport in the unsaturated zone and might be responsible for concentration peaks of herbicides observed in lysimeter drainage.
- Biodegradation is assumed to contribute to some extent to the fate of the studied herbicides in the unsaturated zone.
- Biodegradation leads to characteristic isotopic shifts in carbon isotopes of herbicides terbuthylazine and metolachlor in lysimeter drainage. Stable carbon isotopes ($^{13}C/^{12}C$) can be used in the unsaturated zone as a powerful tool to describe pesticide degradation qualitatively.
- Plant uptake of herbicides can contribute to the fate of the studied herbicides in the unsaturated zone.
- Sorption may lead to chemical accumulation within the soil matrix. However, with time sorption sites will be occupied, and the leaching of contaminants to lysimeter drainage will be increased.
- Soil texture influences the hydraulic and (bio)geochemical process in the unsaturated zone, notably. We speculate that a higher clay content in Lysimeter 2 results in a decreased mass flux of pesticides in the lysimeter drainage compared to Lysimeter 1.

3.4 A review on risk assessment in managed aquifer recharge

During my employment at the chair of Hydrogeology at TUM, I was also involved in the Central Europe Interreg project DEEPWATER-CE. This project investigated the potential to implement managed aquifer recharge (MAR) schemes in four partner countries: Hungary, Poland, Slovakia, and Croatia. Socio-economic, geological, hydrogeological, technical, and regulatory influences on MAR implementation were assessed. Results from this assessment were interpreted, and guidelines for MAR implementation in Central Europe were developed (DEEPWATER-CE, 2020).

This project introduced me to MAR and how knowledge and understanding of the unsaturated zone are important for designing and implementing MAR schemes. Accordingly, the following study was conducted as part of this thesis (Chapter 7): “A review on risk assessment in managed aquifer recharge,” published in Integrated Environmental Assessment and Management (Imig et al., 2022b). An increase of 1 to 10 km^3/year of abstracted groundwater from MAR schemes has been documented between 1965 and 2015 (Dillon et al., 2019). With an increased dependency on water supply on MAR sites, potential risks of increased infiltration of pollutants into aquifers are connected (Kazner et al., 2012; Lawrence et al., 2008). Bekele et al. (2018) mention the dissolution of compounds or minerals of the aquifer matrix and the mobilization of metals due to MAR operation. Mismanagement of MAR sites can also result in the salinization of the aquifer or clogging of the infiltration surface (Jakeman et al., 2016; Martin, 2013; Olsthoorn, 1982). An improved understanding of flow and transport processes can help to mitigate these risks since the prediction of contamination spreading or clogging processes in greater detail will be possible.

Potential risks of MAR schemes can be evaluated during MAR scheme planning, implementation and operation by applying suited risk assessment methods. Such methods include identifying hazards, analysing and evaluating their risks and developing an adequate risk treatment approach (ISO, 2008).

Within the publication by Imig et al. (2022b), we aimed to summarize existing MAR risk assessment methodologies and identify frequently considered risks. Further, we highlighted limitations and lessons learned from MAR risk assessment documented in the literature. As a description of state of the art, this publication may serve as a starting point for further evaluating potentially suitable methods for MAR risk assessment, improving safety, and decreasing risks related to MAR schemes.

Hypotheses include:

- An overview of existing MAR risk assessment methodologies will support planners and operators of MAR schemes in selecting an appropriate risk assessment method. Moreover, an overview of the potential risks of MAR schemes will further facilitate the risk assessment process and hence support the development of risk treatment options to ensure safe MAR operation.

- The review will highlight the limitations of existing risk assessment methods and may facilitate the development of specific MAR guidelines, which include holistic risk assessment approaches.

Chapter 4 Improved lumped-parameter and numerical modelling of unsaturated water flow and stable water isotopes

These chapters include the following publication, with some modifications: Imig, A., Shajari, F., Augustin, L., Einsiedl, F., Rein, A., 2022. Improved lumped-parameter and numerical modelling of unsaturated water flow and stable water isotopes. Groundwater 1–13. https://doi.org/10.1111/gwat.13244

Anne Imig and Fatemeh Shajari share the first authorship for this publication, where Anne Imig carried out numerical modelling (HYDRUS-1D), and Fatemeh Shajari conducted lumped-parameter modelling. A statement from the doctoral candidate concerning her contribution to publications was submitted within the framework of a publication-based dissertation, together with a statement of confirmation from the co-authors according to Article 7, section 3, clause 2 of the TUM Doctoral Regulations (PromO) was submitted along with the publication.

Anne Imig did neither collect nor analyse samples taken at the study site. Stable water isotopes in precipitation and lysimeter drainage were analysed at the Chair of Hydrogeology at TUM. The Bavarian Environment Agency (Bayerisches Landesamt für Umwelt, LfU) collected meteorological data, water samples from precipitation and lysimeter drainage and measured lysimeter drainage rates and lysimeter weight. Arno Rein initially drafted Appendix A2.

In the case of this publication, not all chapters have been written by Anne Imig. In cooperation with the co-authors, Anne Imig's primary thematical involvement was as follows:

- Introduction section: background, numerical modelling approaches
- Methods section: water flow and stable water isotope transport in the unsaturated zone, consideration of preferential flow paths and the influence of immobile water, numerical model setup, estimation of median transit time, model curve fitting procedure
- Results and discussion section: numerical flow and stable water isotope transport modelling; comparison of LPM application and numerical modelling
- Summary and conclusion section: results of numerical modelling, comparison with lumped-parameter modelling, outlook

Graphical Abstract

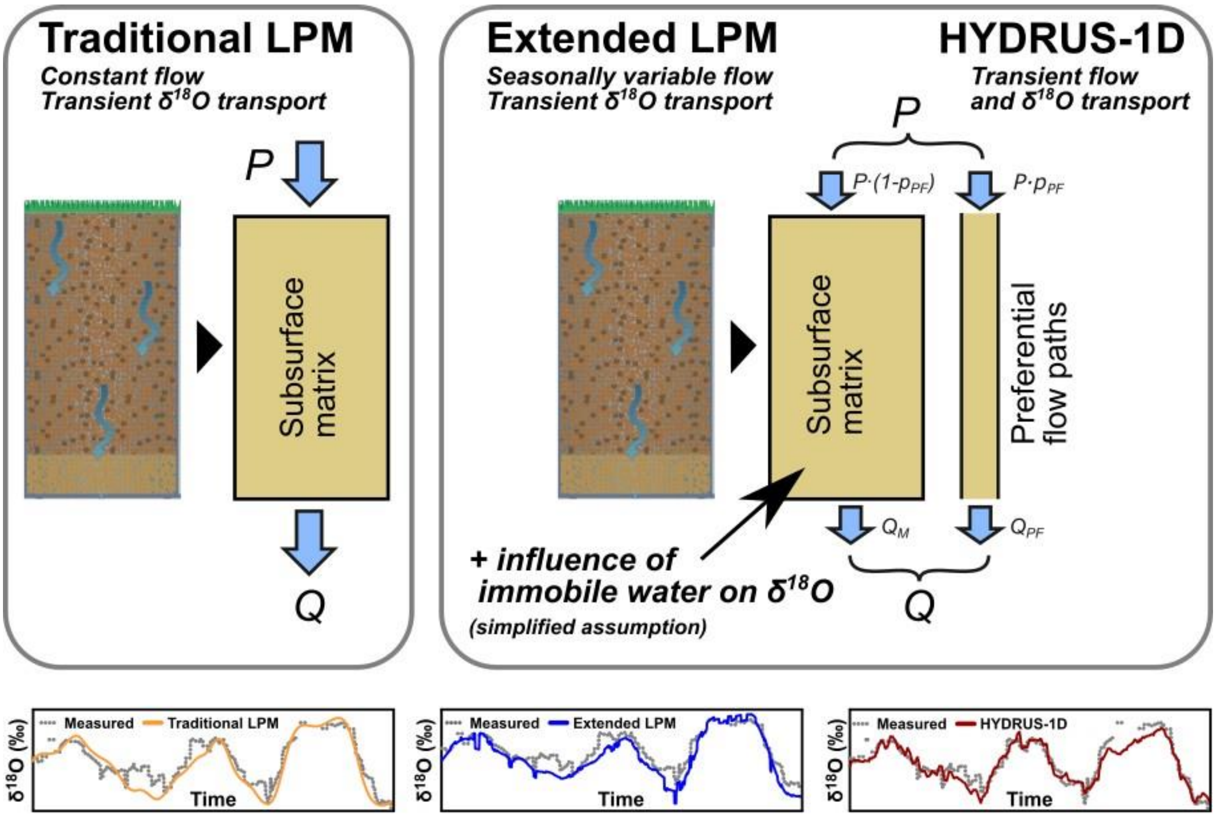

Abstract

Characterizing unsaturated water flow in the subsurface is a requirement for understanding effects of droughts on agricultural production or impacts of climate change on groundwater recharge. By employing an improved lumped-parameter model (LPM) approach that mimics variable flow we have interpreted stable water isotope data ($\delta^{18}O$ and $\delta^{2}H$), taken over three years at a lysimeter site located in Germany. Lysimeter soil cores were characterized by sandy gravel (Ly1) and clayey sandy silt (Ly2), and both lysimeters were vegetated with maize. Results were compared to numerical simulation of unsaturated flow and stable water isotope transport using HYDRUS-1D. In addition, both approaches were extended by the consideration of preferential flow paths. Application of the extended LPM, and thus varying flow and transport parameters, substantially improved the description of stable water isotope observations in lysimeter seepage water. In general, findings obtained from the extended LPM were in good agreement to numerical modelling results. However, observations were more difficult to describe mathematically for Ly2, where the periodicity of seasonal stable water isotope fluctuation in seepage water was not fully met by numerical modelling. Furthermore, an extra isotopic upshift improved simulations for Ly2, probably controlled by stable water isotope exchange processes between mobile soil water and quasi- immobile water within stagnant zones. Finally, although LPM requires less input data compared

to numerical models, both approaches achieve comparable decision-support integrity. The extended LPM approach can thus be a powerful tool for soil and groundwater management approaches.

4.1 Introduction

Characterizing water flow in the unsaturated zone is an important task related to agronomics and environmental issues. Among others, this implies evaluating the effects of climate change, such as droughts on agricultural production, ecosystems and groundwater recharge (Blanchoud et al., 2007; Kundzewicz and Döll, 2009; Varis, 2018; Vbra and Richts, 2015; Woldeamlak et al., 2007). Further understanding and quantification of unsaturated flow is crucial for assessing the fate and transport of pollutants in the unsaturated zone and assessing their impacts on groundwater (Bradford et al., 2003; Dann et al., 2009; Hsieh et al., 2001; Stumpp and Hendry, 2012).

In this context, laboratory experiments and inverse modelling approaches are used to determine soil hydraulic properties. Both have shortcomings; laboratory results may largely differ from those found at a field site, and additional uncertainties might occur from upscaling (Dinelli et al., 2000; Schwärzel et al., 2006; Winton and Weber, 1996). For modelling approaches, detailed site data are required that often are not available, such as initial and boundary conditions (Asadollahi et al., 2020). Simplifying assumptions must be made, accordingly, which often bear considerable uncertainty.

As an alternative, if flow-related parameters such as soil moisture or hydraulic potentials are not available from the field, environmental isotopes coupled with lumped parameter models (LPMs) can be used to obtain information on subsurface flow and relevant flow processes on the field scale (Leibundgut et al. 2009). Comparing with numerical models, LPMs require only a limited number of data (tracer input and output) and fitting parameters (“lumped” parameters). Depending on the hydrological conditions, different tracer transport models, such as advection-dispersion, piston-flow or exponential models, can be combined (Einsiedl et al., 2009; Leibundgut et al., 2009; Małoszewski et al., 2002; Małoszewski and Zuber, 1982; Stockinger et al., 2019; Stumpp et al., 2009a, 2009b, 2009c).

The present study aims at addressing several disadvantages of LPMs and introducing an improved approach. Inherent to the LPM concept, steady-state flow is considered as a pre-requisite of the implemented analytical solutions. Whereas this assumption is adequate for long-term groundwater conditions, it can be problematic for unsaturated flow where pronounced temporal variations often prevail. Our previous study (Shajari et al. 2020) revealed that the consideration of temporally varying flow conditions and tracer transport could potentially improve the simulation of stable water isotopes in seepage water and thus reduce uncertainties related to the fitted parameters. Therefore, in the present study, we have extended the LPM approach and subdivided the whole simulation time into several sub-periods for mimicking transient flow. In this way, each set of parameters (mean transit time and dispersion parameter) is fitted for each sub-period. To this respect, Małoszewski et al. (2006) considered a yearly changing mean transit time for simulating stable water isotope transport in different lysimeters. Stumpp et al. (2009 a, c, 2007) extended this approach by varying the dispersion parameter, in addition to mean transit time, and obtained improved model prediction.

Further, to better describe short time fluctuation and measured peaks we extend the traditional LPM approach by implementing a dual-permeability system (separation of transport through subsurface matrix and along preferential flow paths) and consideration of possible contribution of immobile water. The importance of preferential flow on adequately characterizing unsaturated zone flow and transport processes has been studied intensively by Stumpp et al. (2009c), Isch et al. (2019), Benettin et al. (2019) and Radolinksi et al. (2021). The combination of LPM and preferential flow has successfully been applied by Stumpp et al. (2007) and Shajari et al. (2020).

Another difficulty of LPM models is the adequate description of the tracer input function (Mc Guire et al., 2002; Małoszewski et al. 2006; Stumpp et al., 2009a, b, c). We have considered different input functions to account for seasonal or vegetation-related variation and different assumptions for evapotranspiration (Shajari et al., 2020). To the best of our knowledge, only few lysimeter studies with stable water isotopes are available that consider the same vegetation for different soil types.

In this paper, we applied an extended LPM approach in two lysimeters filled with different soils (sandy gravels and clayey sandy silt) and vegetated by maize. We also carried out numerical simulations of water flow and stable water isotope transport (using HYDRUS-1D) to verify the extended LPM approach.

4.2 Materials and methods

4.2.1 Lysimeter study site and considered soils

Field studies were done at two weighable lysimeters as described in detail by Shajari et al. (2020). These lysimeters are located near Wielenbach, Germany, about 48 km southwest of Munich (elevation 549 m above sea level). They consist of stainless-steel cylinders filled with undisturbed soil cores (surface area of 1 m^2, length of 2 m). Lysimeter 1 (Ly1) contains sandy gravels (taken from a former target shooting area near Garching, Germany), Lysimeter 2 (Ly2) contains clayey sandy silt (taken from an agricultural site at Hutthurm-Auberg near Passau, Germany). The soil of Ly1 is characterized as a calcaric Regosol (according to the Word Reference Base for Soil Resources, WRB 2015). It has developed above sandy to silty calcareous gravels, where 4 distinct soil layers were identified. The soil of Ly2 is a Cambisol (Stagnosol) (WRB, 2015) developed above gneiss, which was sub-divided into 5 layers. Table A-1 and Table A-2 in Appendix A, contain information on soil horizons and measured grain size distributions (only limited data available for Ly1). The lysimeters were vegetated with maize (upper boundary) and had seepage face controlled lower boundaries, allowing drainage if the soil is saturated but no upward water inflow.

4.2.2 Observations and sampling at the study site

Precipitation, seepage water and lysimeter weight were recorded automatically as described in detail by Shajari et al. (2020). Precipitation data prior to 2013 were collected at a meteorological weather station at the lysimeter study site. Samples for stable water isotope analysis were collected from July 2013 to April 2016 on a weekly basis, with greater intervals during dry season and smaller intervals during wet season. Stable water isotopes ($^2H/^1H$, $^{18}O/^{16}O$) were analysed using laser spectroscopy (details are given in Shajari et al. 2020). From measured isotope contents, delta-values ($\delta^{18}O$ and δ^2H) were calculated as δ (‰) = ($R_{Sample} - R_{Standard}$) / $R_{Standard}$ × 1000, with stable water isotope ratio R ($^2H/^1H$ or $^{18}O/^{16}O$) as the sample (R_{Sample}) and the Vienna Standard Mean Ocean Water (V-SMOW) as the standard ($R_{Standard}$). The analyser showed a precision of 0.1‰ for $\delta^{18}O$ and 0.5‰ for δ^2H. Measurements or sampling within the soil cores, such as of water content or hydraulic potential, were not possible due to experimental restrictions.

4.2.3 Soil sampling and measurement of soil hydraulic parameters

Unfortunately, the original sites where the soil cores were taken are not accessible anymore, due to infrastructure. Consequently, for Ly1, soil samples were taken about 1 km West of the original excavation site for the soil core (near Garching, Germany), where soil types and textures are assumed similar. Three replicated soil samples were taken at a fresh hillside cutting from three depths (0-0.1 m, >0.1-0.2 m and 1.0-1.2 m below surface, cf. Table A-2). For these samples, water retention curves and unsaturated hydraulic conductivity were measured using the ku-pF apparatus DT 04-01 (Umwelt-Geräte-Technik GmbH UGT, Germany). Measurements yielded the following soil hydraulic parameters (SHPs): residual and saturated soil water content (θ_r and θ_s), water retention curve shape parameters α and n (van Genuchten-Mualem model) and saturated hydraulic conductivity K_S (cf. Table A-2). For Ly2, soil sampling at a representative site was not possible due to restricted accessibility.

4.2.4 Lumped-parameter modelling

We have used LPM to simulate the transport of stable water isotopes ($\delta^{18}O$, δ^2H) in the lysimeters. LPM simulate tracer transport in the unsaturated zone by solving a convolution integral that includes tracer input and the tracer transfer function (also called weighing function). If tracer transport through the subsurface matrix and along preferential flow paths are considered, the following equation can be applied (Małoszewski and Zuber, 1982; Stumpp et al., 2007; Shajari et al., 2020):

$$C_{\mathrm{out}}(t) = (1 - p_{\mathrm{PF}}) \int_0^t C_{\mathrm{in}}(t - \tau)\, g_{\mathrm{M}}(\tau)\, \mathrm{d}\tau \;+\; p_{\mathrm{PF}} \int_0^t C_{\mathrm{in}}(t - \tau)\, g_{\mathrm{PF}}(\tau)\, \mathrm{d}\tau \qquad (4.1)$$

where C_{out} and C_{in} are tracer output and input concentration as a function of time, respectively, and are delta values (‰) of seepage (lysimeter outflow) and recharging water ($\delta^{18}O$ and $\delta^{2}H$) in this study. g_M and g_{PF} are transit-time distribution functions for the subsurface matrix and preferential flow paths (-), respectively, and τ indicates all possible transit times within the system (d). The first term on the right-hand side of Equation (1) describes tracer transport through the soil matrix, while the second term describes transport along preferential flow paths; p_{PF} denotes the portion of preferential flow (-). Advective-dispersive tracer transport was considered for the subsurface matrix (Kreft and Zuber, 1978; Lenda and Zuber, 1970),

$$g_{\mathrm{M}}(\tau) = \frac{1}{\tau\sqrt{4\pi P_{\mathrm{D}}\, \tau/T}} \exp\left[-\frac{(1 - \tau/T)^2}{4P_{\mathrm{D}}\, \tau/T}\right] \qquad (4.2)$$

while pure advection (piston flow) was assumed for tracer transport along preferential flow paths (Małoszewski and Zuber, 1982):

$$g_{\mathrm{PF}}(\tau) = \delta(\tau - T_{PF}) \qquad (4.3)$$

where T is mean transit time (or mean travel time) of water (d), and P_D is the dispersion parameter (-). T_{PF} is the mean residence time of water within preferential flow paths, which was set to the temporal resolution for modelling (d). Fitting parameters for lumped modelling are thus T, P_D and p_{PF}. For the consideration of tracer transport through the subsurface matrix only, p_{PF} is set to zero.

The sampling interval for the isotope data depended on seepage water availability and varied between 1 day and 2 weeks (in average weekly). Hence for the LPM simulation a time step of 1 day was chosen.

The recharge of stable water isotopes into the unsaturated zone as a function of time was not measured directly but estimated from measured stable water isotopes of precipitation. Two different assumptions for the input function were compared (IF0, IF2), as described by Shajari al. (2020). In summary, IF0 considers precipitation as input (no modification) and IF2 considers weighting over hydrologically relevant time periods and actual evapotranspiration determined from the water balance at the lysimeters. Weighting periods of 1, 3 and 6 months were used to account for short-term effects as well as for seasonal and vegetation-related variations of recharge (based on Grabczak et al. (1984) and Małoszewski et al. (1992), similarly applied by Stumpp et al. (2009a) and (2009b), and Shajari al. (2020)). The consideration of six-month periods, i.e., summer (maize growth, April to September) and winter (October to March), yielded best model curve fits in our previous study (Shajari et al., 2020). Thus, in the present study, we also applied this summer-winter scheme for setting up six sub-periods for the observation time at the lysimeters. The final sub-period was extended from March to April 2016 as measurements ended afterwards. For each lysimeter, it was required to consider a pre-phase prior to the observations period, to ensure complete simulated tracer breakthrough. Based on analytical modelling, pre-phases of one year for Ly1 and five years for Ly2 revealed adequate (cf. SI, section Pre-phase setup). Eight sub-periods were considered for Ly1 (for July 2012 to April 2016) and nine for Ly2 (initial sub-period P1 for July 2008 to June 2012). Thus, eight parameters of T, P_D and p_{PF} for Ly1 and nine for Ly2 were fitted.

4.2.5 Numerical modelling

*Unsaturated flow***.** Unsaturated flow of the studied lysimeter soil cores was simulated numerically with the software package HYDRUS-1D, which solves the Richards equation (Šimůnek et al., 2018). The van Genuchten-Mualem model was applied for the soil hydraulic functions $\theta(h)$ and $K(\theta)$ (van Genuchten 1980 and Mualem (1976), respectively):

$$\theta(h) = \begin{cases} \theta_r + \dfrac{\theta_s - \theta_r}{[1 + |\alpha h|^n]^m} & if\ h < 0 \\ \theta_s & if\ h \geq 0 \end{cases} \tag{4.4}$$

$$K(\theta) = K_s S_e^l \left[1 - \left(1 - S_e^{1/m}\right)^m\right]^2 \tag{4.5}$$

where $\theta(h)$ and $K(\theta)$ are water content ($L^3\ L^{-3}$) and hydraulic conductivity ($L\ T^{-1}$) as a function of hydraulic pressure head h (L); θ_r and θ_s are the residual and saturated water content, respectively (L^3L^{-3}), and K_s is the saturated hydraulic conductivity (LT^{-1}). α , n and m are empirical water retention curve shape parameters, where $m = 1 - 1/n$ ($n > 1$) (-). α is often related to the inverse air-entry suction (L^{-1}), whereas n to the pore-size distribution (-). The effective saturation S_e is given as $S_e = (\theta(h) - \theta_r) / (\theta_s - \theta_r)$ (-). The pore connectivity factor l represents the tortuosity of transport paths within the system (-). To decrease the number of fitting parameters, it was set to 0.5 as proposed by Mualem (1976).

Stable water isotope transport in the unsaturated zone. Solute transport can be described by the advection-dispersion equation for the unsaturated zone as follows (Fetter, 1999):

$$\frac{\partial(\theta C)}{\partial t} = \frac{\partial}{\partial z}\left(\theta D \frac{\partial C}{\partial z}\right) - \frac{\partial(qC)}{\partial z} \tag{4.6}$$

where C is the tracer concentration (M L^{-3}), D is the dispersion coefficient (L^2 T^{-1}), and q is the volumetric fluid flux (L T^{-1}). In this study, for the transport of stable water isotopes, only longitudinal dispersion is considered. D is defined as $D_L = \alpha_L \cdot v$, where α_L is the longitudinal dispersivity (L), while v represents flow velocity (L T^{-1}). The dispersion parameter P_D can be calculated as $P_D = \alpha_L / x$ (-), where x is the flow length (L) (x = 2 m, representing lysimeter length).

For stable water isotope transport modelling with HYDRUS-1D, a modified approach developed by Stumpp et al. (2012) was used. In the standard version of HYDRUS-1D, evaporation leads to an accumulation of solutes at the upper boundary. The modified code contains changes for the upper boundary so that evaporation has no effect on isotope content (Stumpp et al., 2012). Thus, isotopic fractionation due to evapotranspiration is neglected. This is expected to be a valid assumption if the observed regression line of stable isotopes of soil water is very close to the local meteoric water line (LMWL) of precipitation (Stumpp and Hendry 2012). As reported by Shajari et al. (2020), such a similarity was also observed at our study site.

Consideration of preferential flow paths and the influence of immobile water. To account for the presence of a second permeability system, we considered preferential flow paths for numerical modelling. This was done outside of HYDRUS-1D, since currently available HYDRUS-1D approaches cannot simulate stable water isotopes in a dual permeability domain. As a simplified assumption, similar to lumped-parameter modelling, piston flow (advective transport) was assumed for the preferential flow paths. A portion of precipitation (p_{PF}) directly enters preferential flow paths, and the remaining portion (1-p_{PF}) reaches the surface of the subsurface matrix. Mean residence times of preferential flow T_{PF} between 1 and 7 days were considered. Information on preferential flow is restricted by the temporal resolution of measurements, which was one week in average (upper boundary), and modelling was carried out on a 1-day resolution basis (lower boundary; cf. Shajari et al., 2020). The model setup is illustrated in Figure A-1 in the Appendix A. Calculations were done using a Python script, coupled to HYDRUS-1D executables and input files.

Furthermore, we have extended the model approach by including an additional isotopic component that accounts for the mixing of mobile and immobile water. As a simplified assumption, a constant positive delta-value is added to represent the influence of immobile water that is isotopically enriched.

Numerical model setup. For numerical modelling, the soil cores of the two lysimeters (Ly1 and Ly2) are represented by 1D model domains, and each model domain is discretized in 200 model cells with uniform cell size of 1 cm. As initial guess, SHPs for grain size distributions similar to Ly2 were obtained from the Rosetta data base. For Ly1, experimentally measured SHPs were available. For the diffusion coefficient in free water, a value of 10^{-9} m^2/s was used (Stumpp et al., 2012; Stumpp and Hendry 2012).

For water flow, the upper boundary was set as an atmospheric boundary condition with surface layer, and seepage face (h=0) was applied to the lower boundary (lysimeter outflow). At the upper flow boundary, we specified measured precipitation and actual evapotranspiration (ET) determined from the water balance at the lysimeters, as described in detail by Shajari et al. (2020). HYDRUS-1D was modified to estimate actual ET by setting h_{CritA} (the minimum allowed pressure head) to -1,500,0000 cm as applied by Groh et al. (2018). For tracer transport simulation, a time-variable solute flux boundary was applied at the top, and a zero-concentration gradient was applied at the bottom.

Since positive delta-values are required for transport modelling in HYDRUS-1D, a constant offset (23 ‰) was added to the (negative) delta-value input and the offset was subtracted again from the modelling results (Stumpp et al. 2012; Sprenger et al. 2016). For modelling the pre-phase, a pressure head of -340 cm (i.e., water content of field capacity) was set as the initial condition for the entire soil column. A modelling pre-phase of 2.5 years was considered for Ly1 (January 2011 to June 2013) and 5.5 years for Ly2 (January 2008 to June 2013) prior to the observation period for allowing the pore volume to exchange at least one time. Stable water isotope input for the modelling pre-phase was obtained from the meteorological station near Passau-Fürstenzell (as no measurements were available at lysimeter site; cf. Figure A-2). Initial stable water isotope content was set to an arbitrary value of 2 ‰ at all depths.

Estimation of median transit times. Following Sprenger et al. (2016), ideal virtual tracers were injected every day (constant amounts) at the top of the unsaturated zone, and cumulative tracer breakthrough curves were calculated based on modelled concentration with HYDRUS-1D. For each of those curves, the time when median concentration occurred was considered the individual median transit time (MTT).

4.2.6 Model curve fitting procedure

Least-square fitting of predictions to observations was done by manual expert adjustment of model parameters, in an iterative procedure. This was based upon statistical evaluation of curve fits using the root mean square error (RMSE), mean error (ME) and coefficient of determination (R^2) (Stumpp et al. 2009a). For lumped-parameter modelling, $\delta^{18}O$ in seepage water was set as objective function. In an iterative procedure, a set of T, P_D and p_{PF} was first fitted for the whole modelling period, then fitted for yearly and finally fitted for the seasonal (winter/summer) periods.

For numerical modelling, the hydraulic and transport parameters were inversely calibrated by using the model-independent parameter estimation utility PEST developed by Doherty (2020 a,b). Measured delta values in lysimeter outflow, drainage, and water content changes (estimated from recorded lysimeter weight) were used as objective functions (calibration targets). Details on parameter bounds for the fitting procedure are provided in Table A-3 of the Appendix A. Transport of both $\delta^{18}O$ and δ^2H was simulated, yielding very similar fitting parameters. In the following, results for $\delta^{18}O$ are presented in detail.

4.3 Results and discussion

4.3.1 Lumped-parameter modelling

Applying the extended LPM approach with temporally varying flow conditions substantially improved the model fit. For Ly1, R^2 was improved from 0.48 (traditional LPM) to 0.86 (IF0, Table 4-1) and for Ly2, R^2 was improved from 0.19 (traditional LPM) to 0.39 (IF0, Table 4-2). Underestimations were reduced significantly, for Ly1 in particular for the first year and for the final part of the curve (third peak starting in June 2015) (Figure 4-1a) and for Ly2 especially for the first year and the third peak (May to November 2015) (Figure 4-2a).

Application of the extended LPM approach revealed pronounced seasonal variations (winter-summer) and annual differences of model parameters (Table 4-1 and 4-2 and Figure 4-3). In addition, basic statistical data of measured $\delta^{18}O$ in Ly1 and Ly2 as well as seasonal variations are summarized in Table A-4 and Figure A-3.

The fitted parameters for this study are within a typical range for similar soils (discussed in detail in Shajari et al., 2020). As shown in Figure 4-3d and e for Ly 1 and Figure 4-3j and k for Ly2, neither T nor P_D variation revealed a clear pattern with respect to the season (values given in Table 4-1). For a sandy gravel soil, Stumpp et al. (2009b) found seasonal variations of T and P_D between 182-413 days and 0.09-0.14, respectively, where a clear trend of summer-winter oscillation seems not obvious. Parameter variations from year to year, found in the present study, are within a similar range as observed by Stumpp et al. (2009b) and Małoszewski et al. (2006) for different soils.

Modification of the input function led to further modelling improvements. For Ly1, IF2 with 6-month weighting showed the best fit (Table 4-1 and Figure 4-1b) and for Ly2 IF2 with 3- and 6-month weighting (Table 4-2 and Figure 4-2b). The modified input function considers weighted input and thus reflects seasonal changes on a three- and six-month basis as well as shorter (one-month) fluctuations of infiltration.

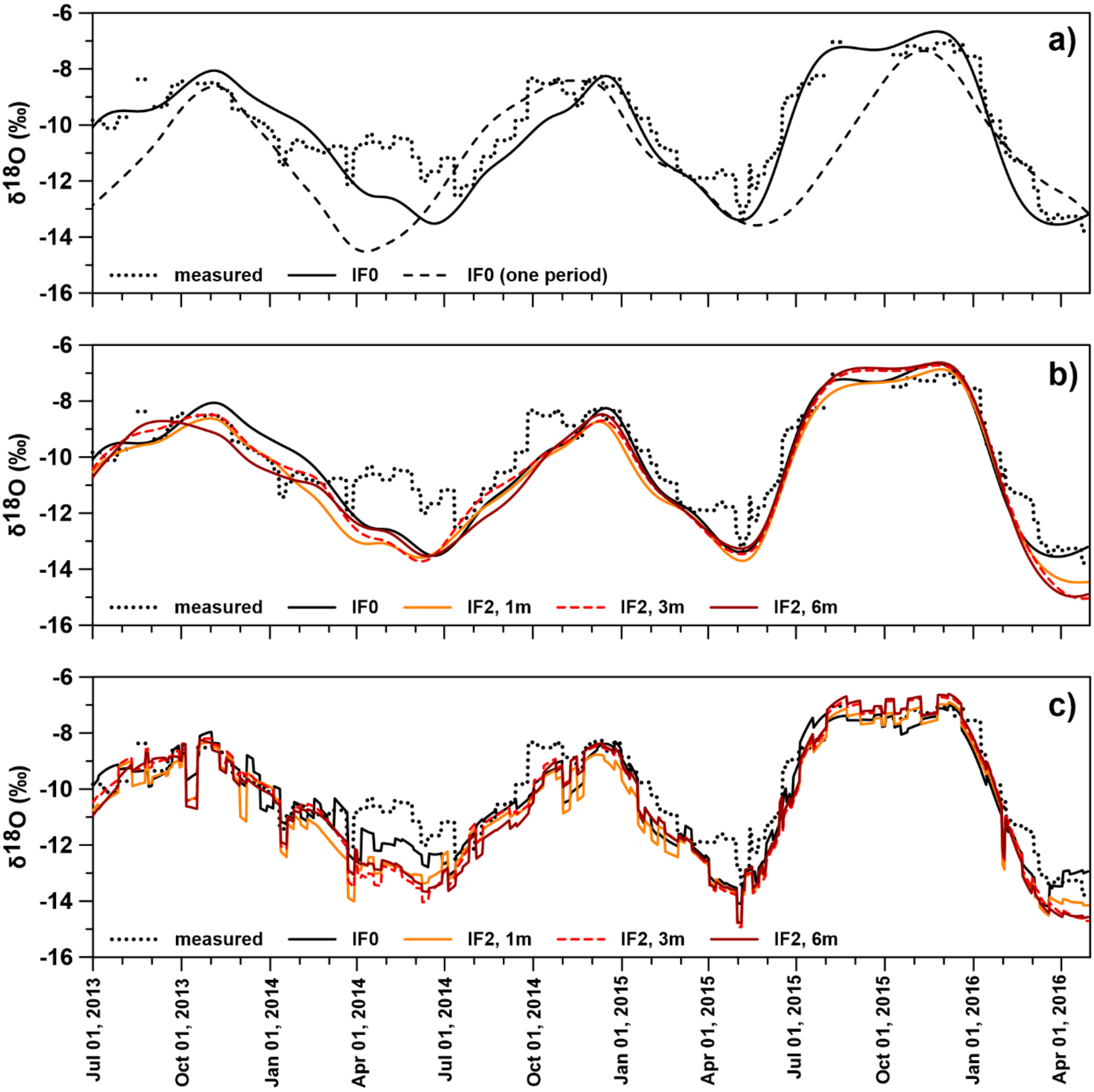

Figure 4-1. Measured and modelled (lumped-parameter model, LPM) δ^{18}O in the seepage water of Ly1 as a function of time. a) Modelling with input function IF0 (δ^{18}O of precipitation as input), considering variable flow (extended LPM, eight sub-periods) and constant flow (“traditional” LPM, one period). b) and c) Modelling with input function IF2 and weighted input within 1, 3 and 6 months (1m, 3m, 6m), considering variable flow. a) and b): stable water isotope transport through the subsurface matrix flow, only; c): transport through the matrix plus along preferential flow paths.

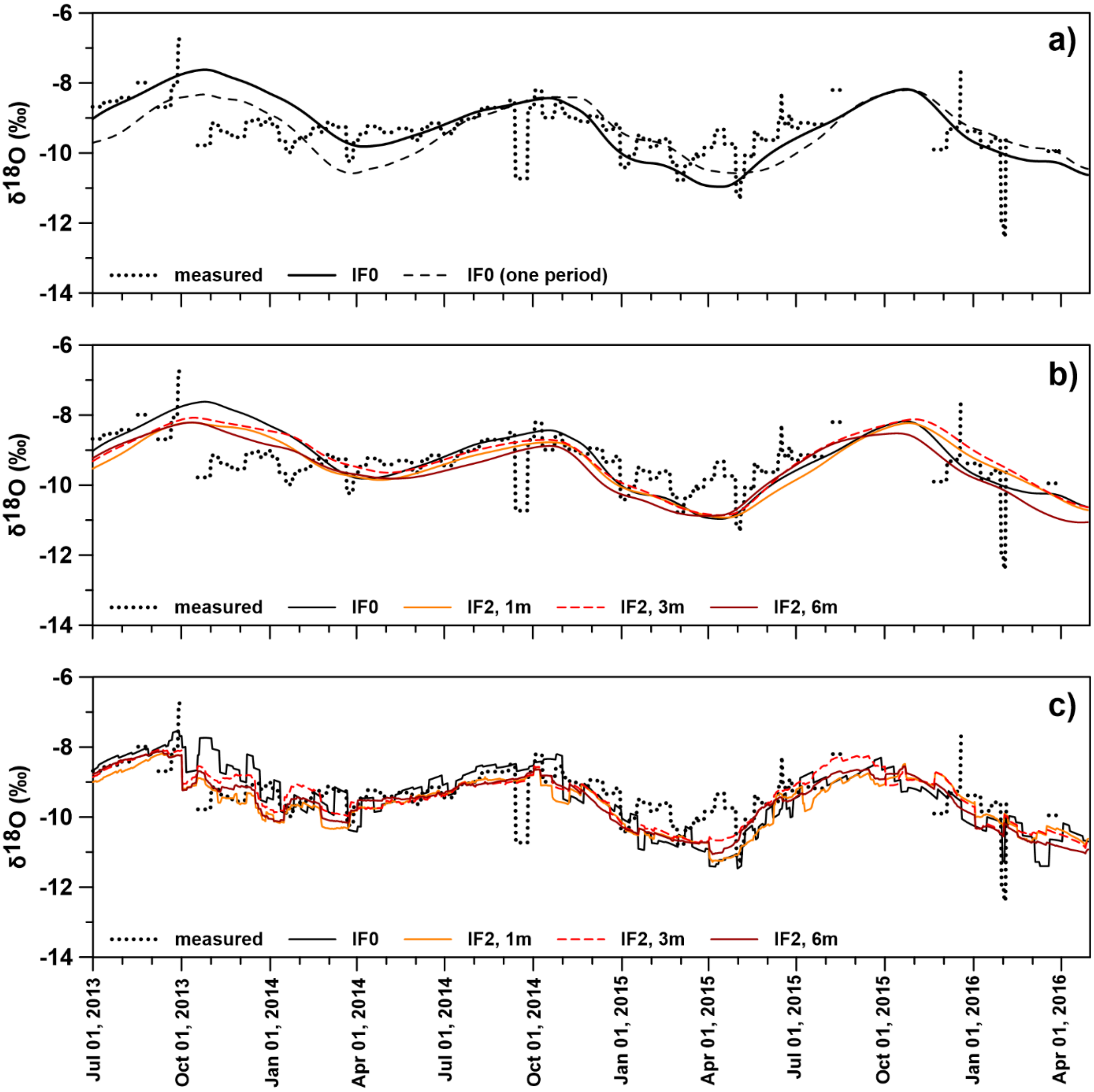

Figure 4-2. Measured and modelled (lumped-parameter model, LPM) $\delta^{18}O$ in the seepage water of Lysimeter 2 as a function of time. a) Modelling with input function IF0 considering variable flow (extended LPM, nine sub-periods) and constant flow ("traditional" LPM, one period). b) and c) Modelling with input function IF2 and weighted input within 1, 3 and 6 months (1m, 3m, 6m), variable flow. a) and b): stable water isotope transport through the subsurface matrix flow, only; c): considers transport through the matrix plus along preferential flow paths.

The implementation of preferential flow paths further improved simulations (cf. Figure 4-1c and Table 4-1 for Ly1 and Table 4-2 and Figure 4-2c for Ly2). Rapid transport of recharging $\delta^{18}O$ along preferential flow paths can explain the observed short-term fluctuations of $\delta^{18}O$ in seepage water. Accordingly, p_{PF} tends to be increased when the precipitation rate is high (see Figure 4-3f versus 4-3c for Ly1, Figure 4-3l versus 4-3i for Ly2). Such a dependency was also found by Stumpp et al. (2007). In contrast, no clear season-dependency of p_{PF} can be seen for Ly2. The difference between the lysimeters could possibly be explained by different contributions of preferential flow paths. For many soils, as found for Ly1 (with some exceptions), contributions of preferential flow tend to be higher in summer (Demand et al., 2019; Täumer et al., 2006). This can be explained by low water contents (that prevail during extended dry periods) and events of high precipitation (Demand et al. 2019).

Gazis and Feng (2004) studied the isotopic composition of precipitation and soil water in sandy loam soils. Their observations suggest that the mixing of percolating water with immobile water can lead to higher $\delta^{18}O$ values (due to the prevalence of isotopically heavy summer water), as observed in our study for Ly2. This finding supports our assumption of a “constant upshift” of modelled isotope values in the seepage water of Ly2, for mimicking contributions of immobile water. A $\delta^{18}O$ upshift of 1 ‰ was found as a best fit. In contrast, mixing between mobile and quasi-immobile water might have a lower influence for the seepage water of Ly1 (no upshift was required there). This might be due to the finer pore structure and thus as a higher effective soil water volume in Ly2 (cf. Shajari et al. 2020). Consideration of the constant isotopic upshift within the LPM did not impact values of T, P_D, and p_{PF}.

Table 4-1. Ly 1: Parameter values fitted from lumped-parameter modelling with different input functions (IF) and statistics. Traditional LP: values taken from Shajari et al. (2020).

	S12	**W12/ 13**	**S13**	**W13/ 14**	**S14**	**W14/ 15**	**S15**	**W15/ 16**	**Av.**	**R^2 (-)**	**RMSE (‰)**	**ME (‰)**
Traditional LPM, Input Function IF0												
T (d)									129	0.48	1.51	-0.61
P_D (-)									0.7			
Input function IF0												
T (d)	121	118	135	145	98	119	165	138	131	0.86	0.81	-0.43
P_D (-)	0.14	0.14	0.08	0.14	0.10	0.09	0.05	0.05	0.10			
p_{PF} (%)	14	9	14	14	13	10	15	12	13			
Input function IF2, 1m												
T (d)	121	88	117	139	112	121	176	135	126	0.87	1.08	-0.79
P_D (-)	0.13	0.13	0.10	0.14	0.14	0.11	0.07	0.05	0.11			
p_{PF} (-)	7	6	12	9	10	8	12	8	9			
Input function IF2, 3m												
T (d)	100	95	115	149	122	119	177	138	127	0.87	1.06	-0.63
P_D (-)	0.13	0.08	0.10	0.16	0.13	0.09	0.07	0.05	0.10			
p_{PF} (%)	7	6	8	6	12	6	12	7	8			
Input function IF2, 6m												
T (d)	100	91	111	152	122	119	178	138	126	0.89	1.03	-0.67
P_D (-)	0.13	0.08	0.10	0.14	0.14	0.09	0.07	0.05	0.10			
p_{PF} (%)	8	7	12	6	10	6	12	7	9			

S: summer, W: winter, Av.: average value for the whole time period

As a major change to our previous study (Shajari et al. 2020), we have considered a longer modelling pre-phase of 5 years (instead of 1 year) for LPM modelling of Ly2. This was done both for constant flow (dashed curve in Figure 4-2a) and varying flow (other model curves in Figure 4-2). This longer pre-phase revealed to be more adequate given the finer-grained structure and higher mean travel time of water within Ly2 (details given in Appendix A Chapter A1 Pre-phase setup).

Table 4-2. Ly 2: Parameter values fitted from lumped-parameter modelling with different input functions (IF) and statistics

Par.	P1	S12	W12/13	S13	W13/14	S14	W14/15	S15	W15/16	Av.	R^2 (-)	RMSE (‰)	ME (‰)
Traditional LPM, Input Function IF0													
T (d)										362	0.19	0.67	-0.05
P_D (-)										1.2			
Input function IF0													
T (d)	350	370	300	360	430	320	380	300	375	354	0.39	0.73	-0.09
P_D (-)	0.7	0.7	0.8	0.5	0.8	0.5	0.9	0.4	0.8	0.7			
p_{PF} (%)	7	8	7	6	10	9	8	12	12	9			
Input function IF2, 1m													
T (d)	350	350	300	350	445	310	370	330	375	354	0.38	0.68	-0.30
P_D (-)	0.7	0.7	0.8	0.7	0.8	0.5	0.7	0.4	0.6	0.7			
p_{PF} (%)	7	8	8	4	11	10	8	12	11	9			
Input function IF2, 3m													
T (d)	350	350	300	390	445	310	370	330	385	360	0.40	0.60	-0.11
P_D (-)	0.7	0.7	0.8	0.7	0.7	0.4	0.7	0.3	0.5	0.6			
p_{PF} (%)	7	8	8	3	9	11	8	7	11	8			
Input function IF2, 6m													
T (d)	350	350	305	365	445	330	390	310	390	361	0.40	0.64	-0.23
P_D (-)	0.7	0.7	0.8	0.6	0.7	0.5	0.9	0.4	0.7	0.7			
p_{PF} (%)	7	9	8	3	9	6	5	7	6	7			

P1: additional modelling pre-phase, July 2008 to June 2012

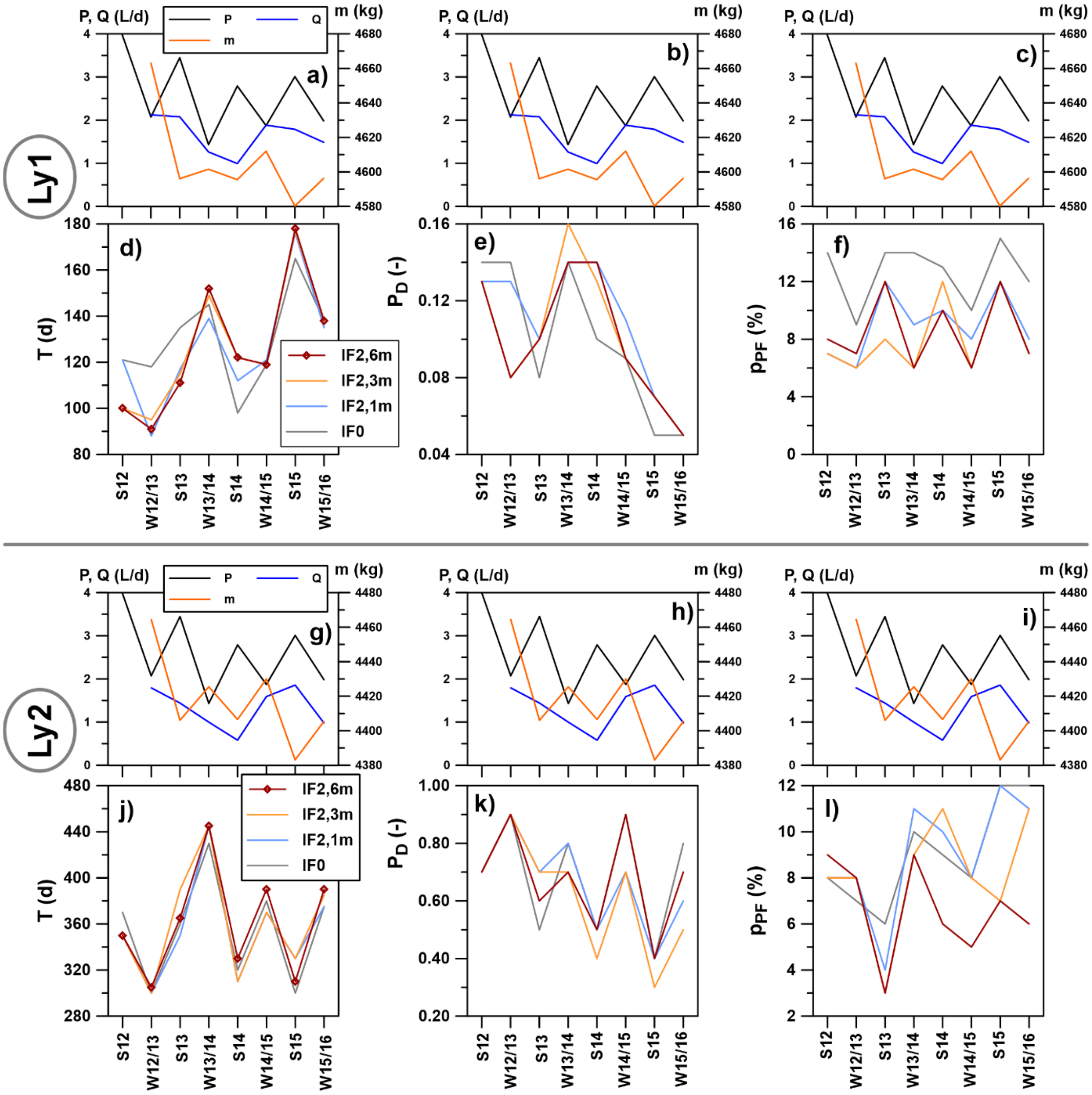

Figure 4-3. Temporal variation of parameters found from applying the extended lumped-parameter model (extended LPM) with different input functions IF for Ly1 (d-f) and Ly2 (j-l) (cf. Table 4-1 and 4-2). Parameters are compared to 6-month-averages of precipitation (P), lysimeter drainage (Q) and lysimeter weight (m) (panels a-c are identical, panels g-i are identical).

4.3.2 Numerical flow and stable water isotope transport modelling

As shown in Figure 4-4a, the modelled curves describe the observed behavior of δ^{18}O for Ly1 well, reproducing seasonal periodicity. As found above for lumped-parameter modelling, the application of stable water isotope transport along preferential flow paths resulted in slightly better overall curve fits. Portions of preferential flow p_{PF} of 8-11% led to similarly good model curve fits, with mean residence times of water within preferential paths (T_{PF}) of 6-7 days. This rather wide range of p_{PF} and T_{PF} indicates a low sensitivity of preferential flow characteristics. This could possibly be explained by the coarse texture of the soil of Ly1, which is characterized by sandy gravels. Connected pores may act as preferential flow paths (enabling rapid transport of the infiltrating water).

For Ly1, fitted values of saturated water content θ_S and dispersion parameter P_D (Table 4-3) are within typical ranges found for sandy gravels (Stumpp et al. 2009b; Sprenger et al. 2015) (Table 4-3 and simulated soil water retention curves shown in Figure A-5). For saturated hydraulic conductivity K_S, fitted values match those found by Stumpp et al. (2009c) and Freeze and Cherry (1979).

Results of numerical modelling for Ly2 are shown in Figure 4-4b. As for LPM application, modelled curves were shifted up by a constant value (0.8 ‰). This value is slightly higher than that found from LPM application (1 ‰) and corresponds to a second component that contributes to delta values in seepage water. The seasonal periodicity seems not fully matched by the simulation. The consideration of preferential flow (Figure 4-3b) substantially improved simulation and reduced under- and overestimations. Moreover, short-term fluctuations were better described (cf. Table 4-3 for statistical evaluation of curve fits with preferential flow). The fitted saturated water content θ_S of 0.28 appears to be at the lower end of frequently reported ranges around 0.3-0.5 (Table 4-3 and simulated soil water retention curves shown in Figure A-5). This could possibly be explained by the relatively high contents of sand (cf. Table A-1 and Table A-2) together with a poor sorting of grain sizes (Durner et al., 2008; Graham et al., 2018; Thoma et al., 2014; Vrugt et al., 2001). Fitted saturated hydraulic conductivity K_S (146.34 cm/d, Table 4-3) is within typical ranges for sandy silt soils (Freeze and Cherry 1979 and Jiang et al. 2010). Observed versus simulated Q for considering matrix flow only or matrix and preferential flow are shown in Figure A-6. In addition to homogeneous conditions, multi-layer scenarios were also modelled, with 4 layers for Ly1 and 5 layers for Ly2 (cf. Table A-1 and Table A-2). Modelled results were very similar to the homogeneous case (results not shown).

Table 4-3. Parameter sets fitted for Ly1 and 2 by inverse numerical flow and isotope transport modelling and statistics.

Depth (cm)	**θ_r (cm^3/cm^3)**	**θ_S (cm^3/cm^3)**	**α (1/cm)**	**n (-)**	**K_S (cm/d)**	**l (-)**	**P_D (-)**	**p_{PF} (%)**	**T_{PF} (d)**	**R^2 (-)**	**RMSE (‰)**	**ME (‰)**
Ly1												
0-200	0.007	0.275	0.35	1.41	6040.20	0.5	0.07	8-11	6-7	0.85	0.67	-0.14
Ly2												
0-200	0.026	0.29	0.005	1.23	146.34	0.5	0.85	12-13	5-7	0.20	0.83	-0.52

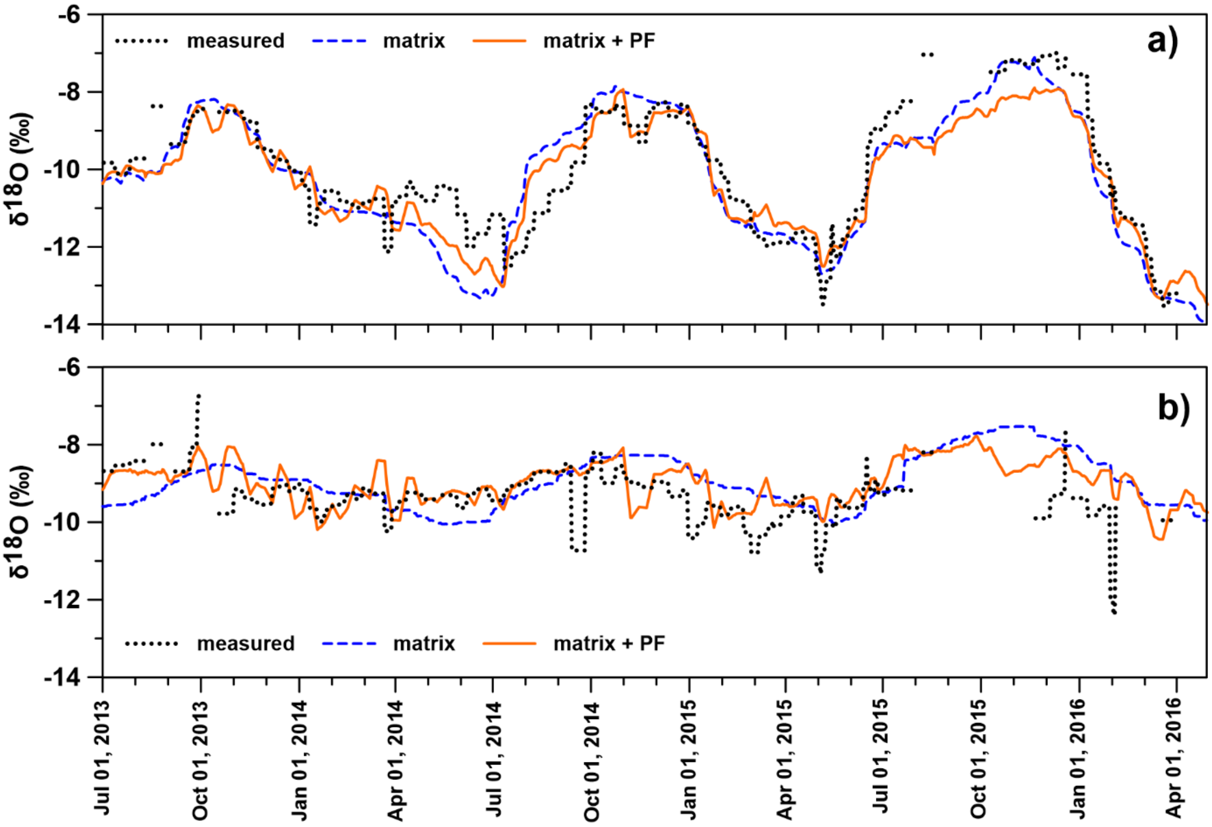

Figure 4-4. Measured versus modelled (HYDRUS-1D) $\delta^{18}O$ in the seepage water of Ly1 (a) and Ly2 (b); transport through the subsurface matrix and along preferential flow paths (PF).

4.3.3 Comparison of LPM application and numerical modelling

Seasonal periodicity of stable water contents in seepage water is met well by both approaches. For Ly2, observations are more difficult to describe (Figure 4-2 and 4-4b). For Ly1, P_D fitted with HYDRUS-1D was lower (0.07) compared to P_D of 0.10-0.11 from LPM modelling. In contrast, for Ly2, P_D obtained from numerical modelling was slightly higher (0.85, Table 4-3) compared to LPM (averages 0.6-0.7, Table 4-2). From numerical modelling studies, Robin et al. (1983) found higher P_D-values when neglecting immobile water as a second porosity system. Similar observations were reported for comparative simulations done by Stumpp et al. (2009c) and Maraqa et al. (1997). Concerning preferential flow, for Ly1, p_{PF} found from numerical modelling (5-7%, Table 4-3) is slightly lower than from LPM application (average 8-13%, Table 4-1). For Ly2, p_{PF} found from numerical modelling (12-13%, Table 4-3) exceeds the LPM best fit (7-9%, Table 4-2).

MTT and *T* are similar for Ly1, with a somewhat lower average for *MTT* (100 d for MTT vs. 126-131 d for LPM, for the different input functions, Table 4-4). For Ly2, *MTT* is much lower than *T*, with 197 d in average vs. 354-361 d. Additional simulation studies with a higher saturated water content θ_s led to an increase in *MTT*, with averages of

274 d (θ_s = 0.4 cm^3/cm^3) and 342 d (θ_s = 0.5 cm^3/cm$^{3)}$ (Table 4-4). Such higher values of θ_s (instead of the fitted values around 0.29 cm^3/cm^3) are also more often reported for silty soils.

Table 4-4. Median transit time (*MTT*) obtained by numerical modelling of virtual tracers for Ly1 und Ly2.

Sub-period	**S12**	**W12/ 13**	**S13**	**W13/ 14**	**S14**	**W14/ 15**	**S15**	**W15/ 16**	**Av.**
Lysimeter 1									
MTT (d)	76	96	91	163	97	103	93	97	100
Lysimeter 2									
MTT (d)	199	242	223	230	187	185	176	162	197
$MTT_{0.4}$ (d)	298	335	293	304	247	254	226	222	274
$MTT_{0.5}$ (d)	393	408	350	365	299	306	267	267	342

$MTT_{0.4}$ and $MTT_{0.5}$: assuming a higher saturated water content θ_s of 0.4 and 0.5 cm^3/cm^3, respectively

4.3.4 Comparison of model concepts and potential improvements

Flow variation is described in a much higher temporal resolution by the numerical model (daily) than by the extended LPM (half-year). As a consequence, the degree of freedom for *T* and P_D value fitting seems higher for the extended LPM approach.

In contrast, the LPM takes an integral view within a “black box”: *T* encompasses the mean transit time of soil water in total, i.e., percolating (mobile) water as well as contributions of (remobilized) immobile water. Accordingly, *MTT* would only be a part of this *T*. This explains the large difference between *T* and *MTT* for Ly2.

The possible overestimation of P_D for Ly2 might be related to shortcomings in our model setup. An extension of our numerical model to a dual-porosity approach could possibly reduce deviations as well. It has the potential of describing immobile water and its influence on flow and stable water isotope transport mechanistically. However, measurements of soil water contents and/or hydraulic potential within soil, at different depths, are recommended (which were not available for this study) for model calibration, to reduce uncertainties associated with such a (more complex) approach.

The numerical model approach could also be extended by considering the uptake of water by plant roots within the soil column. Although root water uptake is not expected to alter the isotopic composition significantly (Allison et al., 1984; Zimmermann et al., 1967), it affects soil water contents during the vegetation period (Sprenger et al. 2016).

4.4 Summary and conclusions

The extended lumped-parameter model (LPM) approach considers temporally variable flow and transport conditions. With simplified assumptions, the model addresses preferential flow and the influence of quasi-immobile water on stable water isotopes, in addition to water flow and stable water isotope transport within the subsurface matrix.

This model was applied successfully to a three-year study with two lysimeters (Ly1 and Ly2) characterized by different soil textures and the same vegetative cover (maize). Improvements were obtained in comparison to “traditional” lumped-parameter modelling that considered steady-state flow. Pronounced seasonal (summer-winter) and year-to-year variations were found for mean transit time of water T, dispersion parameter P_D and portion of preferential flow p_{PF}. Measured stable water isotopes in seepage water were more difficult to explain for Ly2.

Results of the extended LPM approach were compared to results from numerical modelling of HYDRUS-1D. The latter was extended for the consideration of preferential flow and the influence of immobile water (isotopic upshift), in analogy to the extended LPM. In general, model curves from both approaches match each other. For Ly2, in addition to (slight) differences in P_D, transit times of water differed significantly (T vs. MTT). These differences cannot be fully explained: uncertainties for numerical modelling are associated, among others, with missing measurements within the soil columns, such as of water content, pressure head or stable water isotopes. As an advantage of the extended LPM approach, uncertainties of flow characterization are reduced by identifying ranges of plausible parameters as a result of temporally changing flow (and transport) conditions. A step-wise procedure is recommended, with (i) finding one set of parameters (T, P_D and p_{PF}) for the whole simulation time (application of the “traditional” LPM approach) and (ii) finding temporally varying parameters for hydraulically relevant sub-periods, such as seasons or vegetation periods (application of the extended LPM approach for strongly varying flow conditions). This represents a valuable tool for flow characterization, with the advantage of significantly lower data requirements compared to numerical modelling.

Chapter 5 Fate of herbicides in cropped lysimeters: 1. Influence of different model setups on vadose zone flow

These chapters include the following publication, with some modifications: Imig, A., Augustin, L., Groh, J., Pütz, T., Zhou, T., Einsiedl, F., Rein, A., (under review, a) Fate of herbicides in cropped lysimeters: 1. Influence of different model setups on unsaturated flow. Vadose Zone Journal

A statement from the doctoral candidate concerning her contribution to publications was submitted within the framework of a publication-based dissertation, together with a statement of confirmation from the co-authors according to Article 7, section 3, clause 2 of the TUM Doctoral Regulations (PromO) was submitted along with the publication.

Anne Imig did neither collect nor analyse samples taken at the study site. Stable water isotopes in precipitation and lysimeter drainage were analysed at the Chair of Hydrogeology at TUM. The Bavarian Environment Agency (Bayerisches Landesamt für Umwelt, LfU) collected meteorological data, water samples from precipitation and lysimeter drainage and measured lysimeter drainage rates and lysimeter weight.

Abstract

Understanding transport and fate processes in the subsurface are of fundamental importance to identify leaching potentials of, e.g., herbicides to groundwater resources. HYDRUS-1D was used to simulate water flow and solute transport in arable land lysimeters. Simulations were compared to observed drainage rates and stable water isotopes ($\delta^{18}O$) in the drainage. Four different model setups were investigated and statistically evaluated for their model performance to identify dominant processes for water flow characterization in the vadose zone under similar cultivation management and climatic conditions. The studied lysimeters contain soil cores dominated by sandy gravel (Ly1) and clayey sandy silt (Ly2), both cropped with maize located in Wielenbach, Germany. First, a single-porosity setup was chosen. For Ly1, modelling results were satisfactory but for Ly2, the damping observed in the isotope signature of the drainage could not be fully covered. By considering immobile water with a dual-porosity setup, for Ly2, model performance improved. This could be due to a higher fraction of fine pores in Ly2 available for water storage, leading to mixing processes of isotopically enriched summer precipitation water and lighter winter water. Accounting for isotopic evaporation fractionation processes in both model setups did not lead to improved model performance. Consequentially, the difference in soil hydraulic properties between the two lysimeters seem to impact water flow processes. Knowledge of such differences are crucial to prevent contamination and mitigate potential risks to soil and groundwater.

5.1 Introduction

Unsaturated flow and transport are dependent, amongst others, on water content, hydraulic potential and hydraulic conductivity influencing each other and varying in space and time. Mechanistic descriptions of these highly non-linear processes as well as computational models have been developed, attempting to simplify these processes in an appropriate and efficient way (Haws et al., 2005; J. Šimůnek et al., 2008; Šimůnek et al., 2003). These models allow us, e.g., the prediction of contaminant leaching to groundwater and risk assessment aimed at groundwater protection. Knowledge on model setup and process parameters is crucial to achieve model prediction integrity (Doherty, 2015). Laboratory experiments are usually performed to determine process parameters for specific soils and (small-scale) conditions. However, they have shortcomings to describe changing field conditions of, e.g., water content in the soil or atmospheric conditions (Isch et al., 2019; Šimůnek et al., 2001). Lysimeters can provide a linkage between laboratory and field experiments. Lysimeters have the advantage that initial and boundary conditions can be controlled and realistic conditions of environmental processes can be reproduced (Pütz et al., 2018). Lysimeter studies have been successfully applied in the past and can provide important data for the investigation of soil hydraulic properties on the water flow, the chemical cycle, as well as the dynamics of water and chemical plant uptake (e.g., Francaviglia and Capri, 2000; Leita et al., 1996; Piwowarczyk et al., 2013; Winton and Weber, 1996). Lysimeter experiments are often combined with field measurements and tracer tests or environmental tracers such as stable water isotopes in order to set initial and boundary conditions (Groh et al., 2016; Leibundgut et al., 2009; Stumpp et al., 2009c) for modelled process description (Groh et al., 2018; Shajari et al., 2020; Sprenger et al., 2015).

The numerical modelling software HYDRUS-1D permits the description of the liquid phase in the unsaturated soil with different approaches (Šimůnek et al., 2018). The single-porosity approach is based on the simplification that the complex inter- and intra-aggregation of pores can be described with only one homogenous soil porosity. Uniform flow and transport are considered throughout the liquid phase. Single-porosity systems may be able to describe well-sorted soils but fall short to describe immobile water or preferential flow paths (Haws et al., 2005; Jiang et al., 2010; Šimůnek et al., 2001). To overcome these restrictions in a dual-porosity model, the liquid phase is portioned into mobile and immobile regions to allow the description of different flow and transport velocities (Šimůnek and van Genuchten, 2008). Köhne et al. (2004) inversely fitted dispersivity and soil hydraulic parameters of a dual-porosity model setup in HYDRUS-1D. Bromide was used as a tracer in six undisturbed soil columns filled with loamy soils, and effects of initial soil water content were investigated. Compared to the single-porosity setup, the dual-porosity model appeared to have more pronounced impacts for strong water content variations than for low variations. Jiang et al. (2010) simulated leaching of fecal coliforms and bromide in six lysimeters filled with silt loam and sandy loam soils. In these cases, the single-porosity model was able to plausibly simulate water flow and leaching during natural climatic conditions, but for lysimeters with flood irrigation, the dual-porosity models performed better. Isch et al. (2019) investigated the single- and dual-porosity approach in HYDRUS-1D to describe water flow and bromide transport for six uncropped lysimeters filled with silty loam. The consideration of immobile water with the dual-porosity approach improved the description of the bromide transport, which the authors explained with preferential flow influences.

In this study, we compared different single- and dual-porosity setups within HYDURS-1D for describing flow and stable water isotope transport in two lysimeters located in Wielenbach, Germany. The lysimeters were filled with different soils: Lysimeter 1 (Ly1) was dominated by sandy gravel and Lysimeter 2 (Ly2) by clayey sandy silt. Both were cropped with maize. Stable water isotopes were measured in precipitation and lysimeter drainage between July 2013 and April 2016. Furthermore, between 2013 and 2017, four herbicides (metolachlor, terbuthylazine, prosulfuron and nicosulfuron) were applied at the lysimeter site, and their concentration in the drainage was monitored. In our recent study, we interpreted measured stable water isotopes with help of numerical modelling (uniform flow and transport within HYDRUS-1D) and lumped-parameter modelling (Imig et al., 2022a).Results for Ly2 showed underestimations of stable water isotopes ($\delta^{18}O$) in lysimeter discharge. This could be explained by the contribution of mixing with immobile water, where a constant $\delta^{18}O$ upshift, added to simulated values, was considered as a strong simplification. We assumed that the mixing of percolating water with immobile water can lead to higher $\delta^{18}O$ values, due to the prevalence of isotopically enriched summer water.

In the present paper, we further explored the possible influence of immobile water with help of dual-porosity setups. Moreover, we expanded our view by investigating the contribution of root water uptake and stable water isotope fractionation by evaporation. To the best knowledge of the authors, very few studies are available to date that explore dual-porosity modelling with stable water isotope analysis and reactive transport modelling in the unsaturated zone for a time period of several years. E.g., Huang et al. (2015) calibrated a dual-porosity flow model with stable isotopes and combined this with a reactive transport model of sulphate for a field scale study.With the complexity of a model, the number of fitting parameters increases. Manual calibration of fitting parameters of more complex models, such as dual-porosity setups, can require higher efforts and might be prone to errors. Parameter optimization algorithms can identify optimal parameter sets and support the fitting procedure to inversely calibrate models of the vadose zone (e.g., Groh et al., 2018; Šimůnek et al., 2018; Sprenger et al., 2015). Thus, for the different model calibrations, we used the parameter optimization algorithm PEST developed by Doherty (2020a, 2020b).

Main research goals were thus 1) to determine the soil hydraulic and solute transport parameters by inverse modelling and 2) to identify dominant processes on water flow and stable water isotope transport for each soil, including mobile-immobile water dynamics and isotopic fractionation due to evaporation. Our consecutive paper (Imig et al., under review, b) investigates herbicide leaching by extending the flow model of this study with a reactive transport model. Additionally, stable carbon isotopes of herbicides are analysed for investigating biodegradation.

5.2 Materials and Methods

5.2.1 Study Site

The research site in Wielenbach is located in the south of Germany (47° 53' 3.3" N, 11° 9' 26.2" E, 549 m amsl) and managed by the Bavarian Environmental Agency. It is characterized by moderately continental climate with annual mean precipitation of 928 mm and temperature of 8.9 °C. We investigated two weighable lysimeters, consisting of stainless-steel cylinders with a surface area of 1 m² and a depth of 2 m. The lysimeters were lined with high density polyethylene and filled with undisturbed monolithic soil cores from two different soils (Shajari et al., 2020). Lysimeter 1 (Ly1) contains sandy gravels originating from a former target shooting range near Garching, Germany (48° 13’ 51” N, 11°36’13.4” E). Soils at this site are characterized by a calcaric Regosol developed above sandy to silty calcareous gravels. Lysimeter 2 (Ly2) contains a clayey sandy silt, and the soil core was excavated from an agricultural site at Hutthurm-Auberg, Germany (48°40’21” N, 13°28’17” E) where Cambisol (Stagnosol) developed above gneiss. More information on the grain size distribution can be taken from the Appendix B (Table B-1 and B-2). Maize was cultivated at the site of both lysimeters during the observation period. Further information on maize cultivation is given in Table B-3. The lysimeters were not irrigated, with the exception of summer 2015, when maize plants were irrigated in small amounts to prevent wilting and water was accidentally released to Ly2 from a hose.

5.2.2 Observation and Sampling

Lysimeter weight, drainage (by a balance) and precipitation (Pluvio, OTT Hydromet) were automatically monitored at a temporal resolution of 0.5 h as described in detail by Shajari et al. (2020). Further meteorological data on air temperature and air humidity were measured at the research site, operated by the German Meteorological Service (Deutscher Wetterdienst DWD). Precipitation and drainage samples were collected at weekly intervals from July 2013 to April 2016 and adjusted to shorter intervals only during periods of higher water flow. The samples were analysed on stable water isotopes ($\delta^{18}O$ and $\delta^{2}H$) with a liquid water isotope analyser (Los Gatos, Inc., model 912 0050; Shajari et al., 2020). The isotope values were express in the δ notation relative to the Vienna Standard Mean Ocean Water (V-SMOW). Average air temperatures in the lysimeter cellar were ~15 °C in summer and ~5 °C in winter. Four herbicides (metolachlor, terbuthylazine, prosulfuron and nicosulfuron) were applied to the lysimeters between 2013 and 2017, in late May or early June according to common agricultural practice.

5.2.3 Flow and transport modelling

5.2.3.1 Single-porosity model

Transient water flow and stable water isotope transport in the lysimeters were simulated with the numerical software package HYDRUS-1D (Šimůnek et al., 2018). In this model, unsaturated flow is simulated by solving Richards equation (e.g., Delleur, 1999), while applying the van Genuchten-Mualem approach to describe water content θ and hydraulic conductivity K as a function of hydraulic pressure head h (van Genuchten, 1980 and Mualem, 1976):

$$\theta(h) = \begin{cases} \theta_r + \dfrac{\theta_s - \theta_r}{[1 + |\alpha h|^n]^m} & if\ h < 0 \\ \theta_s & if\ h \geq 0 \end{cases} \tag{5.1}$$

$$K(\theta) = K_s S_e^l \left[1 - \left(1 - S_e^{1/m}\right)^m\right]^2 \tag{5.2}$$

where θ_r is residual water content [L^3 L^{-3}], θ_s saturated water content [L^3 L^{-3}] and K_s saturated hydraulic conductivity [L T^{-1}] of the subsurface. α and n are curve shape parameters, where α is often related to the inverse air-entry suction or capillary fringe thickness [L^{-1}] and n to the pore-size distribution [-], with $m = 1 - 1/n$ [-] for $n > 1$. S_e is the effective saturation [-], which is defined as $S_e = (\theta - \theta_r)/(\theta_s - \theta_r)$. The parameter l represents the pore connectivity [-] and was set to a value of 0.5 in accordance with other studies (e.g., Graham et al., 2018; Köhne et al., 2006a; Sprenger et al., 2015). For numerical modelling with HYDRUS-1D, the lysimeters were represented as 1D model domains, discretized in 201 nodes with an equal distance of 1 cm. Using this approach, Imig et al. (2022a) have compared homogeneous (one-layer) and heterogenous (multi-layer) setups for both lysimeters, where similar results were obtained for simulated water flow and δ^{18}O transport. Following the parsimony principle, we decided to use the simpler (homogenous) setup in the present study.

Lysimeter top was set to an atmospheric boundary condition (with a surface water layer of maximum 5 cm thickness to allow water build-up), where we specified measured precipitation and actual evapotranspiration (ET$_a$). The latter was determined from the water balance at the lysimeters, as described in detail by Shajari et al. (2020). To prevent HYDRUS-1D in modifying input evapotranspiration, we have set the parameter h_{CritA} to -1,500,000 cm, as also applied by Groh et al. (2018) and Imig et al. (2022a). A modelling pre-phase of 2.5 years was considered for both lysimeters (January 2011 to

June 2013) for allowing complete pore volume exchange and tracer ($\delta^{18}O$, $\delta^{2}H$) breakthrough before the observation period. As initial condition, a pressure head of -340 cm was set for the whole soil column (corresponding to field capacity, due to a moist period; no measured data were available). For the lower boundary condition, seepage face (h = 0) was chosen (e.g., Groh et al., 2018; Stumpp et al., 2009b). Accordingly, five soil-hydraulic parameters (SHP) were calibrated per lysimeter: θ_r, θ_s, α, n and K_s.

5.2.3.2 Dual-porosity model

To allow an investigation of the mobile and an immobile flow region, a dual-porosity (DP) setup was compared to a single-porosity (SP) setup. The DP setup assumes that the soil contains (i) a mobile zone, also called matrix domain, where water can flow and (ii) an immobile region, where no flow occurs. Non-equilibrium can be considered for absent or slow water mass transfer, while an equilibrium between the regions can be assumed in the case of very fast transfer (Köhne et al., 2004). θ, the total soil water content [L^3 L^{-3}], is obtained as the sum of water contents in the mobile (θ_{mo}) and immobile (θ_{im}) region:

$$\theta = \theta_{mo} + \theta_{im} \tag{5.3}$$

The water dynamics in the mobile region of a dual-porosity system (index *mo*) can be described with Richard's equation, while the water content in the immobile region (index *im*) originates from water exchange:

$$\frac{\partial \theta_{mo}(h)}{\partial t} = \frac{\partial}{\partial z}\left[K(h)\left(\frac{\partial h}{\partial z} + 1\right)\right] - S_{mo} - \Gamma_w \tag{5.4}$$

$$\frac{\partial \theta_{im}(h)}{\partial t} = -S_{im} + \Gamma_w \tag{5.5}$$

where Γ_w is the transfer rate of water from inter- to intra-aggregated pores [T^{-1}] (influx into the immobile region, corresponding to outflux from the mobile region). S_{mo} and S_{im} are sink terms for the respective region [T^{-1}], e.g., accounting for root water uptake. In the current HYDRUS-1D version (4.17), S_{im} is assumed to be zero. The transfer rate can be described as (Gerke and van Genuchten, 1993; Šimůnek et al., 2003, 2001):

$$\Gamma_w = \omega_w \left(S_{e,mo} - S_{e,im}\right) \tag{5.6}$$

with ω_w the first-order rate coefficient for water transfer between the immobile and mobile phase [T^{-1}]. $S_{e,mo}$ and $S_{e,im}$ are effective fluid saturation in the inter- and intra-aggregate region (mobile and immobile zone), respectively [-]. The intra-aggregate region is characterized by the immobile residual and saturated water content, $\theta_{im,r}$ and $\theta_{im,s}$, respectively [L^3 L^{-3}] (Šimůnek et al., 2001). For the inter-aggregate region, the van Genuchten-Mualem model is applied (Eq. 2.1 and 2.2), however now referring to the mobile zone: with $\theta_{mo,r}$ and $\theta_{mo,s}$ (residual and saturated water content of the mobile zone) replacing θ_r and θ_s of the SP setup. Thus, in the dual-porosity setup, three fitting parameters ($\theta_{im,r}$, $\theta_{im,s}$ and ω_w) were considered in addition to the five fitted SHP ($\theta_{mo,r}$, $\theta_{mo,s}$, α, n and K_s). $\theta_{mo,r}$ was set to be zero, so that residual water is only present in the immobile region, as suggested in comparable studies (e.g., Diamantopoulos et al., 2012; Köhne et al., 2002; Šimůnek et al., 2001).

5.2.3.3 Root water uptake, transpiration and leaf area index

Root water uptake was simulated within HYDRUS-1D using the model of Feddes et al. (1978). Transpiration needed to be set separately as boundary condition, so that it was estimated from measured ETa by applying Beer's law (Ritchie, 1972). Parameters of the Feddes model were adjusted for avoiding alteration of transpiration. Maize root growth (rooting depth) and leaf area index as a function of time were estimated for each growing season (assuming logistic growth), outside of HYDRUS-1D in an excel spreadsheet, and set as boundary conditions within HYDRUS-1D. Furthermore, interception (due to the intermediate storage of precipitation water on the plant canopy) was considered within HYDRUS-1D for correcting infiltration. Further details on procedures and assumptions are given in the Chapters B1-B3 and Table B-3. We assumed that no fractionation of stable water isotopes occurred due to root water uptake (Groh et al., 2018; Stumpp et al., 2012).

5.2.4 Stable water isotope transport

Tracer transport can be simulated using the advection-dispersion equation for the unsaturated zone (e.g., Fetter, 1999; Leibundgut et al., 2009):

$$\frac{\partial(\theta c)}{\partial t} = \frac{\partial}{\partial z}\left(\theta D \frac{\partial c}{\partial z}\right) - \frac{\partial(qc)}{\partial z} - \phi \tag{5.7}$$

where c is concentration of a dissolved compound [M L^{-3}], D the dispersion coefficient that can account for molecular diffusion and hydrodynamic dispersion [L^2 T^{-1}], and q the volumetric fluid flux [L T^{-1}]. ϕ is the sink-source term, which, e.g., can consider plant uptake [M L^{-3} T^{-1}]. For the DP setup, stable water isotope transport can described as follows (Šimůnek and van Genuchten, 2008):

$$\frac{\partial(\theta_{mo} c_{mo})}{\partial t} = \frac{\partial}{\partial z}\left(\theta_{mo} D_{mo} \frac{\partial c_{mo}}{\partial z}\right) - \frac{\partial(q_{mo} c_{mo})}{\partial z} - \phi_{mo} - \Gamma_s \tag{5.8}$$

$$\frac{\partial(\theta_{im} c_{im})}{\partial t} = \Gamma_s - \phi_{im} \tag{5.9}$$

$$\text{with } \Gamma_s = \omega_s(c_{mo} - c_{im}) + \Gamma_w c^* \tag{5.10}$$

where D_{mo} is the dispersion coefficient in the mobile region [L^2 T^{-1}] and q_{mo} the volumetric fluid flux density in the mobile region [L T^{-1}]. ϕ_{mo} and ϕ_{im} is the sink-source term of the mobile and immobile region, respectively [M L^{-3} T^{-1}]. The term Γ_s describes solute mass transfer between the two regions [M L^{-3} T^{-1}], where ω_s is the mass transfer coefficient for solutes [T^{-1}] and Γ_w the mass transfer rate of water [T^{-1}]. c^* is solute concentration, which corresponds to mobile region concentration c_{mo} for $\Gamma_w > 0$ and immobile region concentration c_{im} for $\Gamma_w < 0$. ω_s is set to zero to presume that stable water isotopes are only transported by transfer, i.e. term $\Gamma_w c^*$ in Eq. 5.9, and not by diffusive exchange, term $\omega_s(c_{mo} - c_{im})$ (as similarly applied by Haws et al. (2005) for bromide transport).

For simulating stable water isotope transport in the lysimeters, a modified HYDRUS-1D version developed by Stumpp et al. (2012) was used, which prevents increasing stable water isotope contents in infiltrating water due to evaporation (also applied, e.g., Groh et al., 2018; Huang et al., 2015; Imig et al., 2022a; Sprenger et al., 2016b, 2016a, 2015). Passive root water uptake was assumed that does not lead to stable water isotope fractionation (in accordance, e.g., to Groh et al., 2018 and Stumpp et al., 2012). Thus, source-sink terms were set to zero for stable water isotope transport. For the upper boundary condition, stable water isotope contents in precipitation were considered (measured values for the observation period and values from Passau-Fürstenzell for the modelling pre-phase; cf. Shajari et al. 2020). This study focusses on the simulation of δ^{18}O. A constant offset (+23 ‰) was added to the δ^{18}O input and subtracted again from the modelling results, since positive numbers are needed for transport modelling (as similarly done by Sprenger et al. 2016a, Stumpp et al. 2012 and Imig et al., 2022a). As initial condition we have considered a δ^{18}O value of 2 ‰ for the entire soil profile, since no information were available for the modelling pre-phase (the initial conditions revealed no influence on the observation period). Fitting parameter for transport was longitudinal dispersivity α_L (with $\alpha_L = D/v$ for the SP setup and $\alpha_L = D_{mo}/v$ for the DP setup, where v is flow velocity).

5.2.4.1 *Stable isotope fractionation by evaporation*

For our study site, Shajari et al. (2020) found that regression line slopes of stable water isotope content in lysimeter discharge were close to the local meteoric water line, so that isotopic fractionation in drainage due to evaporation was assumed negligible. Nonetheless, in additional simulation scenarios, we investigated possible fractionation by evaporation (and thus increasing δ^{18}O in infiltrating water) using a HYDRUS-1D code modified by Zhou et al. (2021). This code includes a volatile solute boundary at the top, where the total fractionation factor is estimated according to Gonfiantini (1978). In the present study, this code was further modified to consider interception processes (cf. Chapter B2 in the Appendix B).

5.2.5 Parameter optimization

Flow and transport parameters for all scenarios were calibrated using the software PEST (Model-Independent Parameter Estimation, version 17.2; Doherty, 2020a and 2020b). For this task, Python scripts were set up for carrying out HYDRUS-1D executables and coupling to PEST. Observations of lysimeter drainage (Q), stable water isotope signature in drainage (δ^{18}O) and change in soil water storage (ΔSWS) were used as objective variables (same weight in the objective function). For parameter optimization, modelled δ^{18}O values were averaged over time periods of the measurements in order to obtain data pairs. Initial parameter values and parameter ranges were taken from literature, as summarized in Table B-4 and B-5.

Model performance was evaluated based on the Kling-Gupta Efficiency (KGE) as the main criterion. In addition, the root mean square error (RMSE), mean error (ME), coefficient of determination (R^2) and Kendall rank correlation coefficient (τ) were calculated. ΔSWS varied strongly between negative and positive values, which could not be handled for KGE determination: thus, a constant value of 100 kg was added for calculating KGE, leading to positive values (preventing both the variability error term and the bias term of becoming <1; cf. Knoben et al., 2019). Results of statistical evaluation are presented in Table 5-1 and Table A-6, regression plots for modelled versus measured δ^{18}O, Q and ΔSWS for all model setups are given in Figure B-2.

5.3 Results and Discussion

5.3.1 Flow and transport dynamics

Figure 5-1 shows measured versus modelled drainage rate Q and stable water isotope signature δ^{18}O in the outflow of Ly1 as a function of time. Obtained curve fits are similarly well for the SP and DP model setups (Table 5-1 and Table A-6). Seasonal dynamics of δ^{18}O were captured well by both approaches, however with underestimations in summer/autumn 2015 and slight overestimations in July-October 2014 (Figure 5-1b) Q was described reasonably well, too, with a KGE of 0.80 (Table 5-1). Concerning the change in soil water storage (ΔSWS), lower KGE was found for SP (0.58) than for DP (0.66) (Table 5-1, Figure B-1a). Overall, only slight improvements can be seen with the more complex DP setup, which considers exchange processes between immobile and mobile water. When considering potential effects of evaporation fractionation (EF) on δ^{18}O, slight improvements can be seen between June 2015 and March 2016, however there are also more pronounced overestimations (Aug. 2014 – May 2015, March – April 2016) and underestimations (April – July 2014; Figure 5-1b). Curve fits are slightly worse for δ^{18}O (cf. Table 5-1 for KGE).

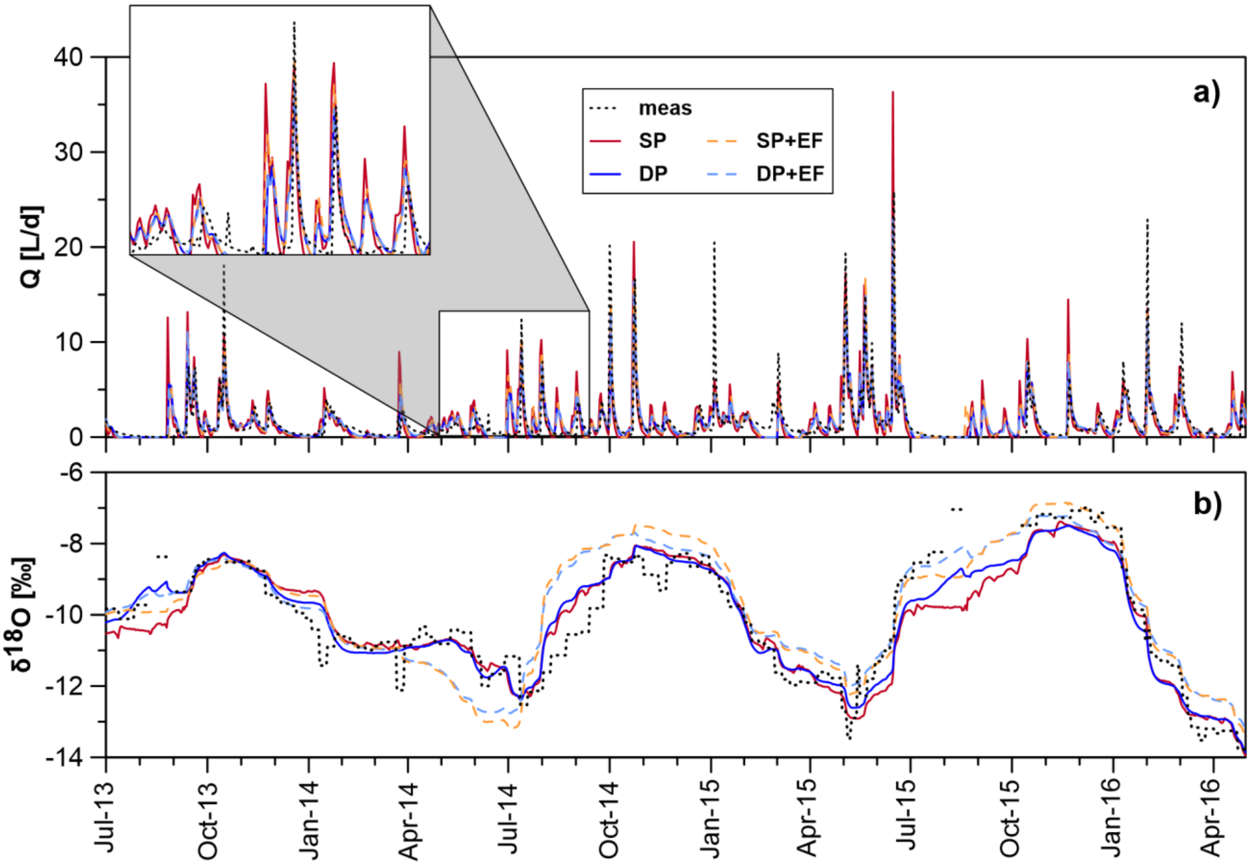

Figure 5-1. Measured and modelled a) discharge rate Q and b) $\delta^{18}O$ in the drainage of lysimeter Ly1 considering single-porosity (SP) and dual-porosity (DP) model setups. EF indicates the combination with evaporation fractionation.

Table 5-1. Statistical evaluation of model curve fits using KGE (Kling-Gupta Efficiency) for the different model setups in lysimeters Ly1 and Ly2 (SP: single porosity, DP: dual porosity; EF indicates the combination with evaporation fractionation). Q: drainage rate, $\delta^{18}O$: isotope signature in lysimeter outflow, ΔSWS: change in soil water storage. Colours indicate statistical performance, with green: good, yellow: intermediate and red: poor.

KGE [-]	Ly1		Ly2	
	SP	SP+EF	SP	SP+EF
Q	0.80	0.83	0.74	0.75
$\delta^{18}O$	0.89	0.85	0.01	0.21
ΔSWS	0.58	0.67	0.45	0.46
	DP	DP+EF	DP	DP+EF
Q	0.80	0.85	0.73	0.70
$\delta^{18}O$	0.89	0.88	0.42	0.14
ΔSWS	0.66	0.67	0.45	0.53

Fitted soil hydraulic parameters (SHP) and α_L are summarized in Table 5-2. Values of θ_s between 0.20 and 0.35 cm^3/cm^3 for Ly1 correspond to ranges of 0.21–0.64 cm^3/cm^3 found for sandy gravels by Sprenger et al. (2015) and Stumpp et al. (2009b). For fitted α_L (0.12–0.5 cm), values are in agreement with ranges between 0.13 and 0.46 cm found by Thoma et al. (2014) for coarse sand and gravel alluvial sediments. For saturated hydraulic conductivity K_s, the fitted value of 6040.2 cm/d corresponds to findings from Thoma et al. (2014) with 1555–42595 cm/d and Freeze and Cherry (1979) with 864–86400 cm/d. Concerning the DP setup, Morvannou et al. (2008) used HYDRUS-1D for simulating unsaturated flow in the subsurface of constructed wetlands. For gravel filters, they found lower ω_w (0.005 compared to 0.06 1/d for Ly1), higher $\theta_{im,r}$ (0.34 versus 0.001–0.007 cm^3/cm^3 for Ly1) and higher $\theta_{im,s}$ (0.36 versus to 0.06 cm^3/cm^3 for Ly1).

The low residual water content we found for the mobile and immobile region (θ_r and $\theta_{im,r}$, respectively) indicates a limited influence of immobile water in Ly1. This also relates to the comparatively small change when extending from SP to DP. Such small differences might be explained with the soil properties: in sandy gravel, wide pores are likely to predominate and hence there are fewer fine pores for water storage, resulting in small immobile water fractions.

Table 5-2: Calibrated parameter sets for modelling water flow and stable water isotope transport in lysimeters Ly1 and Ly2 considering single-porosity (SP), dual-porosity (DP) and combinations with isotopic fractionation due to evaporation (EF).

	θ_r if SP $\theta_{mo,r}$ if DP [cm^3/cm^3]	**θ_s if SP $\theta_{mo,s}$ if DP [cm^3/cm^3]**	**α [1/cm]**	**n [-]**	**K_S [cm/d]**	**$\theta_{im,r}$ [cm^3/cm^3]**	**$\theta_{im,s}$ [cm^3/cm^3]**	**ω_W [1/d]**	**α_L [cm]**
Ly1									
SP	0.0046	0.25	0.50	1.31	6040.2	-	-	-	8.6
DP	0	0.22	0.12	1.38	6040.2	0.001	0.06	0.06	8.0
SP+EF	0.0051	0.35	0.12	1.66	6040.2	-	-	-	9.5
DP+EF	0	0.20	0.16	1.28	6040.2	0.007	0.06	0.02	13.5
Ly2									
SP	0.01	0.35	0.005	1.8	32.5	-	-	-	172
DP	0	0.16	0.007	2.0	80	0.005	0.19	4.99	80
SP+EF	0.005	0.25	0.005	2.0	30	-	-	-	140
DP+EF	0	0.17	0.005	1.45	33	0.043	0.38	0.62	57

Figure 5-2 shows observations and simulations for Ly2. Curve fits of δ^{18}O were much better with the DP setup, compared to SP (KGE of 0.42 versus 0.01, Table 5-1). Seasonal periodicity of δ^{18}O is depicted more accurately with DP, however there are stronger underestimations compared to the SP setup (Figure 5-2b). Fluctuations are less damped, with more pronounced minima. Drainage (Q) and change in soil water storage (ΔSWS) as a function of time could be described similarly well (Figure 5-2a and Table 5-1, Figure 5-1b). In total, the DP setup reveals a clear improvement compared to SP (cf. Table 5-1).

Consideration of EF resulted in an δ^{18}O upshift. Underestimations could be reduced from July 2013 to July 2014, however considerable overestimations occur between July 2014 and March 2016 (Figure 5-2b). Curve fits improved for SP+EF versus SP, however there were no improvements for DP+EF versus DP, except for ΔSWS (Table 5-1).

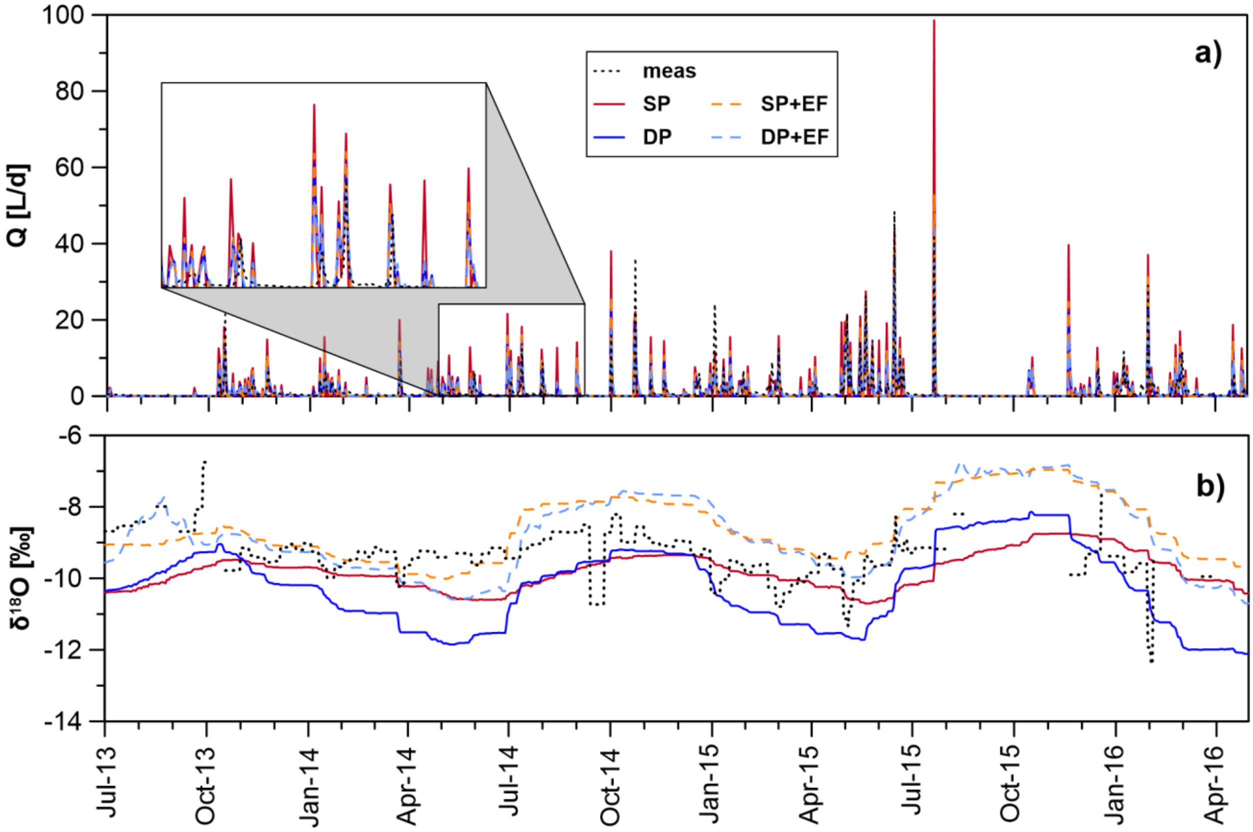

Figure 5-2: Measured and modelled a) discharge rate Q and b) $\delta^{18}O$ in the drainage of lysimeter Ly2 considering single-porosity (SP) and dual-porosity (DP) model setups. EF indicates combination with evaporation fractionation.

For Ly2, fitted parameters from applying DP were in better agreement with literature values compared to the SP setup. Longitudinal dispersivity α_L was higher for SP (172 cm) than for DP (80 cm) (Table 5-2). This is consistent with findings of Robin et al. (1983), who found lower dispersivity values when including immobile water in their model setup. In the DP setup, solute dispersion is covered both via the dispersion term (parameter α_L) and solute exchange between the mobile and immobile region, while it is solely covered via the dispersion term in the SP setup (Glaesner et al., 2018). Longitudinal dispersivity α_L was found to decrease from SP to SP+EF and further to DP and DP+EF setup for Ly2 (172, 140, 80 and 57 cm). This might be an indication that exchange with immobile water and/or evaporation fractionation were contributing to dispersion effects in DP and “+EF” setups, whereas dispersion was covered mainly by α_L in the SP setup. Vanderborght and Vereecken (2007) reported α_L values between 149 and 481.1 cm for ponding conditions in soil core and field experiments with loam and clayey loam soils.

Fitted values of (mobile) saturated, immobile saturated and residual water contents (Table 5-2) are similar in magnitude with findings for loamy soils obtained by Diamantopoulos et al. (2012) and Köhne et al. (2004). Total saturated water content for DP ($\theta_{s,total}$ = $\theta_{mo,s}$ + $\theta_{im,s}$ = 0.35 cm^3/cm^3) is within the range of 0.26-0.54 cm^3/cm^3 reported for similar soils (Diamantopoulos et al., 2012; Graham et al., 2018, Hupet et al., 2003; Köhne et al., 2004; Sprenger et al., 2018). In contrast, $\theta_{s,total}$ fitted with the DP+EF setup (0.55 cm^3/cm^3) is on the upper end of this range.

In additional model runs for Ly1 and Ly2, different weighting of the three observation variables, within the objective function, were compared during the calibration process with PEST. Statistical evaluation of model performance did not improve when weighting the observation variables differently. When giving ΔSWS a higher weight, fitted parameters resulted in a comparable decrease in statistical evaluation of model performance than if Q or $\delta^{18}O$ were given a higher weight.

5.3.2 Effects of soil properties, immobile water and evaporation fractionation

Stable water isotope content in the drainage is stronger damped in Ly2 than in Ly1 (Figure 5-1b versus Figure 5-2b). Climatic conditions and cultivation management were the same for both lysimeters, so that differences in the isotopic signal could be explained by the different soil properties. As a possible explanation, the larger dampening of $\delta^{18}O$ fluctuation in Ly2 can correspond to a higher portion of finer pores, which are available for water storage. This can lead to the mixing of isotopically heavier summer precipitation water with lighter winter water (Gazis and Feng, 2004), resulting in $\delta^{18}O$ reductions.

Differences in simulated $\delta^{18}O$ (lysimeter discharge) between SP and DP were more pronounced for Ly2, than for Ly1 (Figure 5-2b versus 5-1b). This is likely related to the influence of immobile water and soil properties during percolation. Stable water isotopes in precipitation show seasonal variation, with higher $\delta^{18}O$ values in summer when evaporation is most intensive (lighter stable water isotopes are preferred for evaporation). When infiltrated, isotopically heavier summer water can be retained in immobile regions of the lysimeters. It can remobilize and mix with isotopically lighter winter water, thus causing an isotopic upshift in the drainage. Due to the predominance of finer pores in Ly2 (sandy clayey silt), stable water isotopes transport is slower than in Ly1 (sandy gravels). Higher residence times of water in Ly2 thus might lead to more intense remobilization of immobile water and thus increased mixing (eventually leading to isotopic shifts in drainage water).

Considering evaporation fractionation (EF) of infiltrating precipitation water, as an additional process, also had a stronger influence in Ly2 than in Ly1 (Figure 5-1b versus 5-2b, “+EF” curves of simulated $\delta^{18}O$). Interestingly, the $\delta^{18}O$ upshift in Ly2 due to EF consideration was seasonally (~Dec. –May) more pronounced for DP than for SP. This supports the assumptions discussed above, concerning pronounced influences of immobile water on d $\delta^{18}O$ observed in Ly2 outflow. Results demonstrate, however, that accounting for EF had no clear improvement on the simulation of stable water isotopes in the drainage of the two lysimeters, where the most plausible setups are SP and DP for Ly1 and DP for Ly2.

As often expected for silt soils, strong short-term fluctuations may indicate the presence of preferential flow (see Figure 5-2a). On 21 July 2015, a drainage peak of Q = 41.68 L/d was measured, which coincides with an accidental release of water (102.64 L) from a hose placed at Ly2. This peak was more closely modelled with the DP setup (31.90 L/d) than with the SP setup (17.75 L/d), indicating that DP could account for such rapid flow events more accurately. Similarly, Jiang et al. (2010) were able to describe the fast response of drainage via macropores (preferential flow paths) on flood irrigation better by the DP than the SP setup.

Dual-permeability models are often used to mimic preferential flow, as they can provide more flexibility (Köhne et al., 2009a, 2006b). In such models, the hydraulic system is assumed to have different flow domains (matrix and preferential flow), in comparison to one flow domain in the DP setup, where the immobile phase stagnates and can only exchange with the mobile phase (J. Šimůnek et al., 2008). A dual-permeability model setup may thus be better suited to account for the influence of preferential flow. It could not be applied in this work, however, since dual-permeability setups are not yet implemented in currently available versions of HYDRUS-1D for simulating stable water isotope transport (namely in the versions of Stumpp et al., 2012, and Zhou et al., 2021). We recommend investigating this aspect in future works.

A major restriction inherent to the present study is the lack of measurements within the soil profile, such as soil water contents, pressure heads and stable water isotope contents. By prior determination of some parameters based on measurements (e.g., SHPs and dispersivity), the calibration of more complex flow and transport models, involving physical- and chemical-nonequilibrium assumptions, could potentially be accomplished with lower uncertainty. Groh et al. (2018) showed in an inverse modelling study that combining measured flow and transport parameters with tracer data in the objective functions improved model prediction as well as SHP determination. Therefore, additional measurements are recommended for future studies.

Moreover, dual tracer experiments can allow the experimental investigation of a second porosity system. Using two tracers characterized by different diffusion coefficients can give hints on the contribution of diffusion processes, such as diffusive exchange between the mobile and the immobile zone. Such an approach recommended for future experimental investigations.

5.4 Summary and Conclusion

This study allowed the evaluation of various flow and stable water isotope transport processes within two cropped lysimeters. For an inverse modelling process, three objective variables were included into the objective function: (i) lysimeter drainage (Q), (ii) stable water isotopes signature in the drainage water (δ^{18}O), and (iii) the change in the soil water storage (ΔSWS), calculated based on lysimeter weight change.

When applying a single-porosity (SP) model setup within HYDRUS-1D, simulations of transient unsaturated water flow and transport of stable water isotopes yielded plausible results for the sandy gravel soil core of Ly1. The extension to a dual-porosity (DP) setup showed similar model performance. In contrast, for Ly2 filled with clayey sandy silt, the DP setup yielded considerably better results than SP.

Since climatic and cultivation management conditions were the same for both lysimeters, soil properties are identified to be the driving factor in flow and transport of stable water isotopes in the unsaturated zone. For Ly2, the consideration of immobile water (DP setup) yielded better performance. This could be related to a higher portion of fine pores in Ly2 than in Ly1, allowing higher water storage and immobile water formation. For Ly2, the presence of immobile water could explain the damping of the stable water isotope signal in the drainage. Immobile water can retain isotopically enriched (heavier) summer water or lighter winter water, which can remobilize and mix with the mobile water phase. As a result, the mixed water has a less pronounced amplitude in the isotope signature and hence is damped. Further the consideration of evaporation fractionation (EF) was investigated. EF effects led to enrichment of heavier isotopes in water as lighter isotopes tend to evaporate causing an upshift in the measured isotope content in the drainage. However, the DP+EF setup achieved less plausible δ^{18}O simulations than the DP setup, indicating that dampening of the seasonal δ^{18}O signal in the lysimeter drainage of Ly2 may mainly be related to mechanical dispersion and the mixing of water between mobile and immobile regions, instead of EF effects.

The consideration of multi-process modelling to describe water flow and solute transport in the vadose zone is a helpful tool to identify dominant processes and should be an integral part of model calibration. Findings of this study will help modellers and decision makers to identify the contamination potential on groundwater resources and to identify risks to soil and groundwater systems.

Chapter 6 Fate of herbicides in cropped lysimeters: 2. Leaching of four maize herbicides considering different model setups

These chapters include the following publication, with some modifications: Imig, A., Augustin, L., Groh, J., Pütz, T., Elsner, M., Einsiedl, F., Rein, A., (under review, b) Fate of herbicides in cropped lysimeters: 2. Leaching of four maize herbicides considering different model setups. Vadose Zone Journal

A statement from the doctoral candidate concerning her contribution to publications was submitted within the framework of a publication-based dissertation, together with a statement of confirmation from the co-authors according to Article 7, section 3, clause 2 of the TUM Doctoral Regulations (PromO) was submitted along with the publication. Chapter 6.2.2, compound specific isotope analysis (CSIA) and 6.5.4, investigation of biodegradation influences related to the interpretation of the stable carbon isotopes, were not drafted, only edited by Anne Imig.

Anne Imig did neither collect nor analyse samples taken at the study site. Stable water isotopes in precipitation and lysimeter drainage were analysed at the Chair of Hydrogeology at TUM. The Bavarian Environment Agency (Bayerisches Landesamt für Umwelt, LfU) collected meteorological data, water samples from precipitation and lysimeter drainage and measured lysimeter drainage rates, lysimeter weight, herbicide concentration in lysimeter drainage and applied solution. Compound specific isotope analysis for herbicide carbon isotopes was conducted at the Institute of Groundwater Ecology, Helmholtz Zentrum München (Armin Meyer, Martin Elsner).

Abstract

This study investigates the contamination potential of herbicides to groundwater with help of numerical modelling (HYDRUS-1D). Four herbicides, metolachlor, terbuthylazine, prosulfuron and nicosulfuron, were applied over a period of 4.5 years on two lysimeters located in Wielenbach, Germany, and monitored in lysimeter drainage. These lysimeters contained soil cores dominated by sandy gravel (Ly1) and clayey sandy silt (Ly2) and were both cropped with maize. In the preceding study (Imig et al., under review, a), we characterized flow within the lysimeters by using stable water isotopes and unsaturated flow models. Building up on these findings, models were extended for describing reactive transport of the herbicides and investigating the contribution of different processes on chemical fate. At the end of the experiment, 0.9-15.9% of applied herbicides (up to 20.9% if including metabolites) were recovered in lysimeter drainage. Metabolite formation and accumulation was observed, and the presence of biodegradation was also indicated by small changes in carbon isotope signals ($\delta^{13}C$) between applied and leached herbicides. Model setups could describe the dynamics of herbicide concentrations in lysimeter drainage, well. Concentration peaks in drainage were partly also linked with strong precipitation events, indicating an

influence of preferential flow. The soil core with the coarser texture (Ly1) showed less herbicide leaching than the finer texture (Ly2), which can be explained by a larger mobile phase in Ly1. Overall, our approaches and findings contribute to the understanding of multi-process herbicide transport in the vadose zone and leaching potentials to groundwater.

6.1 Introduction

Maize is one of the most important crops worldwide and the second-most cultivated cereal in the European Union (EU). In the EU, 8.7 million ha were cultivated for grain maize and 6.2 million ha for silage (green) maize in 2020 (Eurostat, 2022a, 2022b). More than 90 % of this area is estimated to be treated with pesticides to prevent crop disease and secure higher crop yields (Meissle et al., 2010). Metolachlor, terbuthylazine, nicosulfuron and prosulfuron are among the typical pesticides used on maize cultivation. Pesticides have been substantial in increasing living standards for the growing population worldwide battling hunger and famine (Syafrudin et al., 2021). Besides these positive effects, however, pesticide loss from fields have become an increasing concern. Furthermore, research has highlighted adverse effects including human health risks of agricultural chemicals (e.g., Genuis et al., 2016; Nicolopoulou-Stamati et al., 2016; Trapp and Matthies, 1998), and environmental risks (Arias-Estévez et al., 2008; Ikoyi et al., 2018; Michel et al., 2021). Often, groundwater concentrations of single pesticides and their metabolites exceed the drinking water threshold of 0.1 $\mu g L^{-1}$ (e.g., Delgado-Moreno and Peña, 2007; European Council, 1998; Guzzella et al., 2006; Toccalino et al., 2014).

Physicochemical and subsurface properties influence the retention of pesticides. Herbicides can, e.g., sorb to clay particles or organic matter (Cox et al., 1997; Köhne et al., 2006a; Weber et al., 2000), and degradation processes can influence the fate of pesticides in the subsurface (Barra Caracciolo et al., 2005; Carabias-Martínez et al., 2002; Jaikaew et al., 2017; Vischetti et al., 1998). Additionally, preferential flow can have substantial influence as it may induce concentration peaks in leachate water, which have been documented after strong precipitation events following pesticide application (e.g., Benettin et al., 2019; Isch et al., 2019; Radolinski et al., 2021). In addition, plants can actively influence soil interactions with water and herbicides through, for example, uptake of solutes or microbial transformation processes (e.g., An et al., 2022; Rein et al., 2011; Trapp and Matthies, 1998). A detailed knowledge on the fate of pesticides in the subsurface and their inter-dependencies is a prerequisite for the development of effective methodologies for risk assessment and control of agricultural chemical pollution (e.g., Fantke et al., 2013; Köhne et al., 2009; Michel et al., 2021; Syafrudin et al., 2021).

The combination of experimental data and modelling can be a powerful tool to predict and identify the influence of herbicide transport and fate processes (e.g., Groh et al., 2020; Rein et al., 2011; Stumpp et al., 2009). Limited field experimental and modelling studies of pesticide fate are available to date that combine a multitude of processes such as plant uptake, biodegradation or immobile water in HYDRUS-1D. Sidoli et al. (2016) investigated the transport of metolachlor and two of its metabolites with column experiments combined with numerical modelling in HYDRUS-1D for glaciofluvial soils. Water flow parameters and retardation factors were determined, and the authors found a strong influence of immobile water and soil texture on the transport of metolachlor. Köhne et al. (2006) compared available model setups in HYDRUS-1D for simulating bromide, isoproturon and terbuthylazine transport in loamy and sandy soil in laboratory experiments. Best results were obtained when considering immobile water, preferential flow, and non-linear sorption processes.

As an experimental method, Compound Specific Isotope Analysis (CSIA) permits the identification of degradation processes by analysing environmental stable isotopes. During (bio-) degradation processes the ratio of stable isotopes will often change and thus allows determining the extent of biodegradation (Elsner and Imfeld, 2016; Hunkeler et al., 2008). To date, a limited number of field scale studies investigate CSIA as a method to assess biodegradation of contaminants in the unsaturated zone (e.g., Bouchard et al., 2011, 2008; Torrentó et al., 2021, 2015).

In this work we aim at contributing to a better understanding of transport and fate of four frequently applied herbicides (metolachlor, terbuthylazine, prosulfuron and nicosulfuron) in the unsaturated zone and potential impacts to groundwater. We combine observations at lysimeters and numerical modelling approaches to describe herbicide transport and to determine possible influences of sorption, interaction with immobile water, biodegradation and plant uptake in the unsaturated zone of two cropped lysimeters in Wielenbach, Germany. Results of different multi-process model setups in HYDRUS-1D are compared. Modelling is based on our preceding work (Imig et al., under review, a), where we investigated different model setups for describing unsaturated water flow in the lysimeters with help of stable water isotopes ($\delta^{18}O$). These flow models are extended by reactive transport. Between May 2013 and November 2017, the herbicides were applied to the lysimeters, and concentrations of herbicides and their metabolites were monitored in lysimeter drainage water. Our main research goals include 1) to investigate metabolite concentrations and stable carbon isotope fractionation to improve understanding of biodegradation processes, 2) to identify the dominant processes of herbicide transport and the influence of the soil properties and 3) to estimate sorption and biodegradation parameters by inverse modelling.

6.2 Materials and Methods

6.2.1 Study site and observations

We investigated two lysimeters run by the Bavarian Environmental Agency located in Wielenbach, Germany (549 m asl). Lysimeter 1 (Ly1) is filled with sandy gravel soil and Lysimeter 2 (Ly2) with clayey, sandy silt soil. Detailed grain size distributions and soil origins as well as information on maize cultivation on lysimeters are given in in the preceding paper by Imig et al. (under review, a). The four herbicides metolachlor (MTLC), terbuthylazine (TBA), nicosulfuron (NCS) and prosulfuron (PS) were applied with a commercial pressure sprayer, product Wingart DSG 1,5 Classic. MTLC and TBA were applied yearly, PS and NS irregularly (Table 6-1). Herbicide concentrations were monitored on a weekly basis in lysimeter drainage between May 2013 and November 2017. Measurements were carried out with a high-performance liquid chromatography (HPLC) using tandem mass spectrometric (MS/MS) detection with direct injection (detection limit: 0.01 – 0.03 µg/l). While in the weeks following the application, sampling in drainage took place at the highest possible resolution, the sampling frequency was reduced to about two weeks thereafter, depending on the amount of available discharge. Fertilizer management was done according to good agricultural practice. Monitoring included two metabolites of MTLC (metolachlor ethanesulfonic acid and metholachlor oxanillic acid) and four metabolites of TBA (Desethyl-terbuthylazin, hydroxy-terbuthylazine, terbuthylazin 1 SYN 545666 and terbuthylazin 2 CGA 324007). Physicochemical properties and descriptions of the compounds are given in Table B-1 in the Appendix B.

Table 6-1: Applied herbicide amounts and concentration in applied solution (based on Strauß and Bayer, 2017) and calculated recovery rate (RR) in the drainage of lysimeters Ly1and Ly2 at the end of experiment (10 November 2017). RR, numbers in brackets: metolachlor plus two metabolites, terbuthylazine plus four metabolites.

Substance	**CAS number**	**Applied amount [mg/m^2] (in brackets: concentration in applied solution [g/L])**					**RR [%]**	
		28 May 2013	06 June 2014	03 June 2015	15 June 2016	01June 2017	Ly1	Ly2
Metolachlor	51218-45-2	46.1 (0.69)	117.3 (1.76)	96.0 (1.44)	81.0 (1.22)	70.0 (1.05)	0.9 (12.8)	1.8 (20.9)
Terbuthylazine	5915-41-3	33.2 (0.50)	80.7 (1.21)	78.0 (1.17)	45.0 (0.68)	30.0 (0.45)	1.8 (2.5)	1.3 (2.5)
Nicosulfuron	111991-09-4	7.6 (0.11)	-	-	5.1 (0.08)	5.6 (0.08)	5.3	15.9
Prosulfuron	94125-34-5	-	-	2.5 (0.04)	1.7 (0.03)	1.4 (0.02)	2.1	2

6.2.2 Compound specific isotope analysis (CSIA)

Sampling for compound-specific isotope analysis (CSIA) included (i) the herbicide solution prepared for application and (ii) lysimeter drainage. Samples from the herbicide solution were taken on 3rd June 2015, directly before herbicide application (4 replicates, 100 mL collected in glass vials with screw caps equipped with teflon-coated butyl septa). Drainage was collected at both lysimeters in 2 L aluminium bottles with plastic caps. This was done (i) before herbicide application at 21 May 2015, (ii) 19 days after application (22 June 2015) and (iii) about 7.5 months after application (8 January

2016). Water volumes of 10-12 L were sampled for Ly1 and Ly2, each, at the three sampling campaigns. Samples were frozen directly after sampling.

Subsequently, samples were extracted according to the protocol of Schreglmann et al. (2013). Solid phase extraction discs (Bakerbond Speedisk H_2O -Philic DBV; J.T. Baker, Phillipsburg, USA) were conditioned with ethylacetate, dichloromethane and methanol and dried for 90 seconds. The samples were loaded with a flow rate of 0.1 L min^{-1}, followed by a drying time of 30 minutes. The sorbed analytes were eluted with ethylacetate (once) and dichloromethane (twice) for each 90 seconds followed by 90 seconds air dry time. After complete evaporation of the solvent in the extract, analytes were redissolved in 100 µL of ethyl acetate for subsequent isotope analysis.

Stable carbon isotope values ($\delta^{13}C$) of MTLC and TBA were analysed. The goals were to investigate short- and long-term changes in $\delta^{13}C$ values, as evidence of biodegradation under the influence of preferential flow and matrix flow. Stable carbon isotope analysis was conducted using gas chromatography coupled to isotope ratio mass spectrometry (GC/IRMS) according to a method modified from Reinnicke et al. (2012) and Schreglmann et al. (2013). The system consisted of a TRACE GC Ultra gas chromatograph (Thermo Fisher Scientific, Milan, Italy) coupled with a Finnigan MAT 253 isotope ratio mass spectrometer (IRMS; Thermo Fisher Scentific, Bremen, Germany). The instrument was operated with a helium carrier gas (grade 5.0) at a flow rate of 1.4 mL min^{-1}. One microliter of ethyl acetate extract was injected with a Combi PAL autosampler (CTC Analytics, Zwingen, Switzerland) in a split/splitless injector operated for 1 min in splitless mode and then in split mode with a split flow of 50 mL min^{-1} at a temperature of 230 °C. Helium was used as carrier gas at constant pressure (200 kPa). The gas chromatograph was equipped with a 60 m × 0.32 mm Rxi-5ms column (1 µm film thickness, Restek). The oven temperature program started at 60°C (1 min). Then the temperature was increased by 20 °C min^{-1} from 60 to 175 °C, where it was held for 7 minutes, and subsequently with 15 °C min^{-1} to 280 °C where it was held for 9 minutes. The peak identification was based on retention times in comparison with external standards. The GC/IRMS system and data collection were controlled using Isodat 3.0 software (Thermo).

6.3 Recovery rate determination

Recovery rates (RR) of the herbicides and their metabolites [%], between application concentration (input) and concentration in drainage water (output), were calculated as described in the following. Differences between input and output can be related to processes within the subsurface (including advection and dispersion, sorption, plant uptake, biodegradation) and also to chemical loss by wind drift during application. Based on windspeeds between 2.6 and 4.6 m/s at the application dates (Table B-2), an average spray loss of 4% was assumed based on tabulated values by van de Zande et al. (2007). RR was calculated as RR = m_{out} / m_{in}, where m_{in} is the applied amount of herbicide (Table B-1) referred to lysimeter surface area (1 m^2) and m_{out} is the mass of herbicide (with or without metabolites) recovered in lysimeter drainage:

$$m_{out} = \int_{o}^{t_{end}} F(t)\, dt = \int_{o}^{t_{end}} Q(t) \times c(t)\, dt \tag{6.11}$$

where $F(t)$ is chemical mass flux [M T^{-1}], $Q(t)$ lysimeter drainage rate [L^3/T] and $c(t)$ chemical concentration [M L^{-3}] as a function of time *t* and t_{end} is the end of the observation period. The integral in Eq. (6.1) was solved by using trapezoidal approximation, considering measured concentrations (weekly in average, see above) and the corresponding drainage rates.

6.4 Flow and transport modelling

In the preceding paper Imig et al. (under review, a), flow models for both lysimeters were set up and calibrated within HYDRUS-1D. Best-suited model setups were selected and extended by reactive herbicide transport, as described in the following.

6.4.1 Single-porosity model

For Ly1, both the single-porosity (SP) and dual-porosity (DP) flow model setups revealed plausible results (cf. our preceding paper Imig et al., under review, a). Since the DP setup is more complex and thus associated to higher uncertainties (no measurements within the soil columns were possible for model calibration), the SP setup was chosen for Ly1. It was extended by the equilibrium model (uniform transport) using the standard advection-dispersion equation for the vadose zone (Šimůnek and van Genuchten, 2008):

$$\frac{\partial(\theta c)}{\partial t} + \rho \frac{\partial s}{\partial t} = \frac{\partial}{\partial z}\left(\theta D \frac{\partial c}{\partial z}\right) - \frac{\partial(qc)}{\partial z} - \phi \tag{6.12}$$

where c is the concentration of a dissolved compound [M L^{-3}], θ is soil water content [L^{3}L^{-3}], q is the volumetric flux density [LT^{-1}] and D is the dispersion coefficient, which accounts for molecular diffusion and hydrodynamic dispersion [L^{2}T^{-1}]. For s as the sorbed concentration [MM^{-1}], we considered linear equilibrium sorption with $s = K_D c$, where K_D is the soil to water partition coefficient [L^{3}M^{-1}]. Φ is the source/sink term, where we considered first-order decay and passive chemical plant uptake with $\phi = \mu\theta c + p_a$, where μ is the first-order degradation rate constant [T^{-1}], and p_a is the rate of passive compound root uptake [ML^{-2}T^{-1}]. It can be described as a function of time over the entire root zone as follows (Šimůnek and Hopmans, 2009):

$$p_a(t) = S(h, x, t) \min[c(x,t), c_{max}] \tag{6.13}$$

with $S(h,x,t)$ the sink term defined for root water uptake [T^{-1}] (cf. preceding paper Imig et al., under review, a) and c_{max} a model control parameter associated to the maximum allowed compound concentration for passive uptake [ML^{-3}]. We assumed active plant uptake to be negligible for the considered herbicides. Therefore, to account for passive plant uptake only, maximum allowed concentration was chosen such that $c_{max} > c(x,t)$ at any point in the root zone domain. Parameters K_D and μ were fitted, using α_L found before (8.6 cm for Ly1, Imig et al., under review, a; with $\alpha_L = D/v$, where *v* is flow velocity).

6.4.2 Dual-porosity model

The DP flow model setup revealed more plausible for Ly2 (cf. Imig et al., under review, a). Considering DP, solute transport in the two regions (mobile and immobile region in physical nonequilibrium) can be described as follows (Šimůnek and van Genuchten, 2008):

$$\frac{\partial(\theta_{mo}c_{mo})}{\partial t} + f_{mo}\rho\frac{\partial s_{mo}}{\partial t} = \frac{\partial}{\partial z}\left(\theta_{mo}D\frac{\partial c_{mo}}{\partial z}\right) - \frac{\partial(q_{mo}c_{mo})}{\partial z} - \phi_{mo} - \Gamma_s \tag{6.14}$$

$$\frac{\partial(\theta_{im}c_{im})}{\partial t} + (1-f_{mo})\rho\frac{\partial s_{im}}{\partial t} = \Gamma_s - \phi_{im} \tag{6.15}$$

$$\Gamma_s = \omega_s\,(c_{mo} - c_{im}) + \Gamma_w c^* \tag{6.16}$$

where the indices *mo* and *im* designate the mobile and immobile region, respectively. $\Gamma_s$is the mass transfer rate of chemicals between the mobile and immobile region [M L^{-3} T^{-1}], where ω_s is the first-order chemical mass transfer coefficient [T^{-1}] , Γ_w the mass transfer rate of water [T^{-1}] and c^* the solute concentration [ML^{-3}], which is the mobile region concentration c_{mo} for $\Gamma_w > 0$ and the immobile region concentration c_{im} for $\Gamma_w < 0$ (Šimůnek and van Genuchten, 2008). D is the dispersion coefficient in the mobile region [L^{2}T^{-1}], q_{mo} the volumetric fluid flux density in the mobile region [LT^{-1}]. f_{mo} [-] is the fraction of sorption sites in contact with mobile water, which is assumed to be adequately described by the ratio $\theta_{mo,s}/\theta_s$ (following Nkedi-Kizza et al., 1983, and Köhne et al., 2006). θ_s the total saturated soil water content [L^{3}L^{-3}], obtained as the sum of saturated water content in the mobile ($\theta_{mo,s}$) and immobile ($\theta_{im,s}$) region.

ϕ_{mo} and ϕ_{im} are sink/source terms [$ML^{-3}T^{-1}$] of the mobile and immobile region, respectively, with $\phi_{mo} = \mu\theta c_{mo} + p_a$ (defined above) and ϕ_{im} set to 0 in the current HYDRUS-1D version (4.17) that was used in this study. Chemical equilibrium with linear sorption is considered for both regions, where sorption sites are divided in those being in contact with mobile water and those being in contact with immobile water:

$$s = (1 - f_{mo})s_{im} + f_{mo}s_{mo} = (1 - f_{mo})K_d c_{mo} + f_{mo}K_d c_{mo} = K_d c_{mo} \tag{6.17}$$

Thus, to simulate reactive solute transport with the DP setup, the three parameters K_D, μ and ω_s were fitted. The parameters f_{mo} and α_L were used according to our preceding study (Imig et al., under review, a), with $f_{mo} = \theta_{mo,s}/\theta_s$ = 0.16 / (0.16+0.19) = 0.31 and α_L= 57 cm for Ly2.

6.4.3 Initial and boundary conditions

For reactive transport in both model setups, a Cauchy type condition was applied at the upper boundary for describing chemical input (five inputs corresponding to pesticide application once a year, cf. Table 6-1). The concentration flux was defined from herbicide concentration in applied solution and water infiltration flux. The lower boundary condition of the lysimeters was specified as free drainage, assuming a zero-concentration gradient for the chemicals.

6.4.4 Parameter optimization

Transport parameters were inversely calibrated using the model-independent parameter estimation utility PEST developed by Doherty (2020a and 2020b). Soil hydraulic parameters (SHP) and longitudinal dispersivity were taken from our preceding study (Imig et al., under review, a). As objective variable, herbicide concentration in lysimeter drainage was used. To obtain data pairs (measured versus modelled), we averaged simulated concentrations over periods that correspond to those of the measurements. No measurements within soil columns were available for calibration (such as water contents, hydraulic heads or concentrations). Measurements on degradation or sorption parameters specific to the study site were not available, either, so that initial parameters and parameter ranges for the optimization were taken from literature for similar soils, as summarized in Table B-3. Model performance was evaluated based on the Kling-Gupta Efficiency (KGE) as the main criterion. In addition, the root mean square error (RMSE), mean error (ME), coefficient of determination (R^2) and Kendall rank correlation coefficient (τ) were calculated.

6.5 Results and Discussion

6.5.1 Reactive transport modelling

Fluctuation patterns of herbicide concentrations in lysimeter drainage were generally reproduced by modelling (Figure 6-1 and 6-2). For Ly1, peak concentrations tended to be underestimated (sometimes overestimated), with no clear pattern regarding application year or applied herbicide mass; concentration peaks were simulated slightly too late in 2016 and 2017 (Figure 6-1). KGE values close to zero indicate shortcomings in model performance for MTLC and TBA (Table 6-2).

For Ly2, the timing of herbicide peaks was generally covered well by modelling. Peaks were sometimes simulated too early, however without a clear pattern (e.g., MTLC in 2017, TBA in 2014 and 2017, NCS in 2013). No clear pattern could be identified for over- or underestimations of peak concentrations. For Ly2 the statistical evaluation indicates better model performance of MTLC and TBA than for Ly1 (Table 6-2). On 21 July 2015, a running water hose was accidentally located on top of Ly2, leading to the infiltration of 102.64 L of water. This event is related the highest measured herbicide concentrations in drainage for MTLC, TBA and PS in summer 2015 (Figure 6-1 and 6-2) and might have been induced by preferential flow.

It could be expected that with an increased application of herbicides, the intensity of leached herbicides in the drainage increases. However, neither for Ly1 nor Ly2 strong peaks for MTLC and TBA were observed after the application of the herbicides in the year 2014, even though applied amounts were high (Figure 6-1 and 6-2, Table 6-1). Furthermore, we could identify a relation between precipitation amounts after herbicide application and concentration peaks in lysimeter drainage for both lysimeters. In years with low precipitation amounts after herbicide application, lower peak concentrations were measured in drainage, e.g., in 2014 (22 mm of rain within 21 days after application) and 2017 (58 mm of rain within 21 days after application). In contrast, in years with high precipitation after application, high peaks were observed in drainage (such as 2013, with 170 mm of rain within 21 days after application). An exception is the “water hose accident” of 21 July 2015.

Both in Ly1 and Ly2, elevated NCS concentrations were observed in the first half of 2016 (Figure 6-1c and 6-2c). These could not be related to an application event of herbicides. Remobilization seems also not likely since such elevated concentrations (without prior application) only occurred once for NCS.

In a review, Köhne et al. (2009) compared different pesticide transport models and argued that a satisfactory prediction might be reached if the deviation between measured and modelled concentrations is around factor 3-5. They documented deviations by one or several orders of magnitude for blind validation studies. We reached factor 2-5, so that we may consider our fitting reasonably well.

Fitted biodegradation rate constants μ for Ly1 correspond well to those found in studies with similar soils for MTLC, TBA and NCS (e.g., Carretta et al., 2018; EFSA, 2007). Concerning the soil to water partition coefficient K_d, fewer observations were found for similar soils; ranges generally match our findings (Zsolnay,1994; cf. Chapter C1 in the Appendix C for details). More observations were found with soils similar to Ly2, where fitted K_d and μ correspond well to our findings (Marín-Benito et al., 2014 and Vischetti et al., 1998). The solute mass transfer rates ω_s found for Ly2 were in agreement with studies of Haws et al. (2005).

Table 6-2. Statistical evaluation of simulated herbicide concentration in the drainage of Ly1 and Ly2 (Kling-Gupta efficiency, KGE). Results are depicted in form of a heatmap (from green for good statistical performance to red for poor statistical performance).

	KGE [-], Ly1	**KGE [-], Ly2**
Metolachlor (MTLC)	-0.06	0.63
Terbuthylazine (TBA)	0.06	0.42
Nicosulfuron (NCS)	0.30	0.52
Prosulfuron (PS)	0.50	0.57

Table 6-3. Fitted parameters for reactive transport of metolachlor, terbuthylazine, nicosulfuron and prosulfuron.

	Lysimeter 1		**Lysimeter 2**	
Metolachlor (MTLC)	K_d [cm³/mg]	0.013	K_d [cm³/mg]	0.0002
	μ [1/d]	0.1	μ [1/d]	0.046
			ω_s [1/d]	0.026
Terbuthylazine (TBA)	K_d [cm³/mg]	0.01	K_d [cm³/mg]	0.023
	μ [1/d]	0.08	μ [1/d]	0.057
			ω_s [1/d]	0.035
Nicosulfuron (NCS)	K_d [cm³/mg]	0.037	K_d [cm³/mg]	0.0003
	μ [1/d]	0.055	μ [1/d]	0.019
			ω_s [1/d]	0.005
Prosulfuron (PS)	K_d [cm³/mg]	0.00009	K_d [cm³/mg]	0.00004
	μ [1/d]	0.025	μ [1/d]	0.02
			ω_s [1/d]	0.003

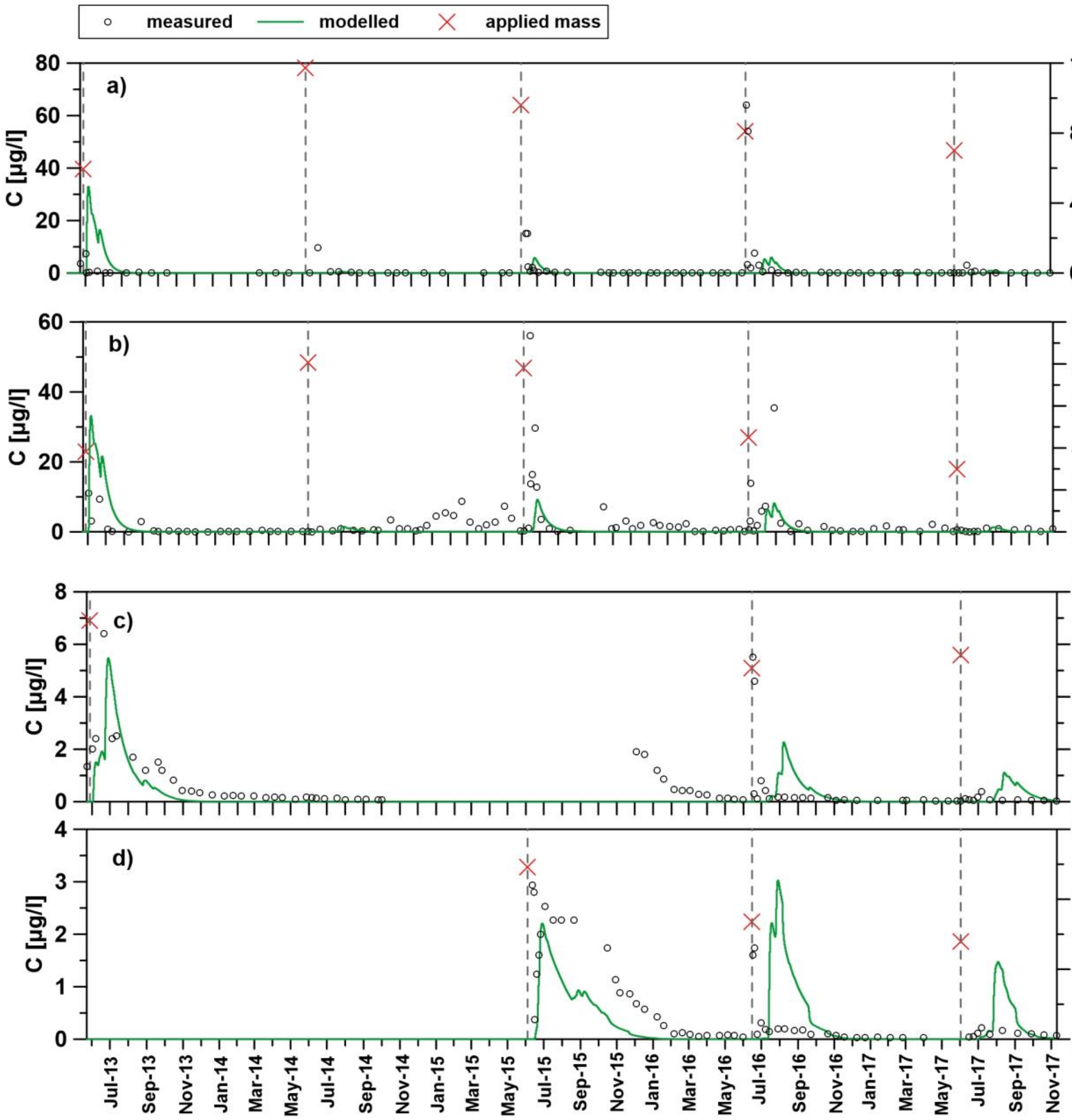

Figure 6-1. Measured (black circles) and modelled (green lines) herbicide concentration of a) metolachlor, b) terbuthylazine, c) nicosulfuron and d) prosulfuron as a function of time in the drainage of Lysimeter 1, together with herbicide input (red crosses; dashed vertical lines indicate application date).

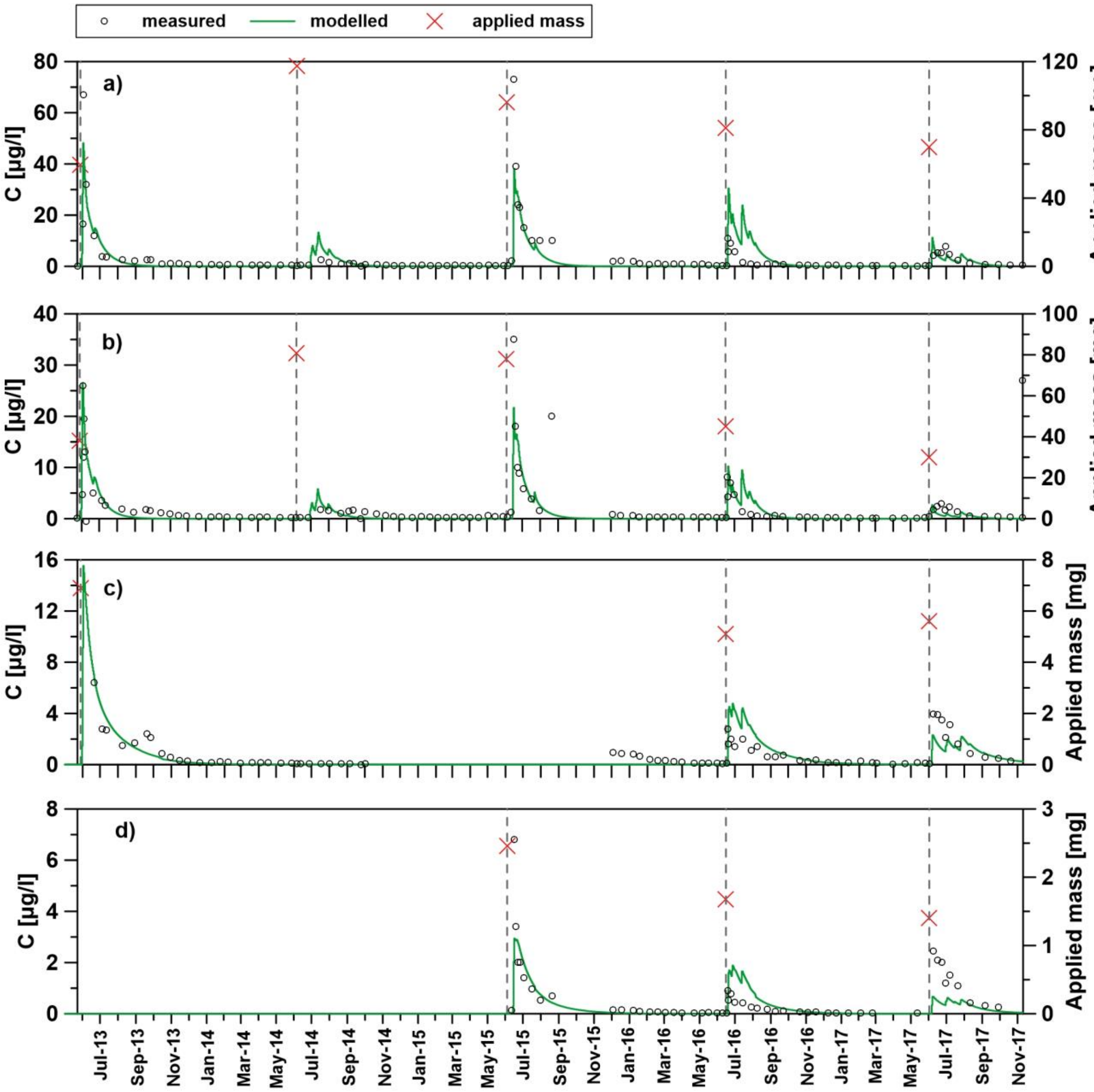

Figure 6-2. Measured (black circles) and modelled (green lines) herbicide concentration of a) metolachlor, b) terbuthylazine, c) nicosulfuron and d) prosulfuron over time in the drainage of Lysimeter 2, together with herbicide input (red crosses; dashed vertical lines indicate application date).

In the currently available literature, we found no comparable long-term, multi-application modelling studies. Existing shorter term, single-application studies might fail in describing the longer-term studies with several applications on bigger scales. We found studies that applied the contaminant only once, and not like in this study, five times over the modelling period (e.g, Celestino Ladu and Zhang, 2011; Jiang et al., 2010; Noshadi et al., 2019; Pot et al., 2005). The longest investigated time frame was half a year and in soil columns of 1.2 m length (Noshadi et al., 2019). We suggest to investigate the influence of time-dependency of herbicide sorption as, e.g., documented by Mamy and Barriuso (2007) and the implementation of time-dependent sorption in future HYDRUS-1D versions.

6.5.2 Influences of model setup

In Ly2, concentration peaks are less frequently underestimated than in Ly1 (Figure 6-1 and 6-2). It could therefore be assumed that the Ly2 model is able to describe peak concentration amplitudes more adequately. The fast responses of the system to herbicide application (measured peak concentrations) could also be related to preferential flow influences. As discussed in our preceding paper (Imig et al., under review, a simulations with the dual-porosity (DP) setup were able to describe short-term fluctuations of δ^{18}O in lysimeter drainage slightly better than the single-porosity (SP) setup. In the present study, we applied a SP setup for Ly1 and a DP setup for Ly2. Better model performance was found for Ly2 than for Ly1 (Table 6-2, Table B-4).

To the best of the authors knowledge, to date, very few studies are available that combine DP considerations with stable water isotope analysis and reactive transport modelling. For example, Huang et al. (2015) calibrated a DP flow model with stable isotopes and extended this model for reactive transport of sulphate (field-scale study). Isch et al. (2019) simulated bromide tracer transport with HYDRUS-1D (DP setup) for six uncropped lysimeters filled with silty loam. Similar to our results, tracer breakthrough was difficult to describe, where peaks were mostly underestimated.

Jiang et al. (2010) simulated leaching of faecal coliforms and bromide in six lysimeters filled with silt loam and sandy loam, which were planted with grass grub. The authors explained fast response of drainage after flood irrigation with preferential flow path influences. Modelled peak concentrations of faecal coliforms after flooding events underestimated measured concentrations by factor two or three.

As also discussed in Imig et al. (under review, a), a dual-permeability model could potentially be better suited to describe preferential flow influences and hence observed concentration peaks. However, the current HYDRUS-1D version does not allow the implementation of a dual-permeability approach for stable water isotope modelling. Therefore, it was not possible to couple stable water isotope observations (for flow characterization) with herbicide measurements (for reactive transport modelling). Since two mobile regions are considered, the dual-permeability setup requires the parameterization of a second soil-hydraulic and transport parameter set. We refrained of such a procedure, which would solely be based on herbicide measurements in lysimeter discharge: limited availability of measurements (such as missing observations within the soil column) and reactivity of the herbicides are associated to considerable uncertainties (cf. also discussion in Imig et al. (2022a)).

In this study, we used a chemical equilibrium approach with linear sorption, however chemical non-equilibrium may describe natural conditions more adequately, by accounting for ad- and desorption kinetics.

We have compared different assumptions concerning sorption processes, including equilibrium linear and non-linear sorption (Freundlich and Langmuir isotherms), as well as two-site kinetic sorption. Compared to equilibrium linear sorption, the other more complex approaches did not improve model performance for Ly1 and Ly2 (results not shown). These more complex approaches might be able to describe sorption processes more adequately, however no measurements of sorption (and biodegradation) parameters were available for our soils and compounds, so that we had to estimate these parameters. This implied additional uncertainties, and following the parsimony principle, we applied the simpler (equilibrium linear sorption) approach, requiring less input parameters.

In other studies, Pot et al. (2005) applied metribuzin and isoproturon to two undisturbed grassed silty loam soil cores under different irrigation intensity, where consideration of chemical non-equilibrium improved model performance. Köhne et al. (2006) compared chemical and physical non-equilibrium setups in HYDRUS-1D for describing the fate of isoproturon and terbuthylazine in undisturbed loamy and sandy soil columns (20-day experiment). Best results were obtained when combining chemical non-equilibrium (two-site kinetic sorption) with physical non-equilibrium (dual-permeability immobile-mobile model) for describing reactive herbicide transport.

6.5.3 Recovery rates if chemicals in drainage

Recovery rates (RR) of the applied chemicals in lysimeter discharge were determined, assuming a wind drift loss of 4% during application (cf. section 2.2). RR showed pronounced differences between compounds and lysimeters, where values at experiment end are shown in Table 6-1 and temporal development is depicted in Figure C-1 and C-2. Highest RR at experiment end was found for MTLC plus metabolites, with 20.9% in Ly2 and 12.8% in Ly1. RR for NCS was about three times higher in Ly2 than in Ly1 (5.3 versus 15.9%). Lower RR was found for TBA plus metabolites and for PS (2.0 – 2.5%)

Remaining chemical fractions might have been sorbed to soil, taken up by plants, mineralized or transformed into metabolites that were not measured. No measurements of respective rates were available for the site, so that possible influences of such processes were investigated by modelling, only. We assume that sorption played the most important role. Sorption was estimated in our study, due to the absence of measurements such as soil organic carbon, soil pH or cation exchange capacity.

A considerable difference in RR between the lysimeters can be seen for MTLC and NCS (higher RR in Ly2 than in Ly1), whereas RR was similar for TBA and PS (Table

6-1). Corresponding to this finding, fitted sorption (K_d) and biodegradation (μ) were lower for MTLC and NCS in Ly2 (however higher K_d and lower μ for TBA, lower K_d and μ for PS; Table 6-3). In line with higher recovery rates in Ly2, Sadeghi et al. (2000) reported 40% more atrazine leaching for silt loam compared to sandy loam soils.

Singh et al. (2002) conducted leaching experiments for MTLC and TBA in column experiments with silt loam and loamy silt soils. The authors found that the mobile phase had a higher influence on solute transport than the immobile phase. For Ly2, an immobile phase was considered in the model setup and the smaller mobile phase was dominating solute transport. For peak flow events, the immobile water phase will not be available for mixing, so that the solute will be mixed within the available mobile region, only. This can lead to higher solute concentrations in the drainage, resulting from the smaller mobile phase in Ly2 during peak flow events. In our case, the dominance of the mobile phase for solute transport was supported by a low fitted solute mass transfer coefficient ω_S (Table 6-3). Such low values indicate almost uniform flow with very slow equilibration of concentrations between the mobile and immobile region (Šimůnek and van Genuchten, 2008).

6.5.4 Investigation of biodegradation influences

The observed formation and accumulation of metabolites (for MTLC and TBA, cf. Figure C-1 and C-2) indicates the activity of biotic degradation pathways in both lysimeters. Biodegradation for these compounds was similarly observed in other studies (e.g., Caracciolo et al., 2001; Guzzella et al., 2003; Torrentó et al., 2021; Zemolin et al., 2014). Comparing calculated recovery rates for herbicides and herbicides plus metabolites (Table 6-1), higher degradation can be assumed for Metolachlor, as a first estimate, with a low to moderate biodegradation activity, in total.

In addition, stable carbon isotopes were analysed to investigate the transformation processes of MTLC and TBA. Measured $\delta^{13}C$ of MTLC and TBA are presented in Figure 6-3 and Table C-5. No analysis was possible for drainage water sampled before herbicide application (21 May 2015, 1st sampling campaign), since concentrations were too low for precise isotope analysis. Also, in samples of the 3rd sampling campaign (8 January 2016), $\delta^{13}C$ could not be measured for both compounds in the drainage of Ly2 and for TBA in the drainage of Ly1, because the peak amplitudes were below the limit of quantification for carbon isotope analysis.

Where analysis was possible, findings indicated a slight shift towards higher (less negative) $\delta^{13}C$ values in drainage compared to the applied herbicide solution (cf. Figure 6-3, Table B-5). This is an indication of microbial degradation activity, where kinetic isotope effects during the biochemical reaction are expected to favour light isotopes, leading to an enrichment of heavier isotopes in the remaining substrate (e.g., Meyer and Elsner, 2013). In the following, the $\delta^{13}C$ change between applied pesticide solution ($\delta^{13}C_{Apl}$) and drainage ($\delta^{13}C_W$) is obtained as $\Delta\delta^{13}C = \delta^{13}C_W - \delta^{13}C_{Apl}$.

For the 2nd sampling campaign (19 days after pesticide application), $\Delta\delta^{13}C$ was similar for MTLC in both lysimeters (+1.9‰ in average, thus slight increase). It was a bit lower for TBA in Ly1 (1.4‰) and Ly2 (0.7‰). For the 3rd sampling campaign (~7.5 months after application), the increase was higher (determined for MTLC with 3.8 ‰). This points towards a higher biodegradation activity for the latter case, where the infiltrated (contaminated) water was residing a longer time in the subsurface (presumably dominated by matrix flow) compared to the first case (where herbicide leaching was presumably dominated by rapid flow paths).

In other investigations, Bundt et al. (2001) compared microbial biomass within the preferential flow and matrix phase for a sandy loam forested field site. They explain a higher microbial biomass in the preferential flow paths with preferable conditions for microbes due to better substrate supply than in the matrix phase. However, the authors did not analyse contaminant degradation. Brovelli et al. (2011) numerically studied the effects of increased heterogeneity of filter sand or gravel packs in constructed wetlands on benzene concentrations in filters. Flow in combination with biodegradation was modelled. Results indicate an increase in benzene concentrations in the filter if higher heterogeneity of the filter were considered. The increase in heterogeneity could be interpreted as preferential flow paths leading to lower degradation than in soil with only matrix flow (homogenous).

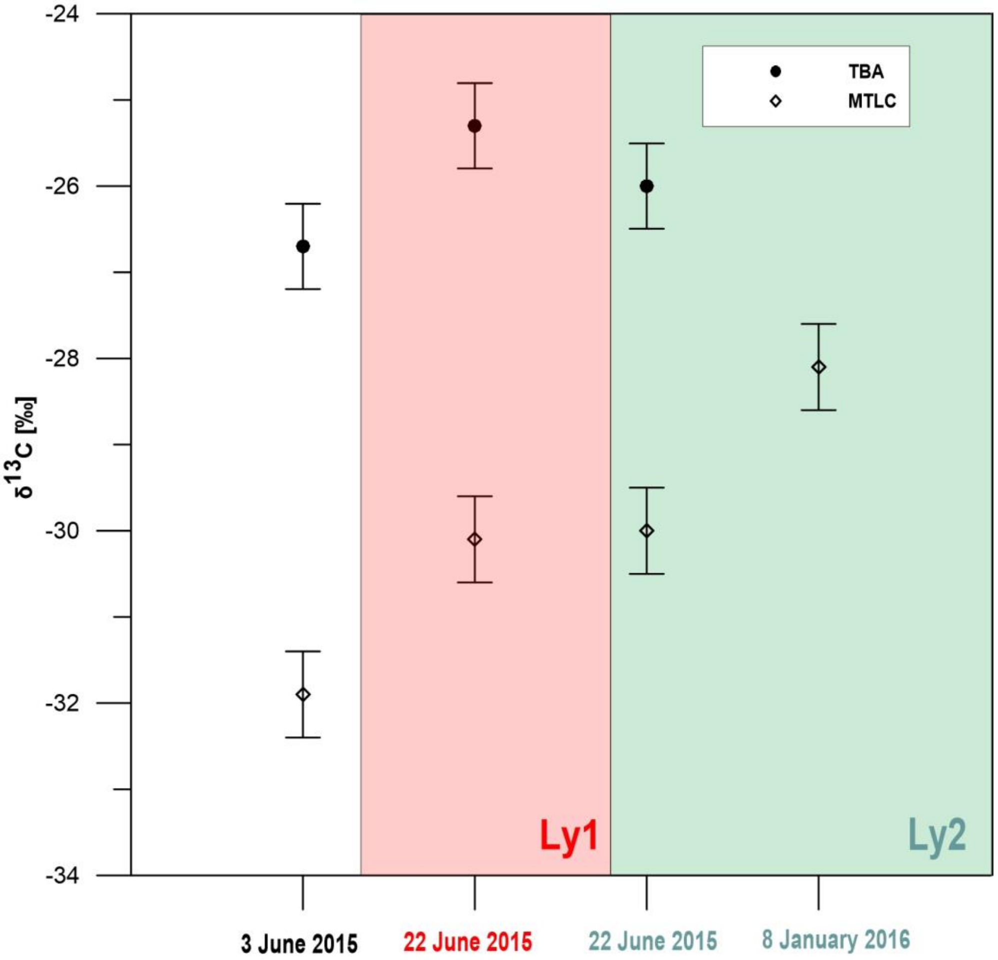

Figure 6-3. $\delta^{13}C$ of terbuthylazine (TBA) and metolachlor (MTLC) in the applied herbicide solution (application day 3 June 2015) and in the drainage of Ly1 and Ly2 at two sampling campaigns (22 June 2015 and 8 January 2016). Error bars indicate total uncertainty of carbon isotope analysis +/- 0.5 ‰.

6.6 Summary and Conclusion

Herbicide transport within two lysimeters filled with sandy gravel (Ly1) and clayey, sandy silt (Ly2) was studied. Four herbicides, MTLC, TBA, NCS and PS, were applied yearly between 2013 and 2017, and concentrations of herbicides and metabolites were monitored in lysimeter drainage. Reactive transport of herbicides was modelled to determine governing processes including biodegradation, sorption, and plant uptake and to estimate their contributions and rates. Generally, modelled herbicide concentrations followed the trend of measured ones and were in the same magnitude. Fitted parameters agree with rate constants of literature values for sorption and degradation processes. Especially interesting are the observed differences in the lysimeters: the clayey, sandy silt of Ly2 showed higher recovery rates of some herbicides in lysimeter drainage than the sandy gravel of Ly1. Furthermore, an immobile phase was considered for Ly2. Thus, the smaller remaining mobile phase in Ly2 was dominating the solute transport and accordingly led to a higher solute concentration in the drainage.

Observed metabolite formation and accumulation let us conclude that biodegradation processes contributed to the fate of herbicides within the lysimeters. Further, carbon isotopes of MTLC and TBA were analysed to identify biodegradation influences. A depletion of heavier isotopes over time in the drainage was found, which points towards higher biodegradation of the infiltrated (contaminated) water residing a longer time in the subsurface compared to water within preferential flow paths.

The considered processes of sorption and biodegradation could be estimated reasonably well with our model, as measured herbicide concentration in drainage fit the modelled concentrations and their processes rates. Limits in describing preferential flow events with the single and dual-porosity flow models became evident as strong peaks were often under- or overestimated by a factor of two or three. The flow description could potentially be improved in the future with a dual-permeability model setup that includes immobile water. Such a setup is currently not available for stable water isotopes in HYDRUS-1D, whose development we recommend in future work. Furthermore, verification of plant uptake with monitored plant concentrations is recommended, where a more detailed model approach might be beneficial, such as considering depth dependency of plant uptake and dynamic feedback with root processes.

Multi-process modelling for herbicide transport in the vadose zone proofed to be a valuable tool for understanding dominant fate and transport processes. Our findings will support modellers and decision makers to predict contamination potential of herbicides to groundwater resources.

Chapter 7 A review on risk assessment in managed aquifer recharge

These chapters include the following publication, with some modifications: Imig, A., Szabó Z., Halytsia, O., Vrachioli, M., Kleinert, V., Rein, A., (2022) A review on risk assessment in Managed Aquifer Recharge. Integrated Environmental Assessment and Management, 00,1-17. doi: 10.1002/ieam.4584

A statement from the doctoral candidate concerning her contribution to publications was submitted within the framework of a publication-based dissertation, together with a statement of confirmation from the co-authors according to Article 7, section 3, clause 2 of the TUM Doctoral Regulations (PromO) was submitted along with the publication. Chapter 7.5.4, social and economic risks, was not drafted but only edited by Anne Imig. Zsóka Szabó and Anne Imig drafted Chapters 7.5.1, 7.5.3, and 7.5.5. together.

Abstract

Managed aquifer recharge (MAR) refers to a suite of methods that is increasingly being applied worldwide for sustainable groundwater management to tackle drinking or irrigation water shortage or to restore and maintain groundwater ecosystems. The potential for MAR is far from being exhausted, not only due to geological/hydrogeological conditions or technical and economic feasibility but also to its lack of acceptance by the public and policymakers. One approach to enable the safe and accepted use of MAR could be to provide a comprehensive risk management, including the identification, analysis and evaluation of potential risks related to MAR. Aims of this paper are to review current MAR risk assessment methodologies and guidelines and summarize possible hazards and related processes. It may help planners and operators select appropriate MAR risk assessment approaches and support the risk identification process. In addition to risk assessment (and subsequent risk treatment) related to the MAR implementation phase, this review also addresses risk assessment for MAR operation. We also highlight limitations and lessons learned from application and development of risk assessment methodologies. Moreover, developments are recommended in the area of MAR-related risk assessment methodologies and regulation. Depending on data availability, collected methodologies may be applicable for MAR sites worldwide.

7.1 Introduction

In their Sixth Sustainable Development Goal, the United Nations aim to ensure the availability and sustainable management of water and sanitation for all by 2030 (UN, 2016). Groundwater is an essential source of water supply worldwide, and an increase in global groundwater extraction from ~100 km³/year in 1950 to 734-1000 km³/year in 2000 reflects growing demand (Shah et al., 2007; Wada et al., 2010). Overexploitations of the aquifers and effects of climate change can lead to a local decrease in groundwater recharge (e.g., Biswas et al., 2018; Green et al., 2007; Kundzewicz and Döll, 2009; Woldeamlak et al., 2007; Casanova et al., 2016; Wada et al., 2012). Pumping groundwater can result in a variety of chemical impacts on the pumped aquifer, including the intrusion of saltwater in case of coastal aquifers, the influx of poor-quality water such as river water or stormwater runoff contaminated by agrochemicals (e.g., Chilton and Foster, 2004; Vbra and Richts, 2015).

One method to address these challenges is managed aquifer recharge (MAR). Excess water from rainfall or flooding, water treatment plants, rivers or desalinated seawater, for example, can be infiltrated into an aquifer to store and recharge groundwater (e.g., Gale, 2005). As a result, the availability of groundwater is maintained or enhanced and groundwater can be extracted in times of need. Moreover, the water quality can be increased by (engineered) natural attenuation processes of the aquifer and soil matrix.

Dillon et al. (2019) document an increase in MAR implementation of about 5 % per year since the 1960s, but this does not match the increasing groundwater abstraction. In countries applying this technology, about 2.4 % of total groundwater abstraction is provided by MAR (or ~1 % worldwide). Even though geological and hydrogeological conditions are among the most predominant factors influencing MAR potentials, psychological and policy-related aspects are also important for the acceptance and implementation of MAR schemes. Such aspects were found to make a considerable contribution to the fact that the full potential for using MAR is often far from being exploited (e.g., Dillon, 2005; Mankad et al., 2015).

Fernández Escalante et al. (2020) and Page et al. (2020) claim that the lack of regulatory frameworks often hinders the implementation of MAR schemes. Building trust in key regulating organisations, such as drinking water regulators, health agencies and public water systems, can potentially influence MAR system promotion (Leviston et al., 2006; Mankad et al., 2015). Nandha et al. (2015) point out that a key step in promoting MAR would be to reduce uncertainties related to MAR implementation and operation such as human health and environmental aspects. Furthermore, authors suggested the development of economic components that aim at ensuring the feasibility and successful implementation of MAR systems (e.g., Casanova et al., 2016; Dillon et al., 2020a). To consider MAR as an integrated water management option for achieving the United Nation’s Sixth Sustainable Development Goal, adequate risk management is required to ensure its safe implementation.

It has been pointed out that MAR risk management should include methodologies that enable a comprehensive assessment of human health, environmental, economic and social risks (e.g., Assmuth et al., 2016). With regard to such a comprehensive approach, Nandha et al. (2015) reviewed existing risk assessment methods that can be applied for MAR when establishing risk assessment guidelines for the United Kingdom. Furthermore, the World Health Organization (WHO) reported the state-of-the-art risk assessment and management approaches for aquifer recharge, focusing on human health risks (Aertgeerts and Angelakis, 2003). Recently, Rodríguez-Escales et al. (2018) have summarized possible causes on a multidimensional level of MAR failure in order to establish a new fault tree-based probabilistic risk assessment approach. Fernández Escalante et al. (2020) reviewed the current state of MAR policies and identified a lack of risk assessment approaches, with the known exception of the Australian policies.

The aim of this paper is therefore to provide a review of current and applied risk assessment guidelines and methods, as well as frequently considered types of risk. This review is intended to provide an overview of existing methods and guidelines and their application, rather than evaluating their applicability. As a description of the state-of-the-art, it may serve as a starting point for further evaluating potentially suited methods/guidelines and selecting associated literature. We also highlight limitations and lessons learned from application and development of the summarized risk assessment methodologies.

7.2 Risk management process

Harm can describe an injury or damage to human health, as well as damage to property or the environment. Hazard is the potential source of harm, which can, for example, be a biological, chemical, physical or radioactive agent, and a hazardous event is an event that can cause harm. The combination of probabilities for the identified hazard to occur in a specific time frame and the magnitude of its harm is termed risk (ISO and IEC, 2014; NRMMC, 2006).

The International Organization of Standardization (ISO) proposes an iterative process for risk management (ISO, 2018), as summarized in Figure D-1. After establishing the scope and context of the evaluation, risk assessment is carried out followed by risk treatment. The risk assessment procedure consists of three steps, i.e. risk identification, risk analysis and risk evaluation (Figure D-1). Risk identification is conducted in order to identify and describe hazards that aid or prevent the achievement of an aim. Risk analysis describes the likelihood of a hazard or hazardous event by taking into consideration consequences and their sensitivities. Risk evaluation intends to identify risks for which actions have to be undertaken such as further analysis, maintain existing control structures or risk treatment options (ISO and IEC, 2014; ISO, 2018).

7.3 **Reviewing Procedure**

Publications were selected according to the following criteria: (i) scientific quality (articles in peer-reviewed scientific journals were preferred, followed by reports of recognized research projects and guidance documents prepared by regulatory agencies) and (ii) recent research. Referring to the latter, we have focused our review on studies published between 2000 and October 2020. Selected older publications are mainly related to background and pioneering literature in the field of risk assessment. Publications were searched with common search engines such as Google Scholar and online databases (including Scopus), as well as the software Publish or Perish

(Harzing, 2020); used search phrases are summarized in the Appendix D. Further references were found within reviewed articles and reports.

The literature reviewed in this paper can be subdivided into three categories: (i) articles and reports about risk assessment case studies and methodological papers, (ii) review articles on possible risks and risk assessment approaches for MAR and (iii) risk assessment guidelines. With regard to point (i), selected studies were further evaluated for the application of risk methodologies, such as in case studies. For this goal, 43 papers with 138 case studies from 23 countries were collected (Figure 7-1; further details see Table D-1 (Appendix D) and discussion section, Chapter 7.5).

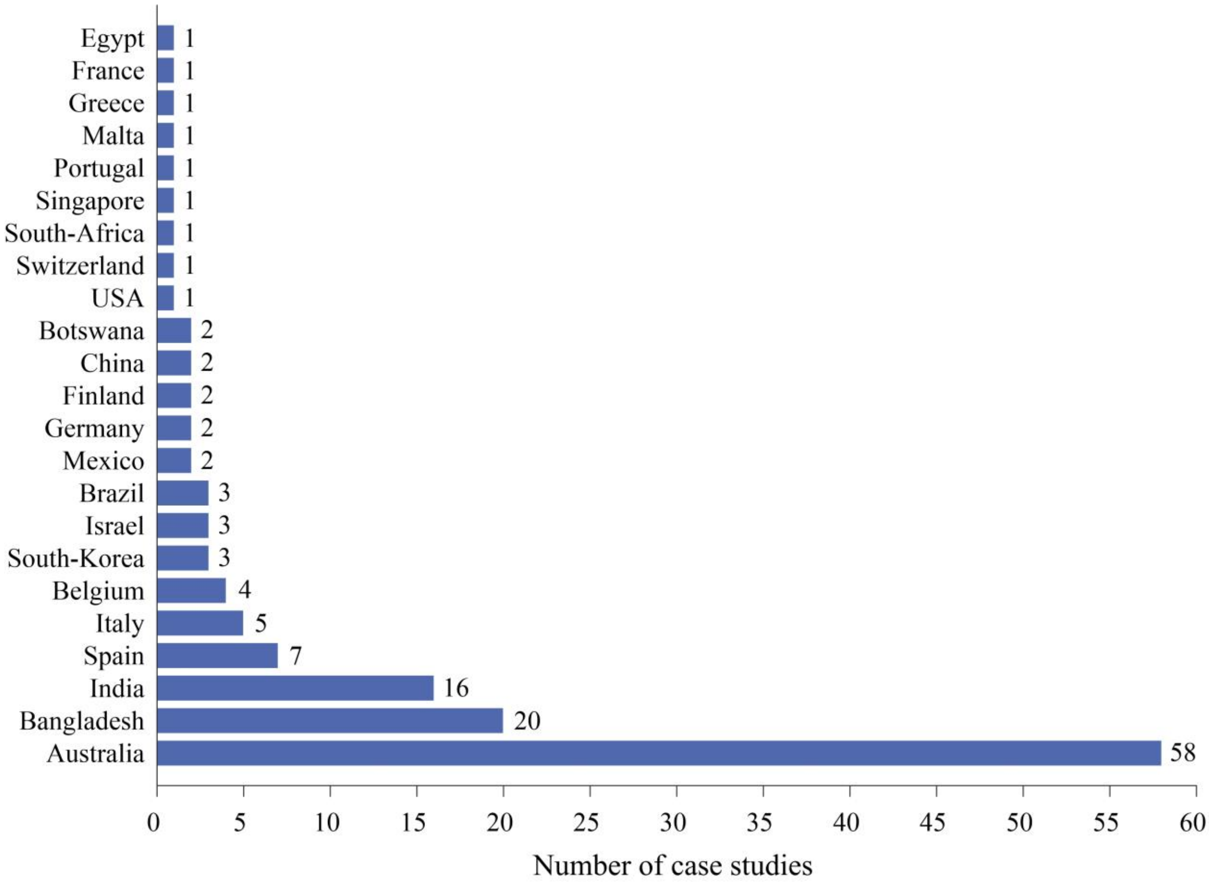

Figure 7-1. Number of reported case studies per country in the reviewed publications (based on Table D-1).

7.4 Risk assessment approaches

Several of the risk assessment approaches described in this section are involving two international frameworks that have been developed for risk assessment in general (without specific attention to MAR): (i) the framework of hazard analysis and critical control points (HACCP) and (ii) the framework of water safety plans (WSP) suggested by the WHO.

Hazard analysis and critical control points. The HACCP framework was developed in the 1960s as a universal, scientifically based approach for food safety (Havelaar, 1994; WHO, 1997; WHO and FAO, 2006). In a twelve-step procedure, a control system is established by identifying hazards and their critical control points. A critical control point is defined as a step in the procedure where control can be applied and can lead to hazard prevention, hazard elimination or the reduction of a hazard to an acceptable level. An effective HACCP plan focuses on prevention, by defining precautions for preventing hazards (EC, 2015). Application of the HACCP framework is compulsory in EU countries where water utilities fall under the provision of food safety (EC, 2015).

Water safety plans. The WHO published the Stockholm Framework 2001, in which it was agreed that future guidelines for drinking-water, wastewater and recreational water should include risk assessment and risk management (Bartram et al., 2001). Based on this, the creation of water safety plans (WSP) was proposed in 2004 (WHO, 2004). WSP are partly based on principles of the HACCP framework but are tailored to the water industry (Declan Page et al., 2012). Human health risks related to drinking water use (potentially arising from microbial, radiological and chemical hazards) are assessed for the whole process of providing drinking water (“from the catchment to the consumer”). This risk assessment forms the basis for decision-making in order to target the human health risks of the system on a multi-barrier principle (Davison et al., 2005). Operational monitoring and control measures are also defined within the WSP since they are important for ensuring that the health-based targets are met.

7.4.1 Risk assessment guidelines related to MAR

This section describes MAR-related guidelines, which include detailed instructions for risk assessment. Reported strengths and weaknesses of those, together with references for application examples, are summarized in Table 7-1.

Australian guidelines for MAR risk assessment. Australia has recommended specific risk assessment methodologies for MAR, as laid down in national guidelines for water recycling (NRMMC, 2006; NRMMC, 2009). These guidelines aim at developing a twelve-step MAR risk management plan and address a variety of water sources. The risk assessment framework incorporated within the Australian guidelines has four iterative stages for identifying human health and environmental risks: (i) entry-level assessment, (ii) assessment of maximum risks, (iii) assessment of residual risks for MAR pre-commissioning, after having considered preventive measures that could minimize the determined maximum risks, and (iv) assessment of residual risks for the operational phase of MAR.

The Australian guidelines offer advice on adequate management for twelve potential hazards to human health and the environment related to MAR implementation and operation. This includes possible preventive measures, monitoring strategies (validation, verification and operational monitoring) and acceptance criteria for the four risk assessment stages. Methods suggested by the Australian guideline to evaluate acceptable risks are based on qualitative risk assessment for environmental risks, and quantitative risk assessment for human health risks (if data are available also possible for environmental risks).

Indian guidelines for MAR risk assessment. Dillon et al. (2014) developed a water quality guide related to the implementation of managed aquifer recharge in India. This guide is structured by a sequence of steps, including the first stage from the Australian guidelines: entry-level risk assessment combined with sanitary surveys as proposed by the WHO (2017).

Chilean guidelines for MAR risk assessment. As recently reported by Page et al. (2020), the National Irrigation Commission of Chile has developed guidelines for MAR application, which implement risk assessment. The Chilean guidelines address human health and environmental risks and restrict the applicability to non-potable water derived from MAR (e.g., agricultural irrigation, environmental benefit or saline intrusion barrier) (CNR and CSIRO, 2020). The guidelines are based upon the Australian and Indian guidelines, as well as the (interconnected) HACCP, WSP and sanitary survey principles.

Table 7-1. Short overview of reported strengths and weaknesses of risk assessment guidelines applied for MAR, as well as references for application examples (including case studies).

Risk assessment guidelines	**Strengths**	**Weaknesses**	**Examples for guideline application (references)**
Australian guidelines (NRMMC, 2006; NRMMC, 2009)	Tailored to specific MAR-related hazards with detailed indications of acceptable risks	Detailed input data needed (e.g., Nandha et al., 2015; WHO, 2012)	Bartak et al., 2015; Gibert et al., 2015; Page et al., 2010b, 2010c, 2010d; Seis et al., 2015; Sprenger et al., 2020; Vanderzalm et al., 2011
Water safety plans (WSP) (WHO, 2004)	Comprehensive approach "from catchment to customer"	Conservative approach; may tend to overestimate risks (e.g., when available data on likelihood are limited)	Bartak et al., 2015; Dominguez-Chicas and Scrimshaw, 2010
Hazard analysis and critical control points (HACCP) framework (e.g., EC, 2015; Havelaar, 1994; WHO, 1997; WHO and FAO, 2006)	Not limited to specific hazards	Hazard identification is subjective; critical control point identification for MAR is more difficult than for water treatment options (MAR as a complex system); failures and risks are not quantified	Dewettinck et al., 2001; Gonzalez et al., 2015; Page et al., 2009; Swierc et al., 2005
Indian guidelines (Dillon et al., 2014)	Low data need	High-risk schemes (e.g., infiltration of wastewater) cannot be evaluated	Dillon et al., 2016a
Chilean guidelines (CNR and CSIRO, 2020)	Low data need (no application documented to date)	Limited to non-potable water use (no application documented to date)	(no application documented to date)

7.4.2 Risk assessment methodologies related to MAR

This section describes methodologies that are frequently applied for a MAR-related risk assessment. Reported strengths and weaknesses of these methodologies, together with references for application examples, are summarized in Table 7-2.

Qualitative risk assessment. A risk factor score matrix is defined for qualitative risk assessment (Figure D-2). The likelihood of a hazard actually occurring is identified by the expected recurrence of the hazard (indicated in units of years), using a five-step scale on one axis of the matrix, e.g., a hazard recurrence interval of 100 years is defined as "rare" (lowest scale). On the other axis, the severity of the consequence of the hazard is defined in five scales. For example, if the integrity of regional ecosystems is endangered, a catastrophic consequence (highest rank) is specified. If both the likelihood and the consequence of the hazard are ranked high, the resulting risk is identified as being very high (Figure D-2). This method was suggested in the Australian Guidelines as well as in the Stockholm Framework for water (Swierc et al., 2005).

Quantitative risk assessment. The Australian guidelines also propose a methodology for quantitative risk assessment (QRA) for MAR, which is based on chemical risk assessment procedures that have been developed by the U.S. Environmental Protection Agency (US EPA, 2002, 1998, 1987). This methodology compares chemical concentrations in an environmental matrix (such as groundwater) to reference values (such as drinking water limits; e.g., US EPA, 2002, 1998, 1987; WHO, 2017). Four steps are considered for quantitative human health risk assessment, as shown in Figure D-3. The hazard, together with its variability, and related impacts are initially identified. Secondly, the dose-response relationship is quantified, which describes how the likelihood and severity of adverse human health effects (the responses) are related to the amount and condition of exposure to an agent (the dose provided) (e.g., Alcade-Sanz and Gawlik, 2017; US EPA, 2002, 1998, 1987). Subsequently, the size and nature of the exposed population to the hazard is identified, including an assessment of the amount (such as contaminant intake), the exposure route (such as the ingestion of contaminated drinking water) and the duration of exposure. The last step combines the information obtained so as to characterize the risk, i.e. to predict the probability of adverse human health effects, where the magnitude, variabilities and uncertainties are determined (e.g., Haas et al., 1999; NRMMC, 2006).

Quantitative microbial risk assessment. Quantitative microbial risk assessment (QMRA) follows the same steps as QRA, but focuses on the quantification of human health risks arising from indicator microorganisms in water (Haas et al., 1999). Indicator or reference pathogens are assessed to maintain reasonable effort for the determination of concentrations, dose-response relationships and related impacts (NRMMC, 2006; NRMMC, 2009, WHO, 2006). The first step of the proposed QMRA procedure identifies pathogen-related hazards posing potential risks to human health. Then, the likelihood of the occurrence of illness (for a given population) is calculated using dose-response curves of the reference pathogens. In a next step, the daily probability of infection is transformed into a probability of infection occurring per year, taking into account a certain number of exposure events per year. Information from the previous steps is integrated in the final step to determine and evaluate the magnitude of risks. Both the WHO (2006) and the Australian guidelines refer to the disability-adjusted life years (DALYs) method for risk evaluation. This method describes the disease burden by calculating accumulated years of life that are lived with disability and/or are lost due to an early death.

Integrated human health risk framework for MAR. Assmuth et al. (2016) have developed and applied a methodology for the regional-level human health risk assessment of chemical and microbiological water contamination. This methodology aims at aiding water management and also incorporates socio-economic aspects of health risks. A model of risk and its impact chain is proposed, combining the related social and economic aspects, as well as factors related to the ecosystem and technical tasks (e.g., design, application, monitoring and control of the MAR scheme). Input data for evaluating risks and their adverse impacts are collected in a first phase. It is suggested that health risks related to pathogens be quantified by QMRA, determining disability-adjusted life years (DALYs) or quality-adjusted life years (QALYs). The data obtained should then be used for a structurally integrated risk analysis, considering pollutant sources, release mechanisms, environmental transport and fate pathways, exposure routes, health effects and resulting socio-economic impacts, as well as management responses.

Pollutant release and transfer register. Ji and Lee (2016a, 2016b, 2017) proposed and applied a pollutant release and transfer register (PRTR) together with deterministic and stochastic methods to assess potential chemical risks for a MAR site. A PRTR provides data to determine (i) the quantity of emitted chemicals (discharged to water systems, soil and the atmosphere) and (ii) the transfer of these chemicals (from their source to the MAR facilities) as a function of time. Potential accumulated chemical risks are proposed to be determined from the toxicity of the chemicals, the distance from the source to the MAR site and the total quantity of chemicals to be transferred from source over time. If recorded data are lacking or predictions for future developments are intended, Ji and Lee (2016b, 2017) propose the application of PRTR in combination with a stochastic approach to estimate potential risks. PRTRs can be used to carry out risk assessments as part of the HACCP procedure and/or the setup of water safety plans, such as was done by Ji and Lee (2017) for two different MAR sites.

Probabilistic risk assessment based on fault trees. Rodríguez-Escales et al. (2016) developed a probabilistic risk assessment methodology for the operational phase of MAR based on fault trees, which considers a series of quasi-independent events that contribute to the total risk. This subdivision aims at simplifying the risk assessment process, i.e., the events can be managed individually; probabilities are computed for the occurrence of these individual events, and these probabilities are systematically recombined to assess overall risk for the MAR system. The open-source application MAR-RISKAPP is available for this approach (Rodríguez-Escales et al., 2018). A fault tree, to be evaluated by the user, includes 65 basic events that can potentially lead to MAR failure (these basic events were assumed to be potentially relevant, based upon a literature review considering 47 different MAR sites; for details, see Rodríguez-Escales et al., 2018). Probabilities of the individual events and the resulting probability for the failure of the global system are determined, forming the basis for the next step; risk treatment should then be conducted for the events identified as most significant.

Public health and economic risk assessment. Juntunen et al. (2017) proposed a risk assessment methodology for MAR with the aim of decreasing the uncertainty of risk prediction and enabling a more accurate decision making for the mitigation of adverse effects. The authors combine methods for economic, environmental, and human health assessment with different computational techniques. Their proposed methodology is composed of four steps. First, flow and (reactive) transport models are applied to predict contaminant and pathogen transport and related potential risks for the use of MAR. The second and third steps include the prediction of public health risks, where QMRA for the determination of human health risks (related to pathogens causing diarrheal diseases) was combined with chemical risk assessment using acceptable daily intake levels, as proposed by the WHO (2010). The final step investigates, regional economic effects resulting from the assessed health impacts, including the illness probability (and related change in labour productivity) estimated by using a computable general equilibrium model.

Screening-level assessment of human health risks arising from micro-pollutants. Rodriguez et al. (2007b, 2007a) proposed a methodology for human health risk assessment at the screening level to evaluate potential risks to MAR arising from contamination with micro-pollutants (considered as chemicals of concern for indirect potable reuse schemes). In order to calculate health risks arising from a chosen chemical, the risk quotient is calculated by relating measured chemical concentration in the recovered water to a benchmark (no-effect) concentration. Such benchmark values are available for regulated compounds, e.g., defined by the accepted maximum level of the compound in drinking water. The risk quotient can then be used to evaluate potential health risks arising from defined chemicals of concern, and policymakers can include risk quotients within specific guidelines.

Quantitative assessment of socio-economic risks. Currently available literature lacks studies that present a specific approach to quantify economic risks associated with MAR. Nevertheless, sensitivity analysis and quantitative probability modelling are two potential approaches to a socio-economic risk assessment associated with MAR implementation (Maliva, 2014; Maréchal et al., 2020).

Cost-benefit analysis (CBA) can be carried out to obtain the net present value and the economic rate of return. Sensitivity analyses can be used to investigate the economic feasibility of a MAR scheme with substantial variations in critical parameters, such as the willingness-to-pay (WTP) of primary beneficiaries (Damigos et al., 2016). In addition, Arshad et al. (2014) performed a break-even analysis of cross-over points to address uncertainty while conducting CBA. The authors provided thresholds that denote points where MAR and surface storage have equal financial returns for key variables that are characterized by high levels of uncertainty. In order to incorporate uncertainty while conducting CBA, Damigos et al. (2016) also applied sensitivity analysis coupled with the Monte Carlo method to simulate uncertainties that affect the value of the critical parameters.

At the operational stage of MAR, economic risks are mainly a result of the realization of human health, technical and environmental risks. Thus, expected value analysis can be used to address uncertainty and consequently to estimate the magnitude of economic losses. In particular, each potential contingency (e.g., excessive clogging, flooding, insufficient aquifer water level) should be identified and weighted by a probability assigned to its occurrence (based on historical data or expert opinions; Maliva, 2014).

The magnitude of the economic risk can then be proxied by the difference between WTP-values that are calculated with and without accounting for uncertainty.

Rupérez-Moreno et al. (2017) calculated values of profitability indicators for MAR under different scenarios, such as considering climate change or varying irrigation demand (if this is the primary objective of the MAR scheme). Maréchal et al. (2020) incorporated risks and uncertainty within cost-effectiveness analysis (CEA) by performing a systematic sensitivity analysis to determine the effect of various parameters on the levelized cost of the MAR scheme.

Finally, multi-criteria decision analysis (MCDA) coupled with geographic information system (GIS) tools (GIS-MCDA) can help identify suitable sites for MAR by taking social, economic, human health and environmental aspects into account. An overview of different GIS-MCDA approaches applied for MAR is provided by Sallwey et al. (2019). MCDA is based on weights that reflect the relative importance of a criterion and are determined based on experts' opinions or survey outcomes and can vary quite noticeably. Bouwer et al. (2008) proposed a fault-tree analysis for risk assessment to identify a set of weighting criteria for the MCDA.

Assessment of economic risks arising from well clogging. Dillon et al. (2016b) proposed to investigate economic risks arising from groundwater well clogging with prior pilot or laboratory studies in order to support decision making for MAR operation schemes (in particular for aquifer storage and recovery). The cost for managing well clogging, estimated from prior pilot or laboratory studies, can be compared to the costs of water treatment that are required for maintaining human health and environmental requirements.

Environmental impact assessment for MAR. El-Fakharany (2013) applied environmental impact assessment (EIA) for a MAR scheme based on an environmental checklist developed by the International Commission on Irrigation and Drainage (ICID, 1993). Using this checklist, effects from irrigation, drainage and flood control projects can be evaluated by considering eight groups: hydrology, pollution, soils, sediments, ecology, socio-economic criteria, human health and (ecological) imbalances. These groups contain 53 environmental issues, in total, such as “low flow regime” or “soil salinity”. El-Fakharany (2013) applied a semi-quantitative scoring scheme with three categories: either positive, negative or no effects were assigned to each environmental issue.

Table 7-2. Short overview of reported strengths and weaknesses of risk assessment methodologies related to MAR, as well as references for application examples (including case studies).

Risk assessment methodologies	Strengths	Weaknesses	Examples for methodology application (references)
Qualitative risk assessment	Low data need	Detailed processes cannot be highlighted	Sultana and Ahmed, 2016; Swierc et al., 2005
Quantitative microbial risk assessment	Precise predictions possible	Detailed input data needed	Ayuso-Gabella et al., 2011; Bekele et al., 2008; Bloetscher, 2001; Page et al., 2010a, 2010b, 2010c, 2016, 2015b, 2015a, 2013, 2012b; Toze et al., 2010
Quantitative risk assessment	Precise predictions possible	Detailed input data needed	Page et al., 2009, 2008
Integrated human health risk frameworks for MAR	Multidimensionality of risk	Detailed input data needed; limited to human health risks	Assmuth et al., 2016
Pollutant release and transfer register (PRTR)	Low data need for risk quantification; objectivity in hazard identification is made sure	Limited to chemical hazards; detailed input data needed	Ji and Lee, 2016a, 2017
Probabilistic risk assessment based on fault trees	Integrated approach: technical and non-technical risks are incorporated	Probability determination based on MAR operator judgements: methodology suited for existing structures	Rodríguez-Escales et al., 2018
Screening-level assessment of human health risks arising from micropollutants	Unregulated contaminants can be incorporated	Health-based benchmarks are conservative and might lead to overestimation of risks	Rodriguez et al., 2007b, 2007a
Public health and economic risk assessment	Consideration of environmental, economic and human health risks; different steps do not rely on each other's output as input data	Input data for scenarios subject to uncertainty	Juntunen et al., 2017
Assessment of economic risks arising from clogging	Economic viability can be assessed	large amount of input data (e.g., pilot studies)	Dillon et al., 2016b
Environmental impact assessment	Considers a broad range of environmental and ecological risks	Not designed specifically for MAR	El-Fakharany, 2013

7.5 Risks associated with facilities of managed aquifer recharge

Few studies were found that have attempted to collect a comprehensive summary of potential MAR-related risks and their assessment. Rodríguez-Escales et al. (2018) categorized risks into (i) technical risks and (ii) non-technical risks. Technical risks can be structural damage, low amounts of water, inadequate water quality and failure to achieve targeted MAR goals, while non-technical risks may include legal constraints, social unacceptance as well as economic and governance-related problems. In another approach, Nandha et al. (2015) highlighted process-oriented aspects of MAR-related risks, where they distinguished between (i) MAR planning (strategic risk), (ii) water pre-treatment, (iii) recharge, (iv) aquifer storage, (v) groundwater recovery, and

(vi) water post-treatment. The authors highlighted the multidimensionality of one hazardous event as it can be related to, and affect, another. For example, flooding events and droughts may affect water quality in addition to the infrastructure of the MAR scheme. This can lead to MAR malfunction, causing water supply shortage and/or a deterioration of water quality.

Lee and Ji (2016) applied HACCP frameworks to cluster hazardous events based on processes occurring in a drinking water-supply system using the MAR scheme of aquifer storage transfer and recovery. One of their clusters (cluster i) is related to hazardous events that may occur in the catchment area and thus outside the MAR facility. The other clusters are related to the MAR facility, i.e. (ii) intake structure for recharging water, (iii) storage of recharging water, (iv) water pre-treatment, (v) injection to the aquifer, (vi) abstraction from the aquifer, (vii) post-treatment, (viii) storage of treated water (ix) water distribution and (x) water end-users.

In the following, we have differentiated between risk types, i.e. (i) human health risks, (ii) environmental risks, (iii) technical risks, (iv) social and economic risks, and (v) risks related to governance and legislation (e.g., similar to Rodríguez-Escales et al. (2018). Furthermore, we have considered four different stages of MAR implementation and operation: risks may arise from, or relate to, (i) the planning of MAR, (ii) the catchment or water source for MAR, (iii) MAR operation (such as infiltration, storage, recovery) and maintenance, (iv) water distribution and final water use (e.g., similar to Nandha et al., 2015; Lee and Ji, 2016). Risk-related aspects, including potential hazards, can be clustered according to these risk types and defined stages of MAR operation and implementation, as summarized in Table D-2. Table D-3 provides an overview of potential hazards that are frequently reported in literature. In the following, we aimed to describe only the initial ("direct") risk related to the hazard or the hazardous event: the multidimensionality of risk or impact chains are not discussed in detail.

7.5.1 Human health risks

Human health risks related to MAR source water (stage i and ii). The reuse of treated wastewater, in particular from different sources, has the potential to cause human health risks (e.g., Page et al., 2012b). Several guidelines are available globally that address the reuse of treated effluents (e.g., EU, 2020; NRMMC, 2006; NRMMC, 2009; US EPA, 2012; WHO, 2006). Wastewater can contain suspended solids, nutrients, dissolved organic carbon, metals and other inorganic chemicals, pathogenic microorganisms, as well as organic chemicals and emerging pollutants such as pharmaceuticals (e.g., Levantesi et al., 2010; Page et al., 2010a; Rodriguez et al., 2007a; Tchobanoglous et al., 2003; Toze et al., 2010). However, stormwater and surface water also can contain such pollutants, raising concern for human health risks (e.g., Assmuth et al., 2016; Bartak et al., 2015; Page et al., 2013; Vanderzalm et al., 2011). Lee and Ji (2016) propose the consideration of risks related to changing temperatures that may influence source water quality (seasonal temperature changes may cause aerobic conditions at the bottom of lakes and rivers and increased algae growth).

Human health risks related to water quality changes during infiltration and water storage/transport in the subsurface (stage ii and iii). Aquifer and groundwater characteristics can also have a great influence on water quality and hence may impact MAR. Groundwater salinity or sodicity, dissolved reactive minerals (such as fluoride or pyrite), radionuclides or metals (such as arsenic), as well as chemical spills, among other things, can lead to a decrease in the quality of water recovered by MAR, and this may induce human health risks (Assmuth et al., 2016; Bartak et al., 2015; Bouwer et al., 2008; Bugan et al., 2016; Lee and Ji, 2016; NRMMC, 2009; Page et al., 2010c, 2013; Swierc et al., 2005; Vanderzalm et al., 2011). Thus, even if the infiltrated (MAR source) water is of acceptable quality, subsurface contamination can lead to a poor quality of water that is recovered by MAR for drinking water or irrigation use (e.g., Dillon et al., 2014; Ji and Lee, 2017). Heterogeneity of the aquifer and spatially and temporally varying groundwater transit times are among the factors that can influence chemical and pathogen retention or removal by natural attenuation processes (e.g., Swierc et al., 2005; Toze et al., 2010).

Human health risks related to water treatment and MAR operation (stage iii and iv). Pre-treatment can significantly improve the quality of infiltration water (e.g., Casanova et al., 2016). Dillon et al. (2009b) point out that an intensive treatment of MAR source water before recharge does not necessarily protect the aquifer and the recovered water. In addition to unnecessarily high costs and effort, the infiltration of source water that is treated to (almost) meet drinking water quality can be harmful if it allows enhanced dissolution of minerals from the aquifer matrix. Furthermore, using chlorination before infiltration can result in the excessive formation of chloroform in the abstracted water (Dillon et al., 2009b), and the formation of other disinfection by-products can cause environmental and human health problems, as well (Pavelic et al., 2005). Overexploitation of the aquifer can endanger a sustainable water supply and may lead to the intrusion of polluted water or saltwater and hence to a decrease in the quality of the recovered water (e.g., O’Leary et al., 2015).

7.5.2 Environmental risks

Environmental risks arising from MAR implementation and operation (stage iii and iv): The construction and operation of a MAR scheme leads to changes of the natural environment e.g., by excavation, drilling or surface sealing for infrastructure buildings needed for MAR. MAR operation can also influence the environment by changing surface water and groundwater levels. This can have an effect on vegetation and groundwater dependent ecosystems (GDEs), the consistency of the rock framework, as well as stream and spring discharge. It may also cause unwanted flooding or landslides affecting natural and built environments (e.g., Assmuth et al., 2016; Page et al., 2009; Rodríguez-Escales et al., 2018; Swierc et al., 2005). GDEs are especially sensitive to groundwater level changes: falling groundwater levels can for example result in water unavailability and increasing groundwater levels may cause anoxia. Among others, this can induce stress to vegetation and changes can start a chain of events effecting the whole food-chain of the ecosystem (e.g., Bartak et al., 2015; NRMMC, 2009; Page et al., 2009, 2010c, 2010d, 2013; Dillon et al. 2009a; Vanderzalm et al., 2011). MAR implementation can potentially also endanger rare species and animal migration through structural changes in the landscape (e.g., infiltration ponds or fencing around groundwater protection zones) or changing groundwater levels (El-Fakharany 2013).

Moreover, due to differences between the chemical composition of natural groundwater and recharged water, effects such as aquifer dissolution (and resulting instabilities), a decrease in water quality and consequent environmental impacts can occur (NRMMC, 2009). Common groundwater quality issues include, among others, increasing water salinity and sodicity, nutrient overload (that may cause eutrophication), as well as contamination of the aquifer (e.g., pesticides, pharmaceuticals) and hydraulically connected surface water bodies (e.g., Casanova et al., 2016; NRMMC, 2006). Furthermore, risks of increasing energy consumption and greenhouse gas emissions, arising from MAR operation, are considered in several studies (e.g., Bartak et al., 2015; NRMMC, 2009; Page et al., 2010c, 2010d; Page et al., 2013, 2009; Vanderzalm et al., 2011).

Environmental risks related to anthropogenic influences (related to stage i and ii). Agricultural activities such as livestock farming, as well as wastewater release and sewer overflow can change the environmental conditions in the MAR catchment (e.g., Bugan et al., 2016; Juntunen et al., 2017; Lee and Ji, 2016; Swierc et al., 2005). Furthermore, many studies investigate environmental risks arising from chemical spills and accidents (e.g., industry, mining, septic tanks, or illegal sewage inflows) or from sabotage (e.g., related to industry, computer hacking, infrastructure, traffic, households, agriculture) in MAR catchment areas (e.g., Assmuth et al., 2016; Bartak et al., 2015; Ji and Lee, 2016a; NRMMC, 2009; Page et al., 2010c; Page et al., 2013; Swierc et al., 2005; Vanderzalm et al., 2011). However, it has to be noted that contamination can also occur accidently due to natural events, like heavy rainfall and floods (e.g., Assmuth et al., 2016; Lee and Ji, 2016).

7.5.3 Technical risks

During the *MAR planning phase (stage i),* among others, water demand is assessed to define the scale of a MAR project. If water demand is under- or overestimated, or if it changes significantly over time, it can cause operational problems (e.g., Lindhe et al., 2020; Nandha et al., 2015; Rodríguez-Escales et al., 2018). Furthermore, the availability of water, in a sufficient quantity and quality, is fundamental for MAR operation (e.g., Dillon et al., 2016a; Lindhe et al., 2020; Nandha et al., 2015). Hydrogeological characteristics and the ability to store water in the subsurface are critical constraints on the scale of the MAR project (Bouwer et al., 2008; Casanova et al., 2016; NRMMC, 2009; Page et al., 2010c; Seis et al., 2015; Shah, 2014). In the planning phase, the influence of climate change can also be incorporated, e.g., by considering resulting changes of water demand and supply changes in the area and hence ensuring supply reliability (Pasini et al., 2012). Groundwater level changes should be evaluated in view of possible flooding of basements or possible impacts on underground cables, which may require specific management measures (NRMMC, 2006).

Catchment characteristics (stage ii) such as slope instability (e.g., landslides) and erosion can damage MAR infrastructure and lead to malfunctioning or failure of the MAR scheme (Rodríguez-Escales et al., 2018; Swierc et al., 2005). In addition, inadequately low or high infiltration rates can impair an (effective) MAR operation, having an effect, among others, on the amount of water storage, travel and residence times, as well as attenuation processes (e.g., Bartak et al., 2015; de los Cobos, 2018; Rodríguez-Escales et al., 2018). Physical clogging of MAR systems can be caused by suspended particulates such as silt and clay particles or organic matter, entrainment and/or formation of gas bubbles. Physical clogging is often accompanied by biological clogging (biofilm formation and biomass accumulation) and chemical clogging (mineral precipitation) (e.g., Jeong et al., 2018). Furthermore, infiltration water with an increased sodicity can increase the swelling of clay particles in the subsurface and thus decrease the efficiency of water recovery (e.g., Bartak et al., 2015; Bugan et al., 2016; NRMMC, 2009; Page et al., 2010c, 2010d; Page et al., 2016, 2013, 2009; Vanderzalm et al., 2011). A way to mitigate clogging can be pre-treatment, such as the use of sand filters or sedimentation ponds for reducing the turbidity of infiltration water (e.g., Casanova et al., 2016; Page et al., 2010c, 2010d; Sultana and Ahmed, 2016). Also, suited maintenance techniques can be applied for this purpose, like wetting and drying cycles for infiltration basins, or the use of a single well for injection and abstraction (thus changing groundwater flow direction) (e.g., Casanova et al., 2016; Pyne, 1995).

Further issues that can pose technical risks, related to both *MAR operation and maintenance (stage iii) as well as water distribution and final use (stage iv),* can include structural damage of the MAR infrastructure induced by natural hazards like flooding, heavy rainfall or droughts (e.g., Bartak et al., 2015; Bugan et al., 2016; Juntunen et al., 2017; Lee and Ji, 2016; Rodríguez-Escales et al., 2018; Swierc et al., 2005). Moreover, problems may arise from the malfunctioning or failure of technical equipment or infrastructure (e.g., Bartak et al., 2015; Bugan et al., 2016; Ji and Lee, 2016a; Juntunen et al., 2017; Pindoria-Nandha, 2016; Rodríguez-Escales et al., 2018; Swierc et al., 2005) and a lack of (trained) operating staff or of technical knowledge (Assmuth et al., 2016; Dillon et al., 2020a; Rodríguez-Escales et al., 2018; Swierc et al., 2005). If water derived from MAR is used for irrigation and this water has a high salinity or is contaminated, plant health can be affected, leading to reduced agricultural yields (e.g., Eisfeld et al., 2021; ISO, 2015). When water is stored before final use, microbial regrowth, disinfection by-products or algae growth can occur due to malfunctioning or design flaws of the infrastructure (Bouwer et al., 2008; Bugan et al., 2016; Lee and Ji, 2016; Pavelic et al., 2005).

7.5.4 Social and economic risks

Social risks related to social acceptance (stage i). Public concerns about MAR include exploiting scarce water resources and possible contamination of aquifers (Rawluk et al., 2013). Furthermore, concerns about risks to human health and the environment posed by water recovered from MAR are also common (Alexander, 2011; Leviston et al., 2006). Concerns have also been raised about additional costs resulting from new water supply methods, and consumers are often unwilling to pay higher fees for water supplies (Alexander, 2011; Leviston et al., 2006; Rawluk et al., 2013).

Social risks related to the lack of communication and information (stage i and iv). Informing the public about a planned MAR project in written and oral forms is a fundamental step in the early development stage (ASCE and EWRI, 2020). It is essential to communicate and provide open access to information. Educating the public about benefits, potential problems, MAR's unknown factors and their handling can increase the transparency of the project and social acceptability (Alexander, 2011; Bekele et al., 2008). In a study by Leviston et al. (2016), the availability of information and possibilities for learning more about MAR implementation, monitoring and maintenance were identified as being essential and more important than a sole assurance of safety. In contrast, it may often not be intuitive for scientists and engineers to engage stakeholders in the planning of MAR schemes (Richter et al., 2014).

Social risk related to source water (stage ii). The behaviour of the public can affect groundwater quality around MAR scheme, for example e.g., washing/bathing near wells or using buffer zone/groundwater protection zones for recreational purposes (Bartak et al., 2015; Bugan et al., 2016). In a study of El-Fakharany (2013), potential socio-economic issues were addressed that could arise from required resettlement or the loss of farmland, which may result from MAR-site construction.

Economic risks related to the financing of MAR schemes (stage i and iii). Within the planning stage, primary economic risks are related to the financing of the MAR project and the realisation of long-term economic benefits. One of the core discrepancies for financing water projects is that water users, as primary beneficiaries, often have insufficient funds to support such projects; this problem has been identified as being particularly acute in developing countries (Maliva, 2014). Moreover, there is a time lag between paid construction costs and the realization of a project's benefits, which may lead the main beneficiaries to consider the investment in the MAR system infeasible in terms of costs and benefits (Maliva, 2014).

Economic risks related to MAR operation and management (stage iii and iv). When it comes to the operational phase of MAR, failure to meet performance objectives is considered to be a principal source of economic risks and associated uncertainties, e.g., if the recharge of water does not result in an adequate increase of groundwater levels (Maliva, 2014). At the same time, the expectation that adequate pre-treatment would mitigate clogging is not always true, as clogging during recovery may be a consequence of changes in water quality at the storage stage (Nandha et al., 2015). This important operational risk can result in high maintenance costs and consequently lead to unforeseen expenses during the operation and management stage of MAR schemes (Maliva, 2014).

Economic risks related to water demand (stage i). Another source of economic risks can be that revenues realised from MAR operation are lower than anticipated at the design stage because the expected water demand has not been fully realized. Irrigation demand, for example, is highly dependent upon climate conditions and the profitability of MAR schemes may vary noticeably under different climate change scenarios (Rupérez-Moreno et al., 2017). In addition, MAR systems can be sensitive to extreme climate events. Floods can put riverbank filtration wells at risk of contamination and potential damage that may severely affect drinking water production in flood-prone areas (Sandhu et al., 2018). Finally, MAR water demand for drinking purposes, which is particularly high during dry seasons, depends heavily on the consumers' perception of the safety of MAR water for household consumption (Hasan et al., 2019).

7.5.5 Risks related to legislation and governance

Issues related to regulation and legislation are hugely important, even in the MAR planning phase. This includes, among others, construction permits and an appropriate coordination with governmental agencies. In addition to technical skills, a legislative background is essential for successful MAR implementation and operation (Rodríguez-Escales et al., 2018). Risks related to legislation and governance are rarely considered in the reviewed literature. For example, the Australian guidelines (NRMMC, 2006; NRMMC, 2009) highlight potential risks related to inadequate education and information on already permitted MAR uses, which might lead to an unauthorized use of MAR and endanger its proper operation. The absence of clear regulations and the need for several different licenses can make the planning procedure very time consuming and difficult, which may decrease the willingness to start a new MAR project (Nandha et al., 2015). Fernández Escalente et al. (2020) emphasize that a clear approval system and clear water ownership rules have to be defined prior to adapting regulations for MAR. Li and Ji (2016) highlight that government policies can support environmental protection (e.g., by setting up protected natural areas), but may also cause environmental impacts (such as land use changes or urbanization): both can hinder MAR implementation.

7.6 Discussion

7.6.1 History and geographic relation of publications on MAR risk assessment

Whereas the assessment of human health, environmental and socioeconomic risks has been well established for many decades, its specific design and application for MAR implementation and operation has only received increasing attention in recent years Among the reviewed literature, the total number of published studies on MAR risk assessment has increased steadily since the middle of the past decade (Figure 7-2a). Australia plays a pioneering role for the development and application of MAR risk assessment: early publications refer to this continent. Among the reviewed literature, an increasing number of publications related to Europe and other regions have been available since 2010 (Figure 7-2a). This coincides with the publication of the Australian MAR guidelines in 2009, which may have prompted the publication of further studies on MAR-related risk assessment. Also 16 of the 34 considered publications after 2009 refer to the Australian guidelines for their methodology (cf. Table D-1). Publication of MAR research peaked in 2015, which can partly be explained by the publication of results that were obtained from the DEMEAU project (Demonstration of promising technologies to address emerging pollutants in water and waste water; Gibert et al., 2015; Seis et al., 2015). Other contributions to this peak are the publication of Assmuth et al. (2016) (risk assessment methodology) and de los Cobos (2018) (MAR site in Switzerland). When looking at the regions covered by the reviewed studies, about 40 % of the studies available to date refer to Australia (Figure 7-2b), followed by Europe (~21%), Asia (~14%), America (~5%) and Africa (~5%). Around 16% of the analysed publications incorporate several case studies (details can be found in Table D-1). The contents of the publications varied: some focused on special aspects and did not provide any particular insight into the MAR site (e.g., Song et al., 2019) whereas others provided detailed information and analysis for a case study (e.g., Swierc et al., 2005).

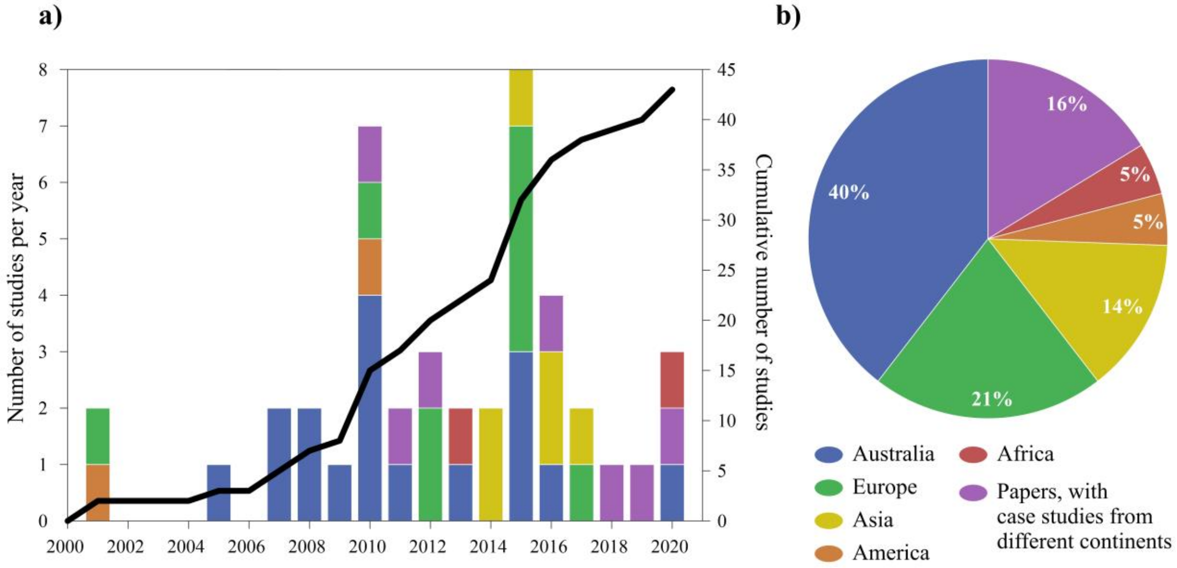

Figure 7-2. Temporal development of publication activity concerning the reviewed literature (based upon data given in Table D-1): a) cumulative number of available studies (black line) and number of papers that appeared per year (bars), b): percentage of studies that refer to MAR risk assessment on a specific continent (percentage of all reviewed publications).

7.6.2 Common MAR risk assessment methodologies and types

The Australian guidelines, including the methodologies of qualitative risk assessment, quantitative risk assessment (QRA) and quantitative microbial risk assessment (QMRA), are applied in about half of the reviewed publications (Table D-1 in the Appendix D). An HACCP analysis was conducted in five case studies accounting for ~12 % of all reviewed case studies. About a third of the considered literature refers to quantitative microbial risk assessment (cf. Table D-1). Among the different risk types, human health and environmental risks were addressed in two thirds of the reviewed publications, followed by technical and socioeconomic risks and risks related to legislation and governance (Figure 7-3). The focus on environmental and human health risks can be related to existing regulations for these risks at a national level. Table D-4 is intended as an overview on methodologies and guidelines that address specific risk types.

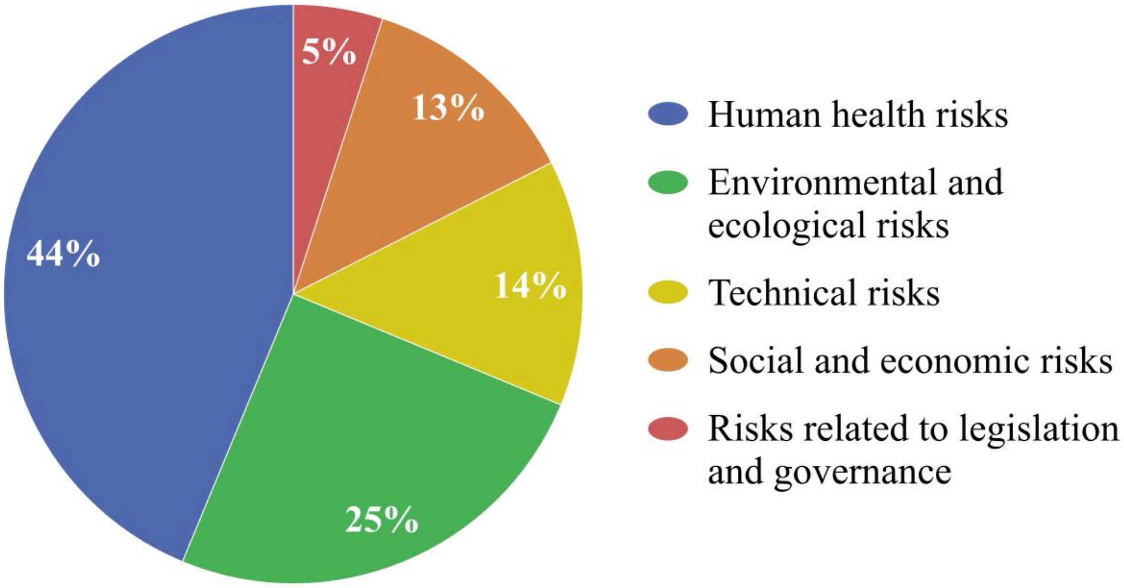

Figure 7-3. Percentages of different risk types in the analysed publications, i.e. (i) human health risks, (ii) environmental risks, (iii) technical risks, (iv) social and economic risks and (v) risks related to legislation and governance. Some of the analysed publications cover two or more risk types (the presented percentages are based upon data provided in Table D-1).

7.6.3 Limitations of risk assessment methodologies and lessons learned from their application and development

Several risk assessment methodologies also recommended in the Australian guidelines, such as QMRA and QRA, require a large amount of detailed input data (e.g., Dillon et al., 2020b; Toze et al., 2010). These data are usually obtained from monitoring and provide the basis of quantitative risk assessments. If such detailed data cannot be obtained with reasonable efforts, stochastic risk assessment approaches can help with the interpretation of the available data (e.g., Ji and Lee, 2017). Another important advantage of using stochastic approaches is that the uncertainty and variability of data and assumptions can be addressed (e.g., Page et al., 2009). Page et al. (2010a; 2010b; 2008) coupled QMRA and Damigos et al. (2016) CBA with Monte Carlo simulation in order to provide a stochastic analysis that accounts for uncertainty and variability and estimate risks based on the outcome.

If no data are available, a qualitative risk assessment (instead of quantitative risk assessment), such as one based upon sanitary surveys, can also be used as an adequate option as proposed by Dillon et al. (2014) in the Indian guidelines. Havelaar (1994) argues that risk identification that implements HACCP frameworks may be biased by the opinions of the planners and operators. To overcome such bias, Ji and Lee (2017) suggested, among others, that all chemicals emitted by a source should be investigated with a pollutant release and transfer function, so that all emitting sources are assessed in the same manner. Nandha et al. (2015) state that the Australian guidelines for MAR focus on potential hazards and thus might not be suitable for process-oriented considerations.

A large number of the reviewed studies focussed on the MAR planning stage, while fewer dealt with the MAR operation and maintenance stage, the assessment of the MAR catchment (or MAR water source) and the distribution and final use of water provided by MAR (cf. Table D-2). However, only five of the recommended risk assessment approaches in the reviewed literature can be applied to cover all four stages of MAR implementation and operation, as well as for the assessment of the four defined risk types. These are (i) the HACCP framework, (ii) the use of water safety plans (WSP) (iii) qualitative risk assessment, (iv) integrated human health risk framework for MAR and (v) the fault tree approach (cf. Table D-4). Nandha et al. (2015), however, found that HACCP and WSP might fail to identify risks specific to MAR-related processes.

The consideration of risk multidimensionality, e.g., via impact chains, is important in order to cover all relevant risk sources and also to take into account influences between different hazards. The following three methodologies were found to include such risk multidimensionality: (i) the fault tree approach developed by Rodríguez-Escales et al. (2018), (ii) the integrated human health risk framework for MAR (Assmuth et al., 2016) and (iii) the public health and economic risk assessment approach developed by Juntunen et al. (2017).

7.6.4 Limitations of reviewed publications

Based on our review focus, we have to take into account certain limitations: we presume that risk assessment studies are often subject of internal reports, prepared by consultancies or MAR operators (e.g., Bloetscher, 2001; Bouwer et al., 2008; Clark et al., 2005), and in many cases they are not publicly available. Furthermore, our review is restricted to publications in English, so that any studies prepared in other languages are not considered. In fact, we assume that aforementioned reasons may explain the limited availability of publications on risk assessments for MAR operations in North and South America, even though MAR is practiced there (e.g., Dillon et al., 2019; Zhang et al., 2020) and a risk assessment is required (ASCE, 2020; MOP, 2014; SEMARNAT, 2009). This is prominent also for MAR in the U.S., which are amongst the countries with the highest installed MAR capacities, worldwide (Dillon et al., 2019).

Apart from Australia, Chile and India, other countries have also published guidelines on MAR implementation and operation: these guidelines acknowledge that a risk assessment should be conducted, but they do not suggest specific methodologies. We found such guidelines for the Netherlands, U.S., Italy and Mexico, amongst others (ASCE and EWRI, 2020; MVROM, 1993; MATM, 2016; SEMARNAT, 2009). A guideline for planning and authorizing MAR schemes is available for South Africa that includes questionnaires for risk identification, however no specific methods for risk analysis or evaluation (Ravenscroft and Murray, 2010).

7.7 Conclusions

Overall, MAR in connection with holistic risk management can be seen as a viable option for reaching the WHOs' Sixth Sustainable Development Goal. Based on the research questions of this review, we can draw the following conclusions:

- Within the past two decades, a strong increase of literature on MAR-related risk assessment started after publication of the Australian MAR guidelines in 2009.

- Human health and environmental risks have most widely been addressed in the considered literature (Figure 4-3), and it can be assumed that the latter risks will be of fundamental importance also in the future. Concerning environmental risks, where in particular groundwater-dependent ecosystems are expected to be directly impacted by MAR, limited data availability is a common problem that needs attention for selecting adequate risk assessment methodologies. We encourage future research to help identify risks of MAR implementation and operation for comprehensive risk management plans, including human health and environmental risks as well as technical risks and risks related to legislation and governance.

- To date, apart from Australia, there is a lack of legally binding MAR frameworks (including risk assessment approaches). It is recommended that policy makers implement holistic risk assessment approaches in their MAR guidelines. Further research could also focus on effective legislative measures in order to enhance the implementation and operation of MAR schemes.

- Only a few risk assessment approaches seem to exist, to date, that consider a holistic risk assessment including human health and environmental risks, technical, social and economic risks as well as risks related to legislation and governance. We encourage that for the development of risk assessment methodology, a process-based approach is used and risks are considered comprehensively.

The development of holistic risk management plans can improve social acceptability and can contribute to a safer implementation and operation of MAR schemes. In addition to a process-based holistic risk assessment approach, we recommend evaluating a MAR scheme also in the context of sustainability, social acceptability and economic feasibility.

Chapter 8 Synoptic discussion

This thesis addresses the characterization of hydraulic and biogeochemical processes in the subsurface related to anthropogenic impacts and the potential use of managed aquifer recharge (MAR). Reactive transport processes are analysed by interpreting carbon isotope measurements of herbicides as well as recovery rates of herbicides and metabolites. Analytical and numerical modelling approaches are deployed to describe stable water isotope and herbicide transport in two vegetated field lysimeters. With different modelling approaches and different modelled constituents, influences of subsurface processes, including preferential flow, immobile water influences, root water, and chemical plant uptake, sorption, and degradation, were investigated. Finally, governing processes for the study site were distinguished to describe observations with the different model approaches adequately. Further, the effects of soil texture on subsurface flow and transport processes were identified.

At the study site in Wielenbach, Germany, the weight and drainage rates of two cropped lysimeters were measured. Additionally, stable water isotope content and herbicide concentration in the lysimeter drainage were analysed. The measurement period was 3,5 years for the stable water isotopes and 4,5 years for the herbicide measurements. Such long data sets have the advantage of representing the environmental conditions for seasonal or vegetative influences at the study site and therefore allow a robust model calibration. Shorter data series (e.g., only measurements in the summer or winter) utilized for boundary conditions of a model might lack the representation of changing environmental conditions and lead to increased uncertainty of the model results. Consequently, we can achieve robust model calibration and derive reliable information on processes and their rates for the unsaturated flow and transport models applied for our study case. To the authors' knowledge, few studies are available that analyse and model an equally long time series of stable isotopes in lysimeters.

Such an extensive data set not only allows to calibrate robust models but also the behaviour and applicability of newly developed models can be tested under different seasonal or vegetative influences. In the publication by Imig et al. (2022a) (cf. Chapter 4), an improved lumped-parameter model was developed, and its capability to describe the data set of the lysimeter site was investigated. Common practice is verifying new model approaches' results by comparing them to the results of existing established models (e.g., Anderson et al., 2015). Therefore, the results of the improved LPM were compared to results from the numerical model HYDRUS-1D. For Lysimeter 1, derived mean transit times of water and dispersion parameters from both modelling approaches were in the same range, whereas for Lysimeter 2, in addition to (slight) differences in the dispersion parameter, mean transit times of water differed notably. These differences could not be fully explained: uncertainties for numerical modelling were associated, among others, with missing measurements within the soil columns, such as of water content, pressure head or stable water isotopes. As an advantage of the extended LPM approach, uncertainties of flow characterization are reduced by identifying ranges of plausible parameters (over the simulation period) because of vegetative or seasonal changing flow (and transport) conditions.

In the publication by Imig et al. (under review, a) (cf. Chapter 5), multi-process models in HYDRUS-1D were investigated to describe stable water isotopes and identify governing processes of flow and transport at the study site. When considering a dual-porosity system for including the description of immobile water, improved statistical model performance for Lysimeter 2 was achieved. For Lysimeter 1, considering a single or a dual-porosity system resulted in very similar statistical model performance. For both lysimeters, the consideration of passive root water and chemical plant uptake slightly improved model fits. In contrast, considering evaporation fractionation of stable water isotopes led to no clear improvements. Differences in how strongly some processes revealed to contribute to flow and transport between the two lysimeters can be related to the soil texture and structure, as vegetative and environmental conditions were the same. For example, a higher fraction of fine pores in Lysimeter 2 is available for water storage, leading to mixing processes of isotopically enriched summer precipitation water and lighter winter water, which could explain the immobile water influences.

With the consideration of additional processes in the model setup, the complexity of a model increases, and with it, the number of fitting parameters. Fitting more parameters will complicate identifying a physically plausible solution with a numerical model (Anderson et al., 2015). For our study case, it could be argued that the lack of information within the lysimeter (e.g., measured hydraulic potential and water content at different depths of the soil columns) makes the identification of a plausible best-fit solution with more fitting parameters difficult and prone to error. Obtaining additional measurements from within the lysimeter, e.g., plants or root lengths, water or stable isotope contents, could help to understand if a good statistical model performance is related to mere fitting success or to the physically based ability of the model to describe the natural environment.

In the publication by Imig et al. (under review, b) (cf. Chapter 6), the concentrations of four herbicides in lysimeter drainage were modelled in addition to stable water isotopes. The calibrated unsaturated zone model of the lysimeters was extended to consider reactive transport to describe herbicide transport. The aim was to identify governing reactive transport processes of the herbicides in the subsurface and determine the leaching potential to groundwater and contamination potential to soil. Recovery rates of 0.9-15.9% of applied herbicides in lysimeter drainage (up to 20.9% if including measured metabolites) were found. Metabolite formation and accumulation were observed in lysimeter drainage. The presence of biodegradation was also indicated by small changes in stable carbon isotope contents of herbicides between input and drainage. Over time, an enrichment in heavier carbon isotopes in the drainage samples was observed. This points towards a higher biodegradation activity over time, where the infiltrated (contaminated) water resided a longer time in the subsurface (presumably dominated by matrix flow) compared to early observations (where rapid flow paths presumably dominated herbicide leaching).

Also, soil structure influences could be identified with the herbicide fate and transport model. Contrary to our initial hypothesis, the clayey, sandy silt of Lysimeter 2 showed higher recovery rates of some herbicides in the lysimeter drainage than the sandy gravel of Lysimeter 1. For Lysimeter 2, an immobile phase was considered in the model setup, and the resulting smaller mobile phase dominated solute transport. For peak flow events, it is expected that the immobile water phase will not be available for mixing, so the solute will only be mixed within the available mobile region. This can lead to higher solute concentrations in the drainage during peak flow events, resulting from a smaller mobile phase in Lysimeter 2.

Herbicide concentration peaks in drainage were connected in time with higher amounts of precipitation, indicating an influence of preferential flow. Further, short-time fluctuations of stable water isotopes were also related to preferential flow influences. The investigated LPM was able to consider preferential flow influences for stable water isotopes and could describe resulting short-term fluctuations. For the HYDRUS-1D model, it was initially hypothesized that the dual-porosity model setup could also cover, to some extent, the influence of preferential flow. The single and dual-porosity setups in HYDRUS-1D under- or overestimated herbicide concentration peaks and fell short of describing short-term fluctuations of stable water isotopes in drainage. It is presumed that a dual-permeability model could be better suited to describe preferential flow influences and hence observed herbicide concentration peaks and short-term fluctuations of stable water isotopes. Unfortunately, currently available HYDRUS-1D versions do not allow the implementation of a dual-permeability approach for stable water isotope modelling. Therefore, it was not possible to investigate the application of a dual-permeability model for coupling an interpretation of observed stable water isotopes (for flow characterization) with herbicide monitoring (for reactive transport modelling). Since two mobile regions are considered, the dual-permeability setup requires the parametrization of two soil hydraulic and transport parameter sets. Therefore, we refrained from such a procedure, which would solely be based on herbicide measurements in lysimeter drainage: limited availability of measurements (such as missing observations within the soil column) and reactivity of herbicides are associated with considerable uncertainties.

Both the applied LPM and the HYDRUS-1D models underestimated stable water isotope contents observed in the drainage of Lysimeter 2. However, since different models (improved LPM and HYDRUS-1D) and model setups (single- and dual-porosity, isotopic fractionation) were compared, we could speculate that shortcomings in describing observations by modelling could also be related to input data and boundary conditions. The input data for the LPM and HYDRUS-1D model describing the stable water isotope content in precipitation was not measured at the study site for the modelling pre-phase. Measurements were available from a location in Passau-Fürstenzell about 200 km to the northeast of Wielenbach and at about 200 m lower elevation. The slope of the local meteoric water line (LMWL) between precipitation sampled at the Wielenbach site and the meteorological station Passau-Fürstenzell were very similar (Shajari et al., 2020). Therefore, the input from Passau-Fürstenzell was considered applicable for the description of the study site Wielenbach within the applied models. In additional tests, sensitivity analyses of the boundary condition of stable water isotope content in precipitation on modelling results were performed. We found that seasonal changes of stable water isotopes in the modelling pre-phase have considerable effects on the stable water isotope content at the beginning of the modelling period. The stable water isotope content from another site (Passau-Fürstenzell) might deviate from the one at the Wielenbach site. Since the mean residence time of water in Lysimeter 2 is higher than in Lysimeter 1, stable water isotope contents of the pre-phase might reside within Lysimeter 2 longer and hence affect the isotopic signature of the drainage. Even though the criterion of similar slopes of the LMWLs for testing the applicability of the measured values at Passau-Fürstenzell was fulfilled, there might still be essential deviations for adequate model description. Furthermore, the lack of water content, hydraulic potential, or stable water isotope content measurements within the lysimeter for numerical model calibration might also explain shortcomings in the isotope signature description.

As described above, different HYDRUS-1D setups were compared to describe both stable water isotope contents and herbicide concentrations in lysimeter drainage (cf. Chapters 5 and 6). Throughout this work, we followed the parsimony principle. In the case of different options, we selected those model setups that use the lowest number of fitting parameters yet achieve an appropriate model fit. Single- and dual-porosity model setups were applied for stable water isotope transport. The more complex dual-porosity setup did improve statistical model performance for Lysimeter 2; however, for Lysimeter 1, only slight improvements were observed. When selecting the model setup for Lysimeter 1 to extend it with reactive transport to describe herbicide concentration in drainage, we thus choose the single-porosity model setup to proceed.

Different setups for describing sorption processes were also compared when modelling reactive herbicide transport in the lysimeters. These included equilibrium sorption (linear isotherm, Freundlich and Langmuir isotherms) and non-linear sorption, including two-site kinetic sorption model setups. Compared to equilibrium linear sorption, the more complex approaches did not improve model performance. These more complex approaches might describe sorption processes more adequately; however, no measurements of sorption (and biodegradation) parameters were available for our soils and compounds, so the parameters had to be estimated. The lack of more detailed measurements implied additional uncertainties, and following the parsimony principle, we applied the simpler (equilibrium linear sorption) approach, requiring fewer input parameters.

Konikow (2011) argued that it might not be expected that subsurface solute transport models can exactly reproduce the measured data but rather be applied to test conceptual model ideas. In a review, Köhne et al. (2009) compared different subsurface pesticide, transport models. They argued that a satisfactory prediction might be reached if the deviation between measured and modelled concentrations is around factors 3-5. For blind validation studies, deviations by one or several orders of magnitude were documented. We reached factors 2-5 in our modelling results so that we may consider our fit reasonably well. Moreover, in the existing literature, we found no comparable long-term, multi-application modelling studies of herbicides in field lysimeters. Approaches are published for shorter terms studies and single herbicide applications; however, these might fail in describing longer-term observations with several herbicide applications on scales bigger than laboratory batch or lysimeter scales. We found studies that applied a compound only once, and not like in the present study, five times over the modelling period (e.g., Celestino Ladu and Zhang, 2011; Jiang et al., 2010; Noshadi et al., 2019; Pot et al., 2005). The longest investigated time frame was half a year and in soil columns of 1.2 m (Noshadi et al., 2019). It can thus be concluded that the development of models to describe reactive transport of herbicides does not have reached final maturity, yet, but research should continue. Our study therefore contributes to the knowledge of long-term behaviour of herbicides in the subsurface considering several application events and compounds. Different influences such as soil texture with the same vegetation and under the same climatic conditions were investigated. Further, information on adequate model description of long-term herbicide transport in the subsurface were obtained.

Furthermore, risk assessment methodologies of MAR were part of this thesis (Imig et al., 2022). The publication aimed to review existing MAR risk assessment methodologies critically and identify frequently considered risks. In addition, we assume that an improved understanding of flow and transport processes (as elaborated in our lysimeter studies) can help mitigate potential risks arising from MAR schemes since the prediction of contamination spreading or clogging processes, in greater detail, will be possible.

In total, we found five risk assessment guidelines and ten risk assessment methodologies which have been applied to date to investigate risks related explicitly to MAR. Within the past two decades, there has been a marked increase in the literature on MAR-related risk assessment following the publication of the Australian MAR guidelines in 2009.

We have differentiated between specific risk types, including (i) human health risks, (ii) environmental risks, (iii) technical risks, (iv) social and economic risks, and (v) risks related to governance and legislation (similar to Rodríguez-Escales et al., 2018). Among the different risk types, human health and environmental risks were addressed in two-thirds of the reviewed publications, followed by technical and socioeconomic risks and risks related to legislation and governance. The focus on environmental and human health risks could be related to existing regulations for these risks at a national level.

Furthermore, we have considered four different stages of MAR implementation and operation: risks may arise from, or relate to, (i) the planning of MAR, (ii) the catchment or water source for MAR, (iii) MAR operation (such as infiltration, storage, recovery) and maintenance, and (iv) water distribution and final water use (similar to Ji and Lee, 2016; Nandha et al., 2015). However, only five of the recommended risk assessment approaches in the reviewed literature can be applied to cover all four stages of MAR implementation and operation and assess the five defined risk types.

Apart from Australia, there is a lack of legally binding MAR frameworks (including risk assessment approaches). Several countries have also published MAR implementation and operation guidelines: these guidelines acknowledge that a risk assessment should be conducted, but they do not suggest specific methodologies. We support the finding of Fernández Escalante et al. (2020) and Page et al. (2020) that the lack of regulatory frameworks often hinders the implementation of MAR schemes. Within the project DEEPWATER-CE, we have collected national legislation of MAR in Central Europe. It was found that currently, no consistency exists in the regulative frameworks, even though all investigated countries (Hungary, Poland, Slovakia, Croatia and Germany) already have transposed EU water framework and drinking water directives into national laws (DEEPWATER-CE, 2021). Building trust in key regulating organizations, such as drinking water regulators, health agencies and public water systems, can potentially help promote the use of MAR systems (Leviston et al., 2006; Mankad et al., 2015).

Chapter 9 Conclusion

The findings obtained from the presented articles contribute to an improved understanding of hydraulic and biogeochemical processes in the subsurface and their description with different modelling approaches.

The extended lumped-parameter model suggested by Imig et al. (2022a) (Chapter 4) was successfully applied to describe measured stable water isotope contents in the drainage of two cropped lysimeters. It can be concluded that the improved LPM represents a valuable tool for flow and transport characterization in the unsaturated zone, with the advantage of lower data requirements compared to numerical modelling.

Moreover, multi-process modelling for stable water isotope and herbicide transport in the unsaturated zone proved to be a powerful means for understanding governing fate and transport processes and their rates. Stable water isotope measurements were successfully utilized to calibrate flow models for the lysimeters. Model results highlight the influence of soil texture and structure on flow and transport. In fine soil textures, immobile water influences were observed to be more pronounced than in coarse textures. The consideration of passive root water and chemical plant uptake slightly improved model fits. Evaporation fractionation processes consideration for stable water isotopes led to no clear statistical improvements of the model performance and was hence considered to be of minor influence.

Observed herbicide metabolite formation and accumulation in lysimeter drainage let us conclude that biodegradation processes contributed to the fate of herbicides within the lysimeters. Further, an enrichment of carbon isotopes of herbicides over time in lysimeter drainage was measured. This points towards higher biodegradation of the infiltrated (contaminated) water residing longer in the subsurface compared to water within preferential flow paths.

Recovery rates of herbicides in lysimeter drainage were higher for finer than for coarser soils, supporting stable isotope modelling results, which indicates that soil structure and texture influence flow and transport. Based on measurements and reactive transport modelling, we presume that sorption dominates the fate of herbicides in the lysimeter, followed by biodegradation.

Findings point towards strong influences of preferential flow on peak herbicide concentrations and short-term fluctuations of stable water isotope contents in the lysimeter drainage.

Furthermore, this thesis gives a summary of existing MAR risk assessment methodologies, and their advantages and limitations are investigated. This evaluation will support planners and operators of MAR schemes in selecting an appropriate risk assessment method. We identified a lack of risk assessment methods that consider a holistic assessment of MAR schemes. A focus on environmental and human health risks taken in current literature distracts from the fact that comprehensible MAR policies and social acceptability are similarly crucial for successful MAR implementation and operation. The highlighted limitations of existing risk assessment methods could facilitate the development of specific MAR guidelines, which include holistic risk assessment approaches. Additionally, an overview of the potential risks of MAR schemes will further facilitate the risk assessment process and hence support the development of risk treatment options to ensure safe MAR operation.

By advancing our understanding of hydraulic and biogeochemical processes in the subsurface we can design effective models to predict groundwater flow and contamination transport and fate. With enhanced prediction abilities, we can protect our aquifers from potential risks arising from, e.g., climate change-induced droughts or contamination with agricultural contaminants. This will lead to improved quantity and quality of groundwater, hence the possibility of sustaining our drinking and irrigation water supply on earth. This thesis recommends the consideration of multi-process modelling to describe water flow and solute transport in the vadose zone to be an integral part of effective model design and calibration. In addition, the information gained from the investigated study sites can be transferred to other contaminated sites with similar subsurface properties and vegetation. The findings of this study will help modellers and decision makers to identify the contamination potential of groundwater resources and risks to soil and groundwater ecosystems, e.g., for MAR implementation, operation, and management.

Chapter 10 Outlook

10.1 Modelling of unsaturated flow and transport

The work presented in Chapters 4-6 about coupling observations and modelling to interpret flow and transport processes allowed the identification of governing hydraulic and biogeochemical prosses and their rates in the unsaturated zone for the two investigated lysimeters in Wielenbach, Germany.

A detailed investigation of the uncertainty of the applied models is strongly recommended. Identifying the input and parameter range that still yields model results that match measured data (to meet the non-uniqueness of the models) could distinguish models or model setups with the most prediction integrity (Anderson et al., 2015). Currently, we are working on a project that intends to compare the uncertainty of the traditional LPM, improved LPM and HYDRUS-1D setups by applying moment-based metrics for global sensitivity analysis, named AMA method (Dell'Oca et al., 2020 and 2017).

Limitations in describing preferential flow events with the HYDRUS-1D single and dual-porosity flow models became evident, as strong herbicide peaks were often under- or overestimated by a factor of two or three and short-term stable water isotope fluctuations were not met by the model. The description could be improved with a dual-permeability model setup encompassing immobile water. Such a setup is currently unavailable for stable water isotopes in HYDRUS-1D, whose development we recommend in future work.

It is highlighted in the literature that only limited models exist to describe chemical plant uptake coupled with unsaturated flow models (e.g., Brunetti et al., 2019; Ruiz et al., 2021). Further model developments are suggested, as agriculture relies on growing plants in unsaturated conditions. Advances in chemical plant uptake models could be invaluable tools for describing and predicting nutrient and agrochemical plant uptake. Modelling results would allow the enhancement of the nutrient composition of an agricultural product. Further, human health risks arising from agrochemical intake with food could be mitigated. Therefore, verifying plant uptake with monitored plant concentrations is recommended for this study case. A more detailed model approach might be beneficial, such as considering the depth dependency of plant uptake and dynamic feedback with root processes (e.g., Brunetti et al., 2019).

With the chosen HYDRUS-1D setups, observed dynamics of herbicide concentrations in lysimeter seepage water could be described reasonably well. However, an exact reproduction of measured data was not possible in many cases. In the existing literature, no long-term, multi-application modelling studies of herbicides in field lysimeters were found that are comparable to our investigation. Reported approaches for shorter term, single herbicide application studies might thus fail in describing longer-term observations with several herbicide applications on scales bigger than laboratory batch or lysimeter scales. Hence, further investigation of herbicide fate and transport in the unsaturated zone is recommended, for example, the influence of time-dependent herbicide sorption and its implementation in HYDRUS-1D, e.g., following Mamy and Barriuso (2007).

10.2 Lysimeter experimental setup

Obtaining measurements within the lysimeter soil core at different depths or further information on soil properties could improve the model description. For example, the importance of organic carbon for the sorption of herbicides is extensively documented in the literature, e.g., by Cabrera et al. (2008), Cox et al. (1997), Jaikaew et al. (2017) and Wang et al. (2010). Because of the absence of measurements of soil organic carbon or other parameters such as pH or cation exchange capacity (e.g., recommended by Sarmah and Sabadie, 2002), we could not investigate their influence on herbicide sorption in the studied lysimeters. Therefore, when setting up a lysimeter experiment, we strongly suggest taking samples from the soil core material at different depths and determining the organic carbon content and other parameters (e.g., pH, temperature, cation exchange capacity). It is further recommended to measure and continuously monitor, e.g., soil water content, hydraulic potential, and stable water isotopes at different depths, which could be especially important for a flow model calibration.

10.3 Limitations of current risk assessment methodologies for MAR

Our research concludes that there is currently a lack of risk assessment methods that consider a holistic assessment of MAR schemes. Thus, we encourage the development of holistic risk assessment methodologies, such as building upon process-based approaches. Currently, we are preparing a manuscript with the working title “Holistic assessment of managed aquifer recharge through technical feasibility and extended cost-benefit analysis - An application for Grand Bahama”, in which we have developed a holistic risk assessment methodology (see Appendix E). Further, concerning environmental risks, limited data availability is a frequent problem that needs attention for selecting adequate risk assessment methodologies. Finally, we encourage future research to help identify risks of MAR implementation and operation for comprehensive risk management plans, including human health and environmental risks, as well as technical and economic risks and risks related to legislation and governance.

References

Abbasi, F., Jacques, D., Simunek, J., Feyen, J., van Genuchten, M.T., 2003. Inverse estimation of Soil Hydraulic and Solute Transport Paarameters from Transient field Experiments: Heterogenous Soil. Trans. Am. Soc. Agric. Eng. 46, 1097–1111.

Aertgeerts, R., Angelakis, A., 2003. State of the Art Report Health Risks in Aquifer Recharge Using Reclaimed Water Water, Sanitation and Health Protection and the Human Environment World Health Organization Geneva and WHO Regional Office for Europe.

Ahmad, K.S., Rashid, N., Azhar, S., 2016. Adsorption and desorption characteristics of chlorosulfuron in selected minerals and Pakistani soils. Eurasian J. Soil Sci. 5, 1. https://doi.org/10.18393/ejss.2016.1.001-012

Ahuja, L.R., Rojas, K.W., Hanson, J.D., Shaffer, J.J., Ma, L., 2000. The Root Zone Water Quality Model. Water Resources Publications LLC, Highlands Ranch, CO.

Alcade-Sanz, L., Gawlik, B.M., 2017. Minimum quality requirements for water reuse in agricultural irrigation and aquifer recharge - Towards a legal instrument on water reuse at EU level. Luxembourg. https://doi.org/10.2760/887727

Alexander, K.S., 2011. Community attitudes towards Managed Aquifer Recharge and stormwater use in Adelaide , Australia. 8th Int. Conf. Water Reclam. Reuse 1–11.

Alfarrah, N., Walraevens, K., 2018. Groundwater overexploitation and seawater intrusion in coastal areas of arid and semi-arid regions. Water (Switzerland) 10. https://doi.org/10.3390/w10020143

Ali, M., Wang, J.J., DeLaune, R.D., Seo, D.C., Dodla, S.K., Hernandez, A.B., 2013. Effect of redox potential and pH status on degradation and adsorption behavior of tylosin in dairy lagoon sediment suspension. Chemosphere 91, 1583–1589. https://doi.org/10.1016/j.chemosphere.2012.12.050

Allison, G.B., Barnes, C.J., Hughes, M.W., Leaney, F.W.J., 1984. Effect of climate and vegetation on oxygen-18 and deuterium profiles in soils. IAEA, International Atomic Energy Agency (IAEA).

An, Q., Wu, Y., Li, D., Hao, X., Pan, C., Rein, A., 2022. Development and application of a numerical dynamic model for pesticide residues in apple orchards. Pest Manag. Sci. https://doi.org/10.1002/ps.6897

Anderson, M.P., Woessner, W.W., Hunt, R.J., 2015. Applied Groundwater Modeling, Applied Groundwater Modeling. https://doi.org/10.1016/c2009-0-21563-7

Arias-Estévez, M., López-Periago, E., Martínez-Carballo, E., Simal-Gándara, J., Mejuto, J.C., García-Río, L., 2008. The mobility and degradation of pesticides in soils and the pollution of groundwater resources. Agric. Ecosyst. Environ. 123, 247–260. https://doi.org/10.1016/j.agee.2007.07.011

References

Arshad, M., Guillaume, J.H.A., Ross, A., 2014. Assessing the feasibility of managed aquifer recharge for irrigation under uncertainty. Water (Switzerland) 6, 2748–2769. https://doi.org/10.3390/w6092748

Asadollahi, M., Stumpp, C., Rinaldo, A., Benettin, P., 2020. Transport and Water Age Dynamics in Soils: A Comparative Study of Spatially Integrated and Spatially Explicit Models. Water Resour. Res. 56, no. https://doi.org/10.1029/2019WR025539

ASCE American Society of Civil Engineering EWRI Environmental and Water Research Institute, 2020. Standard Guidelines for Managed Aquifer Recharge, Standard Guidelines for Managed Aquifer Recharge. https://doi.org/10.1061/9780784415283

Assmuth, T., Simola, A., Pitkänen, T., Lyytimäki, J., Huttula, T., 2016. Integrated frameworks for assessing and managing health risks in the context of managed aquifer recharge with river water. Integr. Environ. Assess. Manag. 12, 160–173. https://doi.org/10.1002/ieam.1660

Ayuso-Gabella, N., Page, D., Masciopinto, C., Aharoni, A., Salgot, M., Wintgens, T., 2011. Quantifying the effect of Managed Aquifer Recharge on the microbiological human health risks of irrigating crops with recycled water. Agric. Water Manag. 99, 93–102. https://doi.org/10.1016/j.agwat.2011.07.014

Barba, C., Folch, A., Gaju, N., Sanchez-Vila, X., Carrasquilla, M., Grau-Martínez, A., Martínez-Alonso, M., 2019. Microbial community changes induced by Managed Aquifer Recharge activities: Linking hydrogeological and biological processes. Hydrol. Earth Syst. Sci. 23, 139–154. https://doi.org/10.5194/hess-23-139-2019

Barbagli, A., Jensen, B.N., Raza, M., Schüth, C., Rossetto, R., 2019. Assessment of soil buffer capacity on nutrients and pharmaceuticals in nature-based solution applications. Environ. Sci. Pollut. Res. 26, 759–774. https://doi.org/10.1007/s11356-018-3515-8

Barra Caracciolo, A., Giuliano, G., Grenni, P., Guzzella, L., Pozzoni, F., Bottoni, P., Fava, L., Crobe, A., Orrù, M., Funari, E., 2005. Degradation and leaching of the herbicides metolachlor and diuron: A case study in an area of Northern Italy. Environ. Pollut. 134, 525–534. https://doi.org/10.1016/j.envpol.2004.08.014

Bartak, R., Page, D., Sandhu, C., Grischek, T., Saini, B., Mehrotra, I., Jain, C.K., Ghosh, N.C., 2015. Application of risk-based assessment and management to riverbank filtration sites in India. J. Water Health 13, 174–189. https://doi.org/10.2166/wh.2014.075

Bartram, J., Fewtrell, L., Stenström, T.-A., 2001. Water Quality — Guidelines, Standards and Health: Assessment of Risk and Risk Management for Water-related Infectious Disease, WHO.

Bear, J., 1972. Dynamics of Fluids in Porous Media. American Elsevier Publishing Company, New York.

References

Bekele, E., Page, D., Vanderzalm, J., Kaksonen, A., Gonzalez, D., 2018. Water recycling via aquifers for sustainable urban water quality management: Current status, challenges and opportunities. Water (Switzerland) 10, 1–25. https://doi.org/10.3390/w10040457

Bekele, E., Toze, S., Higginson, S., Blair, P., Heitz, A., Browne, A., Leviston, Z., Po, M., Nancarrow, B., Tucker, D., Porter, N., Mcguinness, N., Rodriguez, C., Devine, B., 2008. Determining Requirements for Managed Aquifer Recharge in Western Australia : Progress Report. Water.

Bekele, E., Toze, S., Patterson, B., Higginson, S., 2011. Managed aquifer recharge of treated wastewater: Water quality changes resulting from infiltration through the vadose zone. Water Res. 45, 5764–5772. https://doi.org/10.1016/j.watres.2011.08.058

Benettin, P., Queloz, P., Bensimon, M., McDonnell, J.J., Rinaldo, A., 2019. Velocities, Residence Times, Tracer Breakthroughs in a Vegetated Lysimeter: A Multitracer Experiment. Water Resour. Res. 55, 21–33. https://doi.org/10.1029/2018WR023894

Berkowitz, B., Ishai, D., Yaron, B., 2014. Contaminant Geochemistry Interactions and Transport in the Subsurface Environment.

Biswas, A.K., Tortajada, C., Rohner, P., 2018. Assessing Global Water Megatrends, 1st ed, Springer Nature. https://doi.org/10.1007/978-981-10-6695-5_8

Blanchoud, H., Moreau-Guigon, E., Farrugia, F., Chevreuil, M., Mouchel, J.M., 2007. Contribution by urban and agricultural pesticide uses to water contamination at the scale of the Marne watershed. Sci. Total Environ. 375, 168–179. https://doi.org/10.1016/j.scitotenv.2006.12.009

Bloetscher, F., 2001. Risk assessment applications for alternative groundwater injection programs. Bridg. Gap Meet. World’s Water Environ. Resour. Challenges - Proc. World Water Environ. Resour. Congr. 2001 111. https://doi.org/10.1061/40569(2001)153

Blood, M.R., Spagat, E., 2013. Las Posas Basin Aquifer Failure Illustrates Risks of Underground Reservoirs [WWW Document]. Assoc. Press New York City, USA.

BMU, 2008. Grundwasser in Deutschland, Bundesministerium für Umwelt, Naturschutz und Reaktorsicherheit (BMU).

Bouchard, D., Cornaton, F., Höhener, P., Hunkeler, D., 2011. Analytical modelling of stable isotope fractionation of volatile organic compounds in the unsaturated zone. J. Contam. Hydrol. 119, 44–54. https://doi.org/10.1016/j.jconhyd.2010.09.006

Bouchard, D., Hunkeler, D., Gaganis, P., Aravena, R., Höhener, P., Broholm, M.M., Kieldsen, P., 2008. Carbon isotope fractionation during diffusion and biodegradation of petroleum hydrocarbons in the unsaturated zone: Field experiment at Værløse Airbase, Denmark, and modeling. Environ. Sci. Technol. 42, 596–601. https://doi.org/10.1021/es070718f

References

Bouwer, H., Pyne, D., Brown, J., St Germain, D., Morris, T., Brown, C.J., Dillon, P., Rycus, M., 2008. Design, operation, and maintenance for sustainable underground storage facilities, Awwa Research Foundation.

Bradford, S.A., Simunek, J., Bettahar, M., Van Genuchten, M.T., Yates, S.R., 2003. Modeling colloid attachment, straining, and exclusion in saturated porous media. Environ. Sci. Technol. 37, 2242–2250. https://doi.org/10.1021/es025899u

Bradford, S.A., Yates, S.R., Bettahar, M., Simunek, J., 2002. Physical factors affecting the transport and fate of colloids in saturated porous media. Water Resour. Res. 38, 63-1-63–12. https://doi.org/10.1029/2002wr001340

Brooks, R.H., Corey, A.T., 1964. Hydraulic properties of porous media, Hydrol. Paper No. 3,. Fort Collins, Colorado.

Brovelli, A., Rossi, L., Barry, D.A., 2011. Design methodology accounting for the effects of porous medium heterogeneity on hydraulic residence time and biodegradation in horizontal subsurface flow constructed wetlands. Ecol. Eng. 37, 758–770. https://doi.org/10.1016/j.ecoleng.2010.04.031

Brunetti, G., Kodešová, R., Šimůnek, J., 2019. Modeling the Translocation and Transformation of Chemicals in the Soil-Plant Continuum: A Dynamic Plant Uptake Module for the HYDRUS Model. Water Resour. Res. 55, 8967–8989. https://doi.org/10.1029/2019WR025432

Bugan, R.D.H., Jovanovic, N., Israel, S., Tredoux, G., Genthe, B., Steyn, M., Allpass, D., Bishop, R., Marinus, V., 2016. Four decades of water recycling in Atlantis (Western Cape, South Africa): Past, present and future. Water SA 42, 577–594. https://doi.org/10.4314/wsa.v42i4.08

Bundt, M., Widmer, F., Pesaro, M., Zeyer, J., Blaser, P., 2001. Preferential flow paths: Biological “hot spots” in soils. Soil Biol. Biochem. 33, 729–738. https://doi.org/10.1016/S0038-0717(00)00218-2

Carabias-Martínez, R., Rodríguez-Gonzalo, E., Herrero-Hernández, E., Sánchez-San Román, F.J., Prado Flores, M.G., 2002. Determination of herbicides and metabolites by solid-phase extraction and liquid chromatography - Evaluation of pollution due to herbicides in surface and groundwaters. J. Chromatogr. A 950, 157–166. https://doi.org/10.1016/S0021-9673(01)01613-2

Caracciolo, A.B., Giuliano, G., Di Corcia, A., Crescenzi, C., Silvestri, C., 2001. Microbial Degradation of Terbuthylazine in Surface Soil and Subsoil at Two Different Temperatures. Bull. Environ. Contam. Toxicol. 67, 0815–0820. https://doi.org/10.1007/s00128-001-0195-7

Carbo, L., Martins, E.L., Dores, E.F.G.C., Spadott, C.A., Weber, O.L.S., DE-Lamonica-Freire, E.M., 2007. Acetamiprid,carbendazim, diuron and thiamethoxam sorption in two Brazilian tropical soils. J. Environ. Sci. Heal. Part B 42, 499–507.

Carretta, L., Cardinali, A., Marotta, E., Zanin, G., Masin, R., 2018. Dissipation of terbuthylazine, metolachlor, and mesotrione in soils with contrasting texture. J.

Environ. Sci. Heal. - Part B Pestic. Food Contam. Agric. Wastes 53, 661–668. https://doi.org/10.1080/03601234.2018.1474556

Casanova, J., Devau, N., Pettenati, M., 2016. Managed Aquifer Recharge: An Overview of Issues and Options, in: Jakeman, A.J., Barreteau, O., Hunt, J.H., Rinaudo, J.-D., Ross, A. (Eds.), Integrated Groundwater Management. Springer Nature, pp. 619–638. https://doi.org/10.1007/978-3-319-23576-9

Celestino Ladu, J.L., Zhang, D.R., 2011. Modeling atrazine transport in soil columns with HYDRUS-1D. Water Sci. Eng. 4, 258–269. https://doi.org/10.3882/j.issn.1674-2370.2011.03.003

Cheviron, B., Coquet, Y., 2009. Sensitivity Analysis of Transient-MIM HYDRUS-1D: Case Study Related to Pesticide Fate in Soils. Vadose Zo. J. 8, 1064–1079. https://doi.org/10.2136/vzj2009.0023

Chilton, P.J., Foster, S.S.., 2004. Downstream of downtown : urban wastewater as groundwater recharge 115–120. https://doi.org/10.1007/s10040-003-0296-y

Clark, Fritz, 1997. Environmental Isotopes in Hydrogeology. CRC Press LLC. https://doi.org/10.1201/9781482242911

Clark, J.E., Bonura, D.K., Voorhees, R.F. Van, 2005. An overview of injection well history in the United States of America. Dev. Water Sci. 52, 3–12. https://doi.org/https://doi.org/10.1016/S0167-5648(05)52001-X

CNR Ministerio di Agricultura, CSIRO Chile, 2020. Guía Metodológica marco operativo para proyectos de recarga artificial de aquiferos.

Coats, K.H., Smith, B.D., 1964. Dead-End Pore Volume and Dispersion in Porous Media. Soc. Pet. Eng. J. 4, 73–84. https://doi.org/10.2118/647-pa

Cox, L., Koskinen, W.C., Yen, P.Y., 1997. Sorption-Desorption of Imidacloprid and Its Metabolites in Soils. J. Agric. Food Chem. 45, 1468–1472. https://doi.org/10.1021/jf960514a

Custodio, E., 2002. Aquifer overexploitation: What does it mean? Hydrogeol. J. 10, 254–277. https://doi.org/10.1007/s10040-002-0188-6

Damigos, D., Tentes, G., Emmanouilidi, V., Strehl, C., Selbach, J., 2016. Economic Analysis of MAR Technologies.

Dann, R., Close, M., Flintoft, M., Hector, R., Barlow, H., Thomas, S., Francis, G., 2009. Characterization and Estimation of Hydraulic Properties in an Alluvial Gravel Vadose Zone. Vadose Zo. J. 8, 651–663. https://doi.org/10.2136/vzj2008.0174

Darcy, H., 1856. Les fontaines publiques de la ville de Dijon. Exposition et application des principes à suivre et des formules à employer dans les questions de distribution d’eau: Ouvrage terminé par un appendice relatif aux fournitures d’eau de plusieurs villes, au filt. V. Dalmont, Paris.

Davison, A., Howard, G., Stevens, M., Callan, P., Fewtrell, L., Deere, D., Bartram, J., 2005. Water Safety Plans Managing drinking-water quality from catchment to consumer Water, Sanitation and Health Protection and the Human Environment World Health Organization Geneva. Water 82–85.

de los Cobos, G., 2018. The Genevese transboundary aquifer (Switzerland-France): The secret of 40 years of successful management. J. Hydrol. Reg. Stud. 20, 116–127. https://doi.org/10.1016/j.ejrh.2018.02.003

de los Cobos, G., 2015. A historical overview of Geneva's artificial recharge system and its crisis management plans for future usage. Environ. Earth Sci. 73, 7825–7831. https://doi.org/10.1007/s12665-014-3575-0

DEEPWATER-CE, 2021. Comparative transnational report of CE legislation and plicies on MAR, D.T4.1.2.

DEEPWATER-CE, 2020. Common methodological guidance for DEEPQWATER-CE MAR pilot feasibility studies [WWW Document]. URL https://www.interreg-central.eu/Content.Node/DEEPWATER-CE.html

Delgado-Moreno, L., Peña, A., 2009. Compost and vermicompost of olive cake to bioremediate triazines-contaminated soil. Sci. Total Environ. 407, 1489–1495. https://doi.org/10.1016/j.scitotenv.2008.10.047

Delgado-Moreno, L., Peña, A., 2007. Organic amendments from olive cake as a strategy to modify the degradation of sulfonylurea herbicides in soil. J. Agric. Food Chem. 55, 6213–6218. https://doi.org/10.1021/jf0708342

Dell'Oca, A., Riva, M., Guadagnini, A., 2020. Global Sensitivity Analysis for Multiple Interpretive Models With Uncertain Parameters. Water Resour. Res. 56, 1–20. https://doi.org/10.1029/2019WR025754

Dell'Oca, A., Riva, M., Guadagnini, A., 2017. Moment-based metrics for global sensitivity analysis of hydrological systems. Hydrol. Earth Syst. Sci. 21, 6219–6234. https://doi.org/10.5194/hess-21-6219-2017

Delleur, J., 1999. The Handbook of Groundwater Engineering, CRC Press LLC. https://doi.org/10.2136/vzj2008.0079br

Demand, D., Blume, T., Weiler, M., 2019. Spatio-temporal relevance and controls of preferential flow at the landscape scale. Hydrol. Earth Syst. Sci. 23, 4869–4889. https://doi.org/10.5194/hess-23-4869-2019

DERP, 1998. Pesticides and Groundwater. Group 522, 344–351.

Dewettinck, T., Van Houtte, E., Geenens, D., Van Hege, K., Verstraete, W., 2001. HACCP (Hazard Analysis and Critical Control Points) to guarantee safe water reuse and drinking water production - A case study. Water Sci. Technol. 43, 31–38. https://doi.org/10.2166/wst.2001.0708

DHI, 2015. FEFLOW 7.0 User Guide.

References

Diamantopoulos, E., Iden, S.C., Durner, W., 2012. Inverse modeling of dynamic nonequilibrium in water flow with an effective approach. Water Resour. Res. 48, 1–16. https://doi.org/10.1029/2011WR010717

Dillon, P., 2005. Future management of aquifer recharge. Hydrogeol. J. 13, 313–316. https://doi.org/10.1007/s10040-004-0413-6

Dillon, P., Fernández Escalante, E., Megdal, S.B., Massmann, G., 2020a. Managed aquifer recharge for water resilience. Water (Switzerland) 12, 11. https://doi.org/10.3390/w12071846

Dillon, P., Kumar, A., Kookana, R., Leijs, R., Reed, D., Parsons, S., 2009a. Managed Aquifer Recharge - Risks to Groundwater Dependent Ecosystems - A Review. Water for a Healthy Country Flagship Report to Land & Water Australia. Waterlines Rep. Ser. No. 13 64.

Dillon, P., Page, D., Vanderzalm, J., Chadha, D., 2013. Water Quality Considerations in Managed Aquifer Recharge : from Artificial Recharge to Managed Aquifer Recharge in India. J. Groundw. Res. 2, 8–15.

Dillon, P., Page, D., Vanderzalm, J., Sidhu, J., Sandhu, C., Boisson, A., Lakshmanan, E., 2016a. Application of a Water Quality Guide to Managed Aquifer Recharge in India, in: Wintgens, T., Nättorp, A., Lakshmanan, E., Asolekar, S. (Eds.), Natural Water Treatment Systems for Safe and Sustainable Water Supply in the Indian Context: Saph Pani. IWA Publishing, London UK. https://doi.org/10.2166/9781780408392

Dillon, P., Page, D., Vanderzalm, J., Toze, S., Simmons, C., Hose, G., Martin, R., Johnston, K., Higginson, S., Morris, R., 2020b. Lessons from 10 years of experience with Australia's risk-based guidelines for managed aquifer recharge. Water (Switzerland) 12. https://doi.org/10.3390/w12020537

Dillon, P., Pavelic, P., Page, D., Beringen, H., Ward, J., 2009b. Managed Aquifer Recharge: An Introduction, National Water Commission Waterlines Reports Series No.13. https://doi.org/10.1007/BF01929660

Dillon, P., Stuyfzand, P., Grischek, T., Lluria, M., Pyne, R.D.G., Jain, R.C., Bear, J., Schwarz, J., Wang, W., Fernandez, E., Stefan, C., Pettenati, M., van der Gun, J., Sprenger, C., Massmann, G., Scanlon, B.R., Xanke, J., Jokela, P., Zheng, Y., Rossetto, R., Shamrukh, M., Pavelic, P., Murray, E., Ross, A., Bonilla Valverde, J.P., Palma Nava, A., Ansems, N., Posavec, K., Ha, K., Martin, R., Sapiano, M., 2019. Sixty years of global progress in managed aquifer recharge. Hydrogeol. J. 27, 1–30. https://doi.org/https://doi.org/10.1007/s10040-018-1841-z

Dillon, P., Vanderzalm, J., Sidhu, J., Page, D., Chadha, D., 2014. A Water Quality Guide to Managed Aquifer Recharge in India. CSIRO L. Water UNESCO Rep. AusAID PSLP Proj. ROU 14476 67.

Dillon, P., Vanderzalm, J.L., Page, D., Barry, K., Gonzalez, D., Muthukaruppan, M., Hudson, M., 2016b. Analysis of ASR Clogging Investigations at Three Australian ASR Sites in a Bayesian Context. Water 8. https://doi.org/10.3390/w8100442

References

Dinelli, G., Accinelli, C., Vicari, A., Catizone, P., 2000. Comparison of the persistence of atrazine and metolachlor under field and laboratory conditions. J. Agric. Food Chem. 48, 3037–3043. https://doi.org/10.1021/jf991057b

Doherty, J., 2020a. Model-Independent Parameter Estimation User Manual Part II: PEST Utility Support Software.

Doherty, J., 2020b. Model-Independent Parameter Estimation User Manual Part I: PEST, SENSAN and Global Optimisers.

Doherty, J., 2015. Calibration and Uncertainty Analysis for Complex Environmental Models, Groundwater. https://doi.org/10.1111/gwat.12360

Dolfing, J., Harrison, K.B., 1993. Redox and reduction potentials as parameters to predict the degradation pathway of chlorinated benzenes in anaerobic environments. FEMS Microbiol. Ecol. 13, 23–29. https://doi.org/10.1111/j.1574-6941.1993.tb00047.x

Dominguez-Chicas, A., Scrimshaw, M.D., 2010. Hazard and risk assessment for indirect potable reuse schemes : An approach for use in developing Water Safety Plans. Water Res. 44, 6115–6123. https://doi.org/10.1016/j.watres.2010.07.007

Dong, X., Sun, H., 2016. Effect of Temperature and Moisture on Degradation of Herbicide Atrazine in Agricultural Soil. Int. J. Environ. Agric. Res. 2, 2454–1850.

Donn, M., Reed, D., Vanderzalm, J., Page, D., 2020. Assessment of E. coli attenuation during infiltration of treatedwastewater: A pathway to future managed aquifer recharge. Water (Switzerland) 12. https://doi.org/10.3390/w12010173

Durner, W., 1994. Hydraulic conductivity estimations from soil with heterogeneous pore structure. Water Resour. Res. 30, 211–233.

Durner, W., Jansen, U., Iden, S.C., 2008. Effective hydraulic properties of layered soils at the lysimeter scale determined by inverse modelling. Eur. J. Soil Sci. 59, 114–124. https://doi.org/https://doi.org/10.1111/j.1365-2389.2007.00972.x

EC European Commission, 2015. European Union EU general risk assessment methodology (Action 5 of Multi-Annual Action Plan for the surveillance of products in the EU (COM(2013)76). https://doi.org/10.4324/9781849776110-28

Einsiedl, F., Małoszewski, P., Stichler, W., 2009. Multiple isotope approach to the determination of the natural attenuation potential of a high-alpine karst system. J. Hydrol. 365, 113–121. https://doi.org/10.1016/j.jhydrol.2008.11.042

Eisfeld, C., van der Wolf, J.M., van Breukelen, B.M., Medema, G., Velstra, J., Schijven, J.F., 2021. Die-off of plant pathogenic bacteria in tile drainage and anoxic water from a managed aquifer recharge site. PLoS One 16, 1–22. https://doi.org/10.1371/journal.pone.0250338

El-Fakharany, Z., 2013. Environmental Impact Assessment of Artificial Recharge of Treated Wastewater on Groundwater Aquifer System. Case study: Abu Rawash, Egypt. J. Am. Sci. 9.

Elsner, M., Imfeld, G., 2016. Compound-specific isotope analysis (CSIA) of micropollutants in the environment - current developments and future challenges. Curr. Opin. Biotechnol. 41, 60–72. https://doi.org/10.1016/j.copbio.2016.04.014

European Council (EUCO), 2010. Directive 2010/75/EU Industrial Emissions. Off. J. Eur. Union L334, 17–119. https://doi.org/10.3000/17252555.L_2010.334.eng

European Council (EUCO), 2006. Regulation (EC) No 1907/2006 of the European Parliament and of the Council of 18 December 2006 concerning the Registration, Evaluation, Authorisation and restriction of Chemicals (REACH), establishing a European Chemicals Agency, amending Directive 1999/4. Off. J. Eur. Union 1–520. https://doi.org/2004R0726 - v.7 of 05.06.2013

European Council (EUCO), 2000. Directive 2000/60/EC of the European Parliament and of the Council. Off. J. Eur. Union 21, 196.

European Council (EUCO), 1998a. Council Directive 98/83/EC, Ammended by EC 2015/1787 of 6 October 2015. Off. J. Eur. Union 31, 1–32. https://doi.org/2004R0726 - v.7 of 05.06.2013

European Council (EUCO), 1998b. Council Directive 98/83/EC on the quality of water intended for human consumption. Off. J. Eur. Union 31, 1–32. https://doi.org/2004R0726 - v.7 of 05.06.2013

European Environment Agency (EEA), 2022. Europe’s groundwater - a key resource under pressure 1–11.

European Food Safety Authority EFSA, 2007. Conclusion regarding the peer review of the pesticide risk assessment of the active substance nicosulfuron, European Food Safety Authority Journal. https://doi.org/10.2903/j.efsa.2006.55r

European Parliament and European Council, 2020. Regulation (EU) 2020/741 of the European parliment and of the council of 25 May 2020 on minimum requirements for water reuse. Off. Jounal Eur. Union 2019, 32–55.

Europen Council (EUCO), 2004. Directive 2004/35/CE. Off. J. Eur. Union 1–23.

Eurostat, 2022a. Grain maize and corn-cob-mix by area, production and humidity [WWW Document]. URL https://ec.europa.eu/eurostat/web/products-datasets/-/tag00093

Eurostat, 2022b. Green maize by area, production and humidity [WWW Document]. URL https://ec.europa.eu/eurostat/web/products-datasets/-/tag00101

Fantke, P., Friedrich, R., Jolliet, O., 2012. Health impact and damage cost assessment of pesticides in Europe. Environ. Int. 49, 9–17. https://doi.org/10.1016/j.envint.2012.08.001

Feddes, R.A., Kowalik, P.J., Zaradny, H., 1978. Simulation of field water use and crop yield. Wageningen : Centre for agricultural publishing and documentation.

Feddes, R.A., Raats, P.A.C., 2004. Parametrizing the soil-water-plant root system, in: Feddes, R.A., de Rooij, G.H., van Dam, J.C. (Eds.), Proceedings of the Unsaturated Zone Modelling: Progress, Challenges and Applications. https://doi.org/10.2136/vzj2006.0162br

Feng, W., Wei, Z., Song, J., Qin, Q., Yu, K., Li, G., Zhang, J., Wu, W., Yan, Y., 2017. Hydrolysis of nicosulfuron under acidic environment caused by oxalate secretion of a novel Penicillium oxalicum strain YC-WM1. Sci. Rep. 7, 1–11. https://doi.org/10.1038/s41598-017-00228-2

Fernández Escalante, E., Henao Casas, J.D., Vidal Medeiros, A.M., San Sebastián Sauto, J.S.S.S., 2020. Regulations and guidelines on water quality requirements for Managed Aquifer Recharge. International comparison. Acque Sotter. - Ital. J. Groundw. 7–22. https://doi.org/10.7343/as-2020-462

Fetter, C.W., 2001. Applied Hydrogeology.

Fetter, C.W., 1999. Contaminant Hydrogeology. Prentice-Hall, Inc.

Francaviglia, R., Capri, E., 2000. Lysimeter experiments with metolachlor in Tor Mancina (Italy). Agric. Water Manag. 44, 63–74. https://doi.org/10.1016/S0378-3774(99)00084-0

Freeze, R.A., Cherry, J.A., 1979. Groundwater, Prentice-Hall, Inc.

Gale, I., 2005. Strategies for Managed Aquifer Recharge (MAR) in semi-arid areas. UNESCO’s Int. Hydrol. Program. 1–33.

Gallardo, A.H., Marui, A., 2016. The aftermath of the Fukushima nuclear accident: Measures to contain groundwater contamination. Sci. Total Environ. 547, 261–268. https://doi.org/https://doi.org/10.1016/j.scitotenv.2015.12.129

Ganot, Y., Holtzman, R., Weisbrod, N., Bernstein, A., Siebner, H., Katz, Y., Kurtzman, D., 2018. Managed aquifer recharge with reverse-osmosis desalinated seawater: Modeling the spreading in groundwater using stable water isotopes. Hydrol. Earth Syst. Sci. 22, 6323–6333. https://doi.org/10.5194/hess-22-6323-2018

Ganot, Y., Holtzman, R., Weisbrod, N., Nitzan, I., Katz, Y., Kurtzman, D., 2017. Monitoring and modeling infiltration-recharge dynamics of managed aquifer recharge with desalinated seawater. Hydrol. Earth Syst. Sci. 21, 4479–4493. https://doi.org/10.5194/hess-21-4479-2017

Gardner, W.R., 1960. Dynamic aspects of water availability to plants. Soil Sci.

Gazis, C., Feng, X., 2004. A stable isotope study of soil water: Evidence for mixing and preferential flow paths. Geoderma 119, 97–111. https://doi.org/10.1016/S0016-7061(03)00243-X

Genuis, S.J., Lane, K., Birkholz, D., 2016. Human Elimination of Organochlorine

Pesticides: Blood, Urine, and Sweat Study. Biomed Res. Int. 2016. https://doi.org/10.1155/2016/1624643

Gerke, H.H., van Genuchten, M.T., 1996. Macroscopic representation of structural geometry for simulating water and solute movement in dual-porosity media. Adv. Water Resour. 19, 343–357. https://doi.org/10.1016/0309-1708(96)00012-7

Gerke, H.H., van Genuchten, M.T., 1993. A dual-porosity model for simulating the preferential movement of water and solutes in structured porous media. Water Resour. Res. 29, 305–319. https://doi.org/10.1029/92WR02339

Gibert, O., Hernández, M., Kienle, C., Simon, E., Sprenger, C., Besselink, H., Hannappel, S., 2015. Field investigations and risk assessment in La Vall d'Uixó (Castellón, Spain) - DEMEAU.

Glaesner, N., Diamantopoulos, E., Magid, J., Kjaergaard, C., Gerke, H.H., 2018. Modeling Solute Mass Exchange between Pore Regions in Slurry-Injected Soil Columns during Intermittent Irrigation. Vadose Zo. J. 17, 180006. https://doi.org/10.2136/vzj2018.01.0006

Gonfiantini, R., 1978. Standards for stable isotope measurements in natural compounds. Nature 271, 534–536. https://doi.org/10.1038/271534a0

Gonzalez, D., Page, D., Vanderzalm, J., Dillon, P., 2015. Setting water quality trigger levels for the operation and management of a MAR system in Parafield, South Australia. J. Hydrol. Eng. 20, 1–8. https://doi.org/10.1061/(ASCE)HE.1943-5584.0001001

Grabczak, J., Rózański, K., Małoszewski, P., Zuber, A., 1984. Estimation of the tritium input function with the aid of stable isotopes. Catena 11, 105–114. https://doi.org/10.1016/0341-8162(84)90001-8

Graham, S.L., Srinivasan, M.S., Faulkner, N., Carrick, S., 2018. Soil Hydraulic Modeling Outcomes with Four Parameterization Methods: Comparing Soil Description and Inverse Estimation Approaches. Vadose Zo. J. 17, 170002. https://doi.org/10.2136/vzj2017.01.0002

Green, T.R., Bates, B.C., Charles, S.P., Fleming, P.M., 2007. Physically based simulation of potential effects of carbon dioxide-altered climates on groundwater recharge. Vadose Zo. J. 6, 597–609. https://doi.org/10.2136/vzj2006.0099

Groh, J., Stumpp, C., Lücke, A., Pütz, T., Vanderborght, J., Vereecken, H., 2018. Inverse Estimation of Soil Hydraulic and Transport Parameters of Layered Soils from Water Stable Isotope and Lysimeter Data. Vadose Zo. J. 17, 170168. https://doi.org/10.2136/vzj2017.09.0168

Groh, J., Vanderborght, J., Pütz, T., Gründling, R., Rupp, H., Rahmati, M., Sommer, M., Sommer, M., Vereecken, H., Gerke, H.H., 2020. Responses of soil water storage and crop water use efficiency to changing climatic conditions: A lysimeter-based space-for-time approach. Hydrol. Earth Syst. Sci. 24, 1211–1225. https://doi.org/10.5194/hess-24-1211-2020

References

Groh, J., Vanderborght, J., Pütz, T., Vereecken, H., 2016. How to Control the Lysimeter Bottom Boundary to Investigate the Effect of Climate Change on Soil Processes? Vadose Zo. J. 15, vzj2015.08.0113. https://doi.org/10.2136/vzj2015.08.0113

Grünheid, S., Hübner, U., Jekel, M., 2007. Impact of temperature on biodegradation of bulk and trace organics during soil passage in an indirect reuse system, in: 6th IWA Specialist Conference on Wastewater Reclamation and Reuse for Sustainability. p. 8.

Guzzella, L., Pozzoni, F., Giuliano, G., 2006. Herbicide contamination of surficial groundwater in Northern Italy. Environ. Pollut. 142, 344–353. https://doi.org/10.1016/j.envpol.2005.10.037

Guzzella, L., Rullo, S., Pozzoni, F., Giuliano, G., 2003. Studies on Mobility and Degradation Pathways of Terbuthylazine Using Lysimeters on a Field Scale. J. Environ. Qual. 32, 1089–1098. https://doi.org/10.2134/jeq2003.1089

Haas, C.N., Rose, J.B., Gerba, C.P., 1999. Quantitative Microbial Risk Assessment. John Wiley and Sons Inc, New York.

Hainsworth, J.M., Aylmore, L.A.G., 1986. Water Extraction by Single Plant Roots. Soil Sci. Soc. Am. J. 50, 841–848. https://doi.org/10.2136/sssaj1986.03615995005000040003x

Harzing, 2020. Publish or perish [WWW Document].

Hasan, M.B., Driessen, P.P.J., Majumder, S., Zoomers, A., van Laerhoven, F., 2019. Factors affecting consumption of water from a newly introduced safe drinking water system: The case of managed aquifer recharge (MAR) systems in Bangladesh. Water (Switzerland) 11. https://doi.org/10.3390/w11122459

Havelaar, A.H., 1994. Application of HACCP to drinking water supply. Food Control 5, 145–152. https://doi.org/10.1016/0956-7135(94)90074-4

Haws, N.W., Rao, P.S.C., Šimůnek, J., Poyer, I.C., 2005. Single-porosity and dual-porosity modeling of water flow and solute transport in subsurface-drained fields using effective field-scale parameters. J. Hydrol. 313, 257–273. https://doi.org/10.1016/j.jhydrol.2005.03.035

Hildebrandt, A., Guillamón, M., Lacorte, S., Tauler, R., Barceló, D., 2008. Impact of pesticides used in agriculture and vineyards to surface and groundwater quality (North Spain). Water Res. 42, 3315–3326. https://doi.org/10.1016/j.watres.2008.04.009

Howell, T.A., 2004. Lysimetry, in: Encyclopedia of Soils in the Environment. pp. 379–386. https://doi.org/10.1016/B0-12-348530-4/00391-X

Hsieh, P., Bahr, J., Doe, T., Flint, A., Gee, G., Gelhar, L., Solomon, K., van Genuchten, M.T., Wheatcraft, S., 2001. Conceptual Models of Flow and Transport in the Fractured Vadose Zone. https://doi.org/10.2113/1.1.200

Huang, M., Hilderman, J.N., Barbour, L., 2015. Transport of stable isotopes of water and sulphate within reclaimed oil sands saline-sodic mine overburden. J. Hydrol. 529, 1550–1561. https://doi.org/10.1016/j.jhydrol.2015.08.028

Hunkeler, D., Meckenstock, R.U., Lollar, B.S., Schmidt, T.C., Wilson, J.T., 2008. A Guide for Assessing Biodegradation and Source Identification of Organic Ground Water Contaminants using Compound Specific Isotope Analysis (CSIA). USEPA Publ. EPA 600/R-, 1–82.

Hupet, F., Lambot, S., Feddes, R.A., Van Dam, J.C., Vanclooster, M., 2003. Estimation of root water uptake parameters by inverse modeling with soil water content data. Water Resour. Res. 39. https://doi.org/10.1029/2003WR002046

ICID International Commission on Irrigation and Drainage, 1993. The ICID environmental check-list to identify environmental effects of irrigation, drainage and flood control projects. HR Wallingford Ltd.

Igboama, W.N., Hammed, O.S., Fatoba, J.O., Aroyehun, M.T., Ehiabhili, J.C., 2022. Review article on impact of groundwater contamination due to dumpsites using geophysical and physiochemical methods. Appl. Water Sci. 12, 1–14. https://doi.org/10.1007/s13201-022-01653-z

Ikoyi, I., Fowler, A., Schmalenberger, A., 2018. One-time phosphate fertilizer application to grassland columns modifies the soil microbiota and limits its role in ecosystem services. Sci. Total Environ. 630, 849–858. https://doi.org/10.1016/j.scitotenv.2018.02.263

Imig, A., Augustin, L., Groh, J., Pütz, T., Elsner, M., Einsiedl, F., Rein, A., under review, b. Fate of herbicides in cropped lysimeters: 2. Leaching of four maize herbicides considering different model setups. Vadose Zo. J.

Imig, A., Augustin, L., Groh, J., Pütz, T., Zhou, T., Einsiedl, F., Rein, A., under review,a. Fate of herbicides in cropped lysimeters: 1. Influence of different model setups on vadose zone flow. Vadose Zo. J.

Imig, A., Shajari, F., Augustin, L., Einsiedl, F., Rein, A., 2022a. Improved lumped-parameter and numerical modeling of unsaturated water flow and stable water isotopes. Groundwater 1–13. https://doi.org/10.1111/gwat.13244

Imig, A., Szabó, Z., Halytsia, O., Vrachioli, M., Kleinert, V., Rein, A., 2022b. A review on risk assessment in managed aquifer recharge. Integr. Environ. Assess. Manag. 18, 1513–1529. https://doi.org/10.1002/ieam.4584

Isch, A., Montenach, D., Hammel, F., Ackerer, P., Coquet, Y., 2019. A comparative study of water and bromide transport in a bare loam soil using lysimeters and field plots. Water (Switzerland) 11, 1–25. https://doi.org/10.3390/w11061199

ISO/IEC International Organization for Standardization; International Electrotechnical Commission, 2014. Guide 51:2014(en) Safety aspects — Guidelines for their inclusion in standards.

References

ISO International Organization for Standardization, 2008. Guidelines for health risk assessment and management for non-potable water reuse 20426.

ISO International Organization of Standardization, 2015. Guidelines for treated wastewater use for irrigation projects — Part 1: The basis of a reuse project for irrigation 16075-1 2015.

IUSS Working Group WRB, 2015. World Reference base for soil resources 2014, updated 2015 International soil classification system for naming soils and creating legends for soil maps, Nature Nanotechnology. World Soil Resources Reports No. 106. FAO, Rome. https://doi.org/10.1038/nnano.2009.216

Jaikaew, P., Malhat, F., Boulange, J., Watanabe, H., 2017. Aspect of the degradation and adsorption kinetics of atrazine and metolachlor in andisol soil. Hell. Plant Prot. J. 10, 1–14. https://doi.org/10.1515/hppj-2017-0001

Jakeman, A.J., Barreteau, O., Hunt, R.J., Rinaudo, J.-D., Ross, A., 2016. Integrated Goundwater Management, Integrated Groundwater Management. https://doi.org/10.1007/978-3-319-23576-9

James, P., Barcelona, M.J., Ritchey, J.D., Lefaivre, M.H., 1984. Effective Porosity of Geologic Materials: First Annual Report 42.

Jarvis, N.J., 2007. A review of non-equilibrium water flow and solute transport in soil macropores: Principles, controlling factors and consequences for water quality. Eur. J. Soil Sci. 58, 523–546. https://doi.org/10.1111/j.1365-2389.2007.00915.x

Jeong, H.Y., Jun, S.C., Cheon, J.Y., Park, M., 2018. A review on clogging mechanisms and managements in aquifer storage and recovery (ASR) applications. Geosci. J. 22, 667–679. https://doi.org/10.1007/s12303-017-0073-x

Ji, H.W., Lee, S. Il, 2016a. Assessment of risk due to chemicals transferred in a watershed: A case of an aquifer storage transfer and recovery site. Water (Switzerland) 8. https://doi.org/10.3390/w8060242

Ji, H.W., Lee, S. Il, 2016b. Use of pollutant release and transfer register (PRTR) to assess potential risk associated with chemicals in a drinking water supply facility. Desalin. Water Treat. 57, 29228–29239. https://doi.org/10.1080/19443994.2016.1171170

Ji, H.W., Lee, S.-I., 2017. Comparison of potential risk on two managed aquifer recharge sites from river basin. Water (Switzerland) 9. https://doi.org/10.3390/w9090674

Jiang, S., Pang, L., Buchan, G.D., Šimůnek, J., Noonan, M.J., Close, M.E., 2010. Modeling water flow and bacterial transport in undisturbed lysimeters under irrigations of dairy shed effluent and water using HYDRUS-1D. Water Res. 44, 1050–1061. https://doi.org/10.1016/j.watres.2009.08.039

Jones, R.L., 1969. Inhibition of Gibberellic Acid-induced α-Amylase Formation by Polyethylene Glycol and Mannitol. Plant Physiol. 44, 101–104.

https://doi.org/10.1104/pp.44.1.101

Jørgensen, P.R., Hoffmann, M., Kistrup, J.P., Bryde, C., Bossi, R., Villholth, K.G., 2002. Preferential flow and pesticide transport in a clay-rich till: Field, laboratory, and modeling analysis. Water Resour. Res. 38, 28-1-28–15. https://doi.org/10.1029/2001wr000494

Juntunen, J., Meriläinen, P., Simola, A., 2017. Public health and economic risk assessment of waterborne contaminants and pathogens in Finland. Sci. Total Environ. 599–600, 873–882. https://doi.org/10.1016/j.scitotenv.2017.05.007

Juraske, R., Castells, F., Vijay, A., Muñoz, P., Antón, A., 2009. Uptake and persistence of pesticides in plants: Measurements and model estimates for imidacloprid after foliar and soil application. J. Hazard. Mater. 165, 683–689. https://doi.org/10.1016/j.jhazmat.2008.10.043

Karakurt-Fischer, S., Bein, E., Drewes, J.E., Hübner, U., 2020. Characterizing a novel in-situ oxygen delivery device for establishing controlled redox zonation within a high infiltration rate sequential biofilter. Water Res. 182, 1–11. https://doi.org/10.1016/j.watres.2020.116039

Karigar, C.S., Rao, S.S., 2011. Role of microbial enzymes in the bioremediation of pollutants: A review. Enzyme Res. 2011. https://doi.org/10.4061/2011/805187

Karim, K., Guha, S., Beni, R., 2020. Comparative Analysis of Chemical, Physical and Biological Contaminants in Drinking Water in Various Developed Countries around the World. J. Water Resour. Prot. 12, 714–728. https://doi.org/10.4236/jwarp.2020.128043

Kazner, C., Wintgens, T., Dillon, P., 2012. Water Reclamation Technologies for Safe Managed Aquifer Recharge. IWA Publishing.

Kendall, C., McDonnell, J.J., 1998. Isotope Tracers in Catchment Hydrogeology. Elsevier, Oxford, UK.

Knoben, W.J.M., Freer, J.E., Woods, R.A., 2019. Technical note: Inherent benchmark or not? Comparing Nash-Sutcliffe and Kling-Gupta efficiency scores. Hydrol. Earth Syst. Sci. 23, 4323–4331. https://doi.org/10.5194/hess-23-4323-2019

Köhne, J.M., Köhne, S., Gerke, H.H., 2002. Estimating the hydraulic functions of dual-permeability models from bulk soil data. Water Resour. Res. 38, 26-1-26–11. https://doi.org/10.1029/2001wr000492

Köhne, J.M., Köhne, S., Mohanty, B.P., Šimůnek, J., 2004. Inverse Mobile-Immobile Modeling of Transport During Transient Flow: Effects of Between-Domain Transfer and Initial Water Content. Vadose Zo. J. 3, 1309–1321. https://doi.org/10.2136/vzj2004.1309

Köhne, J.M., Köhne, S., Šimůnek, J., 2009a. A review of model applications for structured soils: a) Water flow and tracer transport. J. Contam. Hydrol. 104, 4–35. https://doi.org/10.1016/j.jconhyd.2008.10.002

Köhne, J.M., Köhne, S., Šimůnek, J., 2009b. A review of model applications for structured soils: b) Pesticide transport. J. Contam. Hydrol. 104, 36–60. https://doi.org/10.1016/j.jconhyd.2008.10.003

Köhne, J.M., Köhne, S., Šimůnek, J., 2006a. Multi-process herbicide transport in structured soil columns: Experiments and model analysis. J. Contam. Hydrol. 85, 1–32. https://doi.org/10.1016/j.jconhyd.2006.01.001

Köhne, J.M., Mohanty, B.P., Šimůnek, J., 2006b. Inverse dual-permeability modeling of preferential water flow in a soil column and implications for field-scale solute transport. Vadose Zo. J. 5, 59–76. https://doi.org/10.2136/vzj2005.0008

Konikow, L.F., 2011. The Secret to Successful Solute-Transport Modeling. Groundwater 49, 144–159. https://doi.org/https://doi.org/10.1111/j.1745-6584.2010.00764.x

Kördel, W., Egli, H., Klein, M., 2008. Transport of pesticides via macropores (IUPAC Technical Report). Pure Appl. Chem. 80, 105–160. https://doi.org/10.1351/pac200880010105

Körner, P., Jung, D., Kruse, A., 2019. Influence of the pH Value on the Hydrothermal Degradation of Fructose. ChemistryOpen 8, 1121–1132. https://doi.org/10.1002/open.201900225

Kreft, A., Zuber, A., 1978. On the physical meaning of the dispersion equation and its solutions for different initial and boundary conditions. Chem. Eng. Sci. 33, 1471–1480. https://doi.org/https://doi.org/10.1016/0009-2509(78)85196-3

Krieger, M.S., Pillar, F., Ostrander, J.A., 2000. Effect of temperature and moisture on the degradation and sorption of florasulam and 5-hydroxyflorasulam in soil. J. Agric. Food Chem. 48, 4757–4766. https://doi.org/10.1021/jf000009k

Kumar, R., Shankar, V., Jat, M.K., 2015. Evaluation of root water uptake models - A review. ISH J. Hydraul. Eng. 21, 115–124. https://doi.org/10.1080/09715010.2014.981955

Kundzewicz, Z.W., Döll, P., 2009. Will groundwater ease freshwater stress under climate change? Hydrol. Sci. J. 54, 665–675. https://doi.org/10.1623/hysj.54.4.665

Lahvis, M., Baehr, A.L., 1997. Documentation of R-UNSAT, A Computer Model for the Simulation of Reactive, Multispecies Transport in the Unsaturated Zone. USGS Open-File Rep. 97–630, 1–112.

Lapworth, D.J., Baran, N., Stuart, M.E., Ward, R.S., 2012. Emerging organic contaminants in groundwater: A review of sources, fate and occurrence. Environ. Pollut. 163, 287–303. https://doi.org/10.1016/j.envpol.2011.12.034

Lawrence, A.R., Morris, B.L., Foster, S.S.D., 2008. Hazards induced by groundwater recharge under rapid urbanization. Geol. Soc. London, Eng. Geol. Spec. Publ. 15, 319–328. https://doi.org/10.1144/gsl.eng.1998.015.01.32

Le Corre, K., Aharoni, A., Cauwenberghs, J., Chavez, A., Cikurel, H., Ayuso Gabella, M.N., Genthe, B., Gibson, R., Jefferson, B., Jeffrey, P., Jimenez, B., Kazner, C., Masciopinto, C., Page, D., Regel, R., Rinck-Pfeiffer, S., Salgot, M., Steyn, M., van Houtte, E., Tredoux, G., Wintgens, T., Xuzhou, C., Yu, L., Zhao, X., 2012. Water reclamation for aquifer recharge at the eight case study sites: a cross case analysis, in: Kazner, C., Wintgens, T., Dillon, P. (Eds.), Water Reclamation Technologies for Safe Managed Aquifer Recharge. pp. 11–31.

Lee, S. Il, Ji, H.W., 2016. Identification of hazardous events for drinking water production process using managed aquifer recharge in the Nakdong river delta, Korea. Malaysian J. Anal. Sci. 20, 365–372. https://doi.org/10.17576/mjas-2016-2002-20

Legind, C.N., Rein, A., Serre, J., Brochier, V., Haudin, C.S., Cambier, P., Houot, S., Trapp, S., 2012. Simultaneous Simulations of Uptake in Plants and Leaching to Groundwater of Cadmium and Lead for Arable Land Amended with Compost or Farmyard Manure. PLoS One 7, 1–13. https://doi.org/10.1371/journal.pone.0047002

Leibundgut, C., Małoszewski, P., Külls, C., 2009. Tracers in Hydrology. Wiley-Blackwell a John Wiley& Sons, Ltd., Publications. https://doi.org/10.1002/9780470747148

Leita, L., Ceccon, P., Marucchini, C., Mondini, C., 1996. Behaviour of metolachlor and terbuthylazine in cultivated field lysimeters. Zeitschrift fur Pflanzenernahrung und Bodenkd. 159, 177–182. https://doi.org/10.1002/jpln.1996.3581590212

Lenda, A., Zuber, A., 1970. Tracer dispersion in groundwater experiments, in: Isotope Hydrology. Vienna, pp. 619–641.

Levantesi, C., La Mantia, R., Masciopinto, C., Böckelmann, U., Ayuso-Gabella, M.N., Salgot, M., Tandoi, V., Van Houtte, E., Wintgens, T., Grohmann, E., 2010. Quantification of pathogenic microorganisms and microbial indicators in three wastewater reclamation and managed aquifer recharge facilities in Europe. Sci. Total Environ. 408, 4923–4930. https://doi.org/10.1016/j.scitotenv.2010.07.042

Leviston, Z., Nancarrow, B.E., Tucker, D.I., Porter, N.B., 2006. Predicting Community Behaviour: Indirect Potable Reuse of Wastewater through Managed Aquifer Recharge; Land and Water Science Report 2906, Land and Water Science Report 2906.

Lindhe, A., Rosén, L., Johansson, P.O., Norberg, T., 2020. Dynamic water balance modelling for risk assessment and decision support on MAR potential in Botswana. Water (Switzerland) 12, 1–13. https://doi.org/10.3390/w12030721

Liu, Y., Zhu, K., Su, M., Zhu, H., Lu, J., Wang, Yuxia, Dong, J., Qin, H., Wang, Ying, Zhang, Y., 2019. Influence of solution pH on degradation of atrazine during UV and UV/H2O2 oxidation: Kinetics, mechanism, and degradation pathways. RSC Adv. 9, 35847–35861. https://doi.org/10.1039/c9ra05747a

Maliva, R.G., 2014. Economics of managed aquifer recharge. Water (Switzerland) 6, 1257–1279. https://doi.org/10.3390/w6051257

Małoszewski, P., Rauert, W., Trimborn, P., Herrmann, A., Rau, R., 1992. Isotope hydrological study of mean transit times in an alpine basin (Wimbachtal, Germany). J. Hydrol. 140, 343–360. https://doi.org/10.1016/0022-1694(92)90247-S

Małoszewski, P., Stichler, W., Zuber, A., Rank, D., 2002. Identifying the flow systems in a karstic-fissured-porous aquifer, the schneealpe, austria, by modelling of environmental 18o and 3h isotopes. J. Hydrol. 256, 48–59. https://doi.org/10.1016/S0022-1694(01)00526-1

Małoszewski, P., Zuber, A., 1982. Determining the turnover time of groundwater systems with the aid of environmental tracers. 1. Models and their applicability. J. Hydrol. 57, 207–231. https://doi.org/10.1016/0022-1694(82)90147-0

Mamy, L., Barriuso, E., 2007. Desorption and time-dependent sorption of herbicides in soils. Eur. J. Soil Sci. 58, 174–187. https://doi.org/10.1111/j.1365-2389.2006.00822.x

Mangelsdorf, K., 2017. Stabile Kohlenstoffisotope – Ein Schlüssel zu biologischen Prozessen und Quellen organischer Biomasse in Sedimentsystemen 32–37. https://doi.org/10.2312/GFZ.syserde.07.01.5

Mankad, A., Walton, A., Alexander, K., 2015. Key dimensions of public acceptance for managed aquifer recharge of urban stormwater. J. Clean. Prod. 89, 214–223. https://doi.org/10.1016/j.jclepro.2014.11.028

Mann, M.E., Gleick, P.H., 2015. Climate change and California drought in the 21st century. Proc. Natl. Acad. Sci. U. S. A. 112, 3858–3859. https://doi.org/10.1073/pnas.1503667112

Maraqa, M.A., Wallace, R.B., Voice, T.C., 1997. Effects of degree of water saturation on dispersivity and immobile water in sandy soil columns. J. Contam. Hydrol. 25, 199–218. https://doi.org/10.1016/S0169-7722(96)00032-0

Maréchal, J.-C., Bouzit, M., Rinaudo, J.-D., Moiroux, F., Desprats, J.-F., Caballero, Y., 2020. Mapping Economic Feasibility of Managed Aquifer Recharge. Water 12, 680. https://doi.org/doi:10.3390/w12030680

Marín-Benito, J.M., Pot, V., Alletto, L., Mamy, L., Bedos, C., Barriuso, E., Benoit, P., 2014. Comparison of three pesticide fate models with respect to the leaching of two herbicides under field conditions in an irrigated maize cropping system. Sci. Total Environ. 499, 533–545. https://doi.org/10.1016/j.scitotenv.2014.06.143

Martin, R., 2013. Clogging issues associated with managed aquifer recharge methods. IAH Comm. Manag. Aquifer Recharg. Aust.

MATM Ministero dell'ambiente e della tutela del territorio e del mare, 2016. Decreto 2 maggio 2016, n. 100., Decreto 2 maggio 2016, n. 100., Gazzetta Ufficiale della Repubblica Italiana, n 136 13 giugno 2016, serie generale, Decree 2 may 2016,

n. 100. Gazzetta Ufficiale della Repubblica Italiana, n 136 13 june 2016, general series.

McGrath, G.S., Hinz, C., Sivapalan, M., 2009. A preferential flow leaching index. Water Resour. Res. 45, 1–10. https://doi.org/10.1029/2008WR007265

Meissle, M., Mouron, P., Musa, T., Bigler, F., Pons, X., Vasileiadis, V.P., Otto, S., Antichi, D., Kiss, J., Pálinkás, Z., Dorner, Z., van der Weide, R., Groten, J., Czembor, E., Adamczyk, J., Thibord, J.B., Melander, B., Nielsen, G.C., Poulsen, R.T., Zimmermann, O., Verschwele, A., Oldenburg, E., 2010. Pests, pesticide use and alternative options in European maize production: Current status and future prospects. J. Appl. Entomol. 134, 357–375. https://doi.org/10.1111/j.1439-0418.2009.01491.x

Meyer, A.H., Elsner, M., 2013. 13C/12C and 15N/14N isotope analysis to characterize degradation of atrazine: Evidence from parent and daughter compound values. Environ. Sci. Technol. 47, 6884–6891. https://doi.org/10.1021/es305242q

Michel, C., Baran, N., André, L., Charron, M., Joulian, C., 2021. Side Effects of Pesticides and Metabolites in Groundwater: Impact on Denitrification. Front. Microbiol. 12, 1–17. https://doi.org/10.3389/fmicb.2021.662727

Minaduola, M., Tumarbay, H., Jiao, P., 2021. Application of a root water uptake model and numerical simulation to walnut trees in arid areas of northwest China. Arab. J. Geosci. 14. https://doi.org/10.1007/s12517-021-06609-2

Minister van Volkshuisvesting Ruimtelijke Ordening en Milieubeheer, 1993. The Infiltratiebesluit Bodembescherming (Infiltration Decree Soil Protection).

Moeck, C., von Freyberg, J., Schirmer, M., 2018. Groundwater recharge predictions in contrasted climate: The effect of model complexity and calibration period on recharge rates. Environ. Model. Softw. 103, 74–89. https://doi.org/10.1016/j.envsoft.2018.02.005

Molz, F.J., Remson, I., 1970. Extraction term models of soil moisture use by transpiring plants. Water Resour. Res. 6.

MOP Ministerio de Obras Públicas, 2014. Diagnóstico de metodología para la presentacion y análisis de proyectos de recarga artificial de acuíferos. Elaborado por: AMPHOS 21 Consulting Chile Ltda. 1-288pp.

Morvannou, A., Forquet, N., Vanclooster, M., Molle, P., 2008. Which Hydraulic Model to Use for Vertical Flow Constructed Wetlands ?, in: 13th International Conference on Wetland Systems for Water Pollution Control. p. 9.

Mualem, Y., 1976. A new model for predicting the hydraulic conduc. Water Resour. Res. 12, 513–522. https://doi.org/10.1029/WR012i003p00513

Nandha, M., Berry, M., Jefferson, B., Jeffrey, P., 2015. Risk assessment frameworks for MAR schemes in the UK. Environ. Earth Sci. 73, 7747–7757. https://doi.org/10.1007/s12665-014-3399-y

Neukum, C., Azzam, R., 2012. Impact of climate change on groundwater recharge in a small catchment in the Black Forest, Germany. Hydrogeol. J. 20, 547–560. https://doi.org/10.1007/s10040-011-0827-x

Nicolas, M., Bour, O., Selles, A., Dewandel, B., Bailly-Comte, V., Chandra, S., Ahmed, S., Maréchal, J.C., 2019. Managed Aquifer Recharge in fractured crystalline rock aquifers: Impact of horizontal preferential flow on recharge dynamics. J. Hydrol. 573, 717–732. https://doi.org/10.1016/j.jhydrol.2019.04.003

Nicolopoulou-Stamati, P., Maipas, S., Kotampasi, C., Stamatis, P., Hens, L., 2016. Chemical Pesticides and Human Health: The Urgent Need for a New Concept in Agriculture. Front. Public Heal. 4, 1–8. https://doi.org/10.3389/fpubh.2016.00148

Nimmo, J.R., 2009. Vadose Water. Encycl. Inl. Waters 1, 766–777. https://doi.org/10.1016/B978-012370626-3.00014-4

Nkedi-Kizza, P., Biggar, J.W., van Genuchten, M.T., Wierenga, P.J., Selim, H.M., Davidson, J.M., Nielsen, D.R., 1983. Modeling tritium and chloride 36 transport through an aggregated oxisol. Water Resour. Res. 19, 691–700. https://doi.org/10.1029/WR019i003p00691

Noshadi, M., Foroutani, A., Sepaskhah, A., 2019. Evaluation of HYDRUS-1D and modified PRZM-3 models for tribenuron methyl herbicide transport in soil profile under vetiver cultivation. Int. J. Phytoremediation 21, 878–891. https://doi.org/10.1080/15226514.2019.1583632

NRMMC-EPHC-AHMC, 2006. Australia Guidelines for Water Recycling: Managing Health and Environmental Risks (Phase 1) Natural Resource Management Ministerial Council;Environment Protection and Heritage Council ; Australian Health Ministers' Conference. Nat. Resour. Manag. Minist. Counc. Prot. Herit. Counc. ; Aust. Heal. Minist. Conf. 415.

NRMMC–EPHC–NHMRC, 2009a. Australian Guidelines for Water Recycling: Managing Health and Environmental Risks (Phase 2) Managed Aquifer Recharge; Natural Resource Management Ministerial Council; Environment Protection and Heritage Council; National Health and Medical Research Counc [WWW Document]. J. Environ. Manage. https://doi.org/10.1016/j.jenvman.2014.01.039

NRMMC–EPHC–NHMRC, 2009b. Australian Guidelines for Water Recycling: Managing Health and Environmental Risks (Phase 2) Managed Aquifer Recharge; Natural Resource Management Ministerial Council; Environment Protection and Heritage Council; National Health and Medical Research Counc [WWW Document]. Nat. Resour. Manag. Minist. Counc. Prot. Herit. Counc. ; Aust. Heal. Minist. Conf.

O'Leary, D.R., Izbicki, J.A., Metzger, L.F., 2015. Sources of high-chloride water and managed aquifer recharge in an alluvial aquifer in California , USA 1515–1533. https://doi.org/10.1007/s10040-015-1277-7

Ogata, A., 1970. Theory of dispersion in a granular medium. U.S Geol. Surv. Prof. Pap. 411–I.

References

Ogata, A., Banks, R.B., 1961. A solution of the differential equation of longitudinal dispersion in porous media. Geol. Surv. (U.S.).; Prof. Pap. A1–A7.

Ojha, C.S., Prasad, K.S., Shankar, V., Madramootoo, C.A., 2009. Evaluation of a Nonlinear Root-Water Uptake Model. J. Irrig. Drain. Eng. 135, 303–312. https://doi.org/10.1061/(asce)ir.1943-4774.0000067

Olsthoorn, T.N., 1982. The Clogging of recharge wells, main subjects. KIWA Communication.

Olvera-Velona, A., Benoit, P., Barriuso, E., Ortiz-Hernandez, L., 2008. Sorption and desorption of organophosphate pesticides, parathion and cadusafos, on tropical agricultural soils. Agron. Sustain. Dev. 28, 231–238. https://doi.org/10.1051/agro:2008009

Page, D., Barry, K., Pavelic, P., Dillon, P., 2008. Preliminary quantitative risk assessment for the Salisbury stormwater ASTR Project. CSIRO Water a Heal. Couuntry Natl. Res. Flagsh.

Page, D., Dillon, P., Toze, S., Bixio, D., Genthe, B., Jiménez Cisneros, B.E., Wintgens, T., 2010a. Valuing the subsurface pathogen treatment barrier in water recycling via aquifers for drinking supplies. Water Res. 44, 1841–1852. https://doi.org/10.1016/j.watres.2009.12.008

Page, D., Dillon, P., Toze, S., Sidhu, J.P.S., 2010b. Characterising aquifer treatment for pathogens in managed aquifer recharge. Water Sci. Technol. 62, 2009–2015. https://doi.org/10.2166/wst.2010.539

Page, Declan, Dillon, P., Vanderzalm, J., Bekele, E., Barry, K., Miotlinski, K., Levett, K., 2010. Managed aquifer recharge case study risk assessments. Natl. Res. FLAGSHIPS.

Page, D., Dillon, P., Vanderzalm, J., Toze, S., Sidhu, J., Barry, K., Levett, K., Kremer, S., Regel, R., 2010c. Risk Assessment of Aquifer Storage Transfer and Recovery with Urban Stormwater for Producing Water of a Potable Quality. J. Environ. Qual. 39, 2029–2039. https://doi.org/10.2134/jeq2010.0078

Page, D., Gonzalez, D., Bennison, G., Burrull, C., Claro, E., Jara, M., Valenzuela, G., 2020. Progress in the development of risk-based guidelines to support managed aquifer recharge for agriculture in Chile. Water Cycle 1, 136–145. https://doi.org/10.1016/j.watcyc.2020.09.003

Page, D., Gonzalez, D., Dillon, P., 2012. Microbiological risks of recycling urban stormwater via aquifers. Water Sci. Technol. 65, 1692–1695. https://doi.org/10.2166/wst.2012.069

Page, D., Gonzalez, D., Dillon, P., Vanderzalm, J., Vadakattu, G., Toze, S., Sidhu, J., Miotlinski, K., Torkzaban, S., Barry, K., 2013. Managed Aquifer Recharge and Urban Stormwater Use Options: Public Health and Environmental Risk Assessment Final Report. Goyder Inst. Water Res. Tech. Rep. Ser. No. 13/17.

Page, D., Gonzalez, D., Sidhu, J., Toze, S., Torkzaban, S., Dillon, P., 2016a. Assessment of treatment options of recycling urban stormwater recycling via aquifers to produce drinking water quality. Urban Water J. 13, 657–662. https://doi.org/10.1080/1573062X.2015.1024691

Page, D., Gonzalez, D., Torkzaban, S., Toze, S., Sidhu, J., Miotliński, K., Barry, K., Dillon, P., 2015. Microbiological risks of recycling urban stormwater via aquifers for various uses in Adelaide, Australia. Environ. Earth Sci. 73, 7733–7737. https://doi.org/10.1007/s12665-014-3466-4

Page, Declan, Neus Ayuso-Gabella, M., Kopac, I., Bixio, D., Dillon, P., de Marcay, M., Genthe, B., 2012. Risk assessment and risk management in Managed Aquifer Recharge. Water Reclam. Technol. Safe Manag. Aquifer Recharg. 351–374.

Page, D., Vanderzalm, J., Barry, K., Levett, K., Kremer, S., Ayuso-Gabella, M., Dillon, Toze, S., Sidhu, J., Shackleton, M., Purdie, M., Regel, R., 2009. Operational residual risk assessment for the Salisbury stormwater ASTR project.

Page, D., Vanderzalm, J., Dillon, P., Gonzalez, D., Barry, K., 2016b. Stormwater Quality Review to Evaluate Treatment for Drinking Water Supply via Managed Aquifer Recharge. Water. Air. Soil Pollut. 227. https://doi.org/10.1007/s11270-016-3021-x

Palmgren, M.G., 2001. Plant plasma Membrane H+- ATPases: Powerhouses of Nutrient Uptake. Annu. Rev. plant Physiol. Mol. Biol. 52, 817–845. https://doi.org/10.1146/annurev.arplant.52.1.817

Pasini, S., Torresan, S., Rizzi, J., Zabeo, A., Critto, A., Marcomini, A., 2012. Climate change impact assessment in Veneto and Friuli Plain groundwater. Part II: A spatially resolved regional risk assessment. Sci. Total Environ. 440, 219–235. https://doi.org/10.1016/j.scitotenv.2012.06.096

Pavelic, P., Nicholson, B.C., Dillon, P.J., Barry, K.E., 2005. Fate of disinfection by-products in groundwater during aquifer storage and recovery with reclaimed water. J. Contam. Hydrol. 77, 119–141. https://doi.org/10.1016/j.jconhyd.2004.12.003

Pedretti, D., Barahona-Palomo, M., Bolster, D., Fernàndez-Garcia, D., Sanchez-Vila, X., Tartakovsky, D.M., 2012a. Probabilistic analysis of maintenance and operation of artificial recharge ponds. Adv. Water Resour. 36, 23–35. https://doi.org/10.1016/j.advwatres.2011.07.008

Pedretti, D., Barahona-Palomo, M., Bolster, D., Sanchez-Vila, X., Fernàndez-Garcia, D., 2012b. A quick and inexpensive method to quantify spatially variable infiltration capacity for artificial recharge ponds using photographic images. J. Hydrol. 430–431, 118–126. https://doi.org/10.1016/j.jhydrol.2012.02.008

Pindoria-Nandha, M., 2016. Planning an Aquifer Storage and Recovery scheme in the Sherwood Sandstone aquifer. Cranfield Unviversity.

Piwowarczyk, A., Peng, X., Richards, K.G., Holden, N.M., 2010. A laboratory lysimeter for pesticide transport studies, in: 19th World Congress of Soil Science, Soil

Solutions for a Changing World. Brisbane, Australia., pp. 1–4.

Pot, V., Šimůnek, J., Benoit, P., Coquet, Y., Yra, A., Martínez-Cordón, M.J., 2005. Impact of rainfall intensity on the transport of two herbicides in undisturbed grassed filter strip soil cores. J. Contam. Hydrol. 81, 63–88. https://doi.org/10.1016/j.jconhyd.2005.06.013

Pütz, T., Fank, J., Flury, M., 2018. Lysimeters in Vadose Zone Research. Vadose Zo. J. 17, 180035. https://doi.org/10.2136/vzj2018.02.0035

Pyne, D., 1995. Groundwater recharge and wells - A guide to aquifer storage and recovery. CRC Press.

Radolinski, J., Pangle, L., Klaus, J., Stewart, R.D., 2021. Testing the ‘two water worlds’ hypothesis under variable preferential flow conditions. Hydrol. Process. 35, 1–14. https://doi.org/10.1002/hyp.14252

Rani, S., Sud Sant, D., 2014. Time and temperature dependent sorption behaviour of dimethoate pesticide in various Indian soils. Int. Agrophysics 28, 479–490. https://doi.org/10.2478/intag-2014-0038

Ravenscroft, P., Murray, R., 2010. Planning and Authorising Artificial Recharge Schemes - Strategy and Guideline Development for National Groundwater Planning Requirements WP 9390.

Rawluk, A., Curtis, A., Sharp, E., Kelly, B.F.J., Jakeman, A.J., Ross, A., Arshad, M., Brodie, R., Pollino, C.A., Sinclair, D., Croke, B., Qureshi, M.E., 2013. Managed aquifer recharge in farming landscapes using large floods: an opportunity to improve outcomes for the Murray-Darling Basin? Australas. J. Environ. Manag. 20, 34–48. https://doi.org/10.1080/14486563.2012.724785

Ray, C., Melin, G., Linksy, R.B., 2003. Riverbank Filtration Improving Source-water Quality, Environmental Science and Engineering (Subseries: Environmental Science). https://doi.org/10.1007/0-306-48154-5

Rein, A., Legind, C.N., Trapp, S., 2011. New concepts for dynamic plant uptake models. SAR QSAR Environ. Res. 22, 191–215. https://doi.org/10.1080/1062936X.2010.548829

Reinnicke, S., Juchelka, D., Steinbeiss, S., Meyer, A., Hilkert, A., Elsner, M., 2012. Gas chromatography/isotope ratio mass spectrometry of recalcitrant target compounds: Performance of different combustion reactors and strategies for standardization. Rapid Commun. Mass Spectrom. 26, 1053–1060. https://doi.org/10.1002/rcm.6199

Richards, L.A., 1931. Capillary conduction of liquids through porous mediums. J. Appl. Phys. 1, 318–333. https://doi.org/10.1063/1.1745010

Richter, H.E., Gungle, B., Lacher, L.J., Turner, D.S., Bushman, B.M., 2014. Development of a shared vision for groundwater management to protect and sustain baseflows of the upper san pedro river, Arizona, USA. Water (Switzerland)

6, 2519–2538. https://doi.org/10.3390/w6082519

Ringleb, J., Sallwey, J., Stefan, C., 2016. Assessment of managed aquifer recharge through modeling-A review. Water (Switzerland) 8, 1–31. https://doi.org/10.3390/w8120579

Ritchie, J.T., 1972. Model for predicting evaporation from a row crop with incomplete cover. Water Resour. Res. 8, 1204–1213. https://doi.org/https://doi.org/10.1029/WR008i005p01204

Robin, M.J.L., Laryea, K.B., Elrick, D.E., 1983. Hydrodynamic dispersion during absorption of water by soil 2. Immobile water model. J. Hydrol. 65, 333–348. https://doi.org/10.1016/0022-1694(83)90085-9

Rodríguez-Escales, P., Canelles, A., Sanchez-Vila, X., Folch, A., Kurtzman, D., Rossetto, R., Fernández-Escalante, E., Lobo-Ferreira, J.P., Sapiano, M., San-Sebastián, J., Schüth, C., 2018. A risk assessment methodology to evaluate the risk failure of managed aquifer recharge in the Mediterranean Basin. Hydrol. Earth Syst. Sci. 22, 3213–3227. https://doi.org/10.5194/hess-22-3213-2018

Rodríguez-Escales, P., Fernàndez-Garcia, D., Drechsel, J., Folch, A., Sanchez-Vila, X., 2017. Improving degradation of emerging organic compounds by applying chaotic advection in Managed Aquifer Recharge in randomly heterogeneous porous media. Water Resour. Res. 53, 4376–4392. https://doi.org/10.1002/2016WR020333

Rodríguez-Escales, P., Folch, A., Vidal-Gavilan, G., van Breukelen, B.M., 2016. Modeling biogeochemical processes and isotope fractionation of enhanced in situ biodenitrification in a fractured aquifer. Chem. Geol. 425, 52–64. https://doi.org/10.1016/j.chemgeo.2016.01.019

Rodríguez-Estrella, T., 2012. The problems of overexploitation of aquifers in semi-arid areas: the Murcia Region and the Segura Basin (South-east Spain) case. Hydrol. Earth Syst. Sci. Discuss. 9, 5729–5756. https://doi.org/10.5194/hessd-9-5729-2012

Rodriguez, C., Cook, A., Van Buynder, P., Devine, B., Weinstein, P., 2007a. Screening health risk assessment of micropullutants for indirect potable reuse schemes: A three-tiered approach. Water Sci. Technol. 56, 35–42. https://doi.org/10.2166/wst.2007.831

Rodriguez, C., Weinstein, P., Cook, A., Devine, B., Van Buynder, P., 2007b. A proposed approach for the assessment of chemicals in indirect potable reuse schemes. J. Toxicol. Environ. Heal. - Part A Curr. Issues 70, 1654–1663. https://doi.org/10.1080/15287390701434828

Ronen, D., Sorek, S., 2005. The unsaturated zone - a neglected component of nature, in: Nützmann, G., Viotti, P., Aagaard, P. (Eds.), Reactive Transport in Soil and Groundwater: Processes and Models. Springer Berlin Heidelberg, Berlin, Heidelberg, pp. 3–15. https://doi.org/10.1007/3-540-26746-8_1

Ruiz, S., Fletcher, D.M., Williams, K., Roose, T., 2021. Plant-soil modelling, Annual Plant Reviews Online. https://doi.org/10.1002/9781119312994.apr0755

Rupérez-Moreno, C., Pérez-Sánchez, J., Senent-Aparicio, J., Flores-Asenjo, P., Paz-Aparicio, C., 2017. Cost-Benefit Analysis of the Managed Aquifer Recharge System for Irrigation under Climate Change Conditions in Southern Spain. water 9, 343. https://doi.org/10.3390/w9050343

Sadeghi, A.M., Isensee, A.R., Shirmohammadi, A., 2000. Influence of soil texture and tillage on herbicide transport. Chemosphere 41, 1327–1332. https://doi.org/10.1016/S0045-6535(00)00028-X

Sallwey, J., Bonilla Valverde, J.P., Vásquez López, F., Junghanns, R., Stefan, C., 2019. Suitability maps for managed aquifer recharge: A review of multi-criteria decision analysis studies. Environ. Rev. 27, 138–150. https://doi.org/10.1139/er-2018-0069

Sandhu, C., Grischek, T., Musche, F., Macheleidt, W., Heisler, A., Handschak, J., Patwal, P.S., Kimothi, P.C., 2018. Measures to mitigate direct flood risks at riverbank filtration sites with a focus on India. Sustain. Water Resour. Manag. 4, 237–249. https://doi.org/10.1007/s40899-017-0146-z

Sarmah, A.K., Sabadie, J., 2002. Hydrolysis of sulfonylurea herbicides in soils and aqueous solutions: A review. J. Agric. Food Chem. 50, 6253–6265. https://doi.org/10.1021/jf025575p

Scheffer, F., Schachtschnabel, P., 2018. Lehrbuch der Bodenkunde, Anzeiger für Schädlingskunde und Pflanzenschutz. https://doi.org/10.1007/BF02027629

Schmidt, C.K., Lange, F.T., Brauch, H.J., 2007. Characteristics and evaluation of natural attenuation processes for organic micropollutant removal during riverbank filtration. Water Sci. Technol. Water Supply 7, 1–7. https://doi.org/10.2166/ws.2007.060

Schönenberger, U.T., Simon, J., Stamm, C., 2022. Are spray drift losses to agricultural roads more important for surface water contamination than direct drift to surface waters? Sci. Total Environ. 809. https://doi.org/10.1016/j.scitotenv.2021.151102

Schreglmann, K., Hoeche, M., Steinbeiss, S., Reinnicke, S., Elsner, M., 2013. Carbon and Nitrogen Isotope Analysis of Atrazine and Desethylatrazine at Sub-mug/L Concentrations in Groundwater. Anal. Bioanal. Chem. 405, 2857–2867. https://doi.org/10.1007/s00216-012-6616-0

Schwärzel, K., Šimůnek, J., Stoffregen, H., Wessolek, G., van Genuchten, M.T., 2006. Estimation of the Unsaturated Hydraulic Conductivity of Peat Soils: Laboratory versus Field Data. Vadose Zo. J. 5, 628–640. https://doi.org/10.2136/vzj2005.0061

Seeboonruang, U., 2016. Impact assessment of climate change on groundwater and vulnerability to drought of areas in Eastern Thailand. Environ. Earth Sci. 75, 1–13. https://doi.org/10.1007/s12665-015-4896-3

References

Seis, W., Sprenger, C., Schimmelpfennig, S., 2015. Application of the Australian Guidelines for Water Recycling: Managing Health and Environmental Risks, Part of D11.2: Demonstration of MAR effects on groundwater resources – development and application of different approaches for risk and impact assessmen 308339, 389.

SEMARNAT Secretaría del Medio Ambiente y Recursos Naturales, 2009. Norma Oficial Mexicana NOM-015-CONAGUA-2007, Infiltración artificial de agua a los acuíferos.-Características y especificaciones de las obras y del agua.

Shah, T., 2014. Towards a Managed Aquifer Recharge strategy for Gujarat, India: An economist's dialogue with hydro-geologists. J. Hydrol. 518, 94–107. https://doi.org/10.1016/j.jhydrol.2013.12.022

Shah, T., Burke, J., Villholth, K., Angelica, M., Custodio, E., Daibes, F., Hoogesteger, J., Giordano, M., Girman, J., van der Gun, J., Kendy, E., Kijne, J., Llamas, R., Masiyandama, M., Margat, J., Marin, L., Peck, J., Rozelle, S., Sharma, B., Vincent, L., Wang, J., 2007. Groundwater: A global assessment of scale and significance. Water Food Water Life A Compr. Assess. Water Manag. Agric. 395–424. https://doi.org/10.4324/9781849773799

Shajari, F., Einsiedl, F., Rein, A., 2020. Characterizing Water Flow in Vegetated Lysimeters with Stable Water Isotopes and Modeling. Groundwater 58, 759–770. https://doi.org/10.1111/gwat.12970

Shaler, T.A., Klečka, G.M., 1986. Effects of Dissolved Oxygen Concentration on Biodegradation of. Appl. Environ. Microbiol. 51, 950–955. https://doi.org/10.1128/aem.51.5.950-955.1986

Sharma, S., Bhattacharya, A., 2017. Drinking water contamination and treatment techniques. Appl. Water Sci. 7, 1043–1067. https://doi.org/10.1007/s13201-016-0455-7

Sidoli, P., Lassabatere, L., Angulo-Jaramillo, R., Baran, N., 2016. Experimental and modeling of the unsaturated transports of S-metolachlor and its metabolites in glaciofluvial vadose zone solids. J. Contam. Hydrol. 190, 1–14. https://doi.org/10.1016/j.jconhyd.2016.04.001

Šimůnek, Jirí, Genuchten, M.T., Šejna, M., 2008. Development and Applications of the HYDRUS and STANMOD Software Packages and Related Codes. Vadose Zo. J. 7, 587–600. https://doi.org/10.2136/vzj2007.0077

Šimůnek, J., Hopmans, J.W., 2009. Modeling compensated root water and nutrient uptake. Ecol. Modell. 220, 505–521. https://doi.org/10.1016/j.ecolmodel.2008.11.004

Šimůnek, J., Jarvis, N.J., Van Genuchten, M.T., Gärdenäs, A., 2003. Review and comparison of models for describing non-equilibrium and preferential flow and transport in the vadose zone. J. Hydrol. 272, 14–35. https://doi.org/10.1016/S0022-1694(02)00252-4

Šimůnek, J., Köhne, J.M., Kodešová, R., Šejna, M., 2008. Simulating Nonequilibrium Movement of Water , Solutes and Particles Using HYDRUS – A Review of Recent Applications. Soil Water Res. 3, S42–S51.

Šimůnek, J., Šejna, M., Sakai, M., van Genuchten, M.T., 2018. The HYDRUS-1D Software Package for Simulating the One-Dimensional Movement of Water, Heat, and Multiple Solutes in Variably-Saturated Media, Version 4.17, HYDRUS Software Series 3,. Dep. Environ. Sci. Univ. Calif. Riverside Riverside, 348.

Šimůnek, J., van Genuchten, M.T., 2008. Modeling Nonequilibrium Flow and Transport Processes Using HYDRUS. Vadose Zo. J. 7, 782–797. https://doi.org/10.2136/vzj2007.0074

Šimůnek, J., van Genuchten, M.T., Šejna, M., 2022. The HYDRUS Software Package for Simulating One-, Two-, and Three-Dimensional Movement of Water, Heat, and Multiple Solutes in Variably- Saturated Porous Media, Technical Manual II, Hydrus 2D/3D, Version 5.x. Prague, Czech Republic.

Šimůnek, J., Wendroth, O., Wypler, N., van Genuchten, M.T., 2001. Non-equilibrium water flow characterized by means of upward infiltration experiments. Eur. J. Soil Sci. 52, 13–24. https://doi.org/10.1046/j.1365-2389.2001.00361.x

Singh, N., Kloeppel, H., Klein, W., 2002. Movement of metolachlor and terbuthylazine in core and packed soil columns. Chemosphere 47, 409–415. https://doi.org/10.1016/S0045-6535(01)00322-8

Singh, S.N., Jauhari, N., 2017. Degradation of Atrazine by Plants and Microbes, Environmental Science and Engineering (Subseries: Environmental Science). https://doi.org/10.1007/978-3-319-45156-5_8

Song, Y., Du, X., Ye, X., 2019. Analysis of potential risks associated with urban stormwater quality for managed aquifer recharge. Int. J. Environ. Res. Public Health 16. https://doi.org/10.3390/ijerph16173121

Sprenger, C., Hartog, N., Hernández, M., Vilanova, E., Grützmacher, G., Scheibler, F., Hannappel, S., 2017. Inventory of managed aquifer recharge sites in Europe: historical development, current situation and perspectives. Hydrogeol. J. 25, 1909–1922. https://doi.org/10.1007/s10040-017-1554-8

Sprenger, C., Panagiotou, K., Fernandes, L., Duzan, A., Baptista, V., Glass, J., 2020. Smart framework for real-time monitoring and control of subsurface processes in managed aquifer recharge (MAR) applications 59.

Sprenger, M., Erhardt, M., Riedel, M., Weiler, M., 2016a. Historical tracking of nitrate in contrasting vineyards using water isotopes and nitrate depth profiles. Agric. Ecosyst. Environ. 222, 185–192. https://doi.org/10.1016/j.agee.2016.02.014

Sprenger, M., Seeger, S., Blume, T., Weiler, M., 2016b. Travel times in the vadose zone: Variability in space and time. Water Resour. Res. 52, 5727–5754. https://doi.org/10.1002/2015WR018077

Sprenger, M., Tetzlaff, D., Buttle, J., Laudon, H., Leistert, H., Mitchell, C.P.J., Snelgrove, J., Weiler, M., Soulsby, C., 2018. Measuring and Modeling Stable Isotopes of Mobile and Bulk Soil Water. Vadose Zo. J. 17, 170149. https://doi.org/10.2136/vzj2017.08.0149

Sprenger, M., Volkmann, T.H.M., Blume, T., Weiler, M., 2015. Estimating flow and transport parameters in the unsaturated zone with pore water stable isotopes. Hydrol. Earth Syst. Sci. 19, 2617–2635. https://doi.org/10.5194/hess-19-2617-2015

Stephenson, G.R., Ferris, I.G., Holland, P.T., Nordberg, M., 2006. Glossary of terms relating to pesticides (IUPAC Recommendations 2006). Pure Appl. Chem. 78, 2075–2154. https://doi.org/10.1351/pac200678112075

Stockinger, P.M., Reemt Bogena, H., Lücke, A., Stumpp, C., Vereecken, H., 2019. Time variability and uncertainty in the fraction of young water in a small headwater catchment. Hydrol. Earth Syst. Sci. 23, 4333–4347. https://doi.org/10.5194/hess-23-4333-2019

Storlazzi, C.D., Gingerich, S.B., Van Dongeren, A., Cheriton, O.M., Swarzenski, P.W., Quataert, E., Voss, C.I., Field, D.W., Annamalai, H., Piniak, G.A., McCall, R., 2018. Most atolls will be uninhabitable by the mid-21st century because of sea-level rise exacerbating wave-driven flooding. Sci. Adv. 4, 1–10. https://doi.org/10.1126/sciadv.aap9741

Strauß, C., Bayer, A., 2017. Lysimeteruntersuchungen zum Austragsverhalten von im Maisanbau eingesetzten Herbiziden unter Freilandbedingungen (Standort Wielenbach). Höhere Bundeslehr- und Forschungsanstalt für Landwirtschaft- und Forschungsanstalt Raumberg-Gumpenstein, L17. Gumpensteiner Lysimetertagung 27–32.

Stumpp, C., Hendry, M.J., 2012. Spatial and temporal dynamics of water flow and solute transport in a heterogeneous glacial till: The application of high-resolution profiles of d18O and d2H in pore waters. J. Hydrol. 203–214.

Stumpp, C., Małoszewski, P., Stichler, W., Fank, J., 2009a. Environmental isotope (δ18O) and hydrological data to assess water flow in unsaturated soils planted with different crops: Case study lysimeter station “Wagna” (Austria). J. Hydrol. 369, 198–208. https://doi.org/10.1016/j.jhydrol.2009.02.047

Stumpp, C., Małoszewski, P., Stichler, W., Maciejewski, S., 2007. Quantification of the heterogeneity of the unsaturated zone based on environmental deuterium observed in lysimeter experiments. Hydrol. Sci. J. 52, 748–762. https://doi.org/10.1623/hysj.52.4.748

Stumpp, C., Nützmann, G., Maciejewski, S., Małoszewski, P., 2009b. A comparative modeling study of a dual tracer experiment in a large lysimeter under atmospheric conditions. J. Hydrol. 375, 566–577. https://doi.org/10.1016/j.jhydrol.2009.07.010

Stumpp, C., Stichler, W., Kandolf, M., Šimůnek, J., 2012. Effects of Land Cover and Fertilization Method on Water Flow and Solute Transport in Five Lysimeters: A

Long-Term Study Using Stable Water Isotopes. Vadose Zo. J. 11. https://doi.org/10.2136/vzj2011.0075

Stumpp, C., Stichler, W., Maloszewski, P., 2009c. Application of the environmental isotope δ18O to study water flow in unsaturated soils planted with different crops: Case study of a weighable lysimeter from the research field in Neuherberg, Germany. J. Hydrol. 368, 68–78. https://doi.org/10.1016/j.jhydrol.2009.01.027

Sultana, S., Ahmed, K.M., 2016. Assessing risk of clogging in community scale managed aquifer recharge sites for drinking water in the coastal plain of south-west Bangladesh. Bangladesh J. Sci. Res. 27, 75–86. https://doi.org/10.3329/bjsr.v27i1.26226

Swierc, J., Page, D., Leeuwen, J. Van, 2005. Preliminary Hazard Analysis and Critical Control Points Plan (HACCP) - Salisbury Stormwater to Drinking Water Aquifer Storage Transfer and Recovery (ASTR) Project of Montana. Water.

Syafrudin, M., Kristanti, R.A., Yuniarto, A., Hadibarata, T., Rhee, J., 2021. Pesticides in Drinking Water — A Review. Int. J. Environ. Res. Public Heal. 18. https://doi.org/https://doi.org/10.3390/ijerph18020468

Täumer, K., Stoffregen, H., Wessolek, G., 2006. Seasonal Dynamics of Preferential Flow in a Water Repellent Soil. Vadose Zo. J. 5, 405–411. https://doi.org/10.2136/vzj2005.0031

Tchobanoglous, G., Burton, F.L., Stensel, H.D., 2003. Wastewater Engineering Teatment and Reuse, Metcalf & Eddy, Inc.

Thoma, M.J., Barrash, W., Cardiff, M., Bradford, J., Mead, J., 2014. Estimating Unsaturated Hydraulic Functions for Coarse Sediment from a Field-Scale Infiltration Experiment. Vadose Zo. J. 13, 1–17. https://doi.org/10.2136/vzj2013.05.0096

Toccalino, P.L., Gilliom, R.J., Lindsey, B.D., Rupert, M.G., 2014. Pesticides in groundwater of the United States: decadal-scale changes, 1993-2011. Ground Water 52, 112–125. https://doi.org/10.1111/gwat.12176

Torrentó, C., Bakkour, R., Ryabenko, E., Ponsin, V., Prasuhn, V., Hofstetter, T.B., Elsner, M., Hunkeler, D., 2015. Fate of Four Herbicides in an Irrigated Field Cropped with Corn: Lysimeter Experiments. Procedia Earth Planet. Sci. 13, 158–161. https://doi.org/10.1016/j.proeps.2015.07.037

Torrentó, C., Ponsin, V., Lihl, C., Hofstetter, T.B., Baran, N., Elsner, M., Hunkeler, D., 2021. Triple-Element Compound-Specific Stable Isotope Analysis (3D-CSIA): Added Value of Cl Isotope Ratios to Assess Herbicide Degradation. Environ. Sci. Technol. 55, 13891–13901. https://doi.org/10.1021/acs.est.1c03981

Toze, S., Bekele, E., Page, D., Sidhu, J., Shackleton, M., 2010. Use of static Quantitative Microbial Risk Assessment to determine pathogen risks in an unconfined carbonate aquifer used for Managed Aquifer Recharge. Water Res. 44, 1038–1049. https://doi.org/10.1016/j.watres.2009.08.028

Trapp, S., Matthies, M., 1998. Chemodynamics and environmental modeling: An introduction, Environmental Science and Pollution Research. https://doi.org/10.1007/bf02987670

Trapp, S., Matthies, M., 1997. Chemodynamics and environmental modeling An introduction, Springer Verlag. Elsevier. https://doi.org/10.1029/92WR00607

Tzoraki, O., Dokou, Z., Christodoulou, G., Gaganis, P., Karatzas, G., 2018. Assessing the efficiency of a coastal Managed Aquifer Recharge (MAR) system in Cyprus. Sci. Total Environ. 626, 875–886. https://doi.org/10.1016/j.scitotenv.2018.01.160

UN United Nations, 2016. Sustainable Development Goal 6 [WWW Document].

United Nations, 2022. The United Nations World Water Development Report 2022: Groundwater: Making the invisible visible, Journal of healthcare risk management : the journal of the American Society for Healthcare Risk Management. UNESCO, Paris. https://doi.org/10.1002/jhrm.21236

US EPA United States Environmental Protection Agency, 2012. Guidelines for Water Reuse. US Environ. Prot. Agency Washington, D.C., Off. Wastewater Manag. Off. Water 643.

US EPA United States Environmental Protection Agency, 2002. A review of the reference dose and reference concentration process. Risk Assess. Forum, US Environ. Prot. Agency 1–192.

US EPA United States Environmental Protection Agency, 1998. Human Health Risk Assessment Protocol for Hazardous Waste Combustion facilities. US Environ. Prot. Agency Washington, D.C., Off. Solid Waste 1.

US EPA United States Environmental Protection Agency, 1987. The Risk Assessment Guidelines of 1986-EPA/600/8-87/045. US Environ. Prot. Agency Washington, D.C. 81.

van de Zande, J.C., Michielsen, J.M.G.P., Stallinga, H., 2007. Spray Drift and Off-field Evaluation of Agrochemical in the Netherlands. Plant Res. Int. B.V., Wageningen 149.

van Genuchten, M.T., 1980. A Closed-form Equation for Predicting the Hydraulic Conductivity of Unsaturated Soils. Soil Sci. Soc. Am. J. 44, 892–898. https://doi.org/10.2136/sssaj1980.03615995004400050002x

van Genuchten, M.T., Wierenga, P.J., 1976. Mass Transfer Studies in Sorbing Porous Media I. Analytical Solutions. Soil Sci. Soc. Am. J. 40, 473–480. https://doi.org/10.2136/sssaj1976.03615995004000040011x

Van Ommen, H.C., Van Genuchten, M.T., Van Der Molen, W.H., Dijksma, R., Hulshof, J., 1989. Experimental and theoretical analysis of solute transport from a diffuse source of pollution. J. Hydrol. 105, 225–251. https://doi.org/10.1016/0022-1694(89)90106-6

Van Stempvoort, D.R., Roy, J.W., Grabuski, J., Brown, S.J., Bickerton, G., Sverko, E., 2013. An artificial sweetener and pharmaceutical compounds as co-tracers of urban wastewater in groundwater. Sci. Total Environ. 461–462, 348–3359. https://doi.org/10.1016/j.scitotenv.2013.05.001

Vanderborght, J., Vereecken, H., 2007. Review of Dispersivities for Transport Modeling in Soils. Vadose Zo. J. 6, 29–52. https://doi.org/10.2136/vzj2006.0096

Vanderzalm, J.L., Page, D.W., Dillon, P.J., 2011. Application of a risk management framework to a drinking water supply augmented by stormwater recharge. Water Sci. Technol. 63, 719–726. https://doi.org/10.2166/wst.2011.294

Varis, O., 2018. Population megatrends wand water megatrends, in: Biswas, A.K., Tortajada, C., Rohner, P. (Eds.), Assessing Global Water Megatrends. Springer Nature, Singapore. https://doi.org/10.1007/978-981-10-6695-5_3

Vbra, J., Richts, A., 2015. The global map of groundwater vulnerability to floods and droughts explanatory notes. United Nations Educational, Scientific and Cultural Organization, Paris.

Vischetti, C., Leita, L., Marucchini, C., Porzi, G., 1998. Degradation and mobility of metolachlor and terbuthylazine in a sandy clay loam soil. Agronomie 18, 131–137. https://doi.org/10.1051/agro:19980203

Vrba, J., 2002. The impact of aquifer intensive use on groundwater quality. Intensive Use Groundw. Challenges Oppor. 113–132.

Vrugt, J.A., Bouten, W., Weerts, A.H., 2001. Information Content of Data for Identifying Soil Hydraulic Parameters from Outflow Experiments. Soil Sci. Soc. Am. J. 65, 19–27. https://doi.org/10.2136/sssaj2001.65119x

Wada, Y., Van Beek, L.P.H., Bierkens, M.F.P., 2012. Nonsustainable groundwater sustaining irrigation: A global assessment. Water Resour. Res. 48. https://doi.org/10.1029/2011WR010562

Wada, Y., Van Beek, L.P.H., Van Kempen, C.M., Reckman, J.W.T.M., Vasak, S., Bierkens, M.F.P., 2010. Global depletion of groundwater resources. Geophys. Res. Lett. 37, 1–5. https://doi.org/10.1029/2010GL044571

Weber, J.B., Wilkerson, G.G., Michael Linker, H., Wilcut, J.W., Leidy, R.B., Senseman, S., Witt, W.W., Barrett, M., Vencill, W.K., Shaw, D.R., Mueller, T.C., Miller, D.K., Brecke, B.J., Talbert, R.E., Peeper, T.F., 2000. A proposal to standardize soil/solution herbicide distribution coefficients. Weed Sci. 48, 75–88. https://doi.org/10.1614/0043-1745(2000)048[0075:aptsss]2.0.co;2

Weng, J.H., 2000. The role of active and passive water uptake in maintaining leaf water status and photosynthesis in tomato under water deficit. Plant Prod. Sci. 3, 296–298. https://doi.org/10.1626/pps.3.296

WHO World Health Organization, 2017. Guidelines for Drinking Water quality 4th edition. Geneva.

References

WHO World Health Organization, 2012. Water Safety Planning for Small Community Water Supplies 1–66.

WHO World Health Organization, 2010. WHO Human Health Risk Assessment Toolkit: Chemical Hazards (IPCS Harmonization Project Document; No. 8). Int. Program. Chem. Saf. 106.

WHO World Health Organization, 2006. WHO Guidelines for the safe use of wastewater, excreta and greywater - Volume 1 policy and regulatory aspects.

WHO World Health Organization, 2004. Guidelines for drinking water quality, third edition, Vol. 1. Recommendations, World Health Organization. Geneva. https://doi.org/10.1016/0143-1471(85)90051-0

WHO World Health Organization, 1997. HACCP: introducing the hazard analysis critical control point system. World Health Organization.

WHO World Health Organization, FAO Food and Agriculture Organization of the United Nations, 2006. FAO/WHO guidance to governments on the application of HACCP in small and/or less-developed food businesses. WHO 86, 1–74.

Winton, K., Weber, J.B., 1996. A review of field lysimeter studies to describe the environmental fate of pesticides. Weed Technol. 10, 202–209. https://doi.org/10.1017/s0890037x00045929

Woldeamlak, S.T., Batelaan, O., De Smedt, F., 2007. Effects of climate change on the groundwater system in the Grote-Nete catchment, Belgium. Hydrogeol. J. 15, 891–901. https://doi.org/10.1007/s10040-006-0145-x

Yamaguchi, K., Fuse, E., Takashima, M., Yasuzawa, T., Kuwabara, T., Kobayashi, S., 1998. Fate of organics during soil-aquifer treatment: sustainability of removals in the field. J. Chromatogr. B Biomed. Appl. 713, 447–451. https://doi.org/10.1016/S0378-4347(98)00185-6

Zarebanadkouki, M., Kroener, E., Kaestner, A., Carminati, A., 2014. Visualization of root water uptake: Quantification of deuterated water transport in roots using neutron radiography and numerical modeling. Plant Physiol. 166, 487–499. https://doi.org/10.1104/pp.114.243212

Zemolin, C.R., Avalia, L.A., Cassol, G.V., Massey, J.H., Camargo, E.R., 2014. Environmental fate of s-metolachlor- a review. Planta daninha, Viçosa-MG 32, 655–664. https://doi.org/https://doi.org/10.1590/S0100-83582014000300022

Zhang, H., Xu, Y., Kanyerere, T., 2020. A review of the managed aquifer recharge : Historical development , current situation and perspectives. Phys. Chem. Earth 118–119, 102887. https://doi.org/10.1016/j.pce.2020.102887

Zhao, L., Ma, J., Sun, Z., Liu, H., 2009. Influencing mechanism of temperature on the degradation of nitrobenzene in aqueous solution by ceramic honeycomb catalytic ozonation. J. Hazard. Mater. 167, 1119–1125. https://doi.org/10.1016/j.jhazmat.2009.01.116

Zhou, T., Šimůnek, J., Braud, I., 2021. Adapting HYDRUS-1D to simulate the transport of soil water isotopes with evaporation fractionation. Environ. Model. Softw. 143. https://doi.org/10.1016/j.envsoft.2021.105118

Zimmermann, U., Ehhalt, D., Muennich, K.O., 1967. Soil-water movement and evapotranspiration: Changes in the isotopic composition of the water. IAEA, International Atomic Energy Agency (IAEA).

Zsolnay, A., 1994. The lack of effect of the dissolved organic material in soil on the water solubility of the herbicide, terbuthylazine. Sci. Total Environ. 152, 101–104.

Appendices

Appendix A Supporting Information to Chapter 4

Table A-1. Information on soil layers and grain size distributions. Comp.: components, wt.: weight, a: average of two layers with very similar grain size distribution.

Lysimeter 1					**Lysimeter 2**						
Layer	Horizon	Depth (cm)	Comp. <2 mm (%)	Comp. >2 mm (%)	Layer	Horizon	Depth (cm)	Gravel (wt. %)	Sand (wt. %)	Silt (wt. %)	Clay (wt. %)
1 a	Ah	0-30	50	50	1	Ap	0-40	4	23	49	23
2	Ah	30-40	67	33	2	Bv	40-90	2	20	35	43
3	C	40-50	34	66	3	BvCv	90-130	<1	5	55	39
4 a	C	50-200	20	80	4	Cv	130-180	2	25	45	27
					5	C	180-200	3	21	55	20

Table A-2. Soil hydraulic parameters determined for soil samples taken close to the location of the soil core within Lysimeter 1. θ_r and θ_S: residual and saturated soil water content; α, n: shape parameters (van Genuchten-Mualem model); K_S: saturated hydraulic conductivity.

Sampling depth (cm)	**θ_r (cm^3/cm^3)**	**θ_s (cm^3/cm^3)**	**α (1/cm)**	**n (-)**	**K_s (cm/d)**
0-10	0.023	0.193	0.094	1.499	1685
10-20	0.023	0.257	0.163	1.37	24970
100-120	0.01	0.2	0.069	1.377	38880
Average	0.019	0.22	0.109	1.408	20995

Table A-3. Parameter bounds selected for the application of the parameter optimization algorithm PEST; based on expected value ranges for the considered soils.

Parameter	Lysimeter 1		Lysimeter 2		Main references for the considered bounds
	Lower bound	Upper bound	Lower bound	Upper bound	
θ_r [cm³/cm³]	0.001	0.1	0.01	0.2	Jiang et al. (2010), Stumpp et al. (2009), Sprenger et al. (2015), Thoma et al. (2014), Vanderborght et al. (2000), Abbasi et al. (2003), Cheviron and Coquet (2009)
θ_s [cm³/cm³]	0.1	0.4	0.1	0.5	
α [1/cm]	0.005	0.5	0.005	0.6	
n [-]	1.0	4.0	1.0	4.0	
K_s [cm/d]	4,000	80,000	25	300	
P_D [cm]	0	200	0	200	
p_{pf} [%]	0	15	0	15	
T_{pf} [d]	0	7	0	7	

Table A-4. Basic statistical parameters of measured $\delta^{18}O$ for the whole observation period (Total) and the seasonal (half-year) sub-periods for Ly1 and Ly2 (S13: summer 2013, W13/14: winter 2013/14, etc.). Stdev.: standard deviation, n: number of values.

$\delta^{18}O$ [‰]	Total	S13	W13/14	S14	W14/15	S15	W15/16
Ly1							
Minimum	-13.78	-10.11	-12.12	-12.53	-11.97	-13.48	-13.52
Maximum	-7.00	-8.37	-8.44	-9.82	-8.27	-7.04	-7.00
Average	-10.35	-9.28	-10.08	-11.09	-9.55	-11.06	-9.86
Median	-10.58	-9.35	-10.26	-10.84	-8.88	-11.66	-10.44
Stdev.	1.67	0.66	1.04	0.74	1.31	1.72	2.22
n [-]	126	7	22	19	25	26	23
Ly2							
Minimum	-12.40	-8.69	-10.23	-10.73	-10.79	-11.34	-12.40
Minimum	-6.75	-7.99	-6.75	-8.50	-8.21	-8.20	-7.61
Average	-9.41	-8.40	-9.31	-9.25	-9.46	-9.60	-9.87
Median	-9.36	-8.47	-9.38	-9.23	-9.42	-9.46	-9.58
Stdev.	0.78	0.30	0.65	0.48	0.67	0.76	1.30
n [-]	109	6	22	18	26	25	11

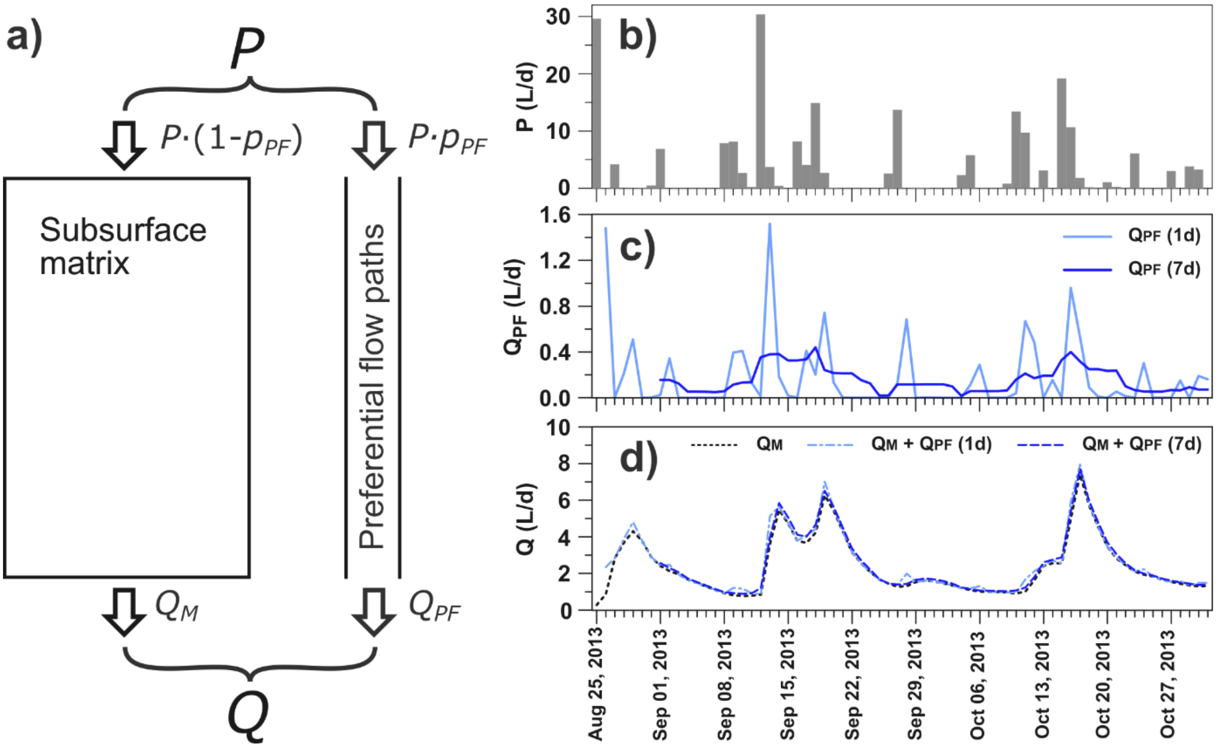

Figure A-1. a): Concept for simulating water flow in the unsaturated zone (numerical modelling). b-d): Example with 5% preferential flow for the time between August and October 2013. b): Observed precipitation (*P*) as a function of time. c): Simulated lysimeter outflow resulting from water flow along preferential flow paths (Q_{PF}), assuming a mean transit time of water within preferential flow paths (T_{PF}) of 1 day (1d) and 7 days (7d). d): Simulated lysimeter outflow within the subsurface matrix (Q_M), without or with consideration of preferential flow. *Q*: total lysimeter outflow, p_{PF}: portion of preferential flow. For a T_{PF} of 1 day, 5% of precipitation (for the example of p_{PF} = 0.05) is transported along preferential flow paths of the lysimeter soil core: at lysimeter outflow, simulated preferential flow corresponds to 5% of precipitation shifted by one day. For higher T_{PF}, moving averages of daily precipitation rates were calculated: as an example, for T_{PF} = 7 days, we assume that precipitation water takes one week for passing the preferential flow paths and reaching lysimeter outflow. Precipitation water present within the preferential flow paths is assumed to be fully mixed. Preferential flow paths were considered for the transport of stable water isotopes, accordingly.

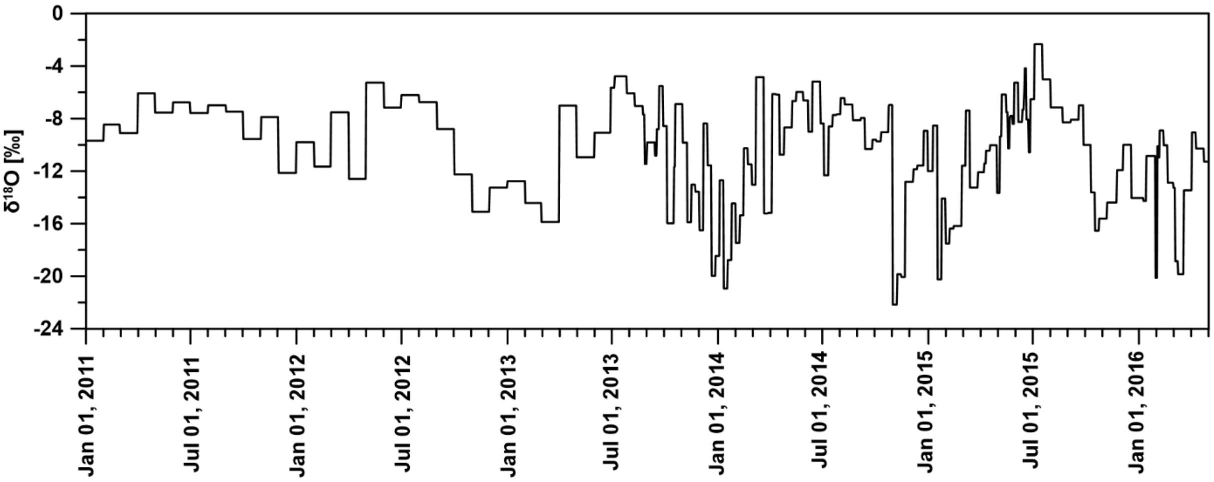

Figure A-2. δ^{18}O as a function of time, measured in precipitation (before 2013: weather station Passau-Fürstenzell, Germany; 2013-2016: lysimeter study site).

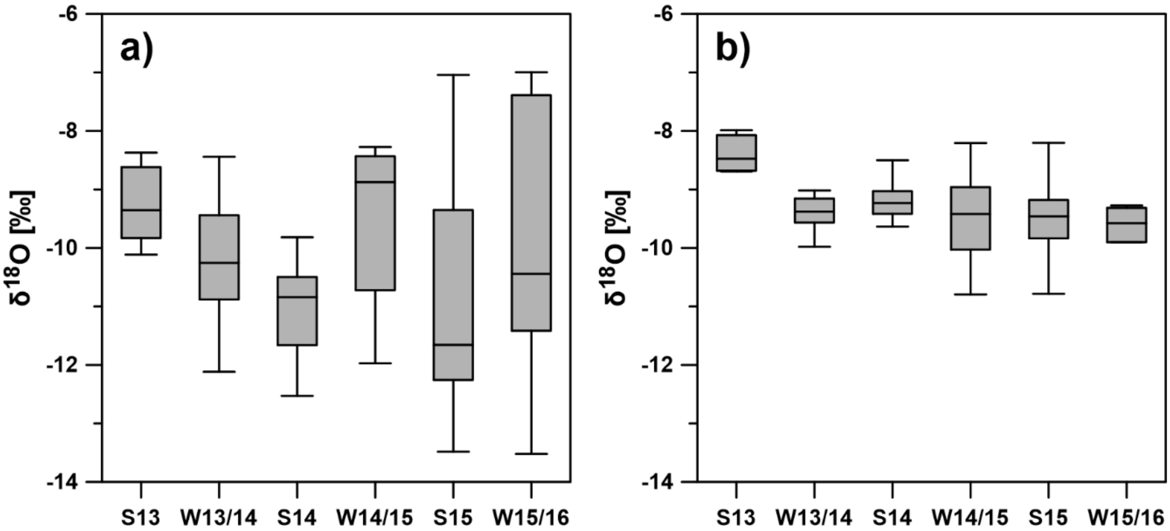

Figure A-3. Variation of measured δ^{18}O in Ly1 (a) and Ly2 (2) within the seasonal sub-periods (cf. Table A-4). Error bars indicate minimum and maximum, boxes the median, lower and upper quartile.

A1. Pre-phase setup

As a major change to our previous study (Shajari et al., 2020), we considered a longer modelling pre-phase of 5 years (instead of 1 year) for LPM modelling of Ly2. This was done both for constant flow (dashed curve in Figure 4-2a, main manuscript) and varying flow (other model curves in Figure 4-2). This longer pre-phase revealed to be more adequate given the finer-grained structure and higher mean residence time of water within Ly2: as seen from the simulated curves of relative recovery (RR) shown in Figure A-4a, about 98% of tracer breakthrough is reached after 5 year (only ~70 % after 1 year). These curves were obtained from applying the analytical solution of Lenda and Zuber (1970) for constant initial tracer concentration:

$$RR(t) = \frac{1}{2}\left[erfc\left(\frac{1-t/T}{\sqrt{4P_D\, t/T}}\right) + exp\left(\frac{1}{P_D}\right) erfc\left(\frac{1+t/T}{\sqrt{4P_D\, t/T}}\right)\right] \qquad \text{(A1)}$$

with T = 362 d and P_D = 0.7 as for Ly2 in our previous study. For Ly1, using a pre-phase of 1 year (as in our previous study) revealed 99 % of tracer breakthrough after one year (curve not shown). However, only considering a second component can explain observations, well: a constant value of $\delta^{18}O$ = 1 ‰ was added to the model curves in order to obtain an upshift and thus correct for underestimation (cf. Figure A-4). This second component, contributing to advective/dispersive isotope transport from lysimeter top, might result from the re-mobilization of immobile water within the soil column of Ly 2, as further discussed in the main manuscript.

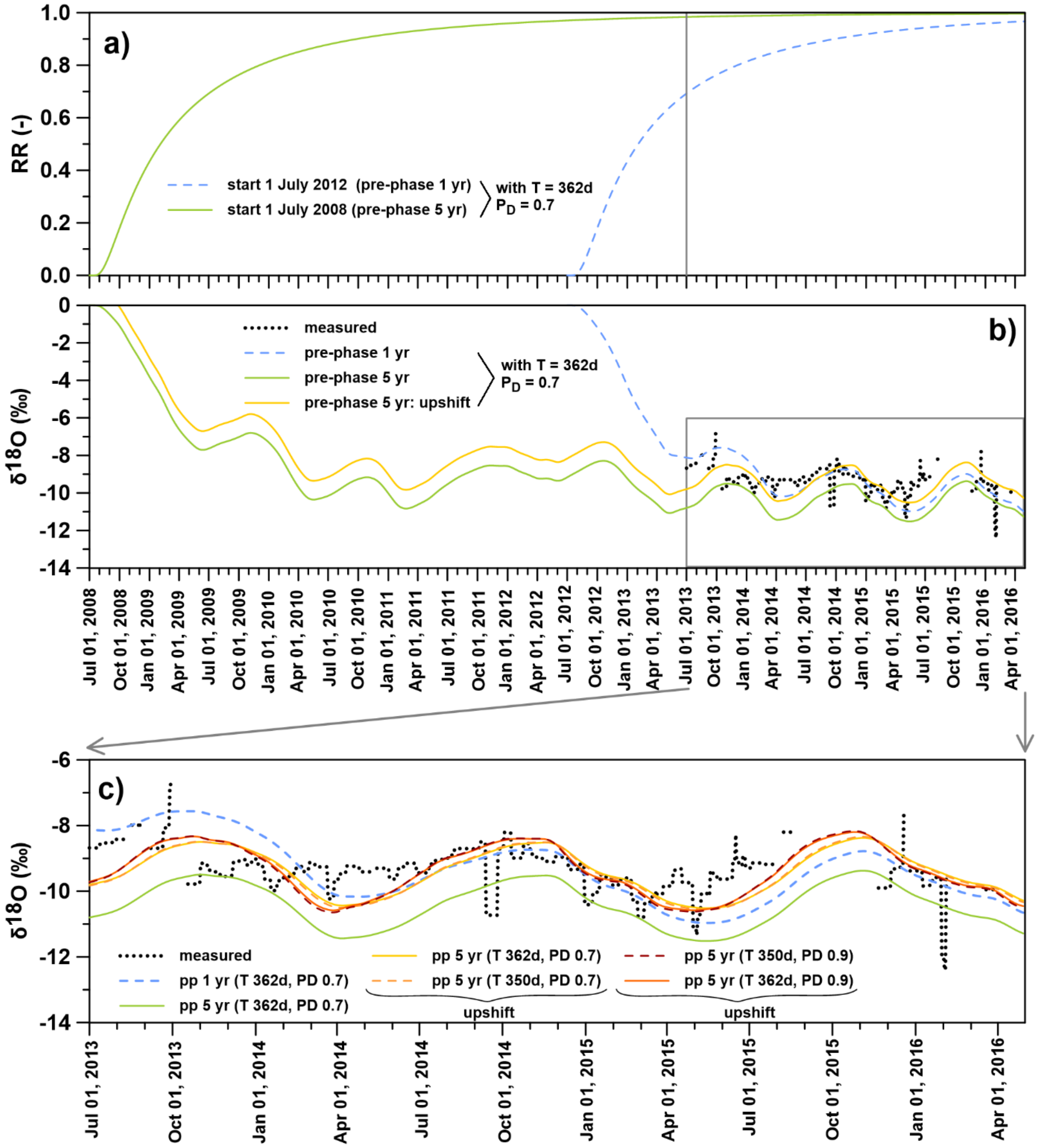

Figure A-4. a) Simulated relative recovery (RR) as a function of time for constant input, with mean transit time T = 362 d and dispersion parameter P_D = 0.7 (analytical solution of Lenda and Zuber 1970, Eq. A1). Input starts at 1 July 2008 (blue dashed curve) and 1 July 2012 (green curve), corresponding to a pre-phase of 5 years and 1 year, respectively. The vertical gray line indicates the start of lysimeter outflow measurements (end of modelling pre-phase). b) Simulated (LPM) versus measured δ^{18}O as a function of time. The orange curve considers a second component that adds to simulated δ^{18}O, leading to constant upshift of 1 ‰. c) Zoom into the time frame of lysimeter outflow measurements (skipping the pre-phase). Consideration of the longer pre-phase (5 years, pp 5 yr) plus the second component ("upshift") could significantly improve curve fits.

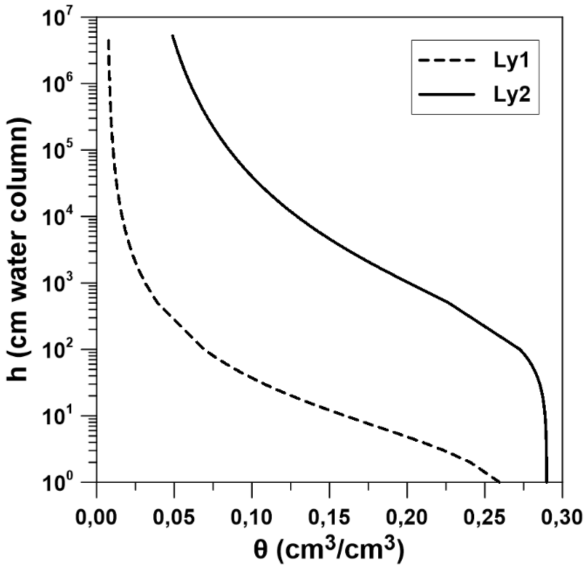

Figure A-5. Water retention curves for Lysimeter 1 and Lysimeter 2 calculated based on fitted soil hydraulic parameters, SHP (cf. Table 3). Due to the lack of in situ measurements in the studied lysimeters, we have analysed these simulated soil water retention curves and compared our findings to those of similar studies. For example, Stauffer and Lu (2012) and Thoma et al. (2014) conclude that the shape of water retention curves can act as a suitable proxy to identify the physical correctness of a fitted set of SHP, which can reduce computational efforts. As expected for coarse soil textures, the water retention curve for Ly1 tends to be S-shaped, a behavior that is controlled by shape parameter *n*. It leads to a steep increase at a higher water content (air entry point), and then the curve is flattening, followed by a strong increase at lower water contents. Such a behavior is typical for the dewatering of considerably different pore sizes. Such differences have been observed for similar soils, e.g., by Stumpp et al. (2009a) and Sprenger et al. (2015). The soil water retention curve for Ly2 is steeper in comparison to Ly1 (lower *n*), as expected due to the finer soil texture.

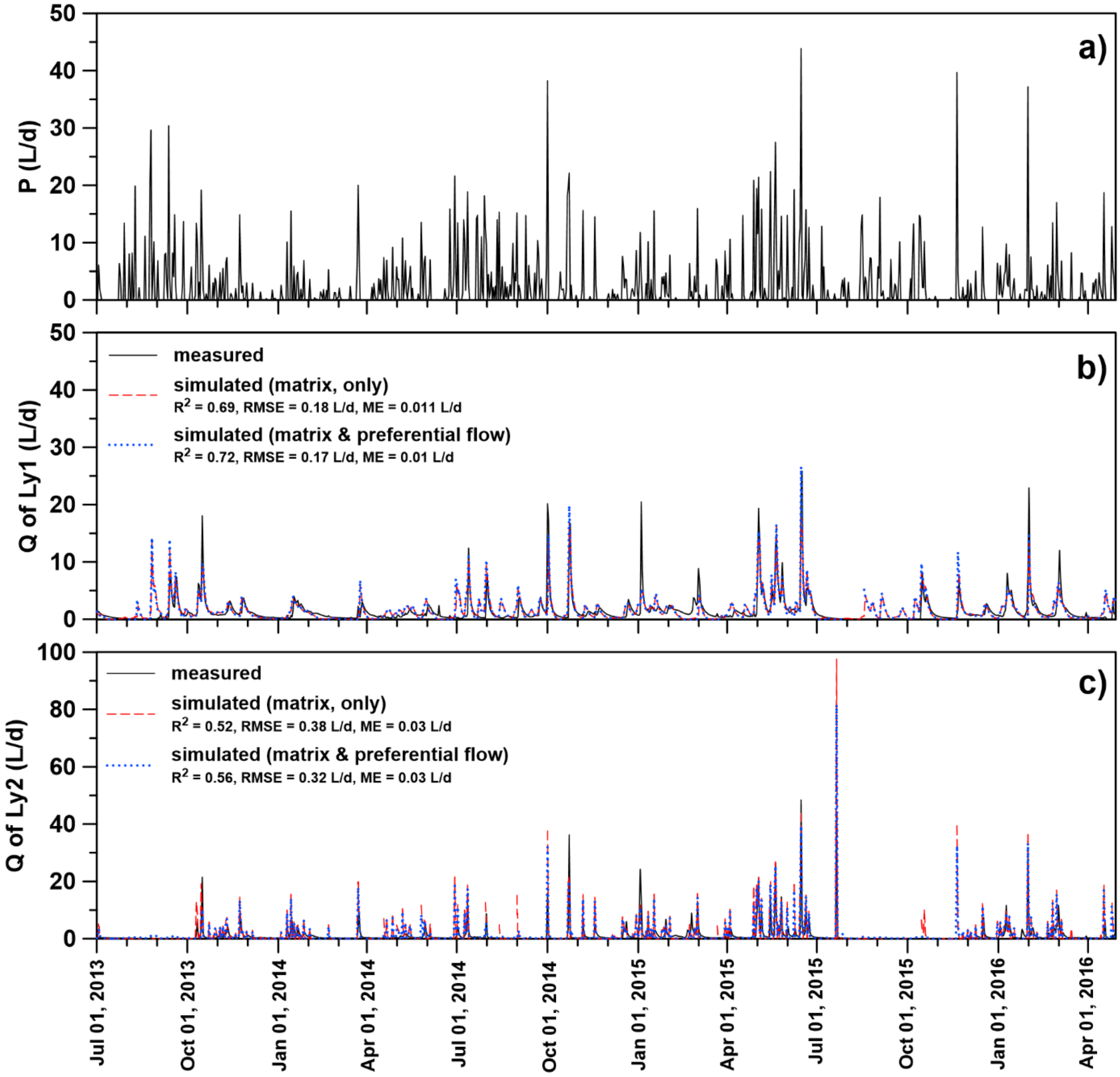

Figure A-6. Precipitation P (a) and discharge rates Q at Lysimeter 1 (b) and Lysimeter 2 (c) as a function of time.

A2. Deuterium excess und line condition excess

We have also calculated the deuterium excess (d-excess) for precipitation and lysimeter seepage water, as well as line-condition-excess (lc-excess) for the seepage water (see Figure below). This is based on data published in Shajari et al. (2020). What we can see is a dampening of d-excess variation in lysimeter seepage water, as well as a reduction (panel a versus panel b). This reflects some influence of evaporation, as expected (cf. also discussion in Shajari et al. 2020). Similar characteristics of d-excess can be seen for both lysimeters (perhaps with a slightly higher seasonal dampening for Lysimeter 2 seepage water), which is also obvious from lc-excess. Since the lower seasonal variations are already discussed in our manuscript based on $\delta^{18}O$, and lc-excess differences between lysimeters are rather low, we decided to not show this graph in the manuscript.

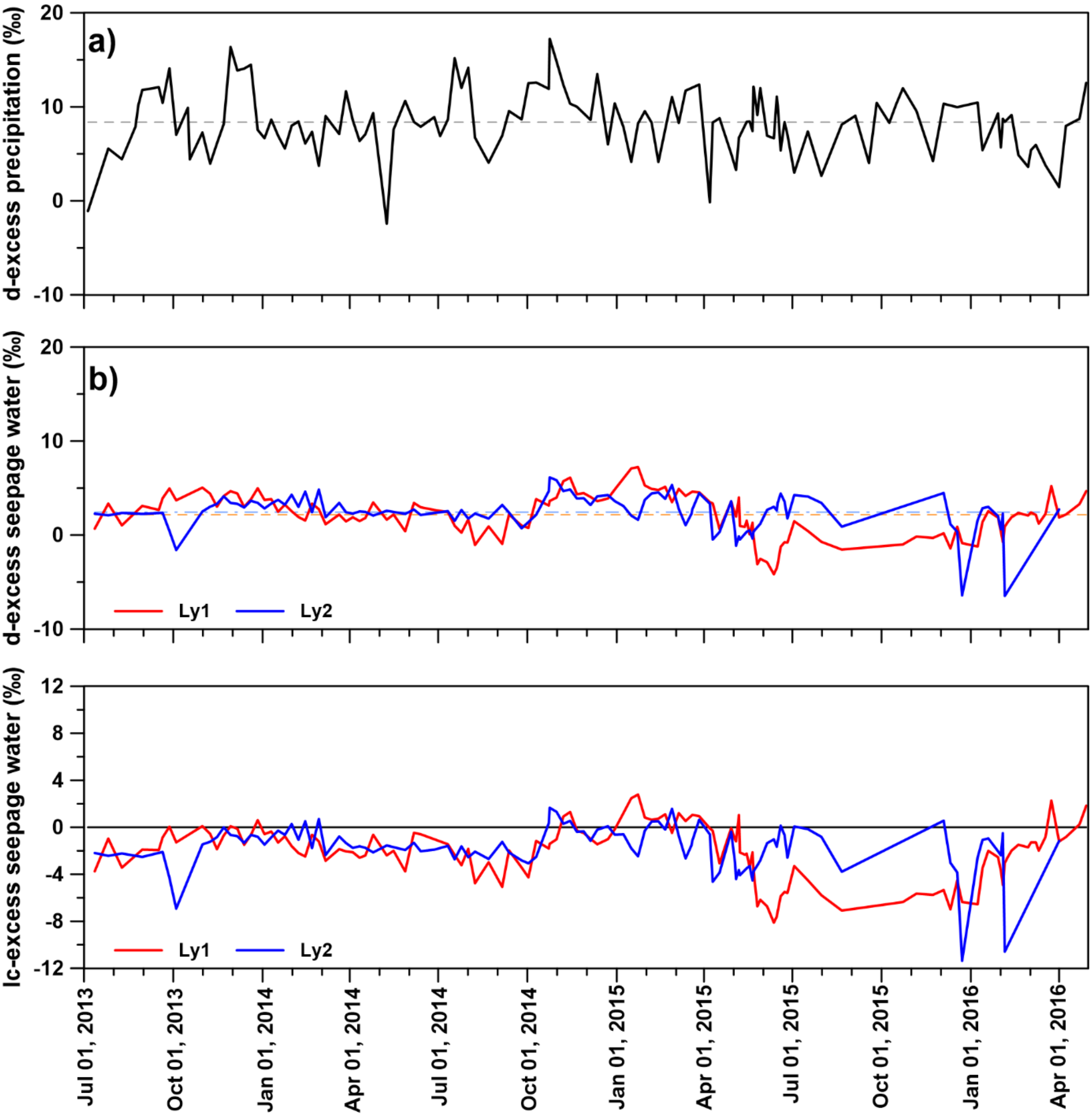

Figure A-7. Deuterium excess as a function of time in precipitation (a) and lysimeter seepage water (b), as well as line-condition excess of lysimeter seepage water (c). a) and b): horizontal lines indicate average of d-excess. c): horizontal line indicates y = 0. Deuterium excess was determined as *d-excess* = δ^2H – *a* · δ^{18}O (e.g., Clark and Fritz, 1997) and line-condition as *lc-excess* = δ^2H – *a* · δ^{18}O – *b* (Landwehr and Coplen, 2006; Liebhard et al. 2022). For the slope *a* and the intercept *b*, values obtained for the local meteoric water line (LMWL) of the lysimeter site were used (7.97 and 8.37, respectively; Shajari et al., 2020).

A3. References

Abbasi, F., Jacques, D., Simunek, J., Feyen, J., van Genuchten, M.T., 2003. Inverse estimation of soil hydraulic and solute transport parameters from transient field experiments: Heterogenous soil. Trans. Am. Soc. Agric. Eng. 46, 1097–1111.

Cheviron, B., Coquet, Y., 2009. Sensitivity Analysis of Transient-MIM HYDRUS-1D: Case Study Related to Pesticide Fate in Soils. Vadose Zo. J. 8, 1064–1079.

Clark, I. D., and P. Fritz. (1997). Environmental Isotopes in Hydrogeology, CRC Press, Boca Raton, Fla.

Jiang, S., Pang, L., Buchan, G.D., Šimůnek, J., Noonan, M.J., Close, M.E., 2010. Modelling water flow and bacterial transport in undisturbed lysimeters under irrigations of dairy shed effluent and water using HYDRUS-1D. Water Res. 44, 1050–1061.

Landwehr, J.M., and Coplen, T.B. (2006). Line-conditioned excess: a new method for characterizing stable hydrogen and oxygen isotope ratios in hydrologic systems. International Conference on Isotopes in Environmental Studies, Monte Carlo, Monaco, 132–135.

Lenda, A., and A. Zuber. 1970. Tracer dispersion in groundwater experiments. In Isotope Hydrology 1970 (pp. 619-641), Vienna: IAEA.

Liebhard, G., Klik, A., Stumpp, C., Nolz, R. (2022). Partitioning evapotranspiration using water stable isotopes and information from lysimeter experiments. Hydrological Sciences Journal 67 (4).

Shajari, F., Einsiedl, F., and A. Rein. 2020. Characterizing water flow in vegetated lysimeters with stable water isotopes and modelling. Groundwater, 58, no. 5: 759–770.

Sprenger, M., Volkmann, T.H.M., Blume, T., Weiler, M., 2015. Estimating flow and transport parameters in the unsaturated zone with pore water stable isotopes. Hydrol. Earth Syst. Sci. 19, 2617–2635.

Stauffer, P.H., Lu, Z., 2012. Quantifying Transport Uncertainty in Unsaturated Rock using Monte Carlo Sampling of Retention Curves. Vadose Zo. J. 11.

Stumpp, C., Nützmann, G., Maciejewski, S., Małoszewski, P., 2009a. A comparative modelling study of a dual tracer experiment in a large lysimeter under atmospheric conditions. J. Hydrol. 375, 566–577.

Stumpp, Christine, Stichler, W., Małoszewski, P., 2009b. Application of the environmental isotope δ18O to study water flow in unsaturated soils planted with different crops: Case study of a weighable lysimeter from the research field in Neuherberg, Germany. J. Hydrol. 368, 68–78.

Thoma, M.J., Barrash, W., Cardiff, M., Bradford, J., Mead, J., 2014. Estimating Unsaturated Hydraulic Functions for Coarse Sediment from a Field-Scale Infiltration Experiment. Vadose Zo. J. 13, 1–17.

Vanderborght, J., Timmerman, A., Feyen, J., 2000. Solute Transport for Steady-State and Transient Flow in Soils with and without Macropores. Soil Sci. Soc. Am. J. 64, 1305–1317.

Appendix B Supporting Information to Chapter 5

B1. Root growth

Root growth of the maize plants at Ly1 and Ly2 was calculated outside of HYDRUS-1D in an excel spreadsheet and implemented as a time-variable boundary condition to consider the different growing seasons and conditions over the years. As suggested in the HYDRUS-1D manual, a logistic growth function was applied to determine the progression of root length L [L] (Šimůnek et al., 2018):

$$L(t) = L_m \cdot \frac{L_0}{L_0 + (L_m - L_0)e^{-rt}} \tag{B1}$$

with L_0 the rooting depth at the start of the growing season [L], L_m the maximum rooting depth [L], r the root growth rate constant [T^{-1}] and t time [T].

In analogy to Hupet et al. (2003) and Stumpp et al. (2012) and adjusted to the site conditions (more intense maize growth in Ly2), the rooting depth of maize plants was assumed to range from L_0=0.01 to L_m=100 cm for Ly1 and from L_0=0.01 to L_m=200 cm for Ly2. Maize growth was more intense in Ly2, as reflected by a higher harvested plant mass (Table B3).

Maize root growth rate constants (r) were estimated from eq. (B1) for each growing season, assuming that half of the maximum rooting depth is reached in the middle of the growing season (Šimůnek et al., 2018; Stumpp et al., 2012). Replacing L(t) in eq. (B1) by $L_m/2$, accordingly, and solving for *r* yields: $r = -1/t \cdot ln[L_0/(L_m - L_0)]$, where *t* corresponds to the middle of the growing season, which can be obtained as *t* = (harvest day - germination day) / 2 (see Table B-3 for germination days and harvest days). As an example, for Ly1 in growing season 2013, *r* = -1/82.5 * ln [0.01/(100-0.1)] = 0.112 d^{-1}. Calculated values for *r* are summarized in Table B-3 for Ly1 and Ly2 in each growing season.

B2. Transpiration, leaf area index and interception

Parameter T is the transpiration rate [L T^{-1}] and can be determined as a proportion of ET, the evapotranspiration rate ET [L T^{-1}] according to Beer's law (Ritchie, 1972):

$$T(t) = ET(t) \cdot \left(1 - e^{-k \cdot LAI(t)}\right) \tag{B2}$$

with k the canopy radiation extinction constant [-] and LAI leaf area index [-] as a function of time t. The extinction constant k can range between 0.5 and 0.75, depending on the angle of the sun, the plant density and the arrangement of the leaves (Šimůnek et al., 2018). In our case, measured (actual) ET is available, and the radiation extinction by the maize canopy was assumed to be 0.6 as suggested by Hupet et al. (2003) and Stumpp et al. (2012) for maize.

The leaf area index LAI indicates the area of leaves per area of soil surface. Since no time-dependent data were available, LAI as a function of time was simulated from logistic plant growth (outside of HYDRUS-1D in an excel spreadsheet). The obtained values (simulated LAI in daily resolution) were used as upper boundary condition in HYDRUS-1D. For this task, eq. (B1) was applied, using minimum and maximum LAI instead of minimum and maximum plant mass. A minimum LAI of 0.01 was used for representing a low value (>0) at the beginning of the growth phase. Breuer et al. (2003) provided averaged LAI values for crops in Europe and Hoyningen-Huene (1983) gave LAI values for maize depending on different planting density. Accordingly, maximum LAI of 3.8 (Ly1) and 4.5 (Ly2) were assumed for the maize fields in 2013 and 2015 to 2017 (12 plants per m²), and 3.4 (Ly1) and 4.3 (Ly2) in 2014 (9 plants per m²). For Ly2, higher LAI values were chosen because a higher plant mass was harvested (cf. Table B-3). For *r* (growth rate constant), the same values as calculated for root growth (cf. previous section and Table B-3) were used, assuming that growth dynamics are comparable.

Furthermore, the HYDRUS-1D code modified by Zhou et al. (2021) was modified to consider interception, the intermediate storage of precipitation water on the plant canopy. Parts of the precipitation hitting vegetation will reach the ground as drip-through, drip-off or stem runoff. Remaining precipitation water is intercepted, i.e., stored temporarily before evaporating directly back into the atmosphere (Hoyningen-Huene, 1983). Thus, the amount of precipitation water is reduced by the amount of intercepted water. The interception rate I [L T^{-1}] can be defined as (Braden, 1985):

$$I(t) = a \cdot LAI(t)\left(1 - \frac{1}{1 + \frac{b \cdot P(t)}{a \cdot LAI(t)}}\right) \tag{B3}$$

where is the precipitation P [L T^{-1}] and empirical constants a [L T^{-1}] and b [-]. For a, a value of $0.025\,cm\,d^{-1}$ is often applied for agricultural crops (Braden, 1985). For the constant b, the SCF soil cover fraction [-] can be used:

$$SCF(t) = 1 - e^{-k \cdot LAI(t)} \tag{B4}$$

Finally, infiltration into the subsurface can be corrected with interception as:

$$Infiltration = \max\begin{cases} Precipitation - Interception \\ 0 \end{cases} \tag{B5}$$

B3. Root water uptake

Within HYDRUS-1D, water uptake by roots can be considered by the sink term in the flow equation for the mobile phase, only (Eq. B4 in the main manuscript; analogously in the single-porosity flow model, Šimůnek and Genuchten, 2008). Root water uptake is defined as the volume of water removed from a unit volume of soil into plant roots per time (Šimůnek et al., 2018):

$$S(h,x,t) = \alpha(h,x,t)b(x,t)T(t) \tag{B6}$$

where $S(h,x,t)$ is the sink term [T^{-1}] depending on the pressure head h, x is soil depth, t is time, $\alpha(h,x,t)$ the water stress response function [-], $b(x,t)$ the normalized root water uptake distribution [L^{-1}] and $T(t)$ the transpiration rate [L T^{-1}] calculated as described in the previous section.

For α, the model of Feddes (1978) was chosen within HYDRUS-1D. It defines values between 0 and 1, depending on the soil water pressure head h: a trapezoidal dependency is described, defined by h_1, h_2, h_3 and h_4. Root water uptake is assumed to be optimal between pressure heads h_2 and h_3, and zero for h_1 and h_4 (no root water uptake at field capacity and permanent wilting point, respectively). The value of h_3 depends on the transpiration rate as follows:

$$h_3 = \begin{cases} h_{3\,low} & if\ T < T_{3\,low} \\ h_{3\,high} + \dfrac{h_{3\,low} - h_{3\,high}}{T_{3\,high} - T_{3\,low}} \cdot \left(T_{3\,high} - T\right) & if\ T_{3\,low} < T < T_{3\,high} \\ h_{3\,high} & if\ T > T_{3\,high} \end{cases} \tag{B7}$$

The values of $T_{3\,low}$ and $T_{3\,high}$ are to be defined in HYDRUS-1D and are suggested to be 0.1 cm d^{-1} and 0.5 cm d^{-1}, respectively, to estimate a typical curve shape that can be expected for crops (Šimůnek et al., 2018). Thus, seven parameters are required for the Feddes model (description of α): the pressure heads h_1, h_2, $h_{3\,high}$, $h_{3\,low}$ and h_4 and the two transpiration rates $T_{3,low}$ and $T_{3,high}$. Since in this work actual transpiration is calculated from measured evapotranspiration, no further reduction of the entered transpiration rate is desired. For this reason, the Feddes parameters are defined in a way to ensure that every computed pressure head is in the optimal range for which the smallest pressure head h_4 is particularly decisive. Accordingly, h_1 and h_2 are set to 0, $h_{3\,high}$ to -500 cm, $h_{3\,low}$ to -900 cm and h_4 to -6 x 10^9 cm.

The normalized root water uptake distribution $b(x)$ accounts for varying root water uptake (Hoffman and van Genuchten, 1983):

$$b(x,t) = \begin{cases} \dfrac{1.667}{L_r(t)} & if\ x > L - 0.2L_r \\ \dfrac{2.0833}{L_r(t)}\left(1 - \dfrac{L-x}{L_r(t)}\right) & if\ x \in (L - L_r; L - 0.2L_r) \\ 0 & if\ x < L - L_r \end{cases} \tag{B8}$$

where $L_r(t)$ is the rooting depth varying with time [L] and L the length of the profile [L]. The x-coordinate is ranging from the bottom of the profile ($x = 0$) to the soil surface ($x = L$).

Furthermore, compensation for reduced root water uptake due to physiological stress can be taken into consideration, using $\omega(t)$ the plant water stress index [-] as suggested by Jarvis (1989) and Šimůnek and Hopmans (2009):

$$\omega(t) = \int_{L_r} \alpha(h,x,t) b(x,t) dx \tag{B9}$$

The critical value of the water stress index ω_c, also known as root adaptability factor, reflects the ability of the plant to revert to the rest of the root profile when faced with stress factors at a certain depth. While for $\omega_c = 1$, no compensation occurs, the local differences are fully compensated for $\omega_c = 0$ (Cai et al., 2018):

$$\frac{T_{act}(t)}{T_{pot}(t)} = \begin{cases} 1 & if\ \omega_c \leq \omega \leq 1 \\ \dfrac{\omega(t)}{\omega_c} & if\ \omega < \omega_c \end{cases} \tag{B10}$$

Since in this work, transpiration is obtained from measured actual evapotranspiration, the threshold value of ω_c is 0. Thus, full compensation is assumed with no further reduction of the determined transpiration rate.

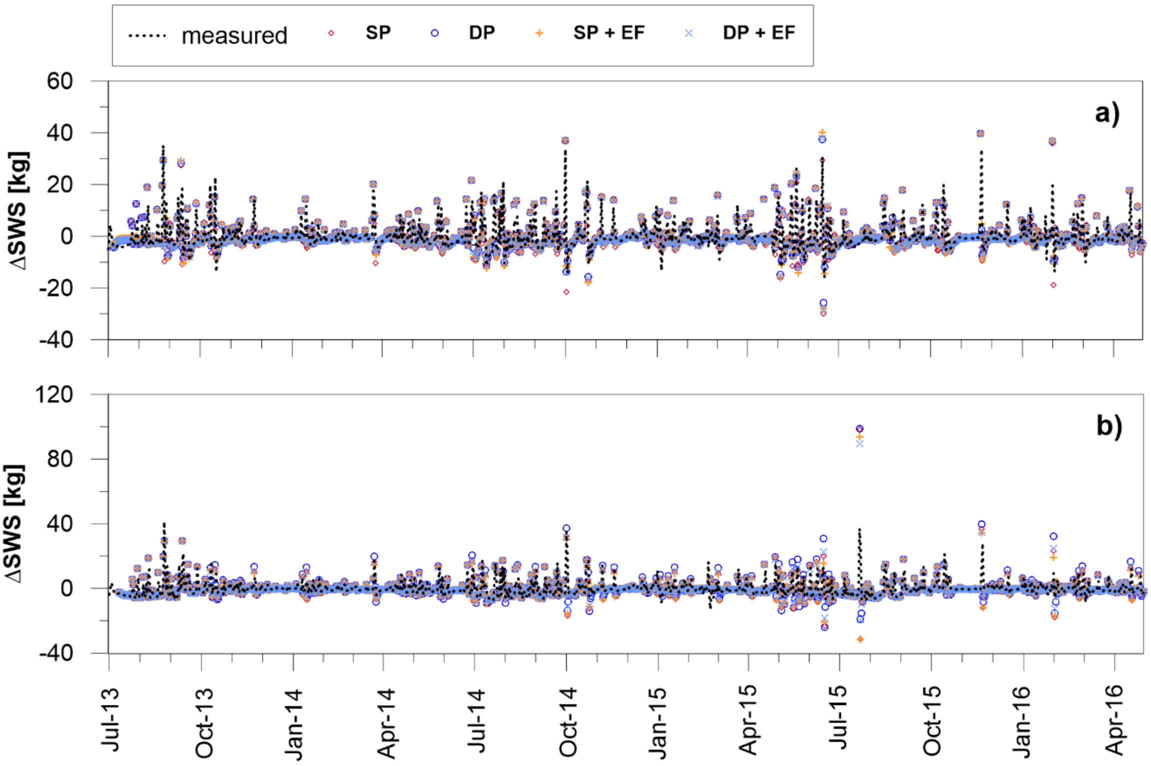

Figure B-1. Measured and modelled soil water storage change ΔSWS as a function of time in (a) Ly1 and (b) Ly2, considering single-porosity (SP) and dual-porosity (DP) model setup. EF: combined with evaporation fractionation**.**

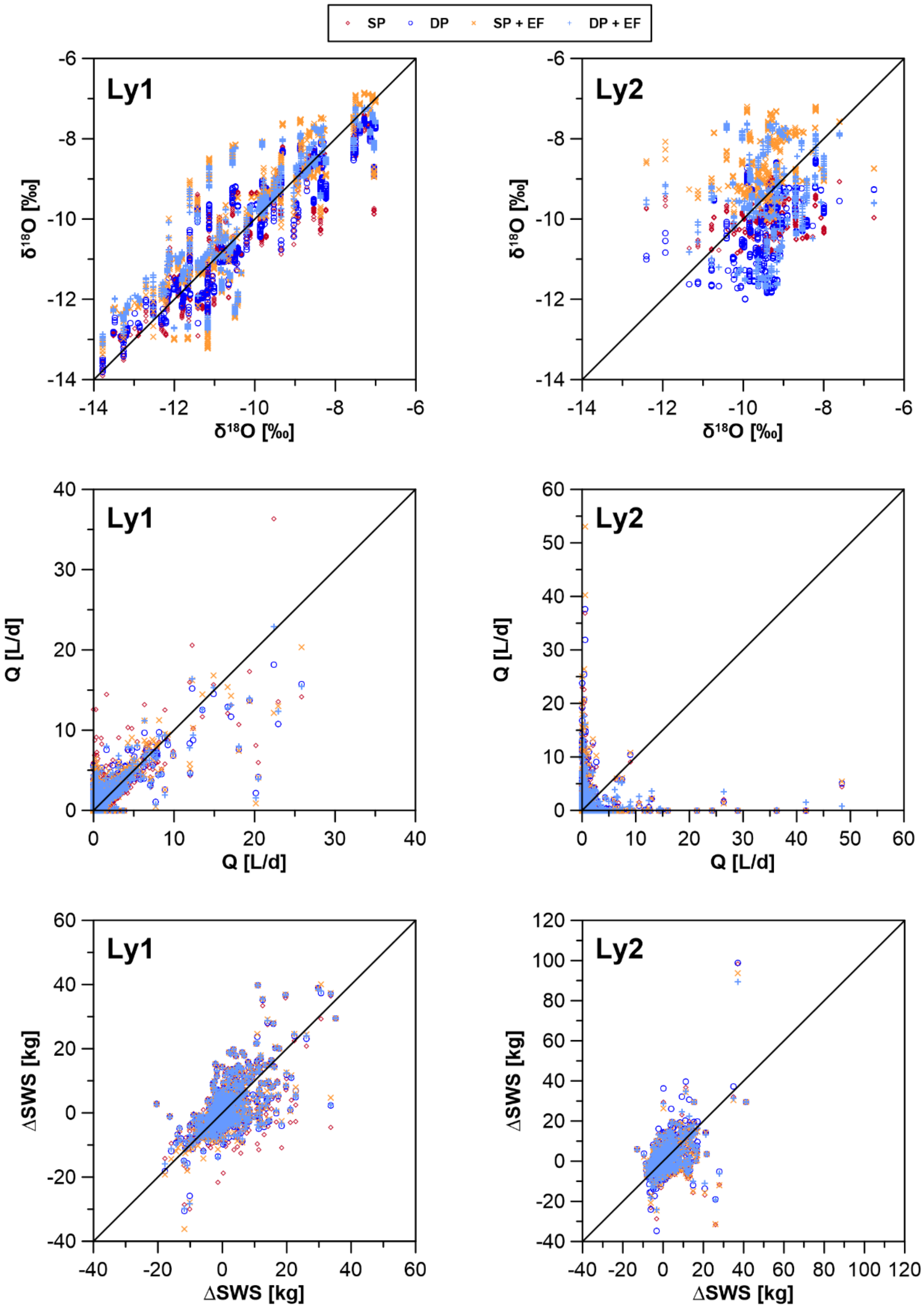

Figure B-2. Modelled (y-axis) versus measured (x-axis) discharge rate Q, ΔSWS and $\delta^{18}O$ in the outflow of Ly1 and Ly2 considering single-porosity (SP) and dual-porosity (DP) model setups. EF: combined with evaporation fractionation.

Table B-1. Grain size distribution of Lysimeter 1 (after Shajari et al., 2020).

Depth [cm]	Horizon	Characteristics	Components < 2 mm [%]	Components > 2 mm [%]
0-20	Ah	Humic upper soil	51	49
20-30	Ah	Humic upper soil	49	51
30-40	Ah	Humic upper soil	67	33
40-50	Ah	Humic upper soil	34	66
50-100	C	C-horizon, Sandy gravel	19	81
100-200	C	C-horizon, Sandy gravel	21	79

Table B-2. Grain size distribution of Lysimeter 2 (after Shajari et al., 2020).

Depth [cm]	Horizon	Characteristics	Gravel [wt. %]	Sand [wt. %]	Silt [wt. %]	Clay [wt. %]
0-40	Ap	A-horizon, ploughed soil	4	23	49	23
40-90	Bv	B-horizon, loamy, brown	2	20	35	43
90-130	BvCv	Transition Bv to Cv	<1	5	55	39
130-180	Cv	C-horizon, loamy, brown	2	25	45	27
180-200	C	C-horizon, gneiss debris	3	21	55	20

Table B-3. Germination and harvest, number of maize plants, estimated growth rate constants and harvested plant mass (2013 to 2017). (a): day 0 is 1 January.

		2013	**2014**	**2015**	**2016**	**2017**
Germination day (a)		130 (10 May)	140 (20 May)	142 (22 May)	144 (23 May)	143 (23 May)
Harvest day (a)		295 (22 Oct)	300 (27 Oct)	272 (29 Sept)	274 (30 Sept)	272 (29 Sept)
Number of maize plants (Ly1 and 2)		12	9	12	12	12
Root growth rate constant r [d^{-1}]	Ly1	0.112	0.115	0.142	0.142	0.143
	Ly2	0.120	0.124	0.152	0.152	0.154
Harvested plant mass [kg-fresh weight]	Ly1	2.0	2.5	1.8	2.0	1.9
	Ly2	3.2	3.8	3.8	3.1	3.8

Table B-4. Initial parameters for modelling water flow and stable water isotope transport in Ly1 and 2 considering single-porosity (SP), dual-porosity (DP) and evaporation fractionation (EF). α_L was initially set to 10% of the total flow length (200cm) for SP and DP setups without EF. For Ly1 and SP, initial SHP were set based on measured values from a similar soil (cf. Shajari et al., 2020) and for Ly2 and SP, based on the Rosetta database implemented in HYDRUS-1D (Schaap et al., 2001). For DP, initial guesses for SHPs of the immobile region were taken based on magnitudes reported in literature, because very limited studies are available to date. For the SP+EF and DP+EF, initial values were set to best fits obtained for SP and DP setups.

		θ_r if SP $\theta_{mo,r}$ if DP [cm³/cm³]	θ_s if SP $\theta_{mo,s}$ if DP [cm³/cm³]	α [1/cm]	n [-]	K_s [cm/d]	$\theta_{im,r}$ [cm³/cm³]	$\theta_{im,s}$ [cm³/cm³]	ω_w [1/d]	α_L [cm]
Lysimeter 1	SP	0.019	0.22	0.109	1.4	20995	-	-	-	20
	DP	0.019	0.22	0.109	1.4	20995	0.01	0.1	0.05	20
	SP + EF	0.0046	0.25	0.5	1.31	6040.2	-	-	-	8.60
	DP + EF	0	0.22	0.12	1.38	6040.2	0.001	0.060	0.063	8
Lysimeter 2	SP	0.1	0.39	0.059	1.48	31.44	-	-	-	20
	DP	0.1	0.39	0.059	1.48	31.44	0.01	0.1	0.05	20
	SP + EF	0.009	0.35	0.005	1.8	32.5	-	-	-	172
	DP + EF	0	0.16	0.007	2.0	30	0.005	0.19	4.99	80

Table B-5. Parameter bounds selected for the application of the parameter optimization algorithm PEST; based on expected value ranges for the considered soils.

Parameter	**Lysimeter 1**		**Lysimeter 2**		**Main references for the considered bounds**
	Lower bound	**Upper bound**	**Lower bound**	**Upper bound**	
θ_r **[cm³/cm³]**	0.001	0.1	0.001	0.1	Abbasi et al.(2003); Cheviron and Coquet (2009); Haws et al. (2005); Köhne et al. (2004)Jiang et al. (2010); Sprenger et al. (2015); Stumpp et al. (2009); Thoma et al. (2014); Vanderborght and Vereecken (2007)
θ_s **[cm³/cm³]**	0.1	0.4	0.1	0.5	
α **[1/cm]**	0.005	0.5	0.0005	0.05	
n **[-]**	1.0	4.0	1.0	4.0	
K_s **[cm/d]**	4000	80000	25	300	
α_L **[cm]**	0	200	0	200	
$\theta_{r,im}$ **[cm³/cm³]**	0.001	0.025	0.001	0.1	
$\theta_{s,im}$ **[cm³/cm³]**	0.01	0.06	0.01	0.5	
ω_s**[1/d]**	0.001	6	0.001	10	

Table B-6. Statistical evaluation of model curve fits (lysimeters Ly1 and Ly2). R²: coefficient of determination, RMSE: root mean square error, ME: mean error, KGE: Kling-Gupta Efficiency, τ: Kendall's Tau. Colours indicate statistical performance, with green: good, yellow: intermediate and red: poor performance. Units for RMSE and ME are [L/d] for Q, [‰] for $\delta^{18}O$ and [kg] for ΔSWS.

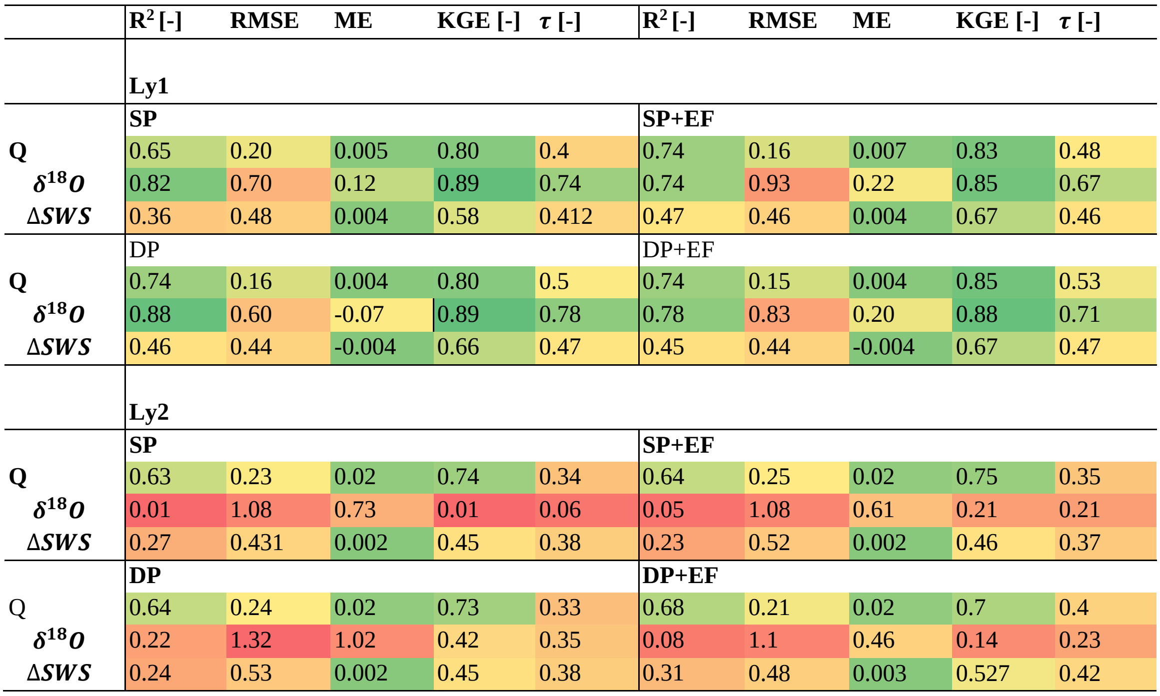

	R² [-]	**RMSE**	**ME**	**KGE [-]**	**τ [-]**	**R² [-]**	**RMSE**	**ME**	**KGE [-]**	**τ [-]**
	Ly1									
	SP					**SP+EF**				
Q	0.65	0.20	0.005	0.80	0.4	0.74	0.16	0.007	0.83	0.48
$\delta^{18}O$	0.82	0.70	0.12	0.89	0.74	0.74	0.93	0.22	0.85	0.67
ΔSWS	0.36	0.48	0.004	0.58	0.412	0.47	0.46	0.004	0.67	0.46
	DP					DP+EF				
Q	0.74	0.16	0.004	0.80	0.5	0.74	0.15	0.004	0.85	0.53
$\delta^{18}O$	0.88	0.60	-0.07	0.89	0.78	0.78	0.83	0.20	0.88	0.71
ΔSWS	0.46	0.44	-0.004	0.66	0.47	0.45	0.44	-0.004	0.67	0.47
	Ly2									
	SP					**SP+EF**				
Q	0.63	0.23	0.02	0.74	0.34	0.64	0.25	0.02	0.75	0.35
$\delta^{18}O$	0.01	1.08	0.73	0.01	0.06	0.05	1.08	0.61	0.21	0.21
ΔSWS	0.27	0.431	0.002	0.45	0.38	0.23	0.52	0.002	0.46	0.37
	DP					**DP+EF**				
Q	0.64	0.24	0.02	0.73	0.33	0.68	0.21	0.02	0.7	0.4
$\delta^{18}O$	0.22	1.32	1.02	0.42	0.35	0.08	1.1	0.46	0.14	0.23
ΔSWS	0.24	0.53	0.002	0.45	0.38	0.31	0.48	0.003	0.527	0.42

B4. References

Abbasi, F., Jacques, D., Simunek, J., Feyen, J., van Genuchten, M.T., 2003. Inverse estimation of Soil Hydraulic and Solute Transport Paarameters from Transient field Experiments: Heterogenous Soil. Trans. Am. Soc. Agric. Eng. 46, 1097–1111.

Braden, H., 1985. Ein Energiehaushalts-und Verdunstungsmodell für Wasser- und Stoffhaushaltsuntersuchungen landwirtschaftlich genutzter Einzugsgebiete. Mitteilungen Dtsch. Bodenkundliche Gesellschaft 42, 294–299.

Breuer, L., Eckhardt, K., Frede, H.G., 2003. Plant parameter values for models in temperate climates. Ecol. Modell. 169, 237–293. https://doi.org/10.1016/S0304-3800(03)00274-6

Cai, G., Vanderborght, J., Couvreur, V., Mboh, C.M., Vereecken, H., 2018. Parameterization of Root Water Uptake Models Considering Dynamic Root Distributions and Water Uptake Compensation. Vadose Zo. J. 17, 160125. https://doi.org/10.2136/vzj2016.12.0125

Cheviron, B., Coquet, Y., 2009. Sensitivity Analysis of Transient-MIM HYDRUS-1D: Case Study Related to Pesticide Fate in Soils. Vadose Zo. J. 8, 1064–1079. https://doi.org/10.2136/vzj2009.0023

Haws, N.W., Rao, P.S.C., Šimůnek, J., Poyer, I.C., 2005. Single-porosity and dual-porosity modelling of water flow and solute transport in subsurface-drained fields using effective field-scale parameters. J. Hydrol. 313, 257–273. https://doi.org/10.1016/j.jhydrol.2005.03.035

Hoffman, G.J., van Genuchten, M.T., 1983. Soil Properties and Efficient Water Use: Water Management for Salinity Control, in: Limitations to Efficient Water Use in Crop Production. American Society of Agronomy, pp. 73–85.

Hoyningen-Huene, J.F., 1983. Die Interzeption des Niederschlags in landwirtschaftlichen Pflanzenbeständen, in: DVWK Schriften 57- Einfluß Der Landsnutzung Auf Den Gebietswasserhaushalt. Kommissionsvertrieb Verlag Paul Parey, p. 73.

Hupet, F., Lambot, S., Feddes, R.A., Van Dam, J.C., Vanclooster, M., 2003. Estimation of root water uptake parameters by inverse modelling with soil water content data. Water Resour. Res. 39. https://doi.org/10.1029/2003WR002046

Jarvis, N.J., 1989. A Simple Empirical Model of Root Water Uptake. J. Hydrol. 107, 57–72.

Jiang, S., Pang, L., Buchan, G.D., Šimůnek, J., Noonan, M.J., Close, M.E., 2010. Modelling water flow and bacterial transport in undisturbed lysimeters under irrigations of dairy shed effluent and water using HYDRUS-1D. Water Res. 44, 1050–1061. https://doi.org/10.1016/j.watres.2009.08.039

Köhne, J.M., Köhne, S., Mohanty, B.P., Šimůnek, J., 2004. Inverse Mobile-Immobile Modelling of Transport During Transient Flow: Effects of Between-Domain Transfer and Initial Water Content. Vadose Zo. J. 3, 1309–1321. https://doi.org/10.2136/vzj2004.1309

Ritchie, J.T., 1972. Model for predicting evaporation from a row crop with incomplete cover. Water Resour. Res. 8, 1204–1213.

Šimůnek, J., Hopmans, J.W., 2009. Modelling compensated root water and nutrient uptake. Ecol. Modell. 220, 505–521. https://doi.org/10.1016/j.ecolmodel.2008.11.004

Šimůnek, J., Šejna, M., Sakai, M., van Genuchten, M.T., 2018. The HYDRUS-1D Software Package for Simulating the One-Dimensional Movement of Water, Heat, and Multiple Solutes in Variably-Saturated Media, Version 4.17, HYDRUS Software Series 3,. Dep. Environ. Sci. Univ. Calif. Riverside Riverside, 348.

Sprenger, M., Volkmann, T.H.M., Blume, T., Weiler, M., 2015. Estimating flow and transport parameters in the unsaturated zone with pore water stable isotopes. Hydrol. Earth Syst. Sci. 19, 2617–2635. https://doi.org/10.5194/hess-19-2617-2015

Stumpp, C., Małoszewski, P., Stichler, W., Fank, J., 2009. Environmental isotope (δ18O) and hydrological data to assess water flow in unsaturated soils planted with different crops: Case study lysimeter station "Wagna" (Austria). J. Hydrol. 369, 198–208. https://doi.org/10.1016/j.jhydrol.2009.02.047

Stumpp, C., Stichler, W., Kandolf, M., Šimůnek, J., 2012. Effects of Land Cover and Fertilization Method on Water Flow and Solute Transport in Five Lysimeters: A Long-Term Study Using Stable Water Isotopes. Vadose Zo. J. 11. https://doi.org/10.2136/vzj2011.0075

Thoma, M.J., Barrash, W., Cardiff, M., Bradford, J., Mead, J., 2014. Estimating Unsaturated Hydraulic Functions for Coarse Sediment from a Field-Scale Infiltration Experiment. Vadose Zo. J. 13, 1–17. https://doi.org/10.2136/vzj2013.05.0096

Vanderborght, J., Vereecken, H., 2007. Review of Dispersivities for Transport Modelling in Soils. Vadose Zo. J. 6, 29–52. https://doi.org/10.2136/vzj2006.0096

Zhou, T., Šimůnek, J., Braud, I., 2021. Adapting HYDRUS-1D to simulate the transport of soil water isotopes with evaporation fractionation. Environ. Model. Softw. 143. https://doi.org/10.1016/j.envsoft.2021.105118

Appendix C Supporting Information to Chapter 6

C1. Discussion of fitted reactive transport parameters

Fitted values of biodegradation rate constant μ in Ly1 for metolachlor (MTLC, 0.1 1/d) and for terbuthylazine (TBA, 0.08 1/d; Table 3) were in agreement with findings from a study by Carretta et al. (2018). The authors investigated degradation of MTLC and TBA for a sandy soil under field conditions. They observed μ values for MTLC of 0.04 – 0.38 1/d and for TBA of 0.03 – 0.25 1/d.

Zsolnay (1994) determined values of the soil to water partition coefficient K_d for TBA between 0.003 and 0.01 cm³/mg in a laboratory experiment for sandy soils, which agree with the fitted K_d of 0.01 cm³/mg in Ly1. Fitted K_d of 0.0002 cm³/mg for MTLC in Ly2 is within ranges reported by Marín-Benito et al. (2014), with $\mathrm{K_d}$ = 0.00014 – 0.0008 cm³/mg under field conditions for clay loam soils in an irrigated maize cropping system. Weber et al. (2000) documented a range of K_d = 0.000108 – 0.002157 cm³/mg for MTLC from different measurements depending on organic matter and clay content of the soil.

The biodegradation rate constant μ = 0.034 1/d found for MTLC for Ly2 is in a comparable range of 0.015-0.035 1/d found by Vischetti et al. (1998) for laboratory degradation tests under different temperature and soil water content conditions for clayey silty soil (Table 3 in main manuscript). For TBA, our fitted K_d of 0.023 cm³/mg and μ of 0.057 1/d (Table 3) correspond in magnitude to findings by Vischetti et al. (1998) with K_d = 0.0047 - 0.024 cm³/mg and μ = 0.006 – 0.024 1/d from lysimeter studies in clayey silty sand lysimeters cropped with maize. The K_d value of 0.0003 cm³/mg fitted for nicosulfuron (NCS) in Ly2 is in the same range as collected by Weber et al. (2000) from different studies (0.0002 – 0.002 cm³/mg).

For NCS, μ values from 0.015 – 0.03 1/d were documented from different field and laboratory experiments with different soil types (EFSA, 2007), which were in agreement with our fitted values of 0.019 1/d for Ly2 and 0.055 1/d for Ly1. For prosulfuron (PS), EFSA (2007) documented K_d values in the range 0.00003 – 0.0014 cm³/mg and μ values in the range 0.019 – 0.14 1/d, and our fitted values (0.00009 cm³/mg for Ly1 and 0.00004 cm³/mg for Ly2) agree with the lower end of the range. Fitted μ values with 0.025 1/d for Ly1 and 0.02/d for Ly 2 also correspond to the lower range of the documented values. The solute mass transfer rates ω_s were calibrated between 0.003 and 0.035 1/d. Haws et al. (2005) fitted ω_s of 0.0006 - 1.2 1/d for chloride transport in silty clay loam on two subsurface-drained cornfield plots.

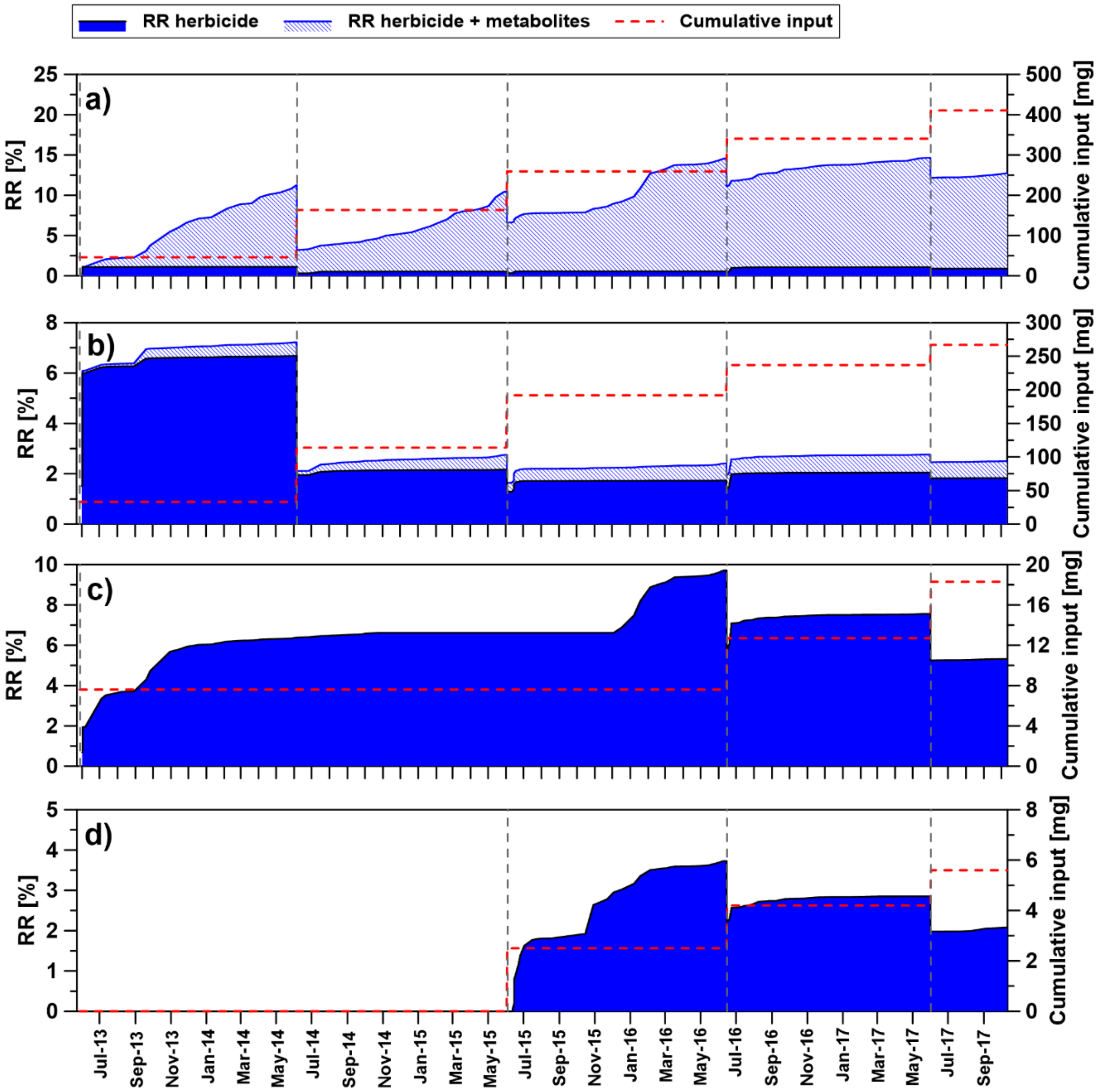

Figure C-1. Recovery rate (RR) of applied chemical mass in the drainage of lysimeter Ly1, together with cumulative input (cumulative amount of herbicides that were applied to the lysimeter). a) Metolachlor without and with two metabolites, b) terbuthylazine without and with two four metabolites, c) nicosulfuron, d) prosulfuron. Grey vertical bars indicate the date of herbicide application (cf. Table 6-1 in Chapter 6).

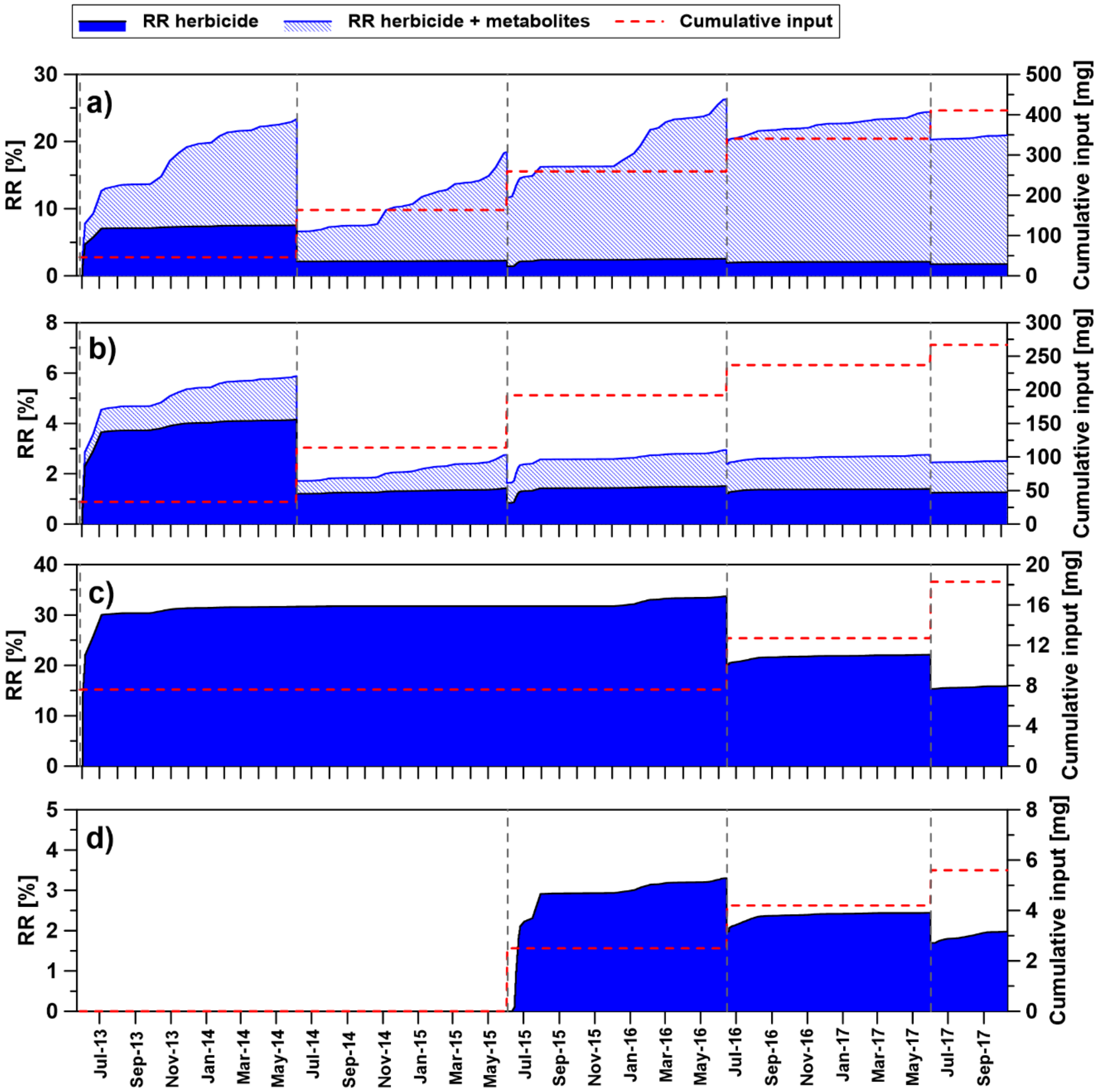

Figure C-2. Recovery rate (RR) of applied chemical mass in the drainage of lysimeter Ly2, together with cumulative input (cumulative amount of herbicides that were applied to the lysimeter). a) Metolachlor without and with two metabolites, b) terbuthylazine without and with two four metabolites, c) nicosulfuron, d) prosulfuron. Grey vertical bars indicate the date of herbicide application (cf. Table 6-1 in Chapter 6).

Table C-1. Physicochemical properties of investigated herbicides and metabolites (after Lewis et al., 2016).

Name	CAS number	Molar mass [g/mol]	Octanol-water portioning coefficient log Kow [-] (pH of 7, 20°C)	Dissociation constant pKa at 20°C	Water solubility at 20°C [mg/L]	Parent Compound
Metolachlor (MTLC)	51218-45-2	283.79	3.4		530	
Metolachlor oxanilic acid (MOXA)	152019-73-3	279.33			360000	MTLC
Metolachlor ethane sulfonic acid (MESA)	171118-09-5	329.4	-1.9		212461	MTLC
Terbuthylazine (TBA)	5915-41-3	229.71	3.4	1.9	6.6	
Desethyl-Terbuthylazine (DET TBA)	30125-63-4	201.66	2.3		327.1	TBA
Hydroxy-terbuthylazine (HT TBA)	66753-06-8	183.21				TBA
TBA 2 CGA 324007	309923-18-0	184.2				TBA GS28620
TBA 1 SYN 545666	unknown	198.22				TBA 2 CGA 324007
Nicosulfuron (NCS)	111991-09-4	410.41	0.61	4.78 (at 25°C)	7500	
Prosulfuron (PS)	94125-34-5	419.38	1.5	3.76	4000	

Table C-2. Measured wind speeds at the lysimeter site during the dates of herbicide application.

Application date	Wind speed [m/s]
28 May 2013	2.6
6 June 2014	2.9
3 June 2015	4.6
15 June 2016	4.1
1 June 2017	2.8

Table C-3. Parameter bounds selected for the application of the parameter optimization PEST, based on expected value ranges for the considered soils.

Parameter	Lysimeter 1		Lysimeter 2		Main references for the considered bounds
	Lower bound	Upper bound	Lower bound	Upper bound	
K_d [cm³/mg]	0	0.1	0	0.1	EFSA (2007); Glaesner et al. (2018); Köhne et al. (2004); Vischetti et al. (1998); Weber et al. (2000)
μ [1/d]	0	0.5	0	0.5	
ω_s [1/d]	-	-	0	10	

Table C-4. Statistical evaluation of model curve fits with the R²: coefficient of determination, RMSE: root mean square error, ME: mean error and KGE: Kling-Gupta Efficiency and τ: Kendall's Tau. Colours indicate statistical performance with green: good, yellow: intermediate and red: poor performance.

	Lysimeter 1					Lysimeter 2				
	R^2 [-]	RMSE [µg/L]	ME [µg/L]	KGE [-]	τ [-]	R^2 [-]	RMSE [µg/L]	ME [µg/L]	KGE [-]	τ [-]
Metolachlor (MTLC)	0	5.5	-0.109	-0.06	0.35	0.36	4.30	-0.67	0.48	0.46
Terbuthylazine (TBA)	0.004	4.69	0.046	0.06	0.28	0.22	2.80	-0.22	0.38	0.48
Nicosulfuron (NCS)	0.24	0.78	-0.14	0.3	0.28	0.27	1.94	-0.14	0.45	0.41
Prosulfuron (PS)	0.26	0.45	0	0.5	0.8	0.20	0.46	-0.03	0.4	0.83

Table C-5. Measured $\delta^{13}C$ of terbuthylazine (TBA) and metolachlor (MTLC) in applied pesticide solution and seepage water of Ly1 and Ly2 (three sample campaigns). Stdev: standard deviation.

δ^{13}C-TBA [‰]			**δ^{13}C-MTLC [‰]**		
Replicates	**Mean**	**Stdev**	**Replicates**	**Mean**	**Stdev**
Applied pesticide solution					
-27.1	-26.7	0.4	-31.9	-31.9	0.1
-26.6			-31.8		
-26.4			-31.9		
-26.6			-31.9		
Ly1 – 1st sampling campaign (21 May 2015, before pesticide application)					
(no analysis possible)			(no analysis possible)		
Ly1 – 2nd sampling campaign (22 June 2015, 19 days after pesticide application)					
-25.2	-25.3	0.3	-30.1	-30.1	0.5
-25.7			-30.5		
-25			-29.5		
-25.3			-30.4		
Ly1 – 3rd sampling campaign (8 Jan 2016, ~7.5 months after pesticide application)					
(no analysis possible)			(no analysis possible)		
Ly2 – 1st sampling campaign (21 May 2015, before pesticide application)					
(no analysis possible)			(no analysis possible)		
Ly2 – 2nd sampling campaign (22 June 2015, 19 days after pesticide application)					
-25.9	-26.0	0.2	-29.9	-30.0	0.3
-25.83			-29.8		
-26.14			-30.28		
Ly2 – 3rd sampling campaign (8 Jan 2016, ~7.5 months after pesticide application)					
(no analysis possible)			-27.9	-28.1	0.3
			-27.9		
			-28.5		

C2. References

Carretta, L., Cardinali, A., Marotta, E., Zanin, G., Masin, R., 2018. Dissipation of terbuthylazine, metolachlor, and mesotrione in soils with contrasting texture. J. Environ. Sci. Heal. - Part B Pestic. Food Contam. Agric. Wastes 53, 661–668. https://doi.org/10.1080/03601234.2018.1474556

European Food Safety Authority EFSA, 2007. Conclusion regarding the peer review of the pesticide risk assessment of the active substance nicosulfuron, European Food Safety Authority Journal. https://doi.org/10.2903/j.efsa.2006.55r

Glaesner, N., Diamantopoulos, E., Magid, J., Kjaergaard, C., Gerke, H.H., 2018. Modelling Solute Mass Exchange between Pore Regions in Slurry-Injected Soil Columns during Intermittent Irrigation. Vadose Zo. J. 17, 180006. https://doi.org/10.2136/vzj2018.01.0006

Haws, N.W., Rao, P.S.C., Šimůnek, J., Poyer, I.C., 2005. Single-porosity and dual-porosity modelling of water flow and solute transport in subsurface-drained fields using effective field-scale parameters. J. Hydrol. 313, 257–273. https://doi.org/10.1016/j.jhydrol.2005.03.035

Köhne, J.M., Köhne, S., Mohanty, B.P., Šimůnek, J., 2004. Inverse Mobile-Immobile Modelling of Transport During Transient Flow: Effects of Between-Domain Transfer and Initial Water Content. Vadose Zo. J. 3, 1309–1321. https://doi.org/10.2136/vzj2004.1309

Köhne, J.M., Köhne, S., Šimůnek, J., 2006. Multi-process herbicide transport in structured soil columns: Experiments and model analysis. J. Contam. Hydrol. 85, 1–32. https://doi.org/10.1016/j.jconhyd.2006.01.001

Lewis, K.A., Tzilivakis, J., Warner, D.J., Green, A., 2016. An international database for pesticide risk assessments and management. Hum. Ecol. Risk Assess. 22, 1050–1064. https://doi.org/10.1080/10807039.2015.1133242

Marín-Benito, J.M., Pot, V., Alletto, L., Mamy, L., Bedos, C., Barriuso, E., Benoit, P., 2014. Comparison of three pesticide fate models with respect to the leaching of two herbicides under field conditions in an irrigated maize cropping system. Sci. Total Environ. 499, 533–545. https://doi.org/10.1016/j.scitotenv.2014.06.143

Vischetti, C., Leita, L., Marucchini, C., Porzi, G., 1998. Degradation and mobility of metolachlor and terbuthylazine in a sandy clay loam soil. Agronomie 18, 131–137. https://doi.org/10.1051/agro:19980203

Weber, J.B., Wilkerson, G.G., Michael Linker, H., Wilcut, J.W., Leidy, R.B., Senseman, S., Witt, W.W., Barrett, M., Vencill, W.K., Shaw, D.R., Mueller, T.C., Miller, D.K., Brecke, B.J., Talbert, R.E., Peeper, T.F., 2000. A proposal to standardize soil/solution herbicide distribution coefficients. Weed Sci. 48, 75–88. https://doi.org/10.1614/0043-1745(2000)048[0075:aptsss]2.0.co;2

Zsolnay, A., 1994. The lack of effect of the dissolved organic material in soil on the water solubility of the herbicide, terbuthylazine. Sci. Total Environ. 152, 101–104.

Appendix D Supporting Information to Chapter 7

D1. List of search phrases

Among others, the following phrases were used in the literature search:

risk assessment managed aquifer recharge, risk framework managed aquifer recharge, risk assessment artificial groundwater recharge, risk framework artificial groundwater recharge, human health risk framework/assessment for managed aquifer recharge, environmental risk framework/assessment for managed aquifer recharge, technical/operational risk framework/assessment for managed aquifer recharge, assessment of managed aquifer recharge failure, risks for managed aquifer recharge failure, failure of managed aquifer recharge sites, economic risks associated with MAR, feasibility of MAR under uncertainty considerations.

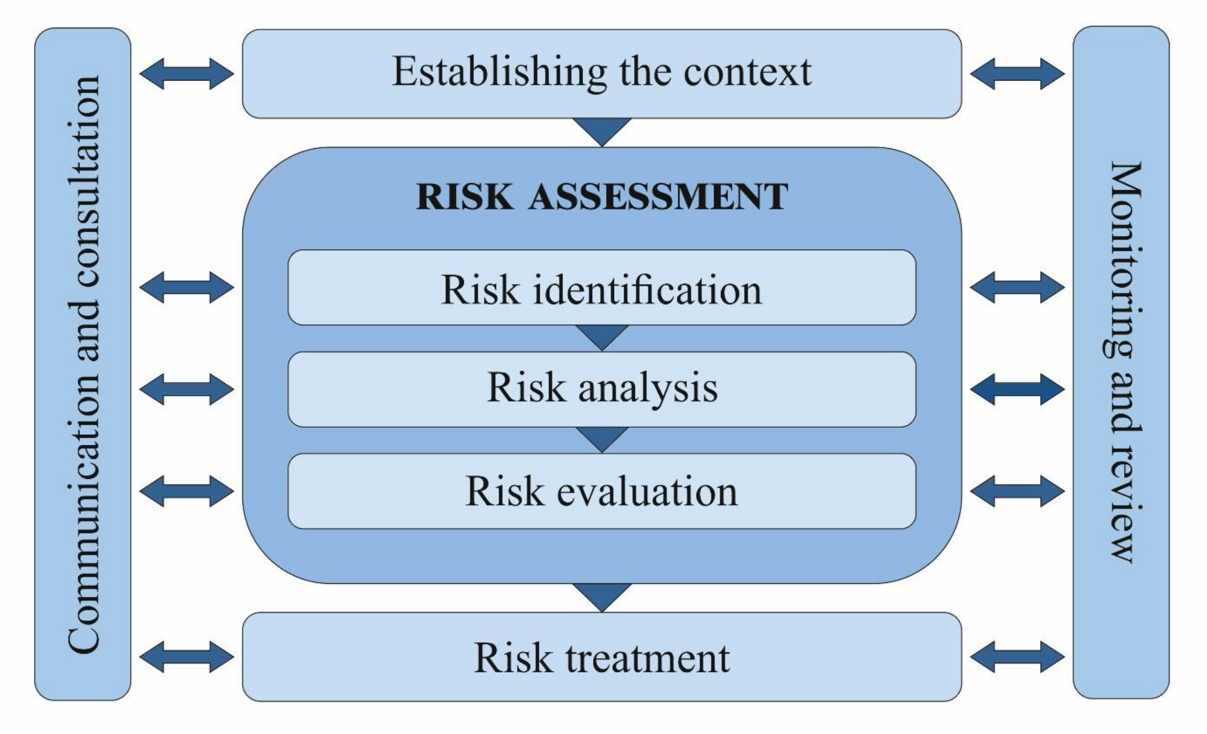

Figure D-1. Steps of the risk management process (after ISO, 2018).

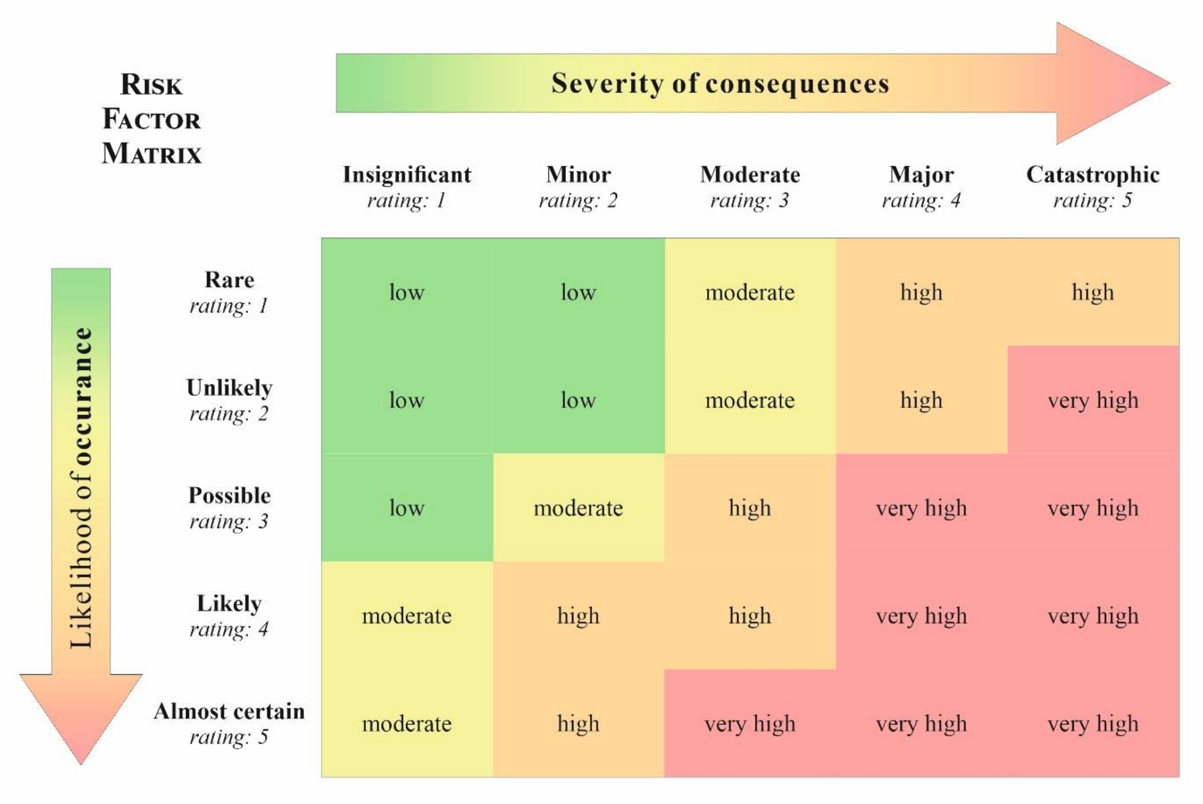

	Insignificant *rating: 1*	Minor *rating: 2*	Moderate *rating: 3*	Major *rating: 4*	Catastrophic *rating: 5*
Rare *rating: 1*	low	low	moderate	high	high
Unlikely *rating: 2*	low	low	moderate	high	very high
Possible *rating: 3*	low	moderate	high	very high	very high
Likely *rating: 4*	moderate	high	high	very high	very high
Almost certain *rating: 5*	moderate	high	very high	very high	very high

Figure D-2. Risk factor score matrix for qualitative risk assessment, relating the likelihood of hazards to the severity of consequences (adapted from Swierc et al., 2005).

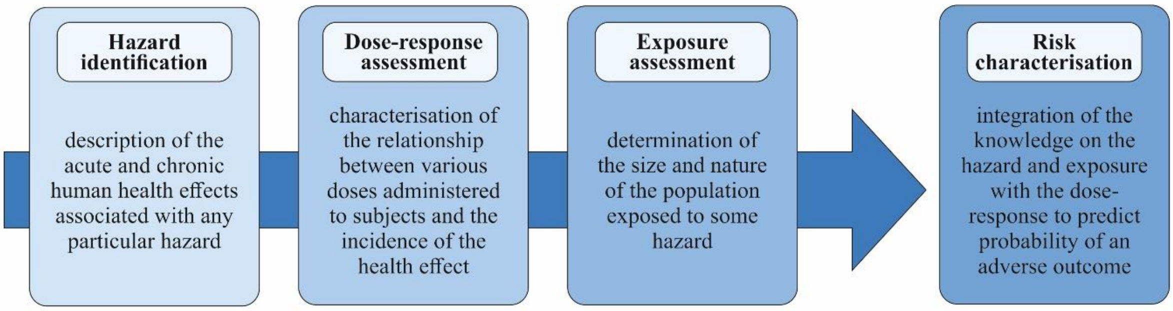
Hazard identification

description of the acute and chronic human health effects associated with any particular hazard

Dose-response assessment

characterisation of the relationship between various doses administered to subjects and the incidence of the health effect

Exposure assessment

determination of the size and nature of the population exposed to some hazard

Risk characterisation

integration of the knowledge on the hazard and exposure with the dose-response to predict probability of an adverse outcome

Figure D-3. Steps of quantitative risk assessment addressing human health risks arising from chemicals (adapted from Haas et al., 1999).

Table D-1. Summary of analysed case studies and methodological publications for MAR risk assessment, including information on the assessed risk type, the continent where research was conducted and the number of case studies. AUS: different methodologies recommended by the Australian guidelines; IND: Indian guidelines; QRA: quantitative risk assessment, HACCP: hazard analysis and critical control points, QMRA: quantitative microbial risk assessment, QualRA: qualitative risk assessment, PRTR: pollutant release and transfer register, WSP: water safety Plans, HHRA cont.: human health risk assessment addressing contaminants, Prob. RA fault trees: Probabilistic risk assessment based on fault trees, Econ. RA clogging: economic risk assessment addressing clogging, Pub. health & econ. RA: public health and economic risk assessment, HHR framew MAR: integrated health risk frameworks for MAR; EIA: environmental impact assessment. Year: year of publication.

No.	Publication	Year	Method	Human health risks	Environ-mental risks	Tech-nical risks	Social & eco-nomic risks	Legislation/ gover-nance risks	Continent	Case studies
1	*Lindhe et al., 2020*	2020				x			Africa	2 from Botswana
2	*Sprenger et al., 2020*	2020		x	x				Europe, America	1 Germany, 1 France, 1 Greece, 3 Brazil
3	*Donn et al., 2020*	2020		x					Australia	17 from Australia
4	*Song et al., 2019*	2019				x				data from different countries
5	*Rodríguez-Escales et al., 2018*	2018	Prob. RA fault trees	x	x	x	x	x	Europe, Asia	1 Portugal, 2 Spain, 1 Italy, 1 Malta, 1 Israel
6	*Ji & Lee, 2017*	2017	PRTR	x	x				Asia	2 from South Korea
7	*Juntunen et al., 2017*	2017	Pub. health & econ. RA	x	x	x	x		Europe	1 from Finland
8	*Page et al., 2016*	2016	QMRA	x	x				Australia, Asia	4 Australia, 1 China, 1 Singapore, 1 India
9	*Ji & Lee, 2016a,b*	2016	PRTR	x	x				Asia	1 from South Korea
10	*Dillon et al., 2016b*	2016	Econ. RA clogging				x		Australia	3 from Australia
11	*Dillon et al., 2016a*	2016	IND	x	x				Asia	3 from India
12	*Page et al., 2015a*	2015	QMRA	x					Australia	1 from Australia
13	*Bartak et al., 2015*	2015	AUS	x	x	x	x	x	Asia	1 from India
14	*de los Cobos, 2015*	2015			x	x	x	x	Europe	1 from Switzerland
15	*Page et al., 2015b*	2015	QMRA	x					Australia	1 from Australia
16	*Assmuth et al., 2015*	2015	HHR framew. MAR	x		x	x		Europe	1 from Finland
17	*Gibert et al., 2015*	2015	AUS	x	x				Europe	1 from Spain
18	*Seis et al., 2015*	2015	AUS	x	x				Europe	1 from Germany
19	*Gonzalez et al., 2015*	2015	HACCP	x					Australia	1 from Australia
20	*Sultana and Ahmed, 2015*	2014	Qual RA	x					Asia	20 from Bangladesh
21	*Shah, 2014*	2014					x	x	Asia	11 from India
22	*Page et al., 2013*	2013	QMRA	x	x				Australia	8 from Australia

Table D-1 (continued)

No.	Publication	Year	Method	Human health risks	Environmental risks	Technical risks	Social & economic risks	Legislation/ governance risks	Continent	Case studies
23	*El-Fakharany, 2013*	2013	EIA	x	x		x			1 from Egypt
24	*Pedretti et al., 2012a,b*	2012							Europe	1 from Spain
25	*Pasini et al., 2012*	2012				x			Europe	1 from Italy
26	*Page et al., 2012*	2012	QMRA	x					Australia, Asia, Europe	2 Australia, 1 China, 1 Italy, 1 Spain, 1 Israel, 1 Belgium
27	*Vanderzalm et al., 2011*	2011	AUS	x	x				Australia	1 from Australia
28	*Ayuso-Gabella et al., 2011*	2011	QMRA	x					Australia, Asia, Europe	1 Israel, 1 Spain, 1 Italy, 1 Australia
29	*Page et al., 2010b*	2010	AUS	x					Australia	1 from Australia
30	*Page et al., 2010c*	2010	QMRA	x	x				Australia	9 from Australia
31	*Page et al., 2010a*	2010	QMRA	x					Australia, America, Europe, Africa	1 from Mexico, 1 Australia, 1 South Africa, 1 Belgium
32	*Levantesi et al., 2010*	2010		x			x		Europe	1 Spain, 1 Italy, 1 Belgium
33	*Toze et al., 2010*	2010	QMRA	x					Australia	1 from Australia
34	*Page et al., 2010d*	2010	AUS		x	x			Australia	1 from Australia
35	*Dominguez et al., 2010*	2010	WSP	x					America	1 from Mexico
36	*Page et al., 2009*	2009	QRA/ HACCP	x	x				Australia	1 from Australia
37	*Page et al., 2008*	2008	QRA/ HACCP	x	x				Australia	1 from Australia
38	*Bekele et al., 2008*	2008	QMRA	x	x	x	x		Australia	1 from Australia
39	*Rodríguez et al., 2007*	2007	HHRA cont.	x					Australia	1 from Australia (planning phase)
40	*Rodriguez et al., 2007a*	2007	HHRA cont.	x					Australia	1 from Australia
41	*Swierc et al., 2005*	2005	QRA/ HACCP	x	x	x			Australia	1 from Australia
42	*Bloetscher et al., 2001*	2001	QMRA	x					America	1 from USA
43	*Dewettnick et al., 2001*	2001	HACCP	x					Europe	1 from Belgium

Table D-2. Aspects of MAR-related risk assessment clustered with respect to the risk type (human health, environmental, technical, social and economic risks, as well as risks related to legislation and governance) and the stage of MAR implementation and operation (i planning, ii assessment of the MAR catchment or water source, iii MAR operation and management, iv water distribution and final use). Examples for aspects frequently reported in literature are given (including possible hazards and related processes, as well as objectives and aims of risk assessment).

Human health risks	Environmental risks	Technical risks	Social and economic risks	Risks related to legislation and governance
MAR planning				
Chemical and microbial risk *(Assmuth et al., 2016; Bartak et al., 2015; Gibert et al., 2015; Ji and Lee, 2016a, 2017; NRMMC, 2009; Page et al., 2009; Page et al., 2010d, 2010d; Page et al., 2013; Pasini et al., 2012; Rodriguez et al., 2007a; Seis et al., 2015; Sprenger et al. 2020; Swierc et al., 2005; Vanderzalm et al., 2011)*.	**Impact on environment from operating MAR scheme.** E.g., impact on ecosystem due to GW level changes, reduction of traffic or agriculture in area, mobilization of pollutants from a nearby contaminated site, energy and Greenhouse gas considerations *(Bartak et al., 2015; Casanova et al., 2016; Dillon et al., 2013; NRMMC, 2009; Page et al., 2010b, 2010c; Page et al., 2009; Vanderzalm et al., 2011)*. **Rare species and animal migration** could be endangered through structural changes in the landscape (e.g., infiltration pond, fencing around groundwater protection zone) or changing groundwater levels *(El-Fakharany, 2013).*	**Water demand and supply** *(Bartak et al., 2015; Casanova et al., 2016; Gibert et al., 2015; Lindhe et al., 2020; Nandha et al., 2015; NRMMC, 2009; Page et al., 2010c; Rodríguez-Escales et al., 2018; Seis et al., 2015; Sprenger et al. 2020;Vanderzalm et al., 2011)*. **Influence of climate change on water supply** *(Pasini et al., 2012)*. **Hydrogeology and storage of water** *(Bouwer et al., 2008; Casanova et al., 2016; NRMMC, 2009; Page et al., 2010c; Seis et al., 2015; Sprenger et al. 2020; Shah, 2014)*. **Flooding of basements, below-ground cables** *(NRMMC, 2009)*.	**Communication & risk perception** *(Bekele et al., 2008; Le Corre et al., 2012)*. **Lack of funding** *(Maliva, 2014; Nandha et al., 2015; Rodríguez-Escales et al., 2017; Shah, 2014)*. **Commitment of stakeholders** *(Casanova et al., 2016)*. **Risk perception & communication with public** *(Alexander, 2011; ASCE, 2020; Bartak et al., 2015; Bekele et al., 2008; Juntunen et al., 2017; Le Corre et al., 2012)*. **Acceptance of MAR scheme by public** *(Alexander, 2011; Leviston et al., 2006; Mankad et al., 2015)*. **Overestimation of potential benefits while assessing economic feasibility of MAR** *(Maliva, 2014).* **Water demand changes due to climate change impacts leading to economic losses** *(Rupérez-Moreno et al., 2017)*.	**Regulatory requirements** *(Casanova et al., 2016; Nandha et al., 2015)*. **Missing land rights** *(Rodríguez-Escales et al., 2017)*. **Subsidies can lead to inefficient water consumption by population** *(Maliva, 2014)*.
Assessing the MAR catchment or water source				
Chemical and microbial risk *(Ayuso-Gabella et al., 2011; Bartak et al., 2015; Bugan et al., 2016; Casanova et al., 2016; Ji and Lee, 2016a, 2017; Juntunen et al., 2017; Lee and Ji, 2016; Nandha et al., 2015; NRMMC, 2009; Page et al., 2009; Page et al., 2010d, 2010c; Page et al., 2016; Rodriguez et al., 2007a; Swierc et al., 2005; Vanderzalm et al., 2011)*. **Pathogens** *(Assmuth et al., 2016; Page et al., 2010b; Page et al., 2008; Swierc et al., 2005)*. **Heterogeneity and transit time as factors influencing pathogen removal** *(Swierc et al., 2005; Toze et al., 2010)*.	**Chemical accidents** *(Bugan et al., 2016; Ji and Lee, 2016b, 2017; Juntunen et al., 2017; Swierc et al., 2005)*. **Stratification according to seasonal changes causing anaerobic conditions on the bottom of lakes and rivers** *(Lee and Ji, 2016).* **Chemical, microbial risks and risks from operating MAR schemes** *(Bartak et al., 2015; NRMMC, 2009; Page et al., 2010c, 2010d; Page et al., 2013, 2009; Vanderzalm et al., 2011)*. **Hydraulics of the aquifer.** E.g., change in pressure head, Water level, volumes, flow rates due to MAR operation *(Bartak et al., 2015; Nandha et al., 2015; NRMMC, 2009; Page et al., 2010b, 2010a; Page et al., 2013, 2009; Pasini et al., 2012; Seis et al., 2015; Sprenger et al. 2020; Vanderzalm et al., 2011).*	**Land use, change of water quality due to flooding and drought** (Bugan et al., 2016; Dillon et al., 2009a; Juntunen et al., 2017; Lee and Ji, 2016; Swierc et al., 2005). **Slope stability, erosion** (Rodríguez-Escales et al., 2018; Swierc et al., 2005). **High and low infiltration rate** (Bartak et al., 2015; de los Cobos, 2015; Rodríguez-Escales et al., 2018).	**Behaviour of public that affects groundwater quality around MAR scheme**. E.g., washing/ bathing near to wells, using buffer zone/GW protection zone for recreational purposes *(Bartak et al., 2015; Bugan et al., 2016)*. **Social disharmony** due to the construction of a MAR site, e.g., because of required resettlements or loss of farm land *(El-Fakharany, 2013).*	**Environmental conservation policies** *(Lee and Ji, 2016)*. **Include policy-makers in the process of protecting the GW quality** *(Bartak et al., 2015)*. **Limited options of communities to protect GW in areas where they lack competency** *(de los Cobos, 2018)*.

Table D-2 (continued)

Human health risks	Environmental risks	Technical risks	Social and economic risks	Risks related to legislation and governance
MAR operation and maintenance				
Pathogen removal *(Ayuso-Gabella et al., 2011; Bartak et al., 2015; Casanova et al., 2016; Donn et al., 2020; Leviston et al., 2006; NRMMC, 2009; Page et al., 2015b, 2012b, 2009, 2008; Page et al., 2010b, 2010d, 2010c; Page et al., 2015a; Swierc et al., 2005; Toze et al., 2010; Vanderzalm et al., 2011)*. **Water Quality aspects** (Bekele et al., 2008; Rodríguez-Escales et al., 2018).	**Chemical, microbial and risks from operating MAR scheme** *(Bartak et al., 2015; NRMMC, 2009; Page et al., 2010c, 2010d; Page et al., 2009; Rodríguez-Escales et al., 2018; Vanderzalm et al., 2011)*.	**Clogging** *(Bartak et al., 2015, 2008; Bugan et al., 2016; Nandha et al., 2015; Page et al., 2010b, 2010c, 2010d; Pedretti et al., 2012; Rodríguez-Escales et al., 2018; Song et al., 2019; Sultana and Ahmed, 2016)*. **Turbidity** (Bugan et al., 2016; Rodríguez-Escales et al., 2018; Swierc et al., 2005). **Malfunctioning of monitoring devices, corrosion of equipment, power failure** (Bartak et al., 2015; Juntunen et al., 2017; Lee and Ji, 2016; Nandha et al., 2015; Rodríguez-Escales et al., 2018; Swierc et al., 2005). **Missing trained operators, operation mistakes** (Assmuth et al., 2016; Dillon et al., 2020a; Rodríguez-Escales et al., 2018; Swierc et al., 2005).	**Unplanned costs** (Rodríguez-Escales et al., 2018). **Economic losses if performance objectives cannot be met** (Blood and Spagat, 2013; Dillon et al., 2016b; Maliva, 2014; Nandha et al., 2015).	**Cross boundary communication actions** *(de los Cobos, 2015).* **Missing land rights** (Bartak et al., 2015; Rodríguez-Escales et al., 2018). **Lack of legislations** (Fernández Escalante et al., 2020; Rodríguez-Escales et al., 2018).
Water distribution and final use				
Pathogens *(Ayuso-Gabella et al., 2011; Bartak et al., 2015; Bugan et al., 2016; Gibert et al., 2015; NRMMC, 2009; Page et al., 2008, 2009; Page et al., 2010a, 2010b, 2010c; Page et al., 2012b, 2012a; Seis et al., 2015; Sprenger et al., 2020; Toze et al., 2010)*. **Turbidity** *(Sultana and Ahmed, 2016; Swierc et al., 2005)*.	**Chemical, microbial and risks from operating MAR scheme** *(Bartak et al., 2015; Gibert et al., 2015; NRMMC, 2009; Page et al., 2010c, 2010c; Page et al., 2009; Seis et al., 2015; Sprenger et al., 2020)*.	**Microbial regrowth during storage, disinfection by-products, algae** *(Bouwer et al., 2008; Bugan et al., 2016; Lee and Ji, 2016; Pavelic et al., 2005)*.	**Economic risk of ill population due to poor water quality** *(Assmuth et al., 2016; Juntunen et al., 2017)*. **Risk perception and communication with public** *(Bartak et al., 2015; Juntunen et al., 2017; Le Corre et al., 2012)*. **Acceptance of MAR scheme by public** *(Alexander, 2011; Leviston et al., 2006; Mankad et al., 2015)*. **Lower benefits than anticipated**. E.g., as a result of insufficient demands for irrigation water due to realization of different climate change scenario *(Maliva, 2014; Rupérez-Moreno et al., 2017)*.	**Adaptation of water quality to changing standards for end-user** *(Nandha et al., 2015)*.

Table D-3. Examples for potential MAR-related (i) human health hazards, (ii) environmental hazards, (iii) technical hazards, (iv) socio-economic hazards and (v) hazards related legislation and governance

Hazard examples	References for the examples
Potential human health hazards	
Pathogens.	*Ayuso-Gabella et al., 2011; Bartak et al., 2015; Bekele et al., 2008; Bugan et al., 2016; Casanova et al., 2016; Dewettinck et al., 2001; Dominguez-Chicas and Scrimshaw, 2010; Donn et al., 2020; Gibert et al., 2015; Gonzalez et al., 2015; Ji and Lee, 2016b, 2017; Lee and Ji, 2016; Levantesi et al., 2010; NRMMC, 2009; Page et al., 2016, 2015b, 2015a, 2013, 2012b, 2009, 2008; Page et al., 2010b; Page et al., 2010a, 2010c, 2010d; Seis et al., 2015; Sprenger et al., 2020; Swierc et al., 2005; Vanderzalm et al., 2011.*
Inorganic and/or organic chemicals.	*Bartak et al., 2015; Bekele et al., 2008; Bugan et al., 2016; Gibert et al., 2015; Ji and Lee, 2016a, 2017; Juntunen et al., 2017; Lee and Ji, 2016; NRMMC, 2009; Page et al., 2016, 2013, 2009, 2008; Page et al., 2010c, 2010c; Rodríguez-Escales et al., 2018; Rodriguez et al., 2007a; Seis et al., 2015; Sprenger et al., 2020; Toze et al., 2010; Vanderzalm et al., 2011.*
Salinity and sodicity.	*Bartak et al., 2015; Bugan et al., 2016; Gibert et al., 2015; Gonzalez et al., 2015; NRMMC, 2009; Page et al., 2010c, 2010c; Page et al., 2016, 2013, 2009; Seis et al., 2015; Sprenger et al., 2020; Vanderzalm et al., 2011.*
Nutrients.	*Bartak et al., 2015; Bugan et al., 2016; Casanova et al., 2016; Gibert et al., 2015; Lee and Ji, 2016; NRMMC, 2009; Page et al., 2010c, 2010d; Page et al., 2016, 2013; Rodríguez-Escales et al., 2018; Seis et al., 2015; Sprenger et al., 2020; Vanderzalm et al., 2011.*
Turbidity and particulates.	*Bartak et al., 2015; Bekele et al., 2008; Bugan et al., 2016; Gibert et al., 2015; Lee and Ji, 2016; NRMMC, 2009; Page et al., 2010c, 2010d; Page et al., 2013, 2009; Rodríguez-Escales et al., 2018; Seis et al., 2015; Sprenger et al., 2020; Sultana and Ahmed, 2016; Swierc et al., 2005; Vanderzalm et al., 2011.*
Radionuclides.	*Gibert et al., 2015; NRMMC, 2009; Page et al., 2010c, 2010d; Page et al., 2016, 2013, 2009; Rodríguez-Escales et al., 2018; Seis et al., 2015; Sprenger et al., 2020; Vanderzalm et al., 2011.*
Adverse land use.	*Bartak et al., 2015; Lee and Ji, 2016; Swierc et al., 2005; Vanderzalm et al., 2011.*
Disinfection by-products (CBPs).	*Lee and Ji, 2016; Pavelic et al., 2005.*
Potential environmental hazards	
Chemical accidents (e.g., industry, road/train/planes, household pesticides, nuclear radiation), sabotage.	*Assmuth et al., 2016; Bartak et al., 2015; Bouwer et al., 2008; Bugan et al., 2016; Lee and Ji, 2016; NRMMC, 2009; Page et al., 2010c; Page et al., 2013; Swierc et al., 2005; Vanderzalm et al., 2011.*
(Illegal) release of waste and wastewater, sewer overflow, (illegal) livestock, contamination by birds.	*Bugan et al., 2016; Juntunen et al., 2017; Lee and Ji, 2016; Swierc et al., 2005.*
Impacts of MAR scheme on GW-dependent ecosystem, e.g., due to changing water levels, quality, pressure, volumes and flow rates leading e.g., to the mobilization and migration of contaminants, dissolution of minerals. Rare species and animal migration could be endangered through structural changes in the landscape (e.g., infiltration ponds, fencing around groundwater protection zone) or changing groundwater levels.	*Assmuth et al., 2016; Bartak et al., 2015; Dillon et al., 2009a; El-Fakharany, 2013; Gibert et al., 2015; Nandha et al., 2015; NRMMC, 2009; Page et al., 2010c, 2010d; Page et al., 2013, 2009; Pasini et al., 2012; Seis et al., 2015; Sprenger et al., 2020; Swierc et al., 2005; Vanderzalm et al., 2011.*
Energy consumption and greenhouse gas emissions.	*Bartak et al., 2015; Gibert et al., 2015; NRMMC, 2009; Page et al., 2010c, 2010d; Page et al., 2013, 2009; Seis et al., 2015; Sprenger et al., 2020; Vanderzalm et al., 2011.*
Potential technical hazards	
Flood, heavy rainfalls (such as monsoon rainfall).	*Bartak et al., 2015; Bugan et al., 2016; Juntunen et al., 2017; Lee and Ji, 2016; NRMMC, 2009; Rodríguez-Escales et al., 2018; Swierc et al., 2005.*
Clogging.	*Bartak et al., 2015; Bekele et al., 2008; Bugan et al., 2016; Lee and Ji, 2016; Nandha et al., 2015; NRMMC, 2009; Page et al., 2010b; Page et al., 2010c, 2010d; Pedretti et al., 2012b; Rodríguez-Escales et al., 2018; Song et al., 2019; Sultana and Ahmed, 2016.*
Drought.	*Juntunen et al., 2017; Lee and Ji, 2016; Nandha et al., 2015; NRMMC, 2009; Rodríguez-Escales et al., 2018; Swierc et al., 2005.*

Table D-3 (continued)

Hazard examples	References for the examples
Potential technical hazards	
Reduced/elevated infiltration rate.	*Bartak et al., 2015; de los Cobos, 2018; Rodríguez-Escales et al., 2018)*
Slope instability, erosion.	*Rodríguez-Escales et al., 2016; Swierc et al., 2005.*
Lack of land.	*Rodríguez-Escales et al., 2018.*
Water demand and supply changes.	*Lindhe et al., 2020; Nandha et al., 2015; NRMMC, 2009.*
Reliability of technology, malfunctioning or failure of technical equipment or infrastructure (including e.g., pre and post treatment, pumps, pipes, monitoring schemes), fires, computer hacking, terrorism.	*Bartak et al., 2015; Bouwer et al., 2008; Bugan et al., 2016; Juntunen et al., 2017; Lee and Ji, 2016; Nandha et al., 2015; Rodríguez-Escales et al., 2018; Swierc et al., 2005.*
Missing trained staff (leading to problems/failure of MAR operation).	*Assmuth et al., 2016; Dillon et al., 2020; Rodríguez-Escales et al., 2018; Swierc et al., 2005.*
Bacterial re-growth, biofilm in distribution system and storage tanks.	*Bugan et al., 2016.*
Potential socio-economic hazards	
Lack of funding /financial support, business case.	*Maliva, 2014; Pindoria-Nandha, 2016; Rodríguez-Escales et al., 2018; Shah et al., 2013.*
Unplanned costs (maintenance, installation etc.).	*Rodríguez-Escales et al., 2018.*
Changing standards for end-user.	*Nandha et al., 2015.*
Insufficient communication and negative risk perception of the public.	*Alexander, 2011; ASCE and EWRI, 2020; Bartak et al., 2015; Bekele et al., 2008; Juntunen et al., 2017; Le Corre et al., 2012.*
Economic losses if performance objectives cannot be met.	*Blood and Spagat, 2013; Dillon et al., 2016b; Maliva, 2014; Nandha et al., 2015.*
Behaviour of public that affects groundwater quality around the MAR scheme (e.g., washing/bathing near to wells, absence of buffer zone or groundwater protection zone for recreational purposes).	*Bartak et al., 2015; Bugan et al., 2016.*
Negative economic effects due to illness originating from poor water quality.	*Assmuth et al., 2016; Juntunen et al., 2017.*
Missing acceptance and trust of public.	*Alexander, 2011; Leviston et al., 2006; Mankad et al., 2015.*
Missing commitment of stakeholders.	*Casanova et al., 2016.*
Benefits are lower than anticipated, e.g., if the actual willingness-to-pay is lower than declared; or if there is an insufficient demand (e.g., for irrigation water under different climate change scenarios).	*Maliva, 2014; Rupérez-Moreno et al., 2017.*
Subsidies can lead to inefficient water consumption by population.	*Maliva, 2014.*
Construction of MAR site could lead to resettlements or the loss of farm land for the local population, which could cause social disharmony (this may also be related to minority groups).	*El-Fakharany, 2013*
Potential hazards related to legislation and governance	
Missing land rights.	*Bartak et al., 2015; Rodríguez-Escales et al., 2018.*
Legislative requirements; regulatory risks such as environmental conservation policies, water quality regulations.	*Bartak et al., 2015; Casanova et al., 2016; de los Cobos, 2018, 2015; Fernández Escalante et al., 2020; Lee and Ji, 2016; Nandha et al., 2015; Rodríguez-Escales et al., 2018.*

Table D-4. Overview of risk types (columns) considered by methodologies and guidelines (lines) for risk assessment of MAR schemes (x: applied in the evaluated literature, +: potentially applicable for the indicated risk types, (x): the Australian guidelines give some suggestions on technical aspects but do not include a defined assessment procedure for technical risks).

	Human health risks	**Environmental risks**	**Technical risks**	**Socio-economic risks**	**Risks related to legislation & governance**
Australian guidelines	x	x	(x)		
Water safety plans	x	x	+	+	+
Hazard analysis and critical control points (HACCP) framework	x	x	+	+	+
Indian guidelines	x	x			
Chilean guidelines	x	x			
Qualitative risk assessment	x	x	+	+	+
Quantitative microbial risk assessment (QMRA)	x				
Quantitative risk assessment	x	x			
Integrated human health risk framework for MAR	x	x	x	x	x
Pollutant release and transfer register (PRTR)	x	x			
Probabilistic risk assessment based on fault trees	x	x	x	x	x
Screening-level assessment of human health risks arising from micro-pollutants	x				
Public health and economic risk assessment	x	x	x	x	
Assessment of economic risks arising from well clogging				x	
Environmental impact assessment of MAR	x	x		x	
Sum	14	12	4 (x) 7 (x,+)	5 (x) 8 (x,+)	2 (x) 5 (x,+)
Percentage (methodologies & guidelines per risk type referred to all 15 methodologies & guidelines)	93%	80%	27% (x) 47 % (x,+)	33% (x) 53% (x,+)	13% (x) 33% (x,+)

D2. References

Alexander, K.S., 2011. Community attitudes towards Managed Aquifer Recharge and stormwater use in Adelaide , Australia. 8th Int. Conf. Water Reclam. Reuse 1–11.

ASCE American Society of Civil Engineering EWRI Environmental and Water Research Institute, 2020. Standard Guidelines for Managed Aquifer Recharge, Standard Guidelines for Managed Aquifer Recharge. https://doi.org/10.1061/9780784415283

Assmuth, T., Simola, A., Pitkänen, T., Lyytimäki, J., Huttula, T., 2016. Integrated frameworks for assessing and managing health risks in the context of managed aquifer recharge with river water. Integr. Environ. Assess. Manag. 12, 160–173. https://doi.org/10.1002/ieam.1660

Ayuso-Gabella, N., Page, D., Masciopinto, C., Aharoni, A., Salgot, M., Wintgens, T., 2011. Quantifying the effect of Managed Aquifer Recharge on the microbiological human health risks of irrigating crops with recycled water. Agric. Water Manag. 99, 93–102. https://doi.org/10.1016/j.agwat.2011.07.014

Bartak, R., Page, D., Sandhu, C., Grischek, T., Saini, B., Mehrotra, I., Jain, C.K., Ghosh, N.C., 2015. Application of risk-based assessment and management to riverbank filtration sites in India. J. Water Health 13, 174–189. https://doi.org/10.2166/wh.2014.075

Bekele, E., Toze, S., Higginson, S., Blair, P., Heitz, A., Browne, A., Leviston, Z., Po, M., Nancarrow, B., Tucker, D., Porter, N., Mcguinness, N., Rodriguez, C., Devine, B., 2008. Determining Requirements for Managed Aquifer Recharge in Western Australia : Progress Report. Water.

Bloetscher, F., 2001. Risk assessment applications for alternative groundwater injection programs. Bridg. Gap Meet. World's Water Environ. Resour. Challenges - Proc. World Water Environ. Resour. Congr. 2001 111. https://doi.org/10.1061/40569(2001)153

Blood, M.R., Spagat, E., 2013. Las Posas Basin Aquifer Failure Illustrates Risks of Underground Reservoirs [WWW Document]. Assoc. Press New York City, USA. URL https://www.washingtonpost.com/national/health-science/millions-spent-on-california-water-storage-plan-that-leaks/2013/08/24/7747a842-0cfb-11e3-b87c-476db8ac34cd_story.html

Bouwer, H., Pyne, D., Brown, J., St Germain, D., Morris, T., Brown, C.J., Dillon, P., Rycus, M., 2008. Design, operation, and maintenance for sustainable underground storage facilities, Awwa Research Foundation.

Bugan, R.D.H., Jovanovic, N., Israel, S., Tredoux, G., Genthe, B., Steyn, M., Allpass, D., Bishop, R., Marinus, V., 2016. Four decades of water recycling in Atlantis (Western Cape, South Africa): Past, present and future. Water SA 42, 577–594. https://doi.org/10.4314/wsa.v42i4.08

Casanova, J., Devau, N., Pettenati, M., 2016. Managed Aquifer Recharge: An Overview of Issues and Options, in: Jakeman, A.J., Barreteau, O., Hunt, J.H., Rinaudo, J.-D., Ross, A. (Eds.), Integrated Groundwater Management. Springer Nature, pp. 619–638. https://doi.org/10.1007/978-3-319-23576-9

de los Cobos, G., 2018. The Genevese transboundary aquifer (Switzerland-France): The secret of 40 years of successful management. J. Hydrol. Reg. Stud. 20, 116–127. https://doi.org/10.1016/j.ejrh.2018.02.003

de los Cobos, G., 2015. A historical overview of Geneva's artificial recharge system and its crisis management plans for future usage. Environ. Earth Sci. 73, 7825–7831. https://doi.org/10.1007/s12665-014-3575-0

Dewettinck, T., Van Houtte, E., Geenens, D., Van Hege, K., Verstraete, W., 2001. HACCP (Hazard Analysis and Critical Control Points) to guarantee safe water reuse and drinking water production - A case study. Water Sci. Technol. 43, 31–38. https://doi.org/10.2166/wst.2001.0708

Dillon, P., Page, D., Vanderzalm, J., Sidhu, J., Sandhu, C., Boisson, A., Lakshmanan, E., 2016a. Application of a Water Quality Guide to Managed Aquifer Recharge in India, in: Wintgens, T., Nättorp, A., Lakshmanan, E., Asolekar, S. (Eds.), Natural Water Treatment Systems for Safe and Sustainable Water Supply in the Indian Context: Saph Pani. IWA Publishing, London UK. https://doi.org/10.2166/9781780408392

Dillon, P., Fernández Escalante, E., Megdal, S.B., Massmann, G., 2020. Managed aquifer recharge for water resilience. Water (Switzerland) 12, 11. https://doi.org/10.3390/w12071846

Dillon, P., Kumar, A., Kookana, R., Leijs, R., Reed, D., Parsons, S., 2009. Managed Aquifer Recharge - Risks to Groundwater Dependent Ecosystems - A Review. Water for a Healthy Country Flagship Report to Land & Water Australia. CSIRO Waterlines Rep. Ser. No. 13 64.

Dillon, P., Page, D., Vanderzalm, J., Chadha, D., 2013. Water Quality Considerations in Managed Aquifer Recharge : from Artificial Recharge to Managed Aquifer Recharge in India. J. Groundw. Res. 2, 8–15.

Dillon, P., Vanderzalm, J.L., Page, D., Barry, K., Gonzalez, D., Muthukaruppan, M., Hudson, M., 2016b. Analysis of ASR Clogging Investigations at Three Australian ASR Sites in a Bayesian Context. Water 8. https://doi.org/10.3390/w8100442

Dominguez-Chicas, A., Scrimshaw, M.D., 2010. Hazard and risk assessment for indirect potable reuse schemes : An approach for use in developing Water Safety Plans. Water Res. 44, 6115–6123. https://doi.org/10.1016/j.watres.2010.07.007

Donn, M., Reed, D., Vanderzalm, J., Page, D., 2020. Assessment of E. coli attenuation during infiltration of treatedwastewater: A pathway to future managed aquifer recharge. Water (Switzerland) 12. https://doi.org/10.3390/w12010173

El-Fakharany, Z., 2013. Environmental Impact Assessment of Artificial Recharge of Treated Wastewater on Groundwater Aquifer System. Case study: Abu Rawash, Egypt. J. Am. Sci. 9.

Fernández Escalante, E., Henao Casas, J.D., Vidal Medeiros, M.A., San Sebastián Sauto, J., 2020. Regulations and guidelines on water quality requirements for Managed Aquifer Recharge . International comparison. Acque Sotter. Ital. J. Groundw. AS33-462, 7–22. https://doi.org/10.7343/as-2020-462

Gibert, O., Hernández, M., Kienle, C., Simon, E., Sprenger, C., Besselink, H., Hannappel, S., 2015. Field investigations and risk assessment in La Vall d'Uixó

(Castellón, Spain) - DEMEAU.

Gonzalez, D., Page, D., Vanderzalm, J., Dillon, P., 2015. Setting water quality trigger levels for the operation and management of a MAR system in Parafield, South Australia. J. Hydrol. Eng. 20, 1–8. https://doi.org/10.1061/(ASCE)HE.1943-5584.0001001

Haas, C.N., Rose, J.B., Gerba, C.P., 1999. Quantitative Microbial Risk Assessment. John Wiley and Sons Inc, New York.

ISO International Organization for Standardization, 2018. Guidelines for health risk assessment and management for non-potable water reuse 20426.

Ji, H.W., Lee, S. Il, 2016a. Assessment of risk due to chemicals transferred in a watershed: A case of an aquifer storage transfer and recovery site. Water (Switzerland) 8. https://doi.org/10.3390/w8060242

Ji, H.W., Lee, S. Il, 2016b. Use of pollutant release and transfer register (PRTR) to assess potential risk associated with chemicals in a drinking water supply facility. Desalin. Water Treat. 57, 29228–29239. https://doi.org/10.1080/19443994.2016.1171170

Ji, H.W., Lee, S.-I., 2017. Comparison of potential risk on two managed aquifer recharge sites from river basin. Water (Switzerland) 9. https://doi.org/10.3390/w9090674

Juntunen, J., Meriläinen, P., Simola, A., 2017. Public health and economic risk assessment of waterborne contaminants and pathogens in Finland. Sci. Total Environ. 599–600, 873–882. https://doi.org/10.1016/j.scitotenv.2017.05.007

Le Corre, K., Aharoni, A., Cauwenberghs, J., Chavez, A., Cikurel, H., Ayuso Gabella, M.N., Genthe, B., Gibson, R., Jefferson, B., Jeffrey, P., Jimenez, B., Kazner, C., Masciopinto, C., Page, D., Regel, R., Rinck-Pfeiffer, S., Salgot, M., Steyn, M., van Houtte, E., Tredoux, G., Wintgens, T., Xuzhou, C., Yu, L., Zhao, X., 2012. Water reclamation for aquifer recharge at the eight case study sites: a cross case analysis, in: Kazner, C., Wintgens, T., Dillon, P. (Eds.), Water Reclamation Technologies for Safe Managed Aquifer Recharge. pp. 11–31.

Lee, S. Il, Ji, H.W., 2016. Identification of hazardous events for drinking water production process using managed aquifer recharge in the Nakdong river delta, Korea. Malaysian J. Anal. Sci. 20, 365–372. https://doi.org/10.17576/mjas-2016-2002-20

Levantesi, C., La Mantia, R., Masciopinto, C., Böckelmann, U., Ayuso-Gabella, M.N., Salgot, M., Tandoi, V., Van Houtte, E., Wintgens, T., Grohmann, E., 2010. Quantification of pathogenic microorganisms and microbial indicators in three wastewater reclamation and managed aquifer recharge facilities in Europe. Sci. Total Environ. 408, 4923–4930. https://doi.org/10.1016/j.scitotenv.2010.07.042

Leviston, Z., Nancarrow, B.E., Tucker, D.I., Porter, N.B., 2006. Predicting Community Behaviour: Indirect Potable Reuse of Wastewater through Managed Aquifer Recharge, CSIRO Land and Water Science Report 2906.

Lindhe, A., Rosén, L., Johansson, P.O., Norberg, T., 2020. Dynamic water balance modelling for risk assessment and decision support on MAR potential in Botswana. Water (Switzerland) 12, 1–13. https://doi.org/10.3390/w12030721

Maliva, R.G., 2014. Economics of managed aquifer recharge. Water (Switzerland) 6, 1257–1279. https://doi.org/10.3390/w6051257

Mankad, A., Walton, A., Alexander, K., 2015. Key dimensions of public acceptance for managed aquifer recharge of urban stormwater. J. Clean. Prod. 89, 214–223. https://doi.org/10.1016/j.jclepro.2014.11.028

Nandha, M., Berry, M., Jefferson, B., Jeffrey, P., 2015. Risk assessment frameworks for MAR schemes in the UK. Environ. Earth Sci. 73, 7747–7757. https://doi.org/10.1007/s12665-014-3399-y

NRMMC–EPHC–NHMRC, 2009. Australian Guidelines for Water Recycling: Managing Health and Environmental Risks (Phase 2) Managed Aquifer Recharge; Natural Resource Management Ministerial Council; Environment Protection and Heritage Council; National Health and Medical Research Counc [WWW Document]. Nat. Resour. Manag. Minist. Counc. Prot. Herit. Counc. ; Aust. Heal. Minist. Conf. URL https://www.nhmrc.gov.au/about-us/publications/australian-guidelines-water-recycling#block-views-block-file-attachments-content-block-1. (accessed 9.28.20).

Page, D., Ayuso-Gabella, M.N., Kopac, I., Bixio, D., Dillon, P., Salgot de Marçay, M., Genthe, B., 2012a. Risk assessment and risk management in Managed Aquifer Recharge, in: Kazner, C., Wintgens, T., Dillon, Peter (Eds.), Water Reclamation Technologies for Safe Managed Aquifer Recharge. IWA Publishing.

Page, D., Barry, K., Pavelic, P., Dillon, P., 2008. Preliminary quantitative risk assessment for the Salisbury stormwater ASTR Project. CSIRO Water a Heal. Couuntry Natl. Res. Flagsh.

Page, D., Dillon, P., Toze, S., Bixio, D., Genthe, B., Jiménez Cisneros, B.E., Wintgens, T., 2010a. Valuing the subsurface pathogen treatment barrier in water recycling via aquifers for drinking supplies. Water Res. 44, 1841–1852. https://doi.org/10.1016/j.watres.2009.12.008

Page, D, Dillon, P., Toze, S., Sidhu, J.P.S., 2010b. Characterising aquifer treatment for pathogens in managed aquifer recharge. https://doi.org/10.2166/wst.2010.539

Page, D., Dillon, P., Vanderzalm, J., Bekele, E., Barry, K., Miotlinski, K., Levett, K., 2010c. Managed aquifer recharge case study risk assessments. CSIRO.

Page, D., Dillon, P., Vanderzalm, J., Toze, S., Sidhu, J., Barry, K., Levett, K., Kremer, S., Regel, R., 2010d. Risk Assessment of Aquifer Storage Transfer and Recovery with Urban Stormwater for Producing Water of a Potable Quality. J. Environ. Qual. 39, 2029–2039. https://doi.org/10.2134/jeq2010.0078

Page, D., Gonzalez, D., Dillon, P., 2012b. Microbiological risks of recycling urban stormwater via aquifers. Water Sci. Technol. 65, 1692–1695. https://doi.org/10.2166/wst.2012.069

Page, D., Gonzalez, D., Dillon, P., Vanderzalm, J., Vadakattu, G., Toze, S., Sidhu, J., Miotlinski, K., Torkzaban, S., Barry, K., 2013. Managed Aquifer Recharge and Urban Stormwater Use Options: Public Health and Environmental Risk Assessment Final Report, Goyder Institute for Water Research Technical Report Series No. 13/17.

Page, D., Gonzalez, D., Sidhu, J., Toze, S., Torkzaban, S., Dillon, P., 2015a. Assessment of treatment options of recycling urban stormwater recycling via aquifers to produce drinking water quality. Urban Water J. 13, 657–662. https://doi.org/10.1080/1573062X.2015.1024691

Page, D., Gonzalez, D., Torkzaban, S., Toze, S., Sidhu, J., Miotliński, K., Barry, K., Dillon, P., 2015b. Microbiological risks of recycling urban stormwater via aquifers for various uses in Adelaide, Australia. Environ. Earth Sci. 73, 7733–7737. https://doi.org/10.1007/s12665-014-3466-4

Page, D., Vanderzalm, J., Barry, K., Levett, K., Kremer, S., Ayuso-Gabella, M., Dillon, Toze, S., Sidhu, J., Shackleton, M., Purdie, M., Regel, R., 2009. Operational residual risk assessment for the Salisbury stormwater ASTR project.

Page, D., Vanderzalm, J., Dillon, P., Gonzalez, D., Barry, K., 2016. Stormwater Quality Review to Evaluate Treatment for Drinking Water Supply via Managed Aquifer Recharge. Water. Air. Soil Pollut. 227. https://doi.org/10.1007/s11270-016-3021-x

Pasini, S., Torresan, S., Rizzi, J., Zabeo, A., Critto, A., Marcomini, A., 2012. Climate change impact assessment in Veneto and Friuli Plain groundwater. Part II: A spatially resolved regional risk assessment. Sci. Total Environ. 440, 219–235. https://doi.org/10.1016/j.scitotenv.2012.06.096

Pavelic, P., Nicholson, B.C., Dillon, P.J., Barry, K.E., 2005. Fate of disinfection by-products in groundwater during aquifer storage and recovery with reclaimed water. J. Contam. Hydrol. 77, 119–141. https://doi.org/10.1016/j.jconhyd.2004.12.003

Pedretti, D., Barahona-Palomo, M., Bolster, D., Fernàndez-Garcia, D., Sanchez-Vila, X., Tartakovsky, D.M., 2012a. Probabilistic analysis of maintenance and operation of artificial recharge ponds. Adv. Water Resour. 36, 23–35. https://doi.org/10.1016/j.advwatres.2011.07.008

Pedretti, D., Barahona-Palomo, M., Bolster, D., Sanchez-Vila, X., Fernàndez-Garcia, D., 2012b. A quick and inexpensive method to quantify spatially variable infiltration capacity for artificial recharge ponds using photographic images. J. Hydrol. 430–431, 118–126. https://doi.org/10.1016/j.jhydrol.2012.02.008

Pindoria-Nandha, M., 2016. Planning an Aquifer Storage and Recovery scheme in the Sherwood Sandstone aquifer. Cranfield Unviversity.

Rodríguez-Escales, P., Canelles, A., Sanchez-Vila, X., Folch, A., Kurtzman, D., Rossetto, R., Fernández Escalante, E., Lobo-Ferreira, J.P., Sapiano, M., San-Sebastián, J., Schüth, C., 2018. A risk assessment methodology to evaluate the risk failure of managed aquifer recharge in the Mediterranean Basin. Hydrol. Earth Syst. Sci. 22, 3213–3227. https://doi.org/10.5194/hess-22-3213-2018

Rodríguez-Escales, P., Fernàndez-Garcia, D., Drechsel, J., Folch, A., Sanchez-Vila, X., 2017. Improving degradation of emerging organic compounds by applying chaotic advection in Managed Aquifer Recharge in randomly heterogeneous porous media. Water Resour. Res. 53, 4376–4392. https://doi.org/10.1002/2016WR020333

Rodríguez-Escales, P., Folch, A., Vidal-Gavilan, G., van Breukelen, B.M., 2016. Modelling biogeochemical processes and isotope fractionation of enhanced in situ biodenitrification in a fractured aquifer. Chem. Geol. 425, 52–64. https://doi.org/10.1016/j.chemgeo.2016.01.019

Rodriguez, C., Cook, A., Van Buynder, P., Devine, B., Weinstein, P., 2007a. Screening health risk assessment of micropullutants for indirect potable reuse schemes: A three-tiered approach. Water Sci. Technol. 56, 35–42. https://doi.org/10.2166/wst.2007.831

Rodriguez, C., Weinstein, P., Cook, A., Devine, B., Van Buynder, P., 2007b. A proposed approach for the assessment of chemicals in indirect potable reuse schemes. J. Toxicol. Environ. Heal. - Part A Curr. Issues 70, 1654–1663. https://doi.org/10.1080/15287390701434828

Rupérez-Moreno, C., Pérez-Sánchez, J., Senent-Aparicio, J., Flores-Asenjo, P., Paz-Aparicio, C., 2017. Cost-Benefit Analysis of the Managed Aquifer Recharge System for Irrigation under Climate Change Conditions in Southern Spain. water 9, 343. https://doi.org/10.3390/w9050343

Seis, W., Sprenger, C., Schimmelpfennig, S., 2015. Application of the Australian Guidelines for Water Recycling: Managing Health and Environmental Risks, Part of D11.2: Demonstration of MAR effects on groundwater resources – development and application of different approaches for risk and impact assessmen.

Shah, T., 2014. Towards a Managed Aquifer Recharge strategy for Gujarat, India: An economist’s dialogue with hydro-geologists. J. Hydrol. 518, 94–107. https://doi.org/10.1016/j.jhydrol.2013.12.022

Shah, T., Burke, J., Villholth, K., Angelica, M., Custodio, E., Daibes, F., Hoogesteger, J., Giordano, M., Girman, J., van der Gun, J., Kendy, E., Kijne, J., Llamas, R., Masiyandama, M., Margat, J., Marin, L., Peck, J., Rozelle, S., Sharma, B., Vincent, L., Wang, J., 2013. Groundwater: A global assessment of scale and significance, in: Molden, D. (Ed.), Water for Food, Water for Life: A Comprehensive Assessment of Water Management in Agriculture. London, UK: Earthscan; Colombo, Sri Lanka: International Water Management Institute (IWMI)., pp. 395–424. https://doi.org/10.4324/9781849773799

Sprenger, C., Panagiotou, K., Fernandes, L., Duzan, A., Baptista, V., Glass, J., 2020. Smart framework for real-time monitoring and control of subsurface processes in managed aquifer recharge (MAR) applications 59.

Song, Y., Du, X., Ye, X., 2019. Analysis of potential risks associated with urban stormwater quality for managed aquifer recharge. Int. J. Environ. Res. Public Health 16. https://doi.org/10.3390/ijerph16173121

Sultana, S., Ahmed, K.M., 2016. Assessing risk of clogging in community scale managed aquifer recharge sites for drinking water in the coastal plain of south-west Bangladesh. https://doi.org/10.3329/bjsr.v27i1.26226

Swierc, J., Page, D., Leeuwen, J. Van, 2005. Preliminary Hazard Analysis and Critical Control Points Plan (HACCP) - Salisbury Stormwater to Drinking Water Aquifer Storage Transfer and Recovery (ASTR) Project of Montana. Water.

Toze, S., Bekele, E., Page, D., Sidhu, J., Shackleton, M., 2010. Use of static Quantitative Microbial Risk Assessment to determine pathogen risks in an unconfined carbonate aquifer used for Managed Aquifer Recharge. Water Res. 44, 1038–1049. https://doi.org/10.1016/j.watres.2009.08.028

Vanderzalm, J.L., Page, D.W., Dillon, P.J., 2011. Application of a risk management framework to a drinking water supply augmented by stormwater recharge. Water Sci. Technol. 63, 719–726. https://doi.org/10.2166/wst.2011.294

Appendix E Contributions to scientific community

E1. Published manuscripts

Imig, A., Szabó Z., Halytsia, O., Vrachioli, M., Kleinert, V., Rein, A., (2022) *A review on risk assessment in Managed Aquifer Recharge*. Integrated Environmental Assessment and Management, 18,1513-1529. doi: 10.1002/ieam.4584

Imig, A., Shajari, F., Augustin, L. Einsiedl, F. Rein, A., (2022*) Improved lumped-parameter and numerical modelling of unsaturated water flow and stable water isotopes*. Groundwater. doi: 10.1111/gwat.13244

Halytsia, O., Vrachioli M., Janik, K., Sławomir, S., Wojtal, G., **Imig, A.,** Rein, A., Sauer, J., (2022) *Assessing economic feasibility of managed aquifer recharge schemes: Evidence from cost-benefit analysis in Poland.* Water Resour. Manag. doi: 10.1007/s11269-022-03303-0

Welsh, K., Bowen-O'Connor, C., Stephens, M., Dokou, Z., **Imig, A.,** Mackey, T., Moxey, A., Nikolopoulos, E., Rein, A., Turner, A., Williams, A., Al Baghdadi, L., Bowleg, J., Chaves, H.L., Davis, A., Guberman, G., Hanek, D., Klausner, S., Medlev, D., Mazzon, N., Miller, I., Williams, W., Wilchcombe, R., (in press) *Potable Water and Terrestrial Resources on Grand Bahama Post-Hurricane Dorian: Opportunities for Climate Resilience***.** International Journal of Bahamian Studies, 28. doi: https://doi.org/10.15362/ijbs.v28i0.467

E2. Submitted manuscripts

Imig, A., Augustin, L., Groh, J., Pütz, T., Zhou, T., Einsiedl, F., Rein, A., (under review) *Fate of herbicides in cropped lysimeters: 1. Influence of different model setups on unsaturated flow.* Vadose Zone Journal

Imig, A., Augustin, L., Groh, J., Pütz, T., Elsner, M., Einsiedl, F., Rein, A., (under review) *Fate of herbicides in cropped lysimeters: 2. Leaching of four maize herbicides considering different model setups.* Vadose Zone Journal

E3. Manuscripts in preparation

Klausner, S., Welsh, K., Iwane Hotta, C., **Imig**, A., McKenzie, Z., Perosa, F., Stephens, M., Turner, A., Thomas, J., Leite Chaves, H., Bowen-O'Connor, C., Moxey, A., Ward, G., Rein, A., (in preparation) *Climate change resilience of freshwater supply on small island states: Research gaps and strategies for a case study in Grand Bahama*

Imig, A., Perosa, F., Iwane Hotta, C., Klausner, S., Welsh, K., Rein, A., (in preparation) *Holistic assessment of managed aquifer recharge through technical feasibility and extended cost-benefit analysis - An application for Grand Bahama*

E4. Presentations

Imig, A., Shajari, F., Einsiedl, F., Rein, A., (2021) *Characterization of soil infiltration by stable water isotopes and an improved lumped-parameter model approach*. EGU General Assembly 2022, online conference, 19.-30. April 2021

Imig, A., Szabo, Z., Halytsia, O., Vrachioli, M., Kleinert, V., Rein, A**.,** (2021) *Current risk assessment approaches applied for managed aquifer recharge (MAR) – An overview.* IAH Congress 2021, Brussels, Belgium 6.-10. September 2021

Imig, A., Klausner, S., Welsh, K., Rein, A. (2022) *A proposed methodology for identifying the feasibility of Managed Aquifer Recharge.* 11th International Symposium on Managed Aquifer Recharge (ISMAR11), Long Beach, United States of America, 11.-15. April 2022

E5. Posters

Imig, A., Augustin, L., Groh, J., Pütz, T., Zhou, T., Elsner, M., Einsiedl, F., Rein, A., *Inverse modelling study for two cropped lysimeters: describing stable water isotope measurements considering different model setups.* Flow and Transport in Permeable Media Gordon Research Conference, Les Diablerets, Switzerland, 11.-17. July 2022.